# DESIGN & ANALYSIS OF ACOUSTICALLY IMPROVED VEHICLE FLOOR CARPETS

A thesis submitted in fulfillment of the requirements for

the degree of Master of Engineering

# THOMAS K JOHN

School of Aerospace, Mechanical and Manufacturing Engineering

RMIT University

December 2008

*Dedicated to my parents, Prof. K C John and Treesa John, and all my teachers, without whose selfless support and love every dream of mine would have been mere dreams.*

# ACKNOWLEDGEMENTS

# DECLARATION

I, **Thomas K John**, hereby submit the thesis entitled "*Design and analysis of Acoustically improved vehicle floor carpets*" for the degree of Masters by Research and certify that except where due acknowledgement has been made, the work is that of the author alone; the work has not been submitted previously, in whole or in part, for any other academic award and that the content of the thesis is the result of work that has been carried out since the official commencement of the program.

Thomas K John

12$^{\text{th}}$ December 2008

# TABLE OF CONTENTS

# 1 Introduction

# 2   Benchmark analysis and target setting for vehicle cabin noise

# 3 Forced vibration analysis of panel systems and sound radiation directivity model

# 4 Design concepts for reducing noise from floor panel sound radiation

# 5 Defining the design process and acoustic tools

# 6  Material simulation, validation and theory

# 7  Virtual modeling and validation, at component and vehicle levels

# 8    Proto-type validation and evaluation of design concept

# 9    Design optimization (Taguchi method based), at material, component and vehicle levels

# 10 Conclusions and recommendations for further research

# LIST OF ABBREVIATIONS

| | |
|---|---|
| **SAC** | Sound Absorption Coefficient |
| **TL** | Transmission Loss |
| **IL** | Insertion Loss |
| **dB** | Decibel |
| **dB(A)** | Decibel, A-weighted |
| **B&K** | Bruel & Kjaer |
| **SEA** | Statistical Energy Analysis |
| **SPL** | Sound Pressure Level |
| **HMS** | Head Measurement System |
| **RPM** | Rotations Per Minute |
| **AC** | Air Conditioner |
| **Hz** | Hertz |
| **AI** | Articulation Index |
| **GSM** | Gram per Square Meter |
| **T60** | Reverberation Time |
| **AFR** | Air Flow Resistance |
| **NCT** | Noise Control Treatment |

# LIST OF FIGURES

# LIST OF TABLES

# SUMMARY

The main objective of this research project is to design, develop and validate an innovative vehicle floor carpet system with improved acoustic performance, and thus reduce noise levels inside the vehicle cabins. The proposed solutions are expected to improve vehicle floor carpet product in areas of acoustic performance, cost, weight and waste reduction, to be environmentally friendly and sustainable in manufacturing.

The following are main research outcomes of the project.

- Acoustically improved vehicle floor carpet with higher sound transmission loss and in-cabin sound absorption coefficient, compared to current production carpet designs.

- Vehicle floor carpet designs that introduce minimum weight and cost penalty for the acoustic performance improvement obtained.

- Material database, i.e. measured acoustic parameters for mathematical modelling, of different vehicle carpet layers.

- Virtual modelling and validation method for design evaluation at component and vehicle levels.

- In-situ vehicle on-road validation test methods for carpet designs

- Optimization methods for further improving the design

In the course of the research, the following questions are also addressed and discussed in the thesis:

- What is the role of vehicle floor carpet in eliminating engine and tyre noise and how good is the current design in achieving it?

- Is virtual modelling and validation an effective tool for designing and evaluating a vehicle carpet acoustically at vehicle level?

- What could be the theoretical limits of noise reduction in the vehicle cabin by acoustically improved vehicle carpets and where are we now?

- Are there simple and efficient methods for in-situ measuring the acoustic performance of carpet design, non-destructively?

- What are the future possibilities in introducing tuned acoustic layers for vehicle carpets?

Initial benchmark analyses and target settings for vehicle cabin noise are conducted to get a clear understanding of the design requirements and constraints. The following observations are worthwhile to be noted from the vehicle tests. Low frequency power train noise has higher sound pressure level (SPL) distribution in the front part of the carpet (front foot well area), which may need more sound barriers. Meanwhile, high frequency tyre-road interaction noise has higher sound pressure level (SPL) distribution in the rear part of the carpet (rear wheel arch and the boot areas), which may need more sound absorption measures.

Based on the benchmark analysis results and review of current carpets systems, the key acoustic parameters for new designs are identified to be Transmission Loss (TL) and in-cabin Sound Absorption Coefficient (SAC), and the various carpet design objectives and constraints are hence defined. This includes design objectives for physical characteristics and functional requirements. A clear understanding of the validation process required for the design evaluation, both virtually and on road, is achieved.

Theoretical analysis of forced vibration of the carpet system is studied by developing mathematical models based on the simple harmonic response and sound radiation directivity of the floor panel and carpet system. The Simple Harmonic Motion oscillator model of analyses of the current carpet design system shows that there is a resonance around the frequency of 323Hz which is in the frequency range of engine or power train noise. This is verified from the sound Transmission Loss measurements of the carpet variants, using the impedance tube method. Further, the theoretical model presented for panel radiation directivity prediction can be used to successfully predict the sound level radiated at a particular angle to the normal of a panel or opening, relative to the sound level radiated in the direction of the normal.

With a basic theoretical understanding of the current carpet design model, four new concept carpet designs are proposed and evaluated in laboratory for acoustic performance. A concept design for both good cabin side sound absorption coefficients and Sound Transmission Loss, identified as Concept 3 design, is developed.

From the above mentioned benchmarking and target setting stage, a systematic design and simulation process flow diagram is formulated. Based on the acoustic targets and the resolution requirement of the results, a suitable simulation tool (Statistical Energy

Analysis) is selected for design and evaluation. A simulation process is defined for carpet systems, which includes material level, component level and vehicle level. Based on this simulation process, the current carpet systems are evaluated, and further new design concepts are identified and proposed based on the simulation results.

Material level simulation validation is conducted for various acoustic samples and measured material sound absorption coefficients have a similar trend to simulated ones and have a variation of only about 10-15% for various samples. The simulation results do not include the low frequency resonance peaks, i.e. below 300Hz, observed in normal incidence absorption measurements. Further, since SEA tools use random incidence Sound absorption Coefficient (SAC) values for simulation inputs, Paris method [53] of converting normal incidence SAC to random incidence is used and validated.

The proposed carpet designs are further simulated and evaluated at component and vehicle levels. In the Alpha Cabin simulation (component level) tests, compared with the current production carpet (MITSUBISHI 380 carpet), Concept 3 carpet consistently reduces about 4.2 dB SPL above 2kHz and reduces up to average of 1 dB below 1 kHz. Concept 3 special mats reduce the noise level by 3 dB above 2 kHz and up to an average of 1 dB below 1kHz, in comparison with the current production carpet (MITSUBISHI 380 carpet).

The vehicle virtual SEA model was evaluated and validated using acoustic transfer function method and well matching results were achieved for engine and tyre noises, except for the coincidence frequency ranges of the backing sheet metal floor. Concept 3 carpet evaluation at the vehicle level shows the reduction of the in-cabin noise level further by up to 3-5 dB, compared to the current production carpet design, for power train noise. The Concept 3 carpet simulation at the vehicle level shows the reduction of the in-cabin noise level further by 2 dB at high frequencies, compared to the current production carpet design, for the tyre-road noise. The Concept 3 mat padded with the current production carpet reduces noise level by about 1dB SPL at high frequencies, compared with the carpet only case for the power train and tyre-road noise. It is illustrated that the proposed the concept 3 carpet has nearly reached the noise reduction limit.

As the component and vehicle simulation results are giving promising results, the proposed Concept 3 mat design is proto-typed for on-road evaluation. A proof of concept mat based on the proposed Concept 3 design (C3-Mat_Prototype) was factory moulded, albeit slight modifications from the original specifications due to material, time and technical constraints. In the impedance tube SAC test, the C3-Mat_Prototype performed

better than the standard mat in the low to mid frequency ranges (up to 3000Hz). Meanwhile, RMIT Alpha Cabin SAC test showed that the C3-Mat_Prototype outperformed the standard mat by an average of 14.2 % for in-cabin side SAC, with the highest improvement of about 40 % of SAC at 800 Hz. On-road vehicle tests show that the C3-Mat_Prototype has better sound absorption at the low to mid frequency range than Standard mat. On road tests using both B&K Pulse and binaural head acoustics were conducted and the data indicates a reduction of in-cabin total SPL by the prototype mat is about 2.1 dB(A) during stationary tests and 0.625 dB(A) during constant driving tests. It is noted that these improvements are measured for the proof of concept factory moulded mat, which points to the fact that a Concept 3 carpet system as a whole can give promising results, as predicted by the simulation model results.

Sensitivity and optimization of the proposed carpet design (Concept 3) are conducted by the Taguchi method. Simulation based Taguchi optimization gives a clear indication for further optimization directions. It is preferred that separate Taguchi loss function calculation be done for various frequency ranges, like Low (315Hz-1kHz), Mid(1kHz-4kHz) and High(4kHz-8kHz) frequency ranges. In Concept 3 carpet layers the AFR and substrate layers have the largest air flow resistivity and therefore they have the largest influence on the sound absorption coefficients in the low frequency range (315 Hz – 1000 Hz). Meanwhile, the foam de-coupler has the largest influence on the sound transmission loss in the low and mid frequency ranges. ON/OFF Taguchi analysis in Alpha Cabin shows that the front foot rest areas consistently dominate in the low, mid and high frequencies and ON/OFF Taguchi analysis for vehicle sound package shows that for engine noise (low frequencies 315Hz to 1 kHz), the headliner and then carpet are the dominating components. Meanwhile, in the case of tyre-road noise, the seats have the highest loss function in all the frequency ranges of interest, followed by carpet treatment, at the mid frequencies (1kHz - 4kHz). An interesting fact identified from the Taguchi analysis results is that the window glasses play a very significant role in the in-cabin sound pressure levels over the low frequency ranges, for both the engine and tyre noises.

The following are identified as recommendations for future design work in improving vehicle carpet acoustics.

- Introducing air-gaps in the range of 10mm in between the heavy layers by use of a honey-comb structure improves the transmission loss by up to 20dB in the frequency range of 1kHz – 2kHz, and up to 10dB in the frequency range of 500Hz – 1kHz, and achieves the best sound transmission loss in these frequency ranges.

- The introduction of honey-comb structure as an air-gap structure does not add any over-head in terms of weight or thickness, compared to foam, nor affects the total absorption of the carpet system.

- Special tuned absorber layers like the perforated facing foam Helmholtz resonator and the corrugated foil faced foam membrane absorbers are excellent in extending the noise reduction frequency ranges to specific low frequency ranges of interest.

# CHAPTER 1

# INTRODUCTION

## 1 GENERAL DESCRIPTION

The study and prediction of sound insulation and absorption of various materials, which includes carpets, trims, heavy sound insulation layers and films, has always been of great significance and interest for acoustic consultants, involved in design of sound packages, especially for vehicle acoustic package designs.

Research has shown that the material acoustic properties can be measured to a desired level of accuracy, which can be used for calculating and predicting the independent acoustical response in a controlled and isolated enclosure with the material samples. Various acoustic evaluation methods like reverberation room measurements, alpha cabin method, Johnson Control method for Transmission loss, etc have been researched and applied for these independent evaluations.

Meanwhile, in the case of an acoustical system which has a combination of various acoustical materials, including structurally linked bodies like in a vehicle cabin, current research shows that a direct addition of the measured acoustical parameters of separate materials may not fully apply. In that case, Statistical Energy Analysis is one of the recommended approaches to predict such a complex acoustical system, as current research shows that it can predict acoustic responses for a wider range of frequencies, even comparable to Finite Element Analysis method.
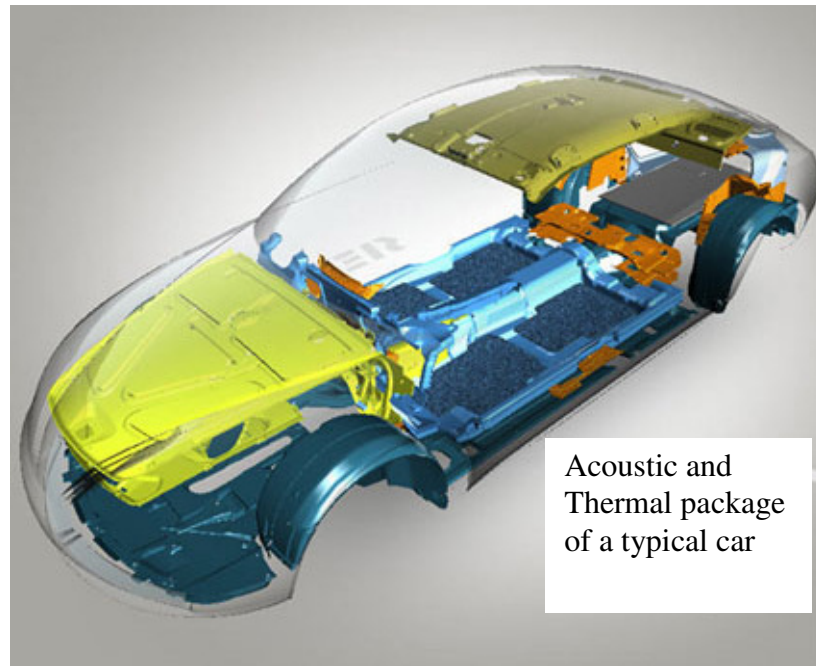
Figure 1.1: Acoustic and thermal package of a typical car
(Courtesy: Rieter automotive, http://www.rieter.com/en/general/products)

A typical car acoustic and thermal package is illustrated in the above Figure 1.1, where this research will be focussed on the improvement of the acoustic insulation and in-cabin absorption of the vehicle floor and carpet, i.e. the blue coloured section of Figure 1.1.

Based on the current research and developments on Statistical Energy Analysis, this research hereby attempts to design acoustically improved vehicle carpets, validate them at component and vehicle levels, and further optimize the design for given constraints, like defined industry standards and targets.

## 2   SCOPE AND OBJECTIVE

As per current research, Statistical Energy Analysis works well with prediction for reasonably complex acoustic systems, with given acoustic parameters of materials, measured using methods like Reverberation room method, Alpha cabin method (preferred for higher frequencies), which are mainly based on random incidence measurements. However, this modelling method has the following drawbacks,

1. Acoustical properties measured using methods like the impedance tube doesn't seem to work well with this modelling method. This requires a study of the influence of angle of sound incidence, as impedance tubes can measure only normal incidence acoustic properties.

2. Material properties like flow resistivity, porosity, tortuosity, etc are required for Statistical Energy Analysis modelling of the material, which are measured generally using various different other methods, which itself brings a dependency on different test setups.

This research also studies the possibilities of providing theoretical explanations for the reasons behind the issues with regards to using impedance tube measurement results (normal incidence) for Statistical Energy Analysis modelling.

There had been large amount of research and development in the area of acoustic insulation and noise reduction for different types of vehicles. There are several set rules applied which have been successful in meeting the current noise standards of the industry. But these methods are generally man power intensive and involve high precision tools and methodologies, which eventually take up time and money. So there comes a need for a quick and portable method for predicting and evaluating an acoustic solution or sound package, for vehicles.

This project contributes significantly to existing technology aiming at dramatically reducing cost and production lead times whilst delivering improved function and performance of an automotive carpet system.

Improved functionality and performance of an automotive carpet system with the opportunity to reduce cost, waste and manufacturing lead-times is one of the focuses of this research. Outcomes of this research project are expected to provide competitive know-how in design and development of automotive carpet systems.

## 3   LITERATURE REVIEW

### 3.1  Carpet Material and Acoustics

Hilyard, et al., [7] described procedures being used to rank the acoustic performance of all diphenylmethane di-isocyanate (MDI) foam backed carpet systems. The procedures were based on the airborne noise Insert Loss (IL) measurement of the carpet composite under laboratory conditions and well established criteria used to assess human response to noisy environments, such as annoyance and speech perception. Data were presented which demonstrated how the interior noise spectrum might be influenced by the unit mass of the heavy layer, and the thickness of the foam backing layer. It was shown that low modulus isolating systems are  superior in Articulation Index performance. Other criteria indicated

that for incident airborne noise the best overall performance should be achieved with a system having a resonance frequency within the 1/3 octave bands centred at 260 Hz and 315 Hz. The influence of system design parameters and foam properties on the resonance frequency was discussed.

Procedures had been described for ranking foam [7] based automotive noise control carpet systems with an assumed airborne noise input, Insert Loss data measured in the laboratory and "noisiness" criteria. The criteria examined were the Articulation Index (AI), the Noise Criteria (NC) and discrete noise component band sound pressure level. Data were presented for the airborne noise IL behaviour of all-MDI polyurethane foam based carpet systems with filled EVA heavy layers. They showed that the resonance frequency trough was shifted to lower frequencies and the IL at resonance enhanced by increasing the unit mass of heavy layer. When the ranking procedures were applied to environmental data it was concluded that the NC approach did not have sufficient sensitivity to differentiate between carpet systems. However, the use of AI, to assess speech perception qualities, and low frequency octave band level, to assess annoyance, showed promise.

Six foam backed carpet systems had been analysed and ranked in terms of potential AI performance [7]. It was found that performance ranked in this way was strongly related to the resonance frequency of the system, systems having low resonance frequency being predicted to perform better than systems with high resonance frequency. System resonance was governed primarily by the effective stiffness and thickness of the foam isolating layer and the unit mass of the steel substrate and heavy layer. Good agreement between predicted and measured resonance frequencies was obtained.

It was demonstrated that systems with good AI performance, which was related to the high frequency IL behaviour, did not perform well at low frequencies. It was concluded that there was potential for optimising the design of a carpet system for a particular vehicle type [7]. This involved designing the system such that the resonance frequency fell within a certain range. For the situation analysed here the optimum range was within the 1/3 octave frequency bands centred at 250 Hz and 315 Hz. Further refinement to performance could be achieved through the control of the damping and airflow resistivity of the MDI foam insulating layer.

One half of interior noise energy penetrates through the floor pan and bulkhead. The two main requirements for the development of improved carpet systems were: (i) criteria for assessing performance and (ii) knowledge of how system design parameters affect their

behaviour. The engine or drive train noise has discrete frequency and controls the noise annoyance, the random broad band noise from the road surface was the major factor contributing to the loudness, and hence interference with speech perception. The main discrete components occurred at low frequencies, below 200 Hz and make no contribution to the AI value [7].

A systematic benchmarking study was performed by Balte, et al., [8] to investigate the acoustic performance of production floor coverings of vehicles. A large number of passenger cars including compact, mid-size, full size, and a truck were selected. The floor coverings were removed from these vehicles and evaluated both on absorption and sound transmission loss performances. It was discovered that the design of the carpet was more important than the materials used. In addition, a carpet with highest absorption did not necessarily have the best sound transmission loss and vice versa. However, an optimum design could achieve high performance in both categories.

Felt-Barrier-Felt-Barrier carpet, a thick carpet provided the best STL. The carpet with nearly 100% coverage of the insulation with the lowest cut-outs provided the best design and acoustic potential. Absorption, transmission loss, homogeneity of material, coverage of insulation, cut-outs and weight determined the acoustic performance of carpets.

Geometric and physical data of selected benchmarking carpets consisted of Dimensions (mm), Area (m$^2$), Cut-outs(%), Absolute Coverage (%), Weight (kg), Draw(mm), Heel Pad, Thickness (mm), Density (kg/m$^3$) and Squared Density (kg/m$^2$).

The use of renewable materials instead of manmade fibres as reinforcement in composite parts provided interesting alternatives for the production of ecologically friendly products [9]. Especially in Europe, renewable materials were of increasing interest because of a directive of the European Parliament that dictated an automotive material recycling rate greater than 80% by the year 2006. This directive was a big opportunity to introduce materials from renewable resources. Therefore, new materials for various interior parts of cars were of interest.

All interior parts of vehicles had different requirements to fulfil regarding acoustics and mechanical performance. Some parts were damping, some parts were absorbing, and some parts fulfilled requirements somewhere in between. In the automotive industry, there were various materials used for acoustic parts and four interesting material compositions were chosen to present in more detail: a standard cotton material, polyester micro-fibre felts,

Lyocell material and natural fibre felts. Nevertheless, it was very difficult to find an optimum material that both fulfilled all requirements and improved passenger comfort.

In general, interior vehicle noise was influenced by various sources; e.g., the engine, exhaust system, gears, wheels, and wind which were so-called primary sound sources. Secondary sound sources were glass and metal sheets. So there was a collection of noise factors that influenced each other.

The use of textiles, especially felts, was based on two major advantages of these materials: low production costs and excellent noise absorption capacity. Felts based on polyester micro-fibres and Lyocell [5] were compared to standard material felts and natural fibre felts. The standard material was a mixture of cotton, polyester bio-component fibres, and polypropylene fibres and represented an ecological solution for good noise absorption. Natural fibre felts were a mixture of natural fibres (flax or hemp) and polypropylene fibres (each 50%). Lyocell felts contained Lyocell (50%), polyester bio-component fibres, and polypropylene fibres. Variations in material weight, thickness, and fibre diameter were considered.

Lyocell is a cellulose fibre based on renewable resources, e.g., wood, and is obtained by an organic solvent spinning process. It is strong, absorbent, wrinkle resistant, biodegradable, and can be fibrillated during processing and has good drapability.

Comparing standard material to Lyocell and to polyester micro-fibre felt showed different advantages of the materials in different frequency ranges. The standard material performed very well in the frequency range above 4000 Hz, whereas it showed some deficits between 1200 Hz and 4000 Hz. Polyester micro-fibre felts showed an improved noise absorption in the middle frequency range of 1200 Hz up to 4000 Hz, which was important for the articulation inside a car. Below 1200 Hz, micro-fibre felts were not as good as standard material because of the homogeneous fibre thickness. Felts made of Lyocell fibres showed the best absorption behaviour over the whole frequency range. Especially below 1600 Hz, the absorption was significantly improved. This range was very important for diesel motors. The comfort for passengers inside a car could be improved by increasing noise absorption with an intelligent application of renewable materials like Lyocell.

Skinners, et al.[10] described trends in the automotive market and then key features determining acoustic absorption of material. They then highlighted the development of a novel technology named ACOUSTIFLEX® from Huntsman Polyurethanes delivering

acoustically active foams straight from production. Physical and acoustic data demonstrated that this technology was suitable for a number of application areas within the automotive market and that the balance of acoustic performance and weight outperformed any other materials currently available on the market. The technology therefore offered producers the opportunity to enhance the acoustic comfort of their vehicles whilst simultaneously lowering the overall weight to achieve this.

## 3.2 Acoustic Simulation and Measurement

Biot's theory provided a framework for the numerical modelling of propagating stress waves in elastic porous materials. Sureshkumar, S., et al. [11] described a finite element method technique based on the adaptation of Biot's theory to acoustic porous material that was applicable for the solution of complex systems consisting of porous, fluid and structural media. Acoustic indicators such as absorption coefficient and transmission loss were calculated for flat samples and these results were compared to known solutions. Finally the transmission loss of a complex dash system was computed and contrasted with the corresponding planar multi-layer results.

Computational simulation tools based on the adaptation of Biot's theory for the modelling served to accurately and effectively predict the acoustical behaviour of porous materials. Prediction of the acoustic behaviour of arbitrary noise control configurations was not feasible using analytical methods and therefore a finite element method based solution technique was used. The validity and applicability of the approach and resulting implementation were demonstrated by solving and verifying example problems.

Duval, et al. [12] first characterized the in-situ diffuse field absorption coefficients using micro-flown p-u probes, showing encouraging results compared to measurements using the reverberation time technique or to poro-elastic simulation.

Obtaining reliable diffuse field absorption coefficients was a key issue for the development of noise control treatment using simulation tools like S.E.A or Ray-Tracing methods [12]. The energy based method called "Vehicle Acoustic Synthesis Method", calculating the sound Pressure Level at ear points from the combination of sound power measurements and acoustic transfer function panel/ear measured or simulated -with Ray-Tracing Methods- for the middle and high frequency range [12].

The 2nd generation of the "Vehicle Acoustic Synthesis Method" (VASM 2) using micro-flown pressure -particle velocity (p-u) [1], for both sound intensity and transfer

functions measurements (without moving the probes), was used to speed up the time to build a validated model of a fully trimmed vehicle in the middle and high frequency range, while increasing accuracy both in terms of source localization and source quantification and while addressing unsteady operating conditions like run-ups [2].

When the transfer functions were measured with a monopole source positioned at ear point applying the reciprocity principle, only the pressure channel of the p-u probe was used. The equation was if it would be possible to get the reflection coefficient of the materials constituting the panels using both pressure and particle velocity channels (from the direct impedance or from the "absorbed" intensity). Unfortunately, an acoustic field hypothesis was needed to answer that question: free-field, standing waves or diffuse field [3].

The reality of a car interior cavity was a semi-statistical field in the middle and high frequency range (315 - 10000 Hz). Nevertheless, upper than a given frequency (typically 1000 Hz in a car), the hypothesis of local diffuse fields could be made like S.E.A. users did. In order to validate this procedure, the absorption coefficients (respectively reflection coefficient $\alpha=1-|R|^2$) of poro-elastic materials in reverberant rooms of different sizes were measured.

Compared to the 1st generation of the "Vehicle Acoustic Synthesis Method" where the source strength characterization was performed using the classical p-p sound intensity technique, the 2nd generation validated the implementation of the micro-flown p-u pressure-particle velocity probes for both sound intensity and transfer functions measurements without moving the probes and without any specific measurement environment [2].

The new measurement technique allowed speeding up the measurement protocol, performing the "Vehicle Acoustic Synthesis Method" on a complete car with all power train operating sources then required only two weeks. Moreover, intensity maps were more refined and unsteady conditions like run-ups became feasible.

The originality of this approach consisted in the simulation of the acoustic package by introducing the insulators in the model as a modification of the power injected in the car compartment (simulated for example by simple Transfer Matrix codes or SEA models or even measured), and as a modification of the cavity transfer functions according to the modification of absorption properties. Using Ray-Tracing simulation, this method became 100% numerical on the acoustic treatment for the middle and high frequency range. The

"Vehicle Acoustic Synthesis Method" was based on an optimized trade-off between good insulation and broadband absorption.

The very good simulation-experiment results had led to the design of an optimized acoustic package reaching the challenging target of a weight reduction of 10%, while maintaining the acoustic performance and the cost.

An important automation effort had been done leading to a comprehensive MATLAB program supporting the modelling effort from the meshing, to the measurements and to the poro-elastic and Ray-Tracing simulation up to 3D colour maps post-treatments.

Three methodical approaches to aid decision making about noise reduction during design stage, using SEA, is being presented in [21].

In order to simulate successively the absorption coefficients of materials for normal and random incidence with Maine 3A V1.3, the Biot parameters of these materials had been determined using an inverse technique based on impedance tube measurements and direct air flow resistivity measurements [4].

In the automotive industry, random incidence sound absorption tests were conducted on flat material samples as well as on finished components such as headliners, seats, and floor carpet systems. Veen, et al. [14] discussed a feasibility study that was being pursued by an SAE task force, under the direction of the Acoustical Materials Committee, to develop a small volume reverberation room test method for conducting random incidence sound absorption tests. This method had the potential to be suitable for the flat material and component testing. A round robin test program was being conducted to determine variability due to test procedures, room size differences and laboratory differences.

The round robin study conducted thus far showed that a properly designed small volume reverberation room, which was significantly smaller than a "full size" room, had the potential to generate comparable results to that of the industry standard full size reverberation room for appropriate frequency ranges. However, the study done thus far also revealed that tests conducted in large rooms had high variations at high frequencies (at and above the frequency where the performance peaks). This variation was larger for higher performing samples than it was for lower performing samples. Also, small size rooms had high variations in the lower frequency range. Therefore, the reason for high variations in test results on similarly designed test rooms needed to be thoroughly understood so that it could

be minimized. Otherwise, there was the potential for larger than acceptable variation in test results from small reverberation room test facilities.

*Design Sensitivity analysis (for final stages, to meet targets) – DSA*

This was an automated analysis (by computer), where the effect of doubling each small components (like even screw hole treatments) was used to measure sensitivity of design changes (for each frequency), which was taken as input and automatically found optimum combination, considering price also.

Once an SEA model was ready, the 3 key parameters, i.e. acoustic performance, cost and weight, could be used by optimisation software to iteratively find the best range of package configuration. A methodology for finding a range of solutions for finding the best sound package relative to cost and weight was considered [22]. Since iterations on an SEA model, by varying properties like absorption, damping and thickness were easy and fast, it was feasible to run an optimiser to work on optimising for cost and weight criteria.

Different cost functions, placing varying emphasis on acoustic performance at target locations and frequencies, plus total cost and weight criteria were used to analyse the SEA model and find an optimum solution. As a first step, a baseline SEA model with a baseline sound package configuration was done. Further the major contributing subsystems were identified. Next, several iterations were run by varying absorption, damping and thickness for these subsystems, to measure the sensitivities of each variation, which was used as input of the optimiser. The 3 parameters mentioned could form a 3D space where the design converges to the optimised package point, visually. A cycle of successive steps would thus converge toward configurations that optimised for the given constraints and emphasis (relative weights) of acoustic performance, cost and weight [22].

With reference to case studies, when a vibration source was known to create a problem at a given frequency, the optimisation was tailored to weight the response at the trouble frequency to be more important than other "non-critical" frequencies. This methodology was also powerful in its flexibility, since the acoustic performance metric could be weighted to stress problem frequencies.

A focused study on the development of treatments to control airborne noise through the dash panels was done [23]. Interior sound levels in trucks continued to be reduced; however, airborne sound transmission through the floor and dash panel (firewall) remained dominant noise paths. There were actually two types of design criteria that must be

established in the sound package development. One was the criterion describing the sound pressure level inside the cab and the other criterion described the quiet sound package treatment.

When establishing the criteria for the interior sound level there were a number of metrics that could be used. These typically included the A-weighted sound level, 1/3 octave band sound pressure level, speech interference level (SIL), preferred speech interference level (PSIL), loudness and articulation index (AI).

The SIL was the arithmetic average of the linear-weighted sound levels in the 500, 1000, 2000 and 4000Hz octave bands. The PSIL was similar to the SIL except that it only averaged the sound level in three octave bands (500, 1000, and 2000Hz). The AI was a measure of the intelligibility of speech with background noise present.

It was important to understand that the noise reduction obtained by the material depended on the substrate to which the material was applied. The truck manufacturers utilized many different substrate materials and constructions so a package developed for one truck might not be optimum for another truck.

Some restrictions included resistance to heat, thickness and weight constraints, limits on how much moisture the de-coupler might absorb and aesthetics.Depending on the substrate and the design of the dash panel, the "optimum" barrier surface weight might be between 3.8 and 9.5 kg/m$^2$.

Component testing had been found to be invaluable as a tool for developing noise control treatments. With full truck on road testing, it was difficult to test actual parts due to space constraints. In addition, variability in the diesel engine sound levels can be of the same order of magnitude as the changes expected due to slight treatment modifications. Loudspeaker tests, involving placing a loudspeaker near the engine block, can also be difficult due to space constraints and flanking paths.

A case study based on the acoustic tools like SEA, insertion loss and sound intensity measurements, was done [24]. A SEA model was constructed to predict the primary paths (panels or area) contributing to the overall interior sound field. Insertion loss measurements were used to verify the primary contributing paths identified using SEA. To provide further details of the primary paths, intensity maps of identified panels were measured allowing detailed construction of the contributory panels.

It was found that SEA predicted the correct airborne acoustic paths in terms of sound transmission loss, and could also provide direction in material changes to improve the TL where necessary. The experimental tools of insertion loss and intensity reinforced the prediction by SEA, and also found highly directive acoustic paths that SEA modelling was unable to consider.

The interior noise of a vehicle usually originated from three major sources: power train/drive line, road/tire interactions, and wind.

SEA was primarily used for noise and vibration analysis in the high frequency range, considering diffuse energy transmission. Therefore this approach was appropriate for reduction of air-borne road noise in the high frequency range. The key concept in SEA was the averaging of energy. The spatial and frequency band averaged energy was used as the primary variables in the governing equations.

The SEA model could contain basic parts, Exterior Subsystems -> Body panels -> Interior subsystems. A SEA model could be an analytical or test-based model. The model in this case was a test-based model. So most of the model parameters were obtained from measurements.

The following two points were to be noted; 1. The exterior subsystems were constrained to have the same energy level as a set of exterior vehicle measurements. The measured SPLs were applied to the exterior cavities as energy constraints in the SEA model. 2. For body panels, the in-vehicle measured STL were used in all area junctions in the model. The coupling areas in those junctions were also from measurements of the size of the panels.

The Damping Loss Factor (DLF) was obtained by using an in-vehicle measured T60 and by following a redistribution procedure.

The concept behind panel contribution was to remove the area junction from the model for the panel under consideration.

1. Insertion loss concept:

To determine the relative contribution of each path, the insertion loss of a barrier material covering each successive partition was measured with reference to the occupant headspace locations.

Limitations: One such limitation was the reduction in cabin absorption by removing the seats; the removal was a necessary consequence for producing reliable insertion loss measurements of all the vehicle partitions. A second limitation was the restriction of the method to airborne acoustic energy transmission only. With the addition of heavy barrier material to the partition, the structural response was obviously changed from the intended in-situ performance that this method tried to encapsulate.

2. Insertion loss measurement procedure:

The following partitions were used: 1 Floor partition 2 Rear gate partition 3 Rear quarter partition 4 Rear door partition 5 Front door partition 6 Front partition. The acoustic excitation was provided by operation on a chassis dynamometer with a coarse road shell installed on the outer roll surface. The resulting sound pressure level for each of the occupant head-space locations before and after the sound barrier layer was installed were subtracted, by insertion loss rule.

3. Sound intensity measurement:

The approach: In order to perform accurate intensity measurements, one must consider the acoustic field in which the measurements are to be performed. An indication of the field might be made from the Reactivity Index (sound pressure level Lp – sound intensity level Li). If RI was zero, the field was perfectly anechoic. A value greater than zero indicated the presence of sound waves in directions other than the incident wave of interest.

On analysis, above 2.5kHz, leaks in the door panel and the coincidence frequency of the glass appeared to be the major paths through the rear door partition. Since SEA did not account for leakage through seals, the path was under predicted in the panel contribution analysis. This result further underscored the need for a reliable method to account for seal and body leakage in SEA.

The ability to utilize existing infrastructure i.e. tools, equipment and machinery to generate a unique acoustic product offering with minimal changes was quite important [25]. New materials, manufacturing processes and concepts regarding the treatment of automotive noise problems had provided the opportunity for enhanced tuning of multi-layered systems.

For carpet and dash systems, it was claimed that a process was developed to control the density over the part, vary the fibre blend and had complete control of the thickness from 2-3mm to in excess of 50mm. With the addition of other acoustic layers, a complete acoustic answer to the challenge of meeting both the absorption and STL requirements was provided.

This along with meeting all of the other customer requirements, for weight, re-cyclability and design parameters, while being cost effective.

Thus the key features of the concept are, 1. The ability to tune the multi-layered system to meet the needs of a specific platform. 2. The ability to vary the density of the de-coupler over the carpet and be able to maintain high lofts. 3. A flexible manufacturing process gives the ability to manipulate the layers to achieve optimum performance 4. Once the influence of each layer was understood, it was possible to manipulate in the poro-elastic properties of each material to then adjust its performance.

A methodology for solving a full vehicle optimization problem for the shape and damping layout of structural panels, by means of FE models, had been developed to meet NVH and weight requirement early in a vehicle program [15]. Numerical results indicated that tackling at the same time the structural shape modifications of the body panels, together with geometry and the materials configuration of the damping viscoelastic layers could lead to improved NVH performance.

Gansen, et al. [16] presented acoustical and physical comparisons among viscoelastic foam, HR foam, and fibre pad. A mass backed carpet in junction with a low density underlay transported by the floor was used to reduce air and structure borne noise which was induced by the road, exhaust, and engine. Commonly used underlay included slab polyurethane (PU) foam (HR foam), cast-in place PU foam, and cotton fibre pad. Fibre pad was pre-dominantly used in the U.S. While, in Western Europe cast-in-place MDI-based viscoelastic PU foam had been a preferred material for carpet underlay. Foam-backed carpets with mass-backing had been produced in Europe for approximately twenty years; only a few North American car makers currently utilized cast-in-place PU foam.

Some of the advantages of the use of foam-in-place over fibre pad for carpet underlay were:

- Good dimensional stability, since the foam was fit to the contour of the floor structure.

- Good moisture resistance

- Easy assembly within the car, which lowered fitting costs

- Foam thickness could be easily varied in order to achieve optimum damping in areas which needed effective damping.

- A variation of sound absorbing characteristics could be achieved by altering the foam formulation.

For air-borne noise absorption, testing method- normal incident sound absorption measurement was the impedance tube method. Viscoelastic and HR foam seemed to parallel each other in sound absorption performance, while they both exhibited better sound absorption performance than fibre pad at all frequencies except 3150 Hz and greater.

For structure borne noise damping, the Geiger Plate Test - attached the PU foam sample to a metal sheet of specified thickness. The metal plate was excited in its fundamental frequency mode and the dampening performance of the foam material was determined by measuring the vibrational decay when the excitation was suddenly removed.

The Complex Modulus Test - A PU foam sample was attached to a thin metal bar (Oberst bar) which was then excited using a random noise signal, FRF was measured and half power band method to determine damping.

The viscoelastic PU foam performed as well as, or better than, the fibre pad and HR foam at all modes of vibration except for the fifth. Viscoelastic PU foam exhibited very high dampening performance around the third and fourth modes of vibrations, where fibre pad had high dampening only at the third mode of vibration within the frequency range of 100 - 1000 Hz. Viscoelastic foam performed well as a vibration dampening material. It was a very effective medium to use as carpet underlay in order to dampen structural-borne noise.

At the same density, viscoelastic PU foam across the board exhibited better physical properties than fibre pad. The most significant differences in physical properties were tensile strength, elongation and compression set which were of importance for a carpet underlay application [16].

## 4  RESEARCH QUESTIONS

The specific research questions that are addressed in this thesis are the following:

- What is the role of vehicle carpet in eliminating engine and tyre noise and how good is the current design in achieving it?

- Is virtual modelling and validation an effective tool for designing and evaluating a vehicle carpet acoustically at vehicle level?

- What could be the theoretical limits of noise reduction in the vehicle cabin by acoustically improved vehicle carpets and what are the current achieved levels?

- Are there simple and efficient methods of in-situ measuring the performance of a design, non-destructively?

- What are the future possibilities in introducing tuned acoustic layers for vehicle carpets?

## 5    OUTCOMES

The basic goal of this research project is to design, develop and validate an innovative car carpet system with improved acoustic performance. The proposed solutions must promote competitive advantage in areas of acoustic performance, cost effectiveness, product weight and waste reduction, and propose environmentally friendly and sustainable manufacturing solutions. The following outcomes are expected as the research yield in the field.

- Acoustically improved vehicle carpet with higher sound transmission loss and in-cabin sound absorption coefficient.

- Vehicle carpet designs that introduce minimum weight and cost penalty for the acoustic performance improvement obtained.

- Material database, i.e. measured acoustic parameters for mathematical modelling, of different vehicle carpet layers.

- Virtual modelling and validation method for design evaluation at component and vehicle levels

- In-situ vehicle on-road validation test methods for carpet designs

- Optimization process methods for further improving the design

A detailed definition of the design target is discussed in section 3 of Chapter 2.

## 6    THESIS STRUCTURE

The development of acoustically optimized vehicle carpets is introduced and further analysis is conducted on vehicles for identifying design targets, in Chapter 2. Chapter 3 is dedicated for mathematical model analysis of the vehicle carpet and for sound radiation model derivation. In Chapter 4 the new concept designs for acoustically improved carpets are

proposed and an initial level of evaluation is being conducted. A study of the process and tools for optimizing and validating the proposed designs, that include new measurement methods and software simulation, is conducted for the project, in Chapter 5. Virtual modelling and validation of the acoustic material layers using acoustic modelling software is the focus of Chapter 6. Meanwhile component level and vehicle level modelling and evaluation of the carpet designs are described in Chapter 7, in detail. The selected concept design is modelled and evaluated at vehicle level using Statistical Energy Analysis, and is tested on-road; the results are analysed and discussed in Chapter 8. Optimization possibilities and sensitivity analysis are conducted on the simulation models for further improvement of the design, in Chapter 9. Chapter 10 discusses about few other possibilities of improving acoustic performance of vehicle carpets, with further research in mind.

# CHAPTER 2

# BENCHMARK ANALYSIS AND TARGET SETTING FOR VEHICLE CABIN NOISE

## 1   INTRODUCTION

This chapter outlines the initial vehicle benchmarking tests and discusses the vehicle cabin noise test results. Further it is followed with a section for defining the design targets of the improved vehicle carpet system, in a systematic approach. The vehicle benchmarking tests measure and compare near field vehicle floor noise for various car models to analyse variable factors and identify the areas to be improved.

Meanwhile, the results from the vehicle tests display the possibilities and potentials of improving the vehicle carpet system to meet tangible targets for both physical and functional requirements. A clear understanding of the listed manufacturing requirements and the similar ones, apart from mere acoustic performance, helps in designing a relevant and marketable solution for vehicle applications.

It is worth noting that emphasis is given to psychoacoustic and subjective evaluation results, while analysing vehicle carpet systems. Hence, subjective analysis of the carpet systems are included well enough in the vehicle cabin noise test procedures.

# 2   VEHICLE NOISE ANALYSIS

Initial benchmark testing for vehicle cabin noise in current vehicle models, specifically Sedan models, is a good start in collecting data required for defining design targets. A multi-point near field data acquisition of the noise distribution just above the vehicle carpet surface is suggested to get a clear picture of the noise transmission paths and noise isolation characteristics of the various vehicle carpets being tested.

The below figure depicts the various points that are appropriate for measuring the in-cabin noise level, following a typical vehicle noise measurement procedure template. Note that the number of measurement points can be optimized and grouped as required, and the irrelevant measurement points (e.g. 1a, 1b and 1c) are not marked in the below diagram. The specific measurement points used for each vehicle are listed in the corresponding test procedure.

**FRONT**
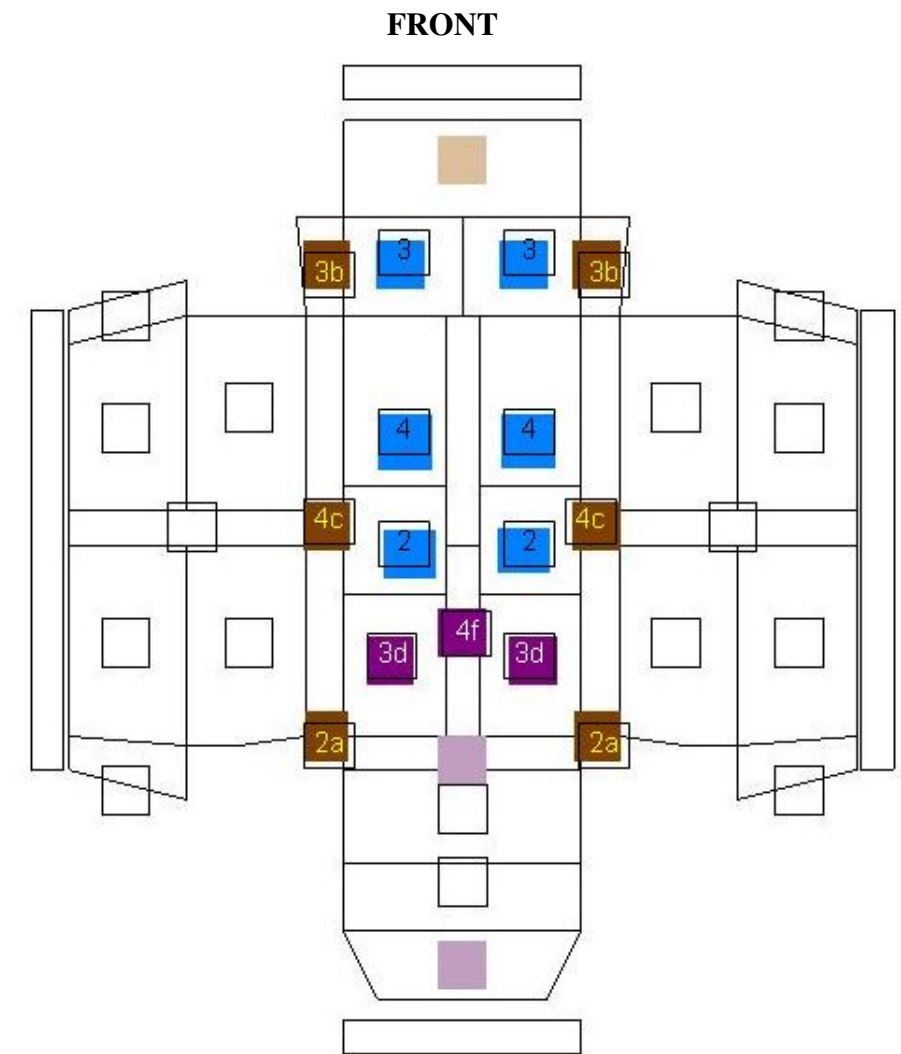


**Figure 2.1: Vehicle cabin noise mapping index for microphone placement**

Two test vehicles of Sedan category are selected for vehicle cabin noise analysis 1) Audi A6 and 2) Hyundai Sonata. Audi A6 fits into the luxury class sedan series and while Hyundai Sonata is from the low price class.

## 2.1 Hyundai Sonata vehicle cabin noise test

The test vehicle details are listed as below:


Hyundai Sonata 2005, Auto Sedan

2.4 littre, 4 cylinders, 16 Valves, TARE 1500

Reg. No. TLH 705,

Engine No. G4JS4138682

VIN No. KMHEM41DR5A162022


Tyre Pressures:

Spec. 30- 33 psi or 230 kPa

Actual Tyre Pressures:

Left Front: 32 psi

Left Rear: 33 psi

Right Front: 31 psi

Right Rear: 30 psi


A PCB accelerometer is glued on the top of engine cover to pick up tacho signals (Figure 2.2). Three G.R.A.S. microphones are at the respective locations (2-3-4 as in Figure 2.1) as shown in Figures 4-5. The distance of microphone tips to the floor carpet surface will be 50 mm. One microphone was placed at the driver's left ear as shown in Figure 2.5. The Bruel & Kjaer Pulse laptop& the front end – the Bruel & Kjaer Pulse intelligent data acquisition system is shown in Figure 2.3. The Hyundai Sonata testing vehicle was mounted on the chassis dynamometer as shown in Figure 2.6.

**Figure 2.2: RPM tacho sensor on top of engine block**



**Figure 2.3: B & K Pulse data acquisition system.**
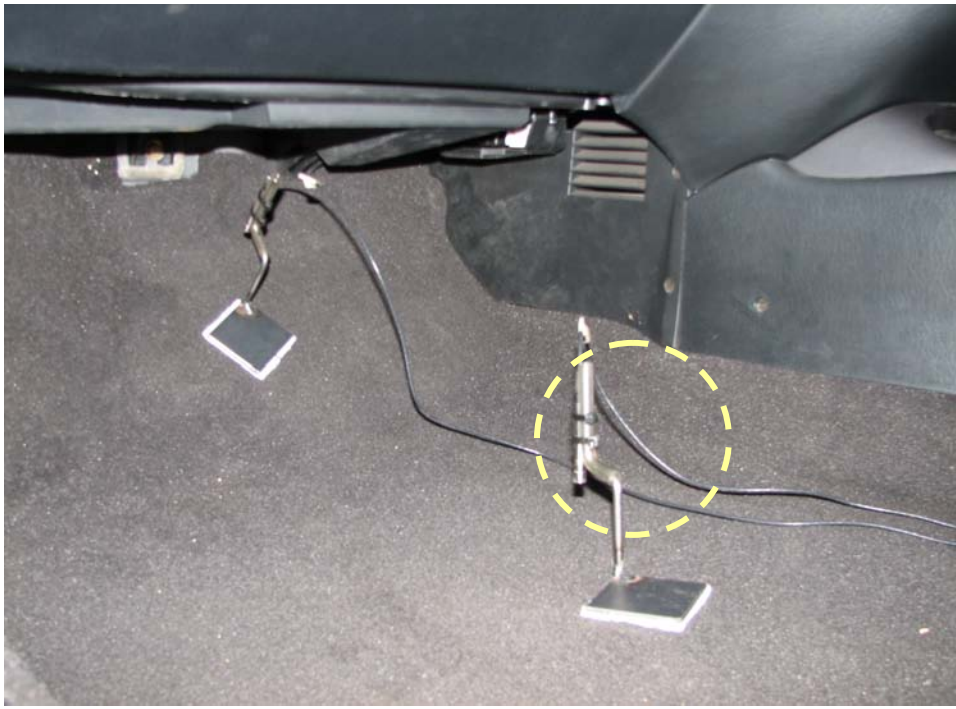
**Figure 2.4: Microphones were placed in the front foot well area**



**Figure 2.5: A microphone was located at the Driver's left Ear (DE).**

**Figure 2.6: Hyundai Sonata testing vehicle was mounted on the chassis dynamometer.**

### 2.1.1  Test procedure

The tests were conducted for both the on-road and chassis dynamometer conditions.

Sound pressure data at idle in drive and neutral, and at constant driving speeds of 40 kph, 60 kph and 80 kph and at the $2^{nd}$ gear slow acceleration were recorded twice with Air Conditioner (A/C) off by the Bruel & Kjaer Pulse intelligent data acquisition system.

The same tests were repeated according to the following microphone placement clusters as shown in Figure 2.4:

- Microphone locations 2, 3 & 4

- Microphone locations 2a, 3b & 4c

- Microphone locations 3d, 4f and at driver ear (DE) level

## *2.2  Hyundai Sonata - Test results and discussion*

The sound pressure waterfall spectra measured from the microphone at DE (Figure 2.7) shows that the on-road second gear slow acceleration test data correlates well with the chassis roll second gear slow acceleration test data above 2500 rpm. Tacho buffer size needs to be increased to catch the right data below 2500 rpm or the testing driver needs to be better trained for the next test runs.
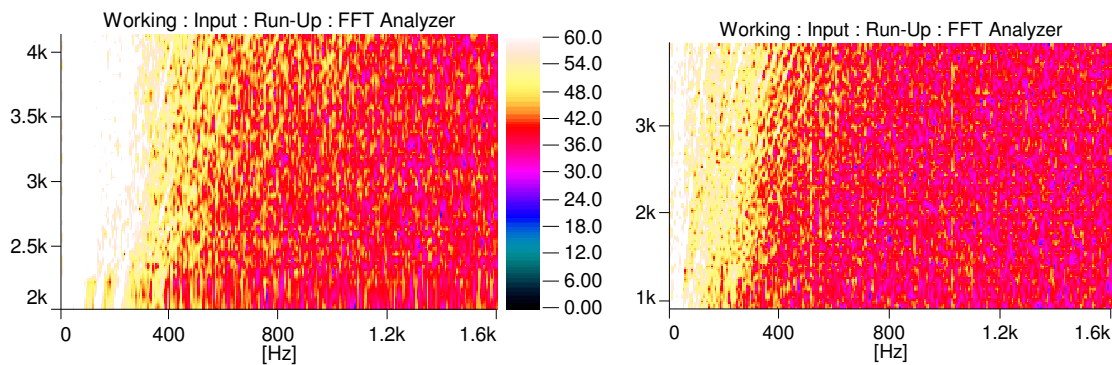
**(a)** On road 2$^{nd}$ gear slow acceleration    **(b)** Chassis dynamometer, 2$^{nd}$ gear slow acceleration

**Figure 2.7:  Sound pressure level water fall spectrum at DE for the 2nd gear slow acceleration tests (a) on the road and (b) the chassis dynamometer**

The previous observation is confirmed by comparison of  the order tracking results of the on-road and chassis dynamometer tests for the second gear slow acceleration, focussing on the engine combustion order of the 2$^{nd}$ as shown in Figure 2.8, where the engine is a four stroke – four cylinder engine.
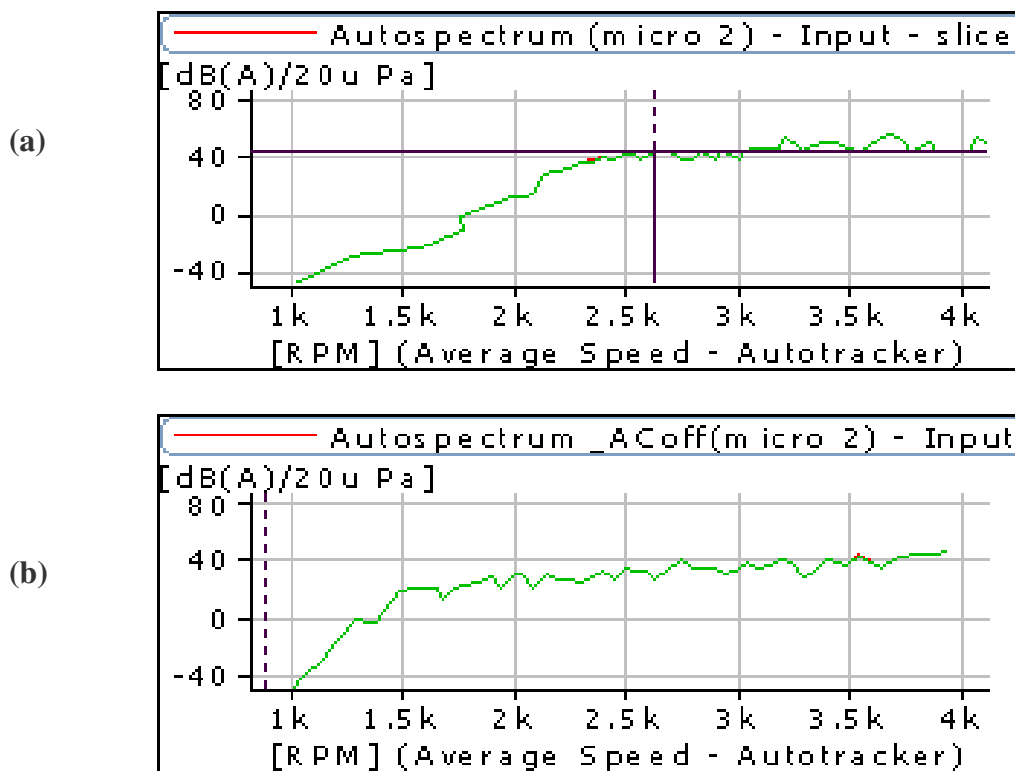


**Figure 2.8: The 2nd order sound pressure level at DE for the 2nd gear slow acceleration on the road (a) and the chassis dynamometer (b)**

Figure 2.9 shows 1/12th octave band SPL readings at the Driver's Ear (DE). Sound pressure levels during the chassis dynamometer test are lower because the tyre-roller interaction is limited on the front wheels.
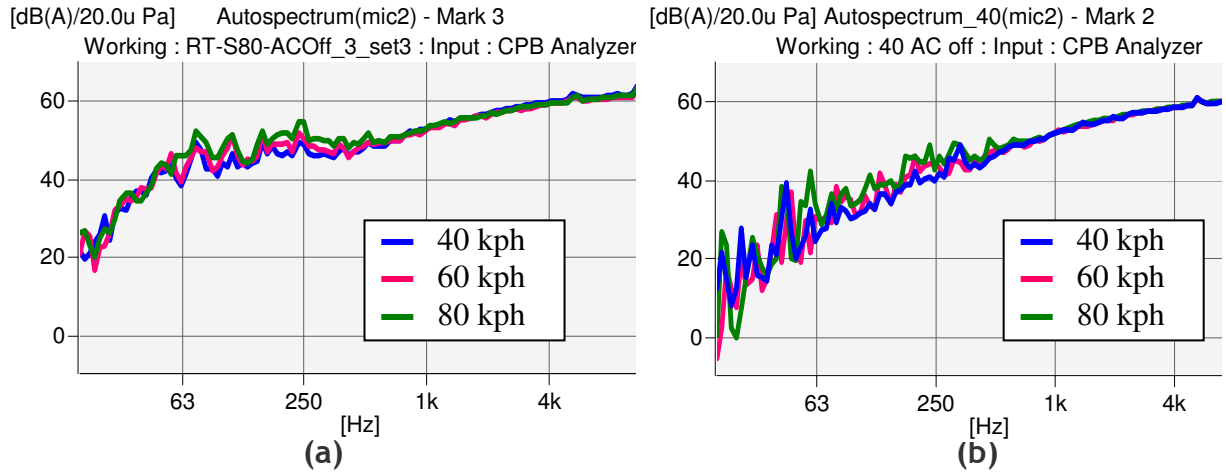


**Figure 2.9: Sound pressure level at DE for constant speeds of 40, 60 and 80 km/h on the road (a) and the chassis dynamometer (b).**

As shown in Figure 2.10, the air flow noise from the car air conditioning unit is in the frequency range less than 300 Hz.
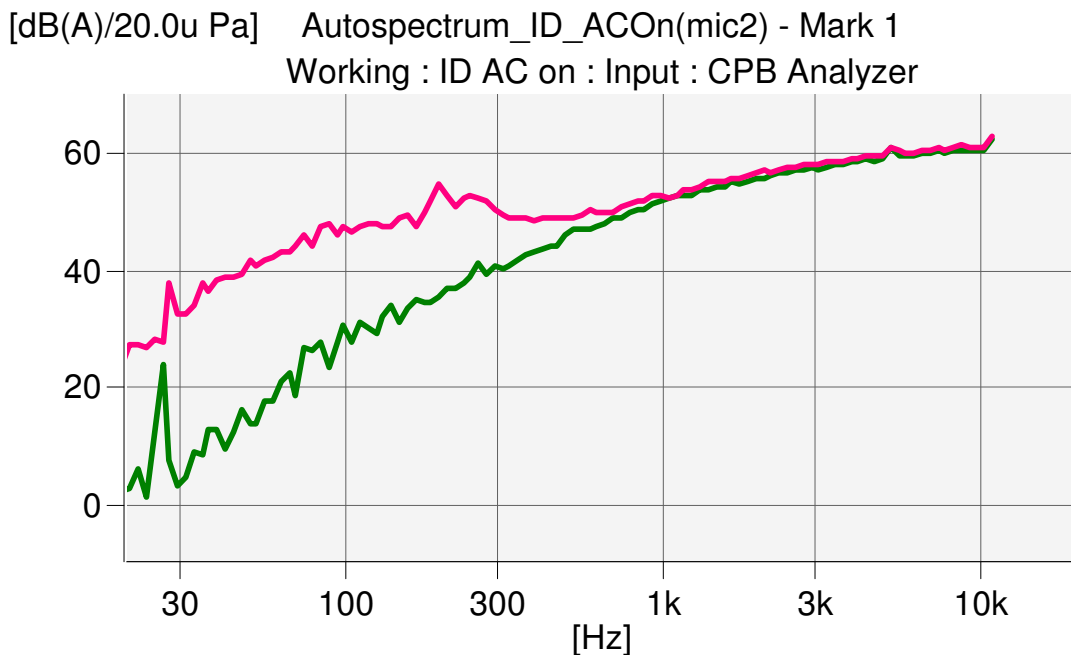


**Figure 2.10: Sound Pressure Auto-spectrum at DE for Idle in Drive_AC On & Off**

During the on-road tests, the front portion of the car floor carpet (eg. front foot well area) is mainly subjected to high SPL, low frequency power train noise as shown in Figure 2.11. whilst higher SPL of high frequency noise (tyre-road interaction noise) is concentrated towards the rear part of the floor carpet (e.g. wheel arch and boot areas) as shown in Figure 2.12. This noise distribution trend applies to all the on-road tests with the SPL increasing with the prescribed driving speeds.

The above findings imply that sound barriers should be applied to the front part of the carpet to block low frequency noise and high frequency absorbing materials should be incorporated in the rear areas of the car carpet assembly.
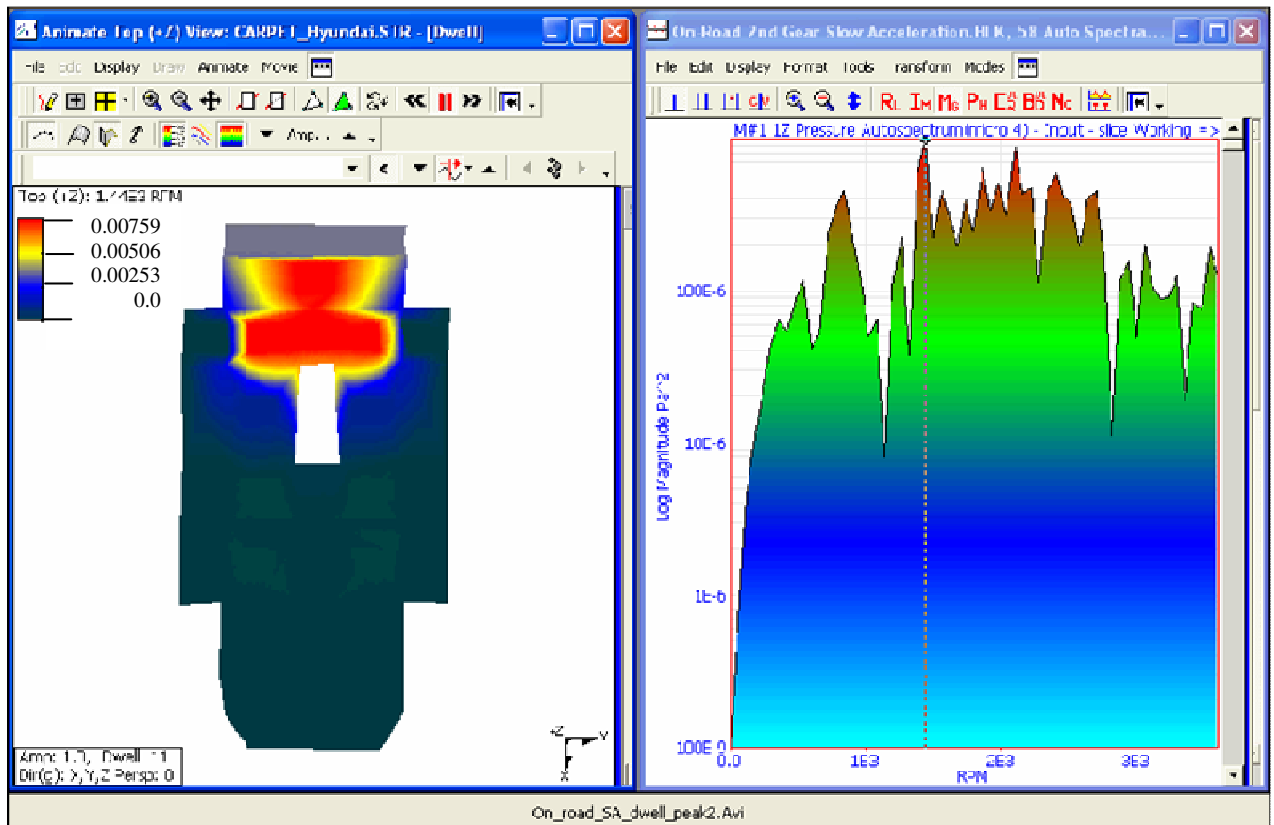


**Figure 2.11: The SPL distribution on the car carpet; 2nd gear slow acceleration on-road test.**
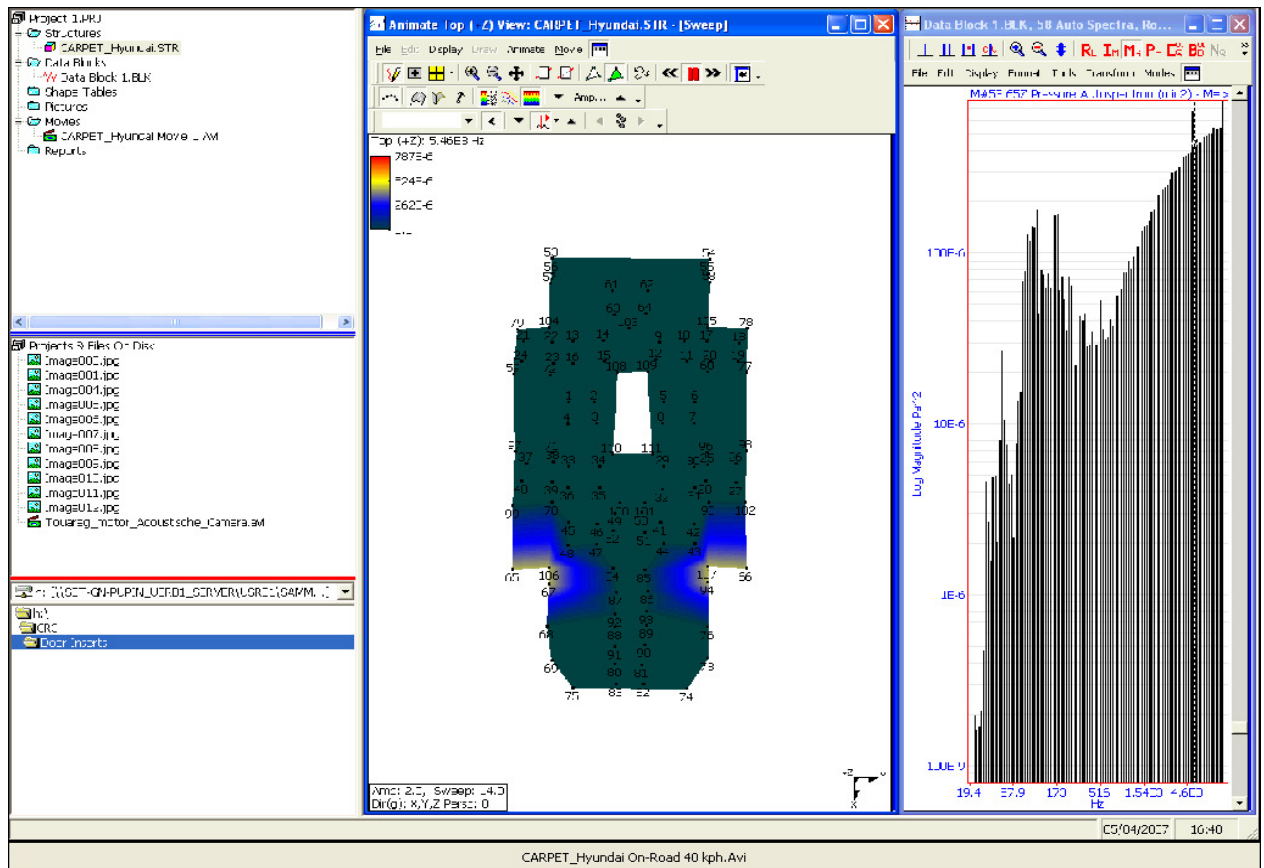
**Figure 2.12: The SPL distribution on the car carpet; 40 kph constant speed on-road test.**

## 2.3  Audi A6 vehicle cabin noise test

The second test vehicle for benchmarking and noise mapping is Audi A6, which relatively falls into the luxury class of sedan category. The test vehicle details are listed as below and Figure 2.13 is a picture of the sedan:

Audi A6 2007, Auto Sedan

2.0 litre, 4 cylinders, FSI Turbo

Reg. No. UMF 487,

VIN No. WAUZZZ4F17N055308

Odometer Reading: 8749 km

Tyre Pressure Specs: 29 psi (front & rear) under normal conditions.

**Figure 2.13: The Audi A6 test vehicle**

For each set of measurements, three (3) G.R.A.S. microphones were used at the locations as shown previously in Figure 2.1. The distance of microphone tips to the floor was 50 mm as shown in Figure 2.3. One microphone was placed at the driver's left ear level as shown in Figure 2.5. The KMT RPM-8000 was used to monitor engine rpm. The Bruel & Kjaer Pulse laptop & the front end – the Bruel & Kjaer Pulse intelligent data acquisition system is shown in Figure 2.3.

### 2.3.1  Test procedure

In-car Sound Pressure Level (SPL) measurements using the Bruel & Kjaer Pulse intelligent data acquisition system were conducted during on-road tests for various driving conditions, to wit:

- Constant speed 40 kph on-road (with and without mats)

- Constant speed 60 kph on-road (with and without mats)

- Constant speed 80 kph on-road (with and without mats)

- Constant speed 100 kph on-road (with and without mats)

- The second gear slow acceleration on-road (with and without mats)

- Idle in-drive AC on and AC off, (with and without mats)

The KMT RPM-8000 was used to tacho the engine rpm during the tests. The output of the RPM-8000 was recorded and integrated in the Bruel & Kjaer Pulse intelligent data acquisition system.

To create an SPL contour map of the floor carpet surface, the above tests were repeated according to the following microphone placement clusters as shown in Figure 2.1:

- Set 1: microphone locations 2, 3 & 4

- Set 2: microphone locations 2a, 3b & 4c

- Set 3: microphone locations 3d, 4f and at driver ear (DE) level

The ME'scopeVES software was then used to generate the SPL contour map of the floor carpet surface using the microphone SPL data from Pulse. Visualization techniques through the use of movie clips from ME'scopeVES were used for comparative analysis of the carpet's acoustic performance.

## 2.4 Audi A6 – Comparative test results and discussion

Comparative sound pressure waterfall spectra (Figure 2.14) measured from the microphone at DE shows that the on-road second gear slow acceleration test data from the Audi A6 correlates well with that of the Hyundai Sonata. This run-up test represents transient conditions occurring during typical driving situations.



(a) Audi A6                    (b) Hyundai Sonata
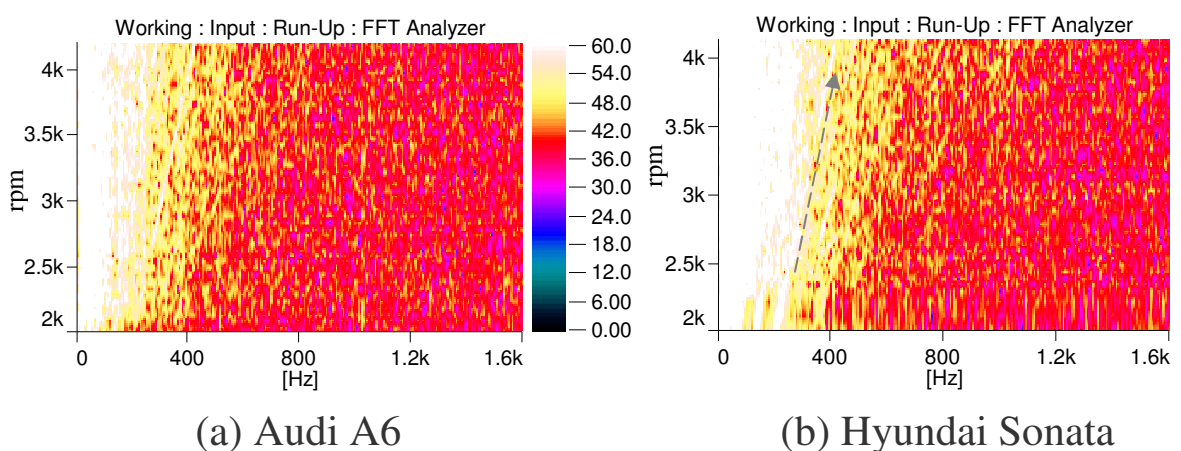
**Figure 2.14: Sound pressure level waterfall spectrum at DE for the 2nd gear acceleration on the road for (a) Audi A6 and (b) Hyundai Sonata.**

Further comparison of the order tracking results of the on-road second gear slow acceleration tests for the engine combustion signature (the 2nd order) as shown in Figure 2.15, suggests that the Audi A6 has a slightly higher total SPL than the Hyundai Sonata. This can be attributed to the turbo charged engine of the Audi A6. The small inconsistency in 2nd order tracking graph for the Audi A6 (Figure 2.15a) below 2500 rpm may be the result of synchronization lapses from the KMT RPM-8000.



(a)

(b)
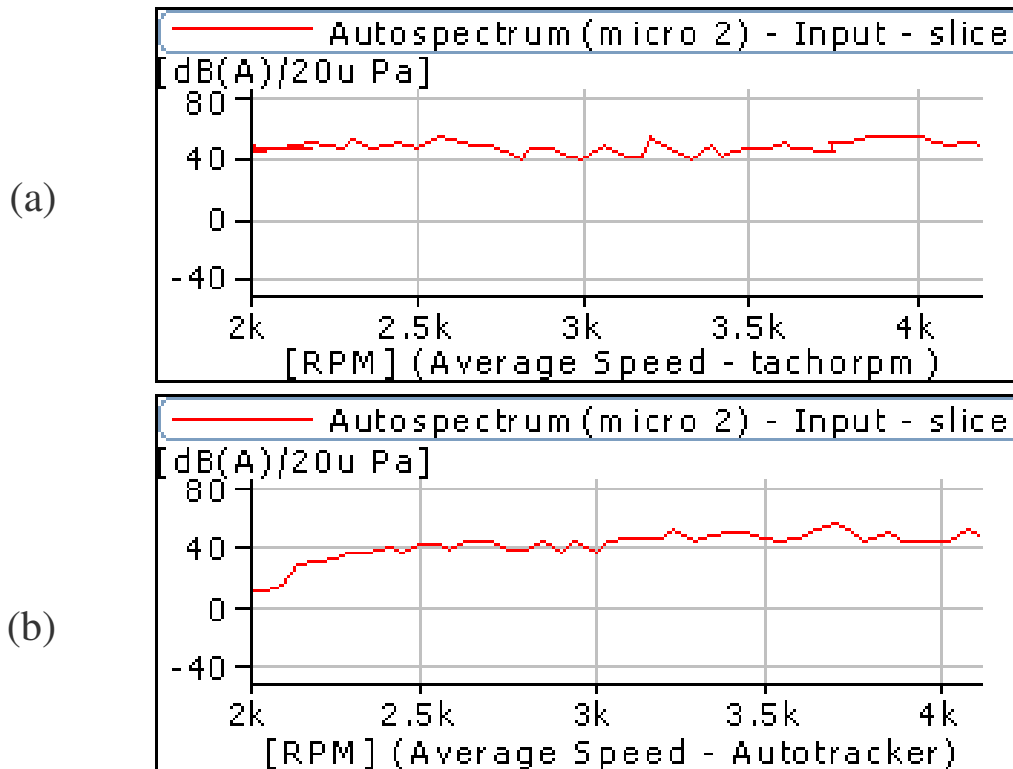
**Figure 2.15: The 2nd order sound pressure level at DE for the 2nd gear slow acceleration on the road (a) Audi A6 and (b) Hyundai Sonata**

Figure 2.16 shows the comparative 1/12th octave band SPL readings at the Driver's Ear (DE) level for the Audi A6 during the constant speed on-road tests. The trend of the SPL increasing with driving speed holds true. Audi A6 registered a slightly higher total SPL compared to the Hyundai Sonata (see Table 1). However, the discrepancy is only on the order of 1-2 dB(A).
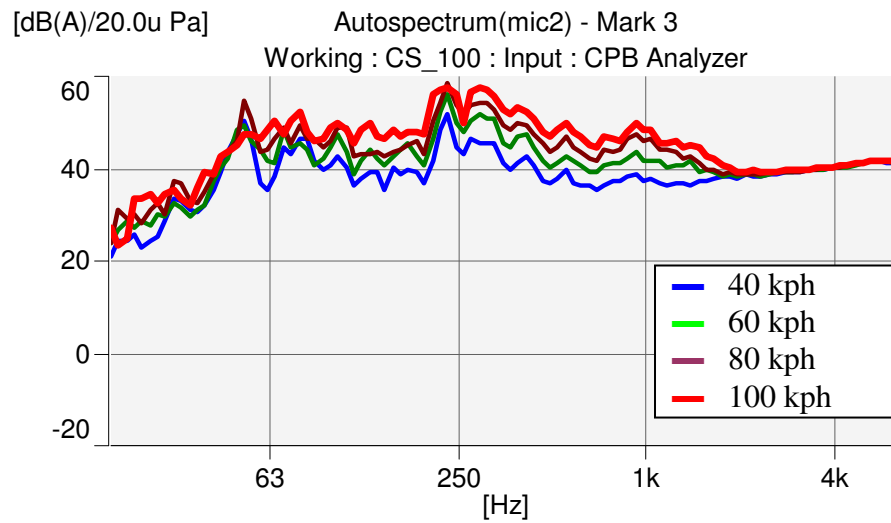
**Figure 2.16: Sound pressure level at DE for constant speeds of 40, 60, 80 and 100 km/h on-road test for Audi A6.**

| On Road Constant Speed Test | | |
|---|---|---|
| **Speed** | **Total Sound Pressure Level [dB(A)] at DE** | |
| | **Hyundai Sonata** | **Audi A6** |
| **40 kph** | **63.0** | 64.7 |
| **60 kph** | **65.6** | **66.8** |
| **80 kph** | **67.6** | **69.5** |
| **100 kph** | **70.9** | **70.3** |

**Table 1. Comparative total SPL's during on-road tests**

Figure 2.17 shows the comparative SPL perceptible at DE for the idling conditions. It should be noted that the introduction of the rubber foot mat have no significant effect on the perceived SPL. This would indicate that the acoustic performance of the Audi A6 carpet is very good.
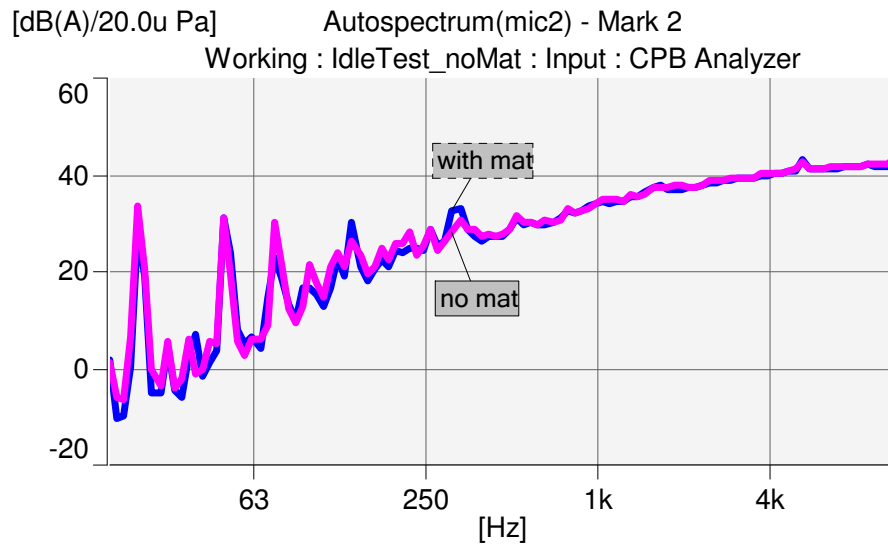
**Figure 2.17: Sound Pressure Auto-spectrum at DE for Idle in drive and A/C off, with and without mats.**

During the on-road tests, the front portion of the car floor carpet (eg. front foot well area) is mainly subjected to high SPL of low frequency (power train) noise as shown in Figure 2.18, whilst high SPL of high frequency noise (tyre-road interaction noise) is concentrated towards the rear part of the floor carpet (e.g. wheel arch and boot areas) as shown in Figure 2.19. This noise distribution trend applies to all the constant speed tests with the SPL magnitudes increasing with the prescribed driving speeds.
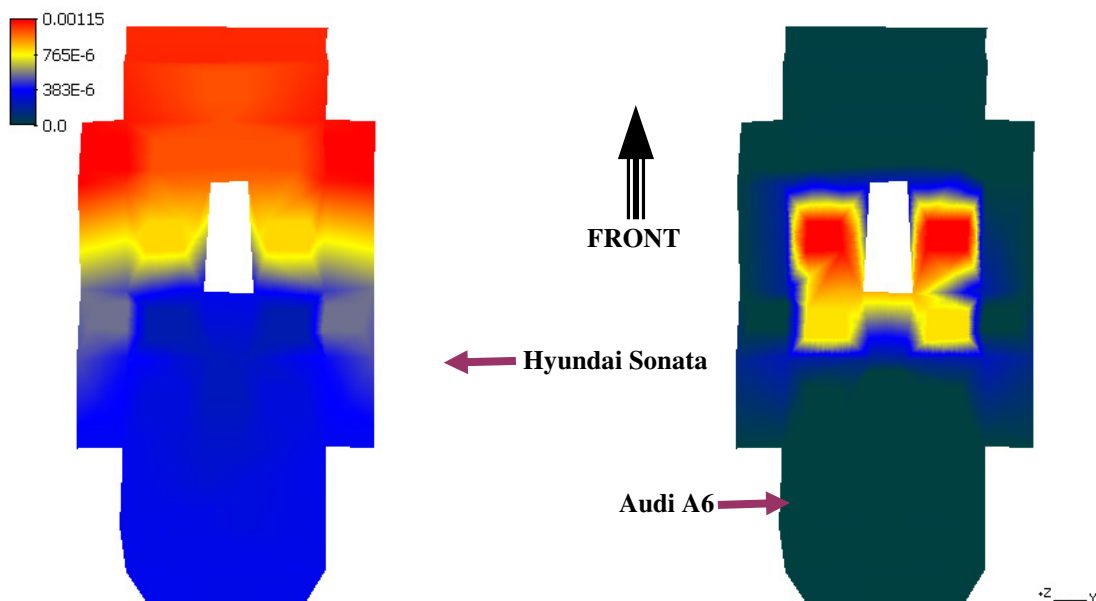


**Figure 2.18: Comparative low frequency (69 Hz) SPL distribution in the car carpet during 80 kph constant speed on-road test.**
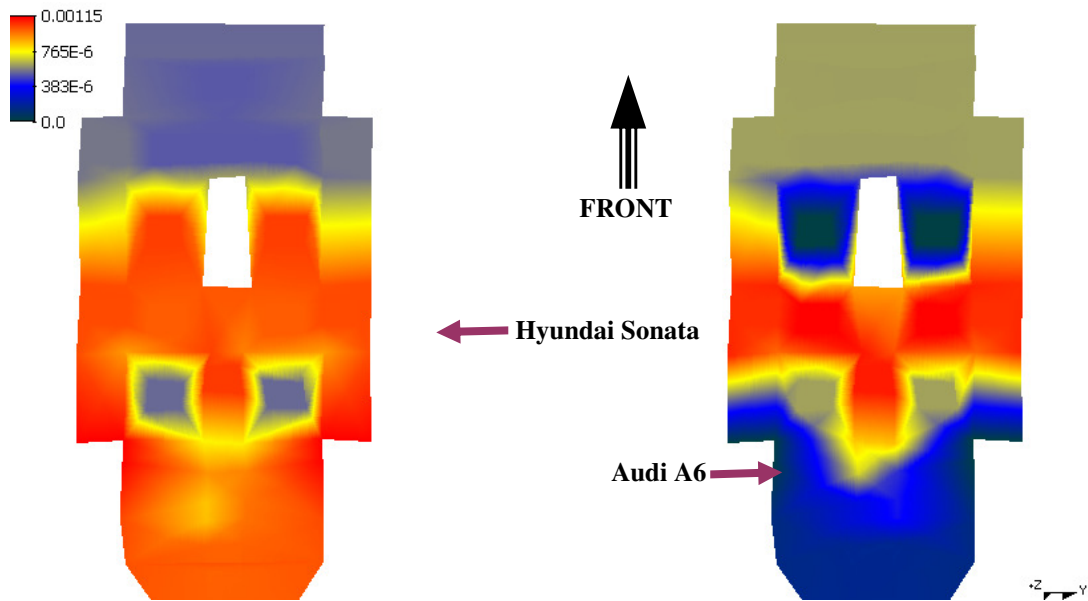
**Figure 2.19: Comparative high frequency (5163 Hz) SPL distribution on the car carpet during 80 kph constant speed on-road test.**

The same carpet SPL mapping trend applies during the acceleration run up as shown in the comparative Figures 20 & 21. It should be mentioned that on run-up (slow acceleration) tests, individual car responses (e.g. spectral peak responses) are unique such that point-to-point comparisons are not always possible. Nevertheless, the carpet surface SPL mapping trends illustrated in Figures 20 & 21 are typical.
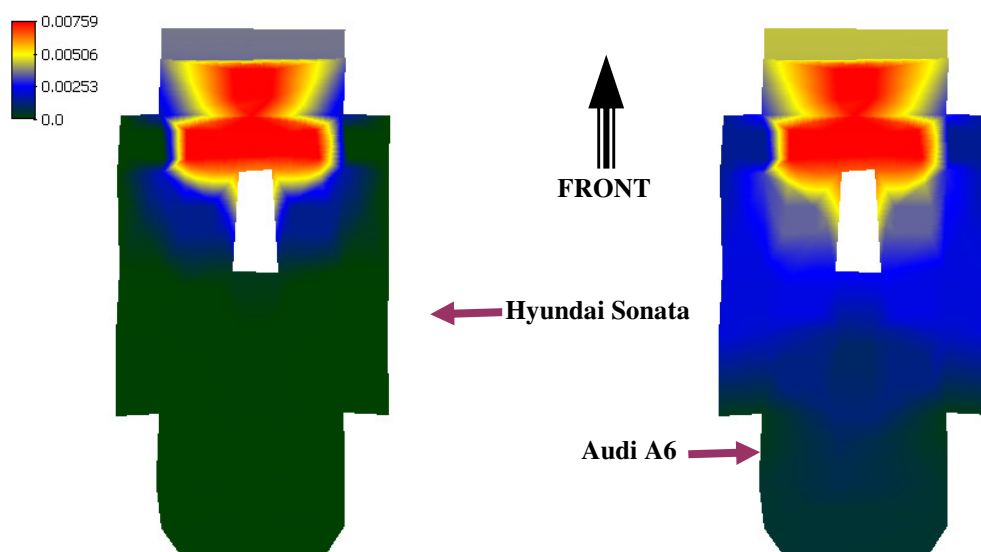


**Figure 2.20: Comparative SPL distribution on the car carpet during slow acceleration on-road test just after starting (low rpm; 840 rpm ≈ 28Hz ).**
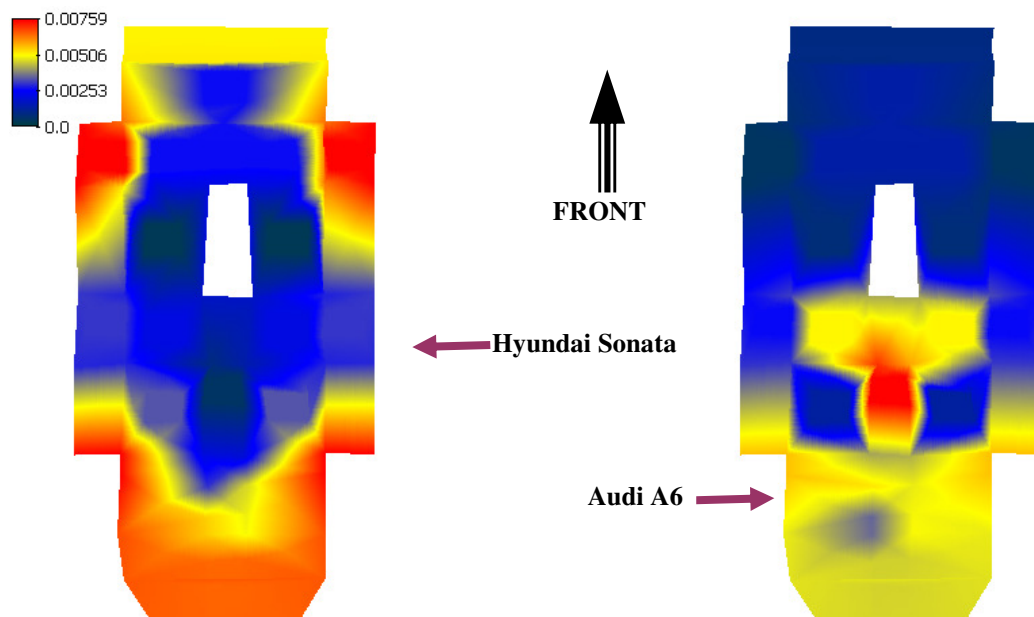
**Figure 2.21: Comparative SPL distribution on the car carpet during slow acceleration on-road test at high engine rpm (3300 rpm ≈ 110Hz).**

The above results indicate that at lower frequencies, where engine noise is mainly concentrated on the frontal areas, the performances of the floor carpets of both test cars are comparable. At 110 Hz, the Audi A6 floor carpet performed better than the Hyundai in reduction of power-train noise in the front part of the floor carpet as evidenced by the reduced 'hot spots' (incidence of high SPL) as shown in Figure 2.21.

## 2.5  Psycho-acoustic and sound quality evaluation

The Head Acoustics HMS III (Figure 2.22) mounted on the front passenger seat of the vehicle was used to measure and record the various sound quality parameters discussed in this report.

**Figure 2.22: Head Acoustics HMS III.**

Six (6) sound quality parameters, directly recorded and analysed using the Head Acoustics HMS III, are listed and discussed herein. The parameters are Articulation Index, Loudness, Fluctuation strength, Roughness, Sharpness and Tonality. Of these parameters, the first three (3) on the list are considered to be of major importance for purposes of our evaluation. Basic description of these sound quality and psychoacoustic parameters are found in Appendix 1 and the comparative parameter plots are included in Appendix 2. The sound quality evaluation is indicative of the overall performance of the car cabin acoustic package.

The $6^{th}$ octave band sound pressure spectra were measured from the right ear microphone of the HMS III as shown in Figure 2.23. Figure 2.24 shows that the on-road constant speed test results of the Audi A6 correlate well with those of the Hyundai Sonata. Total SPL variation is in the order of 1-2 dB(A) and the total SPL increasing with higher driving speeds. The introduction of the foot mats to the Audi A6 has no significant effect on the perceived SPL in the car interior (Figure 2.24).
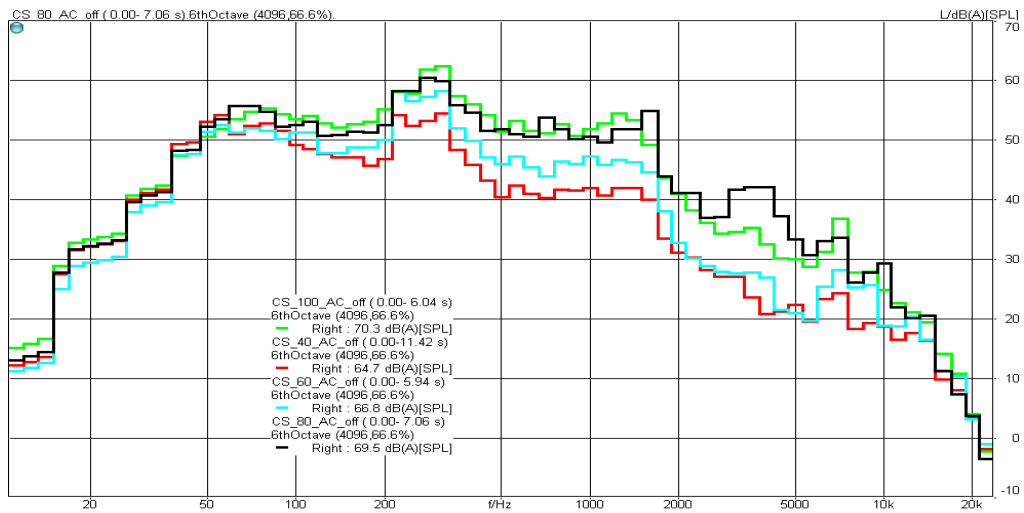
**Figure 2.23 The 6$^{th}$ Octave Band Spectra**
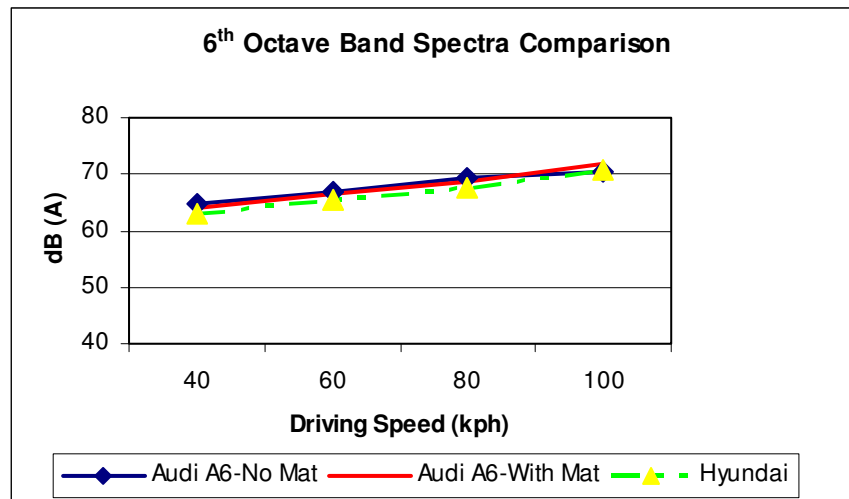


**Figure 2.24: The 6$^{th}$ Octave Band Spectra comparison.**

The articulation index (AI) denotes the ease of holding conversation within an acoustic enclosure. The articulation index is affected by noise, interference, and distortion. The higher the articulation index, the more intelligible is the normal conversation. Figure 2.25 show that the Audi A6 has higher AI values than the Hyundai Sonata inside the vehicle cabins. The AI deteriorates with increasing driving speed due to increased noise levels.

The low AI result for the Hyundai Sonata at 40kph constant speed may be due to inherent flaws in the suspension or chassis design. A poorly responsive suspension for example, can generate resonance resulting to added structural borne noise. The higher AI

exhibited by the Audi A6 can not be explicitly linked to its floor carpet assembly, but it can be surmised that the Audi A6 has a superior overall interior acoustics package.
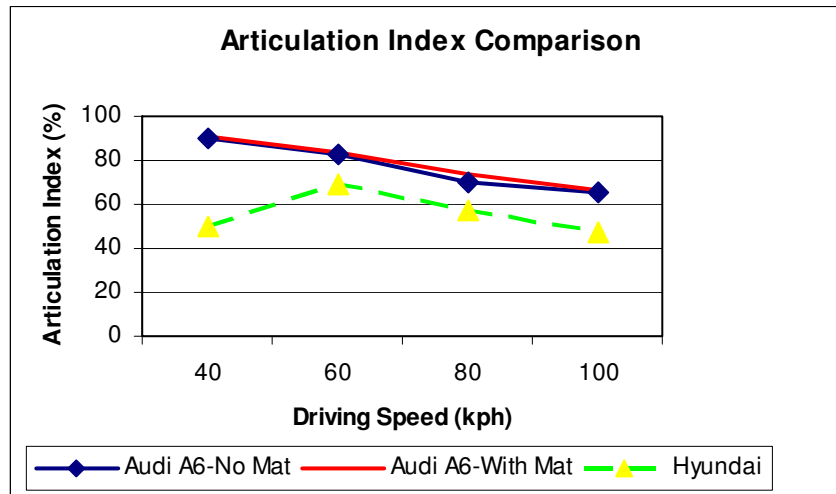


**Figure 2.25: The Articulation Index comparison.**

In terms of loudness index, the Audi A6 cabin interior proved to be better than that of the Hyundai Sonata. Figure 2.26 shows that the comparative loudness index indicated about 10 sonesGF difference between the test cars. The lower loudness index of the Audi A6 (hence quieter) provided a positive impact on the AI as previously discussed.
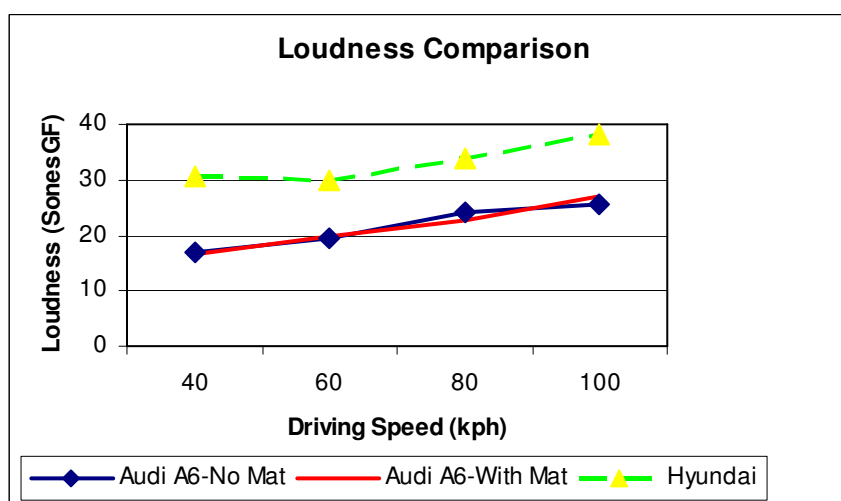


**Figure 2.26: The Loudness Index comparison.**

The fluctuation strength is related to low frequency modulation and Figure 2.27 shows that the Audi A6 registered a slightly higher fluctuation strength index than the Hyundai Sonata. In addition, the variation in the Audi's fluctuation strength indices for the "with mat" and "without mat" cases were not significant.
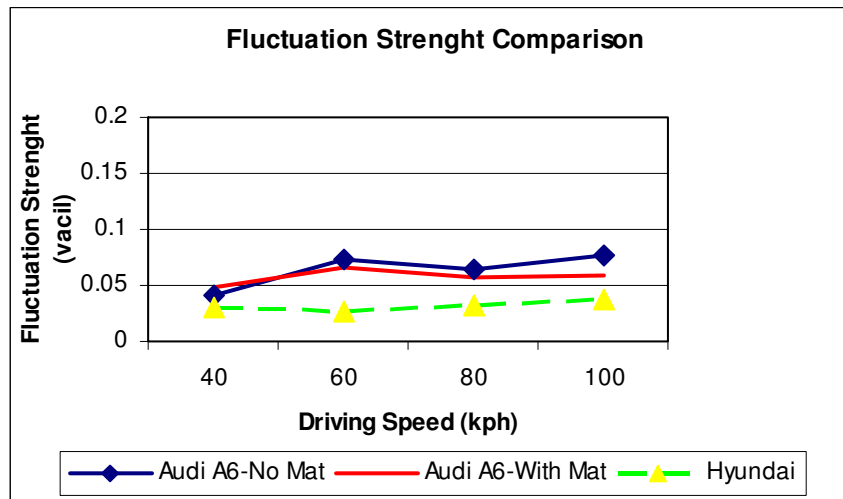


**Figure 2.27: The Fluctuation Strength comparison.**

The comparative sound roughness indices inside the test car cabins are shown in Figure 2.28. Apart from the extreme case for the 40kph constant speed, the Hyundai Sonata had a higher roughness than the Audi A6. The Hyundai Sonata exhibited a trend of elevated roughness index with increasing driving speed which impact negatively on the AI. Since roughness is mostly associated with low frequency sounds, the comparative results indicate that the Audi A6 acoustic package handles engine noise better than that of the Hyundai Sonata.
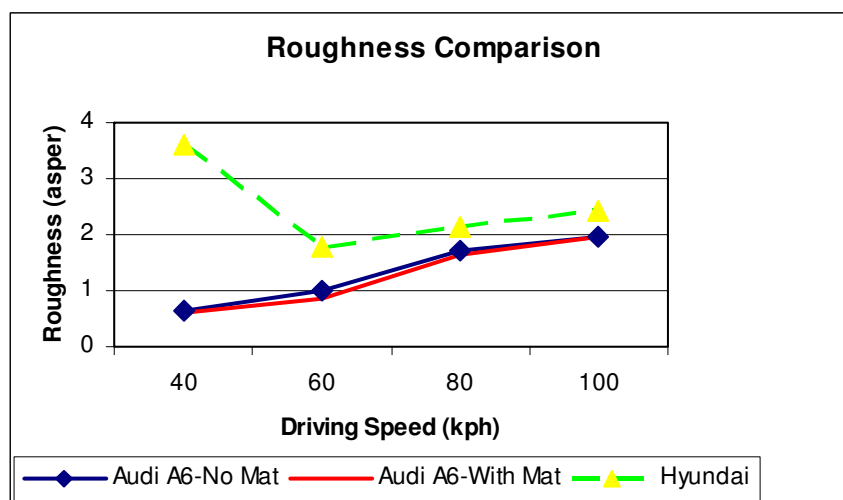


**Figure 2.28: The Roughness comparison.**

The same trends and elevated results of the sharpness index are found for both the Audi A6 and the Hyundai Sonata as shown in Figure 2.29. A better "balanced" sound envelop contributes well to the overall perception of a pleasant acoustic environment. The high reading for the Hyundai Sonata at 40kph may be the result of suspension and chassis design flaws as mentioned earlier.
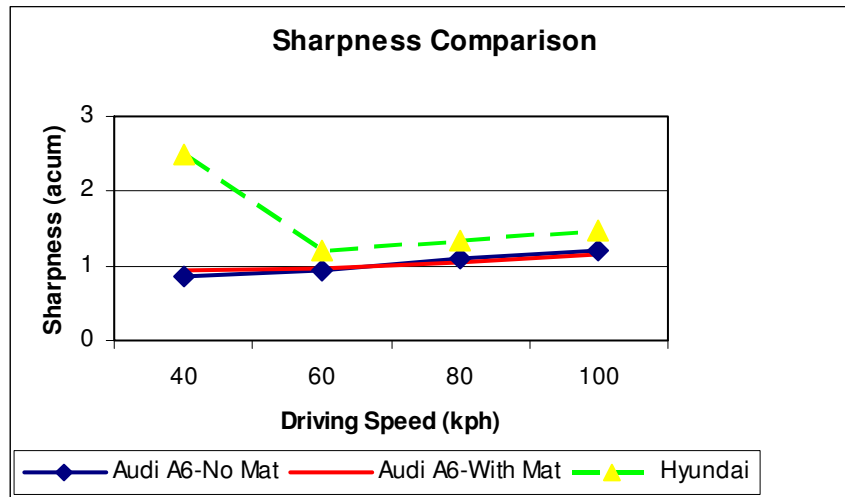


**Figure 2.29: The Sharpness comparison.**

There are no appreciable differences in the comparative tonality indices between the two test cars as shown Figure 2.30. The high measurement value for the Hyundai Sonata at 40kph may be attributed to reasons earlier mentioned. The tonalities for the Audi A6 with and without the "mats" are almost identical.
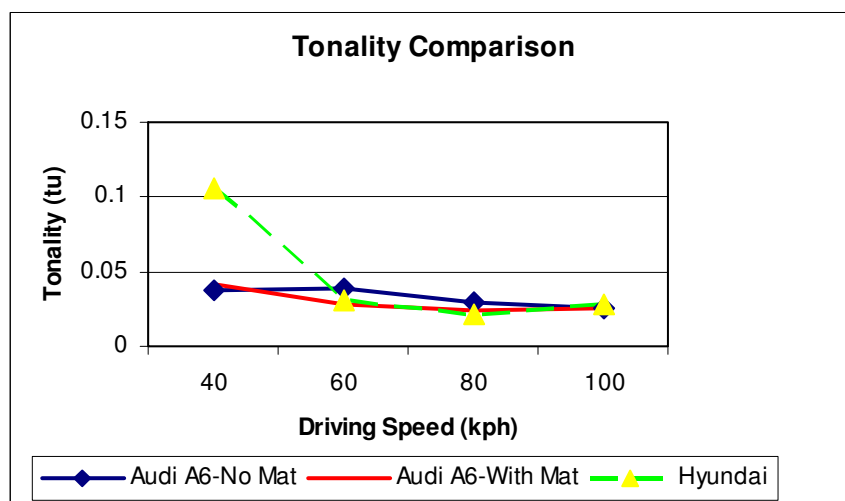


**Figure 2.30: The tonality comparison.**

# 3   TARGET DEFINITION

## 3.1  The carpet system

The vehicle floor carpet assembly refers to the whole floor covering attached to the dash partition and floor pan of the vehicle. The basic function of the floor carpet is to provide suitable cover (e.g. to the bare metal car floor) and comfort to the occupant as well as offer shock, thermal, and acoustic insulation. The carpeting is an integral component of the aesthetics of the car interior.  It can enhance the perception of a luxurious ambiance to the car cabin interior.

The typical floor carpet is constructed with multiple layers of materials. The major carpet components are the tufting and the carpet backing. The former is usually made from woven natural or synthetic materials while the later can be comprised of one or more layers of suitable materials such as felt, foam or latex depending on the intended application. Floor carpet components are mostly bonded together by thermoforming and pressing. The finished product is then cut and finished to size. For standardized applications, the carpet can be moulded to shape and form to fit the surface application.

## 3.2  Carpet design objectives and constraints

The goal of this R&D project is to design, develop and validate an innovative car carpet system with improved acoustic performance. The proposed solutions must promote competitive advantage in areas of acoustic performance, cost effectiveness, product weight and waste reduction, and propose environmentally friendly and sustainable manufacturing solutions. The objectives of the vehicle carpet system design can be categorized into a) Physical characteristics and b) Functional requirements, as given below.

### 3.2.1 Objectives - Physical Characteristics

The new carpet system shall feature improvements or an alternative design to the conventional vehicle floor carpet's heavy layer construction and under layer material. The new design includes a novel composite layered structure with improved noise reduction performance tailored to be compatible with the Futuris' "footprint" concept. The introduction of new heavy layer components, layouts, and structural arrangements will be considered in the design.

**Materials**

New materials or combination of materials that will constitute the new product design will be explored whilst focusing on improving acoustic performance as the primary design consideration.

*Surface layer, Tufting / Velour Needle Punching*

The look, feel and wear durability are strong drivers in the selecting the carpet surface.   These may override acoustic performance criteria.   CSIRO does not have any tufting or velour needle punching equipment.  Making experimental samples would need to be carried out with a manufacturer.  Thus it would be CSIRO's preference to concentrate on the under layers where it has the capability to produce pilot scale sized samples.

*Underlay*

Improvements to noise reduction potential of the carpet underlay shall be investigated through the use of new materials and component arrangements (layering). Particular interest shall be on the construction of improved barrier for low frequency noise control and its selective application to identified critical floor areas. In addition to conventional materials (PU, PEP, felt, latex…), new materials (scrims, microfibre) and alternately methods of construction shall be explored.

Use of microfibres is known to increase the performance of sound absorption particularly at higher frequencies, primarily due to a higher surface area and the potential for a higher tortuosity to be engineered into the construction. There are a number of approaches to creating micro fibre layers and blends worth considering.   Namely electro spun and split able micro fibres.   There are potential novel properties to be exploited with the use of micro fibres, for example it may be possible to have fibres with a range of mechanical resonances in the lower frequency range (100-500Hz). The resonant frequencies are dependent on fibre material properties such as Young's Modulus, fibre diameter and effective length.   These desirable material properties have the potential to be engineered.   It   is   likely   that   a multilayer system will be required for the underlay.

*Material thermoforming property*

In order to facilitate manufacturing and/or production trials to set thermoforming machine temperatures, the new material melting points should be defined.

**Carpet Design**

Carpet design will have to meet vehicle floor pan packaging requirement (assuming Mitsubishi 380 as baseline for example). Design will have to provide acoustic, comfort and aesthetic characteristics. It must be durable, safe and versatile. Preferably, it must be recyclable and low cost.

**Carpet manufacturing process**

Carpet manufacturing starts from tufting, latex/PE coating, heavy layer lamination, heating, moulding, foot pad bonding, foaming and water-jet trimming.

The new design will probably involve additional processes for lamination of air flow resistance layers and microfibre/scrim before thermoforming. The heavy layer may be replaced by light weight heavy layers or air flow resistance layers. The material melting points will have to be considered during heating. After heating, standard processes for trimming and sizing will follow.

Both RMIT and CSIRO do not have production facility. Production trials will have to be conducted in Futuris' manufacturing facility.

**Quality**

Material or component quality must conform to Futuris and OEM clientele specifications as well as all applicable standards:

- Australian / New Zealand Standards

    1. AS/NZS 2111.0-16:1996 (Textile floor coverings)

    2. AS/NZS 2455.2:1996 (Textile floor coverings – Installation practice)

- British Standards Institute / International Standards

    1. BS ISO 11859:1999, BS EN 1307:2005, DD CEN/TS 14159:2004, BS EN 14499:2004

    2. BS 5229:1975

    3. ISO 11859:1999, ISO 1763:1986, ISO 2550:1972

    4. ASTM D3676-01, ASTM D6004-04, ASTM D6005-03, ASTM D6325-98(2004)

- European Standards

    1. IS EN 1307:2005, IS CEN TS 14159:2005, IS EN 14499:2004

2. DIN EN 1307 (2005-05), DIN EN 14499 (2005-02)

**Weight Reduction**

Selection of new materials for the underlay (heavy layer), new design, and the use of alternative methods of manufacture is intended to provide improvements towards overall weight reduction. Should new and lighter materials (eg. microfibre components) with favourable acoustic performance can be utilized, it is likely to lead to a substantial mass reduction of the carpet system.

**Design constraint**

Current Futuris carpet product has a non-permeable heavy layer barrier under the tufting textile which insulates the cabin from exterior noise. Due to a lack of the tufting facilities, working only on the carpet under-layer development may limit carpet acoustic performance enhancement if the carpet heavy layer backing design is not changed. However, the removal of the heavy layer backing from the current carpet design may be constrained by other negative commercial effects on Futuris.

## 3.2.2 Objectives - Functional Requirements

**Acoustic Performance**

The new vehicle floor carpet system is designed to improve acoustics performance inside the vehicle cabin by offering targeted solutions to problematic acoustic areas, to wit:

- Low frequency airborne noise reduction solutions through the use of light weight heavy layers/air flow resistance layers plus air gap in between the component layers, or barriers integrated with mat application/inner dash insulator or as a separate and specific structural treatment – selectively applied to the structure.

- High frequency airborne noise control through better absorption capability by the porous carpet such as moulded cavity absorber or air gap between air flow resistant components inside the moulded floor carpet.

- Improved vibration damping at low frequency and thus reduced low frequency noise infiltration or propagation through the use of porous control layers in place of heavy layer barriers.

The consolidated acoustic performance targets on random incidence absorption coefficient (Figure 2.31) and sound transmission loss/insert loss (Figure 2.32), adopted from the Project Objectives and Constraints Report (0407M2) are presented below.
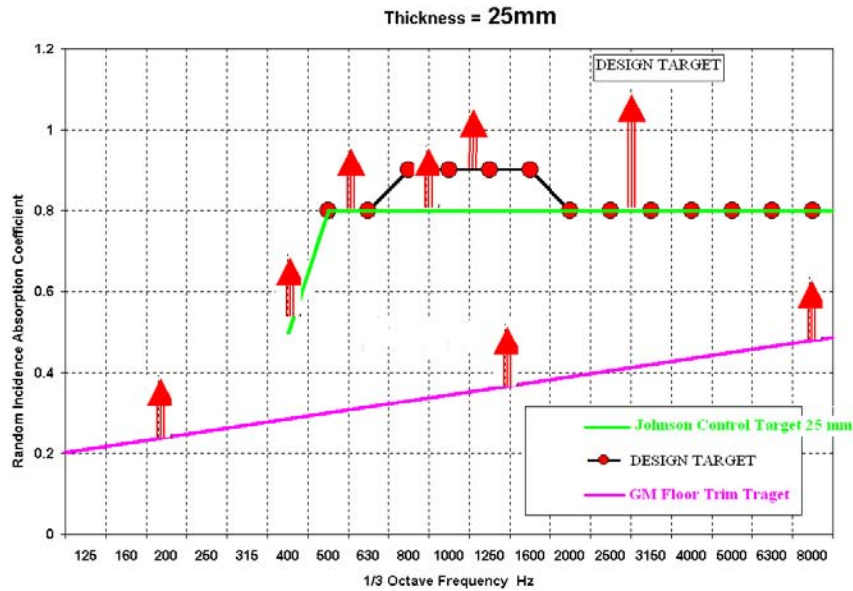


**Figure 2.31: Random incidence sound absorption coefficient design target**
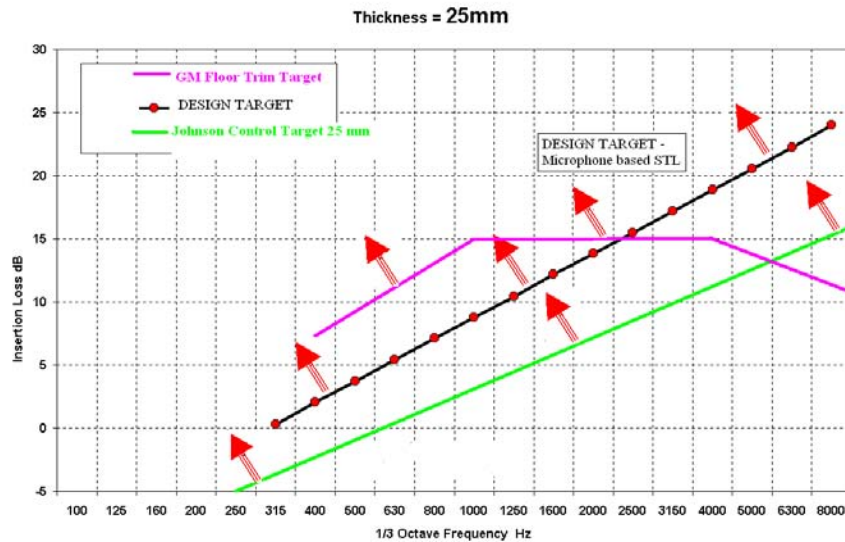


**Figure 2.32: Sound transmission loss/insert loss design target**

**Comfort and Aesthetic Appeal**

The look and feel of the new carpet surface must conform or exceed the typical characteristics of current Futuris carpet products or OEM conventional vehicle floor carpets. The appearance of the conventional tufting will be preserved whilst improving the overall acoustic performance of the carpet assembly.

**Safety**

The product must conform to various safety standards concerning flammability, slip/non-slip, volatile organic compounds emissions, moisture retention, anti-microbial activity, cleaning, and electrical insulation, to wit:

1. HB 37.5-1995 (fire safety)

2. ASTM D7339-07 (volatile organic compounds emission)

3. ASTM E2471-05 (anti-microbial activity)

4. AS/NZS 3733:1995, BS 4088-1.2 -4.0:1994-95, BS 7460:1991, ASTM F1284-04, ASTM F608-03, ASTM F655-06 (cleaning)

5. CSA C22.2.222:1986 (under-carpet wiring)

**Durability**

The new carpet system shall have a product lifespan of 30 years.

**Versatility**

The overall design for the new carpet system shall be adaptable to most car flooring layouts. The integration of the "footprint" concept must not limit the products applicability to specific vehicle cabin design and shall entail minor adjustments in manufacturing methods.

**Service Environment**

Vehicle cabin normal operating conditions:

Temperature            -          -40°C - +50°C

Relative Humidity    -          40 to 85%

**Environmental Impact**

The use of natural fibre and/or recyclable material for the underlay will be pursued. Waste minimization will be addressed through the use of recycled materials and minimizing the number and type of material components of the composite layer. Sustainable manufacturing will be a prime consideration by means of utilizing locally available and/or selected natural material components whenever possible.

Environmental considerations will be factored-in during material selection. There is potential for natural fibres and also for constructing multilayer systems from polymers of compatible chemistry which will allow for the easy reclamation and recycling at the end of product life cycle.

**Cost and Manufacturability**

Cost considerations will be tackled through the combination of simplified or integrated manufacturing techniques (fewer steps, simplified/integrated assembly schemes), use of new materials (resorting to fewer components or material quantity which translate to product weight reduction), and local raw material procurement whenever feasible.

## 3.3  Design validation

The above new carpet design and development will have to be validated through carpet product APQP process following the test verification matrix. RMIT has the capability to validate the designed carpet acoustic performance using AUTOSEA 2 software simulation of material component performance coupled with in-vehicle testing.

Impedance tube test and AUTO SEA 2 material simulation will support CSIRO material development to gain an understanding of the materials acoustic performance and the interaction, and the importance of a variety of material parameters which can be adjusted to engineer and optimise acoustic performance of the material. AUTO SEA 2 parts or component simulation will be used to validate and optimise component design. RMIT intends to develop a simple, portable and reliable methodology or procedure for carpet acoustic evaluations and measurements.

For other carpet design performance such as self-ignition, durability, etc., Futuris development engineers will have to send the parts to relevant NATA certified test labs for testing validations.

# 4  CONCLUSIONS

*Hyundai Sonata cabin noise analysis*

- Low frequency power train noise has higher sound pressure level (SPL) distribution in the front part of the carpet (front foot well area) which may need more sound barriers.

- High frequency tyre-road interaction noise has higher sound pressure level (SPL) distribution in the rear part of the carpet (rear wheel arch and the boot areas) which may need more sound absorption measures.

- The on-road second gear slow acceleration test data correlates well with the chassis roll $2^{nd}$ gear slow acceleration test data above 2500 rpm. Testing driver needs to be better trained or tacho buffer size needs to be increased for the improved data quality for the next test runs.

- AC noise is in the frequency range below 300 Hz.

*Audi A6 cabin noise analysis and sound quality*

- The introduction of foot mats over the floor carpet has no significant effect on the overall acoustic performance of the Audi A6 floor carpet assembly.

- The Audi A6 test car registered a slightly higher total SPL (1-2 dB(A) variation) than the Hyundai Sonata test car under various constant speed driving conditions

- The Audi A6 acoustic package performed better than the Hyundai's in terms of other indices like articulation, loudness, roughness, and sharpness. For fluctuation strength, the Hyundai returned a marginally better performance. The tonality index results are almost identical for the two test cars

- Overall, the acoustic package of the Audi A6 performed better than that of the Hyundai Sonata

# APPENDIX

**SOUND QUALITY PARAMETERS [42]**

### 1. Articulation Index

The Articulation Index indicates the extent to which noise reduces intelligibility of speech. Intelligibility depends on level and the frequency of the background noise. The noise level in the vehicle cabin is thus the factor for intelligibility between vehicle occupants.

Language and the audible range of human hearing can be represented as an area in the vehicle spectrum, limited on one hand by sound pressure level (whispering to shouting), and, on the other hand by sound frequency (200 Hz to 6300 Hz).

### 2. Loudness

A way to quantify loudness is to relate the sensation stimulus to a known standard sound by asking subjects how much louder or softer a test sound is. This method allows subjective loudness to be placed on a linear scale (as opposed to the logarithmic scale of the deciBel).

The standard for this is a 1kHz tone with a sound pressure of 40dB. This reference loudness value is made equal to one (1) sone. Sones GF is the loudness index measured in a free field and sones GD is measured in a diffuse field. For a 1 sone, 1kHz tone to sound twice as loud, its sound pressure must be increased by ~10dB which corresponds to a loudness of 2 sones. So that approximation is used in the definition of the phon: 0.5 sone = 30 phon, 1 sone = 40 phon, 2 sone = 50 phon, 4 sone = 60 phon, etc, where *phon* is another unit of loudness.

Wouldn't it be great to be able to convert from dB to sones (which approximate loudness as perceived by people)? As a crude approximation, it can be said that the A weighting curve approximates the human frequency response at low to moderate sound levels, so dB(A) is *very roughly* the same as phons. The logarithmic relation between sones and phons is shown below.
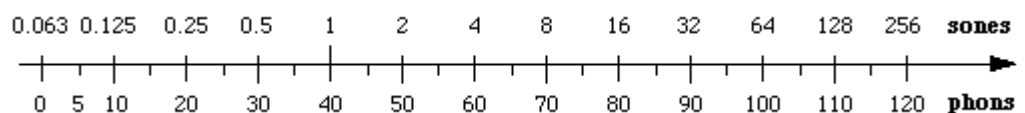
3. **Fluctuation Strength**

Fluctuation Strength measures the sensation of "slow moving" modulation. Sounds modulating at 20 Hz and below can be perceived as fluctuating over time. A good example is a pair of closely spaced tones which cause beating.

The rate of fluctuation, the sound pressure level, and degree of modulation influence fluctuation strength. The reference sound for fluctuation strength: 1kHz tone at 60 dB SPL 100% modulation at 4 Hz gives the reference fluctuation strength = 1 vacil.

4. **Roughness**

Rough sounds are rapidly and repetitively fluctuating noise that contains tones spaced within a critical band amplitude. Sounds which contain modulation between about 20Hz and 200 Hz are considered to be rough-sounding. The sensation of roughness is not limited to true modulating sounds. Noises (broad-band & narrow-band) may also be perceived as rough due to a modulated amplitude envelope.

Parameters important to roughness include the degree of modulation (AM), frequency modulation index (FM) and modulation frequency. Sensitivity to roughness peaks at approximately 70 Hz modulation rate. The modulation frequency range for roughness is ~ 20 Hz - 200 Hz. For centre frequencies at and above 1kHz, the peak roughness sensation occurs at 70 Hz. For centre frequencies below 1kHz, the peak roughness depends upon the width of the critical band.

The reference sound for roughness is: 1 kHz tone at 60 dB, 100% AM modulated at 70 Hz gives the reference roughness equal to 1 asper.

5. **Sharpness**

The basic description of sharpness is the ratio of high frequency level to overall sound frequency level. "Centre of gravity" on frequency scale of spectral envelope describes sharpness: the higher the "centre of gravity", the sharper the sound.

Integration of specific loudness multiplied by a weighting function, divided by total loudness (hence, sharpness is level-independent). Normalized to a reference sound, a narrow band of noise centred at 1kHz at a level of 60dB and a bandwidth of 160Hz, has an agreed sharpness value of 1 acum.

## 6.  Tonality

Sounds can be perceived as tonal when they contain pure tones or noise with bandwidths less than 1 critical band. Tonal sounds exhibit voiced component(s) and periodicity. Non-tonal sounds are noise-like and non-periodic.

Tonality is a measure which can be used to evaluate the overall tonal characteristics of a sound. Takes into account: bandwidth of tonal components, frequency, loudness level with and without tonal components. The reference sound for Tonality: 1kHz tone at 60dB equals 1 tu (tonality unit).

# CHAPTER 3

# FORCED VIBRATION ANALYSIS OF PANEL SYSTEMS AND SOUND RADIATION DIRECTIVITY MODEL

# 1   INTRODUCTION

In this chapter the vehicle carpet system is analysed acoustically using simple, but effective, mathematical models like the Simple Harmonic Motion model. The study helps to quickly identify the acoustic weaknesses like resonant frequencies of the system, where the noise isolation is the minimum, and where could be the focus of development or research.

Further, the study also describes a theoretical method for predicting the directivity of the sound radiated from a panel or opening excited by sound incident on the other side. This directivity needs to be known when predicting the sound level at a particular position due to sound radiation from various kinds of panels like a vehicle floor panel. This is equally applicable to panels like factory roof, wall, ventilating duct or chimney flues. There is surprisingly little information on how to predict this directivity in the scientific literature. Most of this information is based on limited experimental data or its basis cannot be determined.

# 2    SIMPLE HARMONIC ANALYSIS OF VEHICLE FLOOR TRIM PANEL

The current vehicle carpet system in production is the best starting point for both conceptual design and functional analysis studies. The current production carpet we have is based on a three material layer design.

The three layers of the current carpet system are from top to bottom, carpet tufting layer, heavy sound barrier layer and the vibration de-coupler/absorber layer.
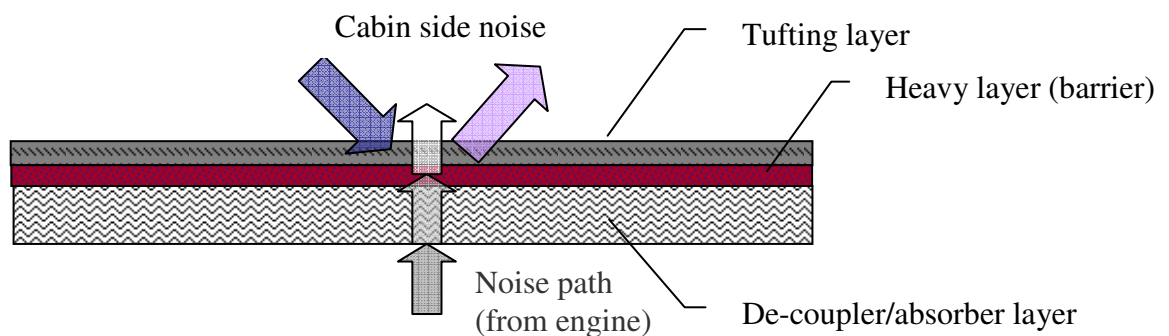


**Figure 3.1:** Current vehicle carpet design

The materials applied in the current production are,

Carpet tufting layer    - 585 gsm carpet fabric & substrate

Heavy layer             - 1.7 kg/m$^2$ heavy layer

De-coupler/absorber   - 1.69 kg/m$^2$ Poly Urethane Foam

The carpet system can be acoustically analyzed by considering it as a spring-mass system in a Simple Harmonic Oscillator (SHM) case, where the de-coupler resonance frequencies are derived from the well established SHM mathematical solution.
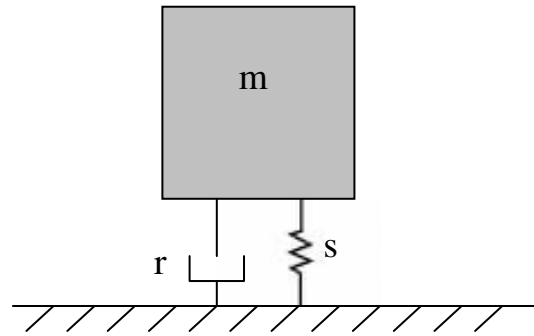
**Figure 3.2:** Simple Harmonic Motion (SHM) oscillator equivalence

$$\frac{x}{F} = \frac{1}{s - m\omega^2 + j\eta\omega} \quad \frac{\text{m}}{\text{N}} \qquad (3.1)$$

Where, "s" it the stiffness of unit area of the carpet panel or the de-coupler layer and $\eta$ is the damping loss factor of the carpet panel.

The resonant frequency is when the denominator is minimum, i.e. when

$$\omega = \omega_0 = \sqrt{\frac{s}{m}} \text{ rad/s} \qquad (3.2)$$

In the case of the carpet system,

$$\text{m} \qquad\qquad = \text{GSM}_{\text{de-coupler}}/2 + \text{GSM}_{\text{tufting}} + \text{GSM}_{\text{heavy layer}} \qquad (3.3)$$

$$\text{GSM}_{\text{de-coupler}} = \rho_{\text{de-coupler}} * t_{\text{de-coupler}} \qquad\qquad (3.4)$$
$$= 49.96 \text{ kg/m}^3 * 0.034\text{m} = 1.6988 \text{ kg/m}^2$$

$$\text{GSM}_{\text{tufting}} \quad = \rho_{\text{tufting\&substrate}} * t_{\text{tufting}} \qquad (3.5)$$

$$= 90 \text{ kg/m}^3 * 0.0065 = 0.585 \text{ kg/m}^2$$

$$\text{GSM}_{\text{heavy layer}} = \rho_{\text{heavy layer}} * t_{\text{heavy layer}} = 1.7 \text{ kgsm} \qquad (3.6)$$

Where, GSM is equivalent surface density in gsm unit, $\rho$ is density and t is the thickness.

Therefore,

$$m \quad = 3.1344 \text{ kg/m}^2$$

$$s \quad = E_{\text{de-coupler}} / t_{\text{de-coupler}} \qquad (3.7)$$

$$= 439.12 * 10^3 / 0.034 = 12.953 * 10^6 \text{ N/m}^3$$

where, $E_{\text{de-coupler}}$ is the Young's modulus (unit area) of the de-coupler layer and $t_{\text{de-coupler}}$ is the thickness of the de-coupler layer.

$$\omega_0 \quad = \sqrt{s/m} \qquad (3.8)$$

$$= \sqrt{(12.953 * 10^6 / 3.1344 \text{ kg/m}^2)} = 2032.86 \text{ radians/second}$$

$$f_0 = \omega_0 / 2\pi = \mathbf{323 \text{ Hz}} \qquad (3.9)$$

Hence, from Simple Harmonic Motion analysis method, the current carpet system is expected to show a normal incidence resonance frequency at **323 Hz**, which is definitely in the power train or engine noise source frequency range. The carpet panel parameters like Young's modulus, density, damping loss factor and GSM were measured in CSIRO material laboratory.

The below graph is a log frequency - amplitude of the x/F transfer function variable values of the current carpet. The resonant peak at 323Hz is clear on the transfer function plot, which is the expected weak link of the current carpet acoustic design.

**Vehicle floor trim SHM response (damped)**

$$\omega = \omega_0 = \sqrt{\frac{s}{m}} \text{ rad/s}$$

**323 Hz**

$$\frac{x}{F} = \frac{1}{s - m\omega^2 + j\eta\omega} \frac{m}{N}$$

Carpet response (SHM damped)

*Amplitude response (x/F)* — 10, 0, -10, -20, -30, -40, -50, -60, -70, -80

100.0 · 1000.0 · 10000.0

$f_o$

**Frequency (Hz)**
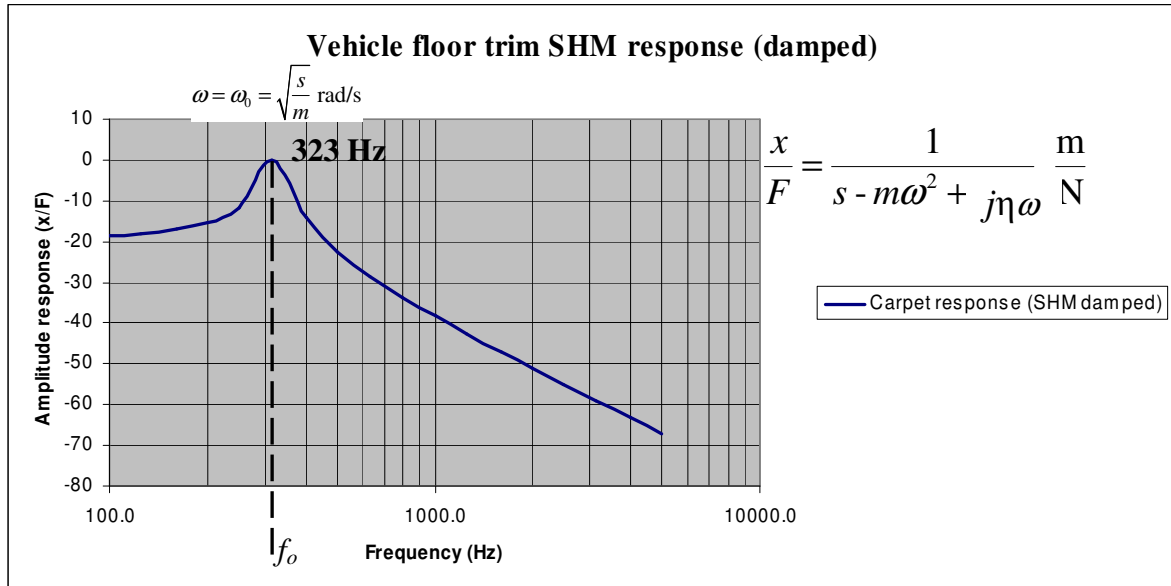
**Figure 3.3:** Simple Harmonic Motion (SHM) oscillator equivalence

Transmission Loss measurements are conducted on the variations of the current carpet design using the B&K impedance tube method, explained in Chapter 5. The results are plotted in the below graph for samples B to K of the current production carpet design.

## Transmission Loss - Set 1

*TL (dB) - 20Log(Inc/Trans)* — 70.0, 60.0, 50.0, 40.0, 30.0, 20.0, 10.0, 0.0, -10.0, -20.0, -30.0

50 · 80 · 125 · 200 · 315 · 500 · 800 · 1250 · 2000 · 3150 · 5000

**Frequency**

Legend: B, C, D, E, F, G, H, I, J, K
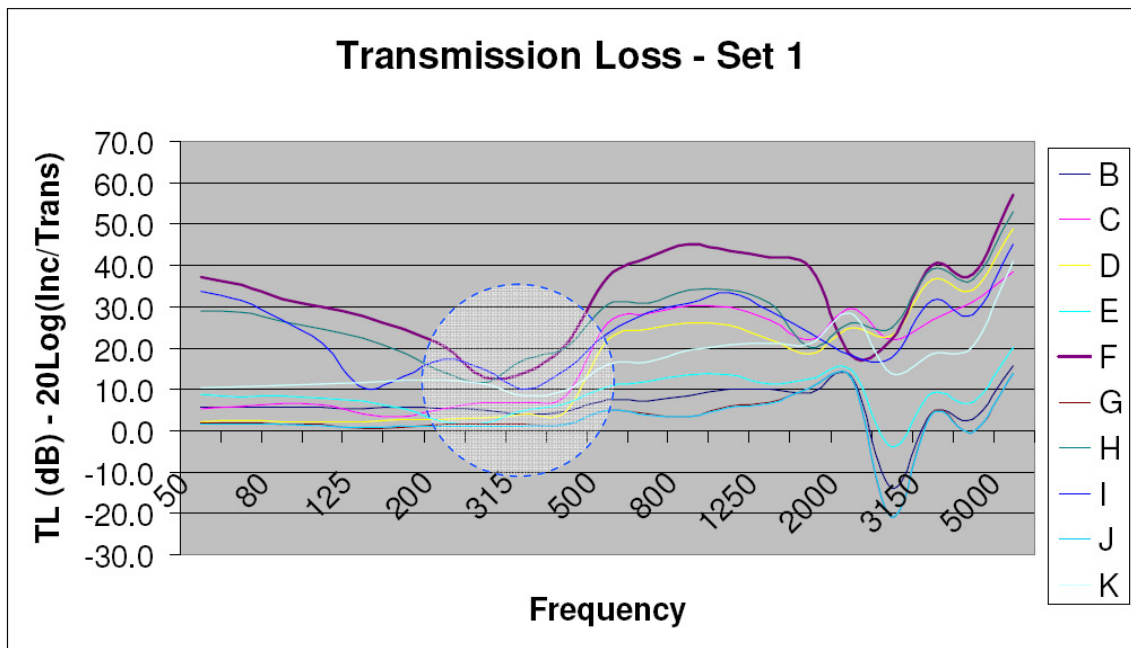
**Figure 3.4:** Transmission Loss results of the current carpet design variants

It is clear from the Transmission Loss results that the carpet design has an evident resonance dip or acoustic weakness at approximately 323 Hz frequency. This is the same case for majority of the samples, with small deviations introduced by factors like the varying GSM of the heavy layer and the fact that the simple spring-mass model is not exact.

# 3  FINITE SIZED PANEL RADIATION – THEORY

A two dimensional method for calculating the directivity of the air-borne radiation of sound from a panel or opening whose vibration is excited by the incidence of sound from the other side, like power train or tyre noise sources, is being presented. The directivity of the radiation depends on the angular distribution of the incident sound energy ($w(\phi)$) or angular weighting function. The proposed method for deriving the angular weighting ($w(\phi)$) is generic and so a variety of cases are studied. For panels or openings like in the wall of a cabin or room, the angular distribution of the incident sound energy is predicted using a physical model which depends on the sound absorption coefficient of the cabin/room reflective surfaces. For an opening, like at the end of a duct, the sound absorption coefficient model is used in conjunction with a two dimensional model for the directivity of the sound source in the duct. The finite size of the panel is taken into account by using a two dimensional model for the real part of the radiation efficiency of the finite size panel or opening.
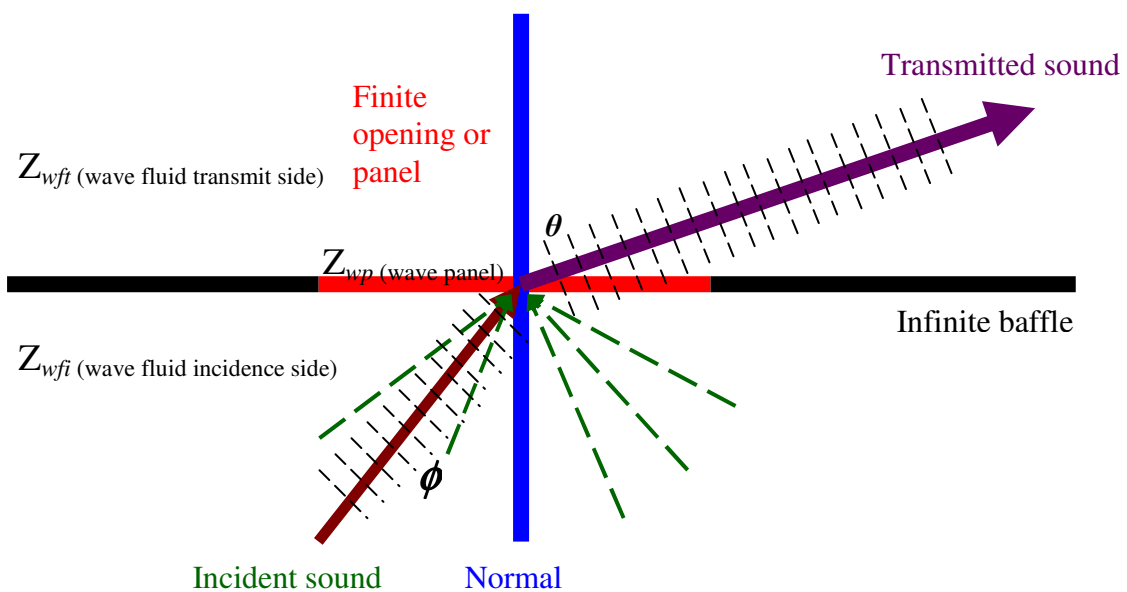


**Figure 3.5:** Panel or opening radiating sound due to forced excitation on the incident side

The directivity of the radiation depends strongly on the length of the radiating object in the direction of the observer and only slightly on the width of the object at right angles to the direction of the observer. For panels, the plate wave impedance of the panel is used. Above its critical frequency or normal incidence resonance frequency a single panel radiates strongly at the angle at which coincidence occurs, i.e. when the angular wavelength coincides with the longitudinal modal frequencies of the panel. The method is compared with published experimental results

The effective impedance $Z_e(\phi)$ of a finite panel in an infinite baffle to a plane sound wave incident at an angle of $\phi$ to the normal to the panel is [45]

$$Z_e(\phi) \text{ (effective)} = Z_{wft}(\phi) \text{ wave fluid transmit side} + Z_{wfi}(\phi) \text{ wave fluid incidence side} + Z_{wp}(\phi) \text{wave panel} \quad (3.10)$$

where

$Z_{wfi}(\phi)$ is the wave impedance of the **fluid** as experienced by the finite panel in an infinite baffle, whose vibration is due a plane sound wave incident at an angle of $\phi$ to the normal to the panel, on the side from which the plane sound wave is incident (this is the fluid loading on the incident side),

$Z_{wft}(\phi)$ is the wave impedance of the **fluid** as experienced by the finite panel in an infinite baffle, whose vibration is due a plane sound wave incident at an angle of $\phi$ to the normal to the panel, on the side opposite to which the sound is incident (this is the fluid loading on the non-incident or transmitted side) and

$Z_{wp}(\phi)$ is the wave impedance of the **finite panel** in an infinite baffle to a plane sound wave incident at an angle of $\phi$ to the normal to the panel, ignoring fluid loading.

It will be assumed that the fluid wave impedances on both sides are the same and the imaginary part of the fluid wave impedance will be ignored [43]. That is

$$Z_{wfi}(\phi) = Z_{wft}(\phi) = \rho c \sigma(\phi) \quad (3.11)$$

where $\rho$ is the density of the fluid, $c$ is the speed of sound in the fluid and $\sigma(\phi)$ is the radiation efficiency into the fluid of one side of the finite panel in an infinite baffle, whose vibration is due a plane sound wave incident at an angle of $\phi$ to the normal to the panel.
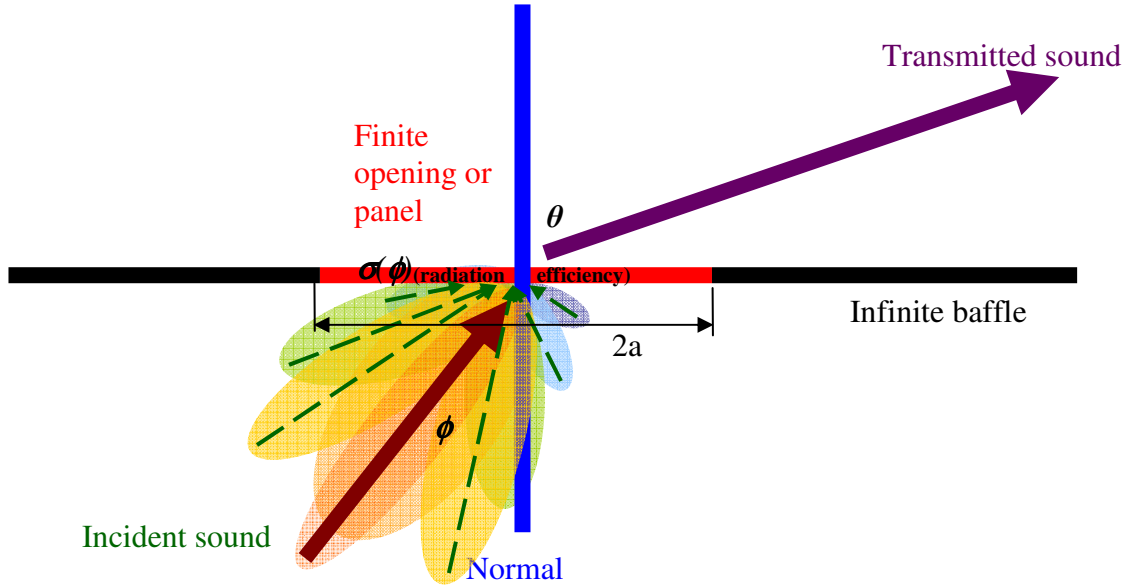


**Figure 3.6:** Sound incident at an angle $\phi$ to the normal to a panel and radiated at an angle of $\theta$

Reflections at the panel edges are ignored [43]. The rms normal velocity $v_{rms}(\phi)$ of the panel due to a plane sound wave incident at an angle of $\phi$ to the normal to the panel which exerts an rms pressure $p_{irms}(\phi)$ is

$$v_{rms}(\phi) = \frac{p_{irms}(\phi)}{\underbrace{2\rho c \sigma(\phi) + Z_{wp}(\phi)}_{Z_e(\phi) \text{ (effective)}}}. \tag{3.12}$$

The transmitted rms sound pressure $p_{trms}(\theta,\phi)$ which is radiated by the panel on the non-incident side to a receiving point, which is at an angle of $\theta$ to the normal to the centre of the panel and a large distance from the panel, is given [44]

$$p_{trms}\left(\theta,\phi\right) \propto v_{rms}\left(\phi\right) \frac{\sin\left[ka\left(\sin\theta - \sin\phi\right)\right]}{ka\left(\sin\theta - \sin\phi\right)} \qquad (3.13)$$

where $k$ is the wave number of the sound and $2a$ is the length of the panel in the plane of the source and observation points. Thus, substituting for $v_{rms}\left(\phi\right)$

$$p_{trms}\left(\theta,\phi\right) \propto \frac{p_{irms}\left(\phi\right)}{2\rho c\sigma\left(\phi\right) + Z_{wp}\left(\phi\right)} \frac{\sin\left[ka\left(\sin\theta - \sin\phi\right)\right]}{ka\left(\sin\theta - \sin\phi\right)}. \qquad (3.14)$$

# 4   DERIVATION OF THE PROPOSED ANGULAR WEIGTHING FUNCTION w(ϕ)

The case where the incident sound is generated by a sound source in an enclosure, like a  room, cabin or duct is now considered. We assume that the sound pressure waves are incident at different angles $\phi$ with random phases and mean squared sound pressures which are proportional to a weighting function $w(\phi)$.

$$\left|p_{irms}\left(\phi\right)\right|^2 \propto w\left(\phi\right). \qquad (3.15)$$

The weighting function is to account for the fact that sound waves at grazing angles of incidence will have had to suffer more wall collisions and therefore be more attenuated before reaching the panel. The total mean square sound pressure $\mid p_{Trms}\left(\theta\right)\mid^2$ at the receiving point is

$$\left|p_{Trms}\left(\theta\right)\right|^2 \propto \int_{-\pi/2}^{\pi/2} \frac{w\left(\phi\right)}{\left|2\rho c\sigma\left(\phi\right) + Z_{wp}\left(\phi\right)\right|^2} \left\{\frac{\sin\left[ka\left(\sin\theta - \sin\phi\right)\right]}{ka\left(\sin\theta - \sin\phi\right)}\right\}^2 d\phi. \qquad (3.16)$$

The case when sound is incident from a source in a free field at an angle $\theta$ to the normal to the panel and the panel radiates at all angles $\phi$ into a room or duct is also of

interest. In this case the weighting function $w(\phi)$ is to account for the fact that sound waves radiated at grazing angles will have had more wall collisions and therefore be more attenuated before reaching the receiving position which is assumed to be a reasonable distance from the panel or opening which is radiating the sound. In this second case, we have to integrate over all angles of radiation $\phi$ because of the reverberant nature of the sound. For this case, the impedance terms in the integral are functions of $\theta$ rather than $\phi$ and can be taken outside the integral. However in this study both cases are calculated using the formula for the first case which is shown above. This is because both cases should be the same by the principle of reciprocity and it is difficult to determine which form of formula is more accurate.

For large values of $ka$, the formula will be similar for the two cases. If $ka$ is much greater than 1, the function

$$\left\{ \frac{\sin\left[ka\left(\sin\theta - \sin\phi\right)\right]}{ka\left(\sin\theta - \sin\phi\right)} \right\}^2 \tag{3.17}$$

has a sharp maximum at $\phi = \theta$ and is symmetrical in both $\theta$ and $\phi$ about the point $\phi = \theta$. We can exploit these facts by evaluating the impedance terms for the first case at $\phi = \theta$ and taking them out side the integral. This gives the formula for the second case.

The relative sound pressure level $L(\theta)$ in the direction $\theta$ is

$$L(\theta) = 20\log_{10}\left(\left|p_{Trms}(\theta)\right|\right) - 20\log_{10}\left(\left|p_{Trms}(0)\right|\right). \tag{3.18}$$
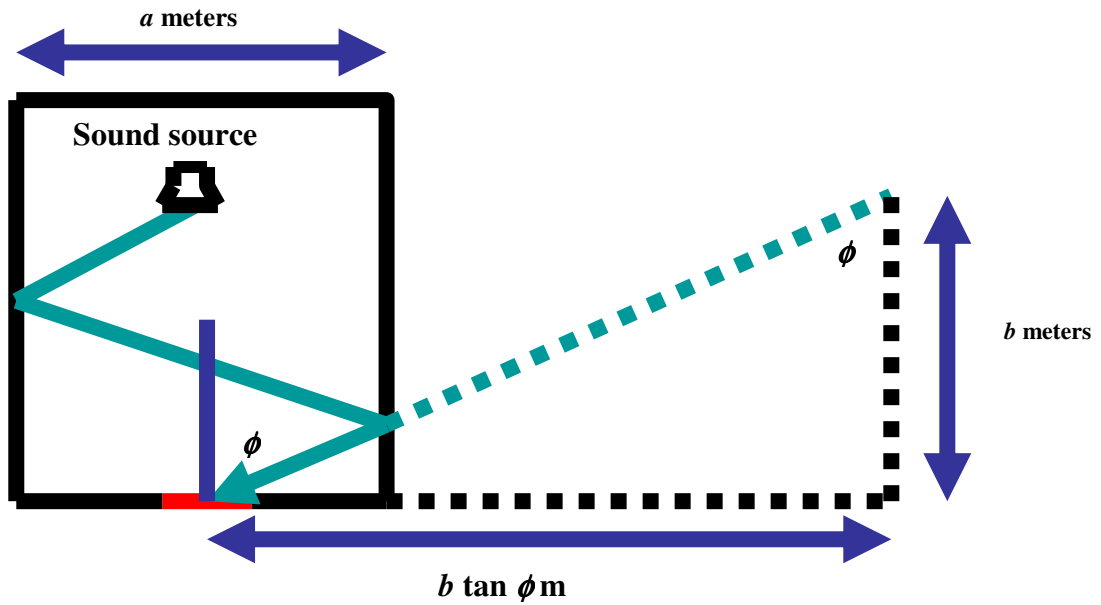
**Figure 3.7:** Calculating the number of wall reflections before sound hits the panel or opening at an angle of $\phi$ to the normal.

Assume that the sound source is distance $b$ from the surface of the room containing the panel or opening and that the room width is $a$ in the plane containing the incident sound ray. If the sound ray is incident at an angle of $\phi$ to the normal to the panel or opening, it travels a minimum distance of $b \tan \phi$ parallel to wall containing the panel or opening before hitting the wall. This is similar to the image source method of predicting reflections in a room. The sound which travels this minimum distance hits the wall the following "n" number of times,

$$n = \frac{b}{a}\tan\phi \tag{3.19}$$

before reaching the panel or opening. If the sound absorption coefficient of the walls of the room is $\alpha$, the sound intensity incident at an angle of $\phi$ to the normal is proportional to

$$w(\phi) = (1-\alpha)^n = (1-\alpha)^{\frac{b}{a}\tan|\phi|}. \tag{3.20}$$

Equation (3.20) gives us the weighting function $w(\phi)$. Uniform diffuse field weighting is obtained when $\alpha$ is zero.

## *4.1  Radiation efficiency function details*

In this study we use the radiation efficiency of a strip of width $2a$, which we approximate with the following equation [44].

$$\sigma(\phi) = \begin{cases} \dfrac{1}{\dfrac{\pi}{2k^2a^2} + \cos\phi} & \text{if } |\phi| \le \phi_l \\[4mm] \dfrac{1}{\dfrac{\pi}{2k^2a^2} + \dfrac{3\cos\phi_l - \cos\phi}{2}} & \text{if } \phi_l < |\phi| \le \dfrac{\pi}{2} \end{cases} \tag{3.21}$$

where

$$\phi_l = \arccos\left(\sqrt{\frac{\pi}{2ka}}\right) \tag{3.22}$$

and $k$ is the wave number of the sound and $2a$ is the length of the panel in the direction of the source.

For an opening with no panel in an infinite baffle we put $Z_{wp}(\phi) = 0$. For a finite panel in an infinite baffle we use the infinite panel result for $Z_{wp}(\phi)$. This result is expected to be the correct result when averaged over frequency, because this approach gives the correct result for point impedances when averaged over frequency and position on a finite panel [45].

$$Z_{wp}(\phi) = m\omega\left\{ j\left[ 1 - \left(\frac{\omega}{\omega_c}\right)^2 \sin^4(\phi)\right] + \eta\left(\frac{\omega}{\omega_c}\right)^2 \sin^4(\phi)\right\} \tag{3.23}$$

where $m$ is the surface density (mass per unit area) of the panel, $\eta$ is the damping loss factor of the panel, $\omega_c$ is the angular critical frequency of the panel and $\omega$ is the angular frequency of the sound.

In the case of a rectangular enclosure like a duct etc, the directivity of the sound source is also included. The sound source is modelled as a line source of length $2r$ where $r$ is the radius of the sound source. The directivity of the sound source is proportional to

$$\left[ \frac{\sin\left(kr\sin\phi\right)}{kr\sin\phi} \right]^2 \tag{3.24}$$

where k rad/m is the wave number.

## 5   COMPARISON WITH PUBLISHED RESULTS ON DIRECTIVITY

In this section, the panel radiation directivity prediction method described in the previous section is compared with experimental results and prediction methods for finite size panels and finite size openings from the literature, which are mainly based on previous glass panel and duct studies, as previous published results are only available in the field of building acoustics. Results are presented on a logarithmic scale of Strouhal number. The Strouhal number is defined as the ratio of the distance across the finite flat panel or finite opening in the direction of the receiver to the wavelength of the sound in the air.

Stead [47] measured the sound insulation of a window installed in one wall of a room. The sound was incident at an angle to the normal to the window from outside the room. This is the opposite direction to the calculation method used in this paper, but is expected to give similar results because of the principle of reciprocity. The window was 1450 mm wide by 2120 mm high. The glass was 6 mm thick. The wall of the room containing the window was part of the external wall of a larger building which served as a baffle. The internal dimensions of the room were 2880 mm wide by 3000 mm high by 5120 mm deep. The loudspeaker was 20 m from the middle of the widow. The edge of the building in the direction of the measurements was 11 m from the centre of the window. Thus the baffle length was set to twice this distance, namely 22 m. To show the result of the diffraction correction, Stead's results at an angle of 90° are compared with the theory presented, in Figure 3.8.
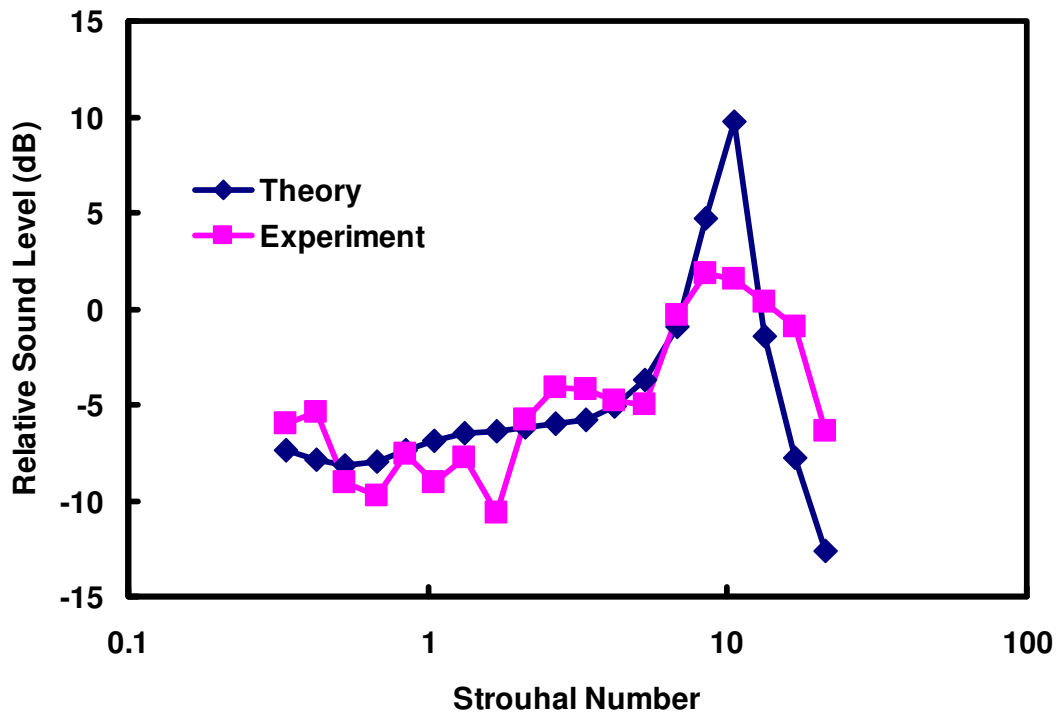
**Figure 3.8:** The sound level at 90° relative to that at 0° as a function of Strouhal number for 6 mm thick glass installed in the wall of a room.
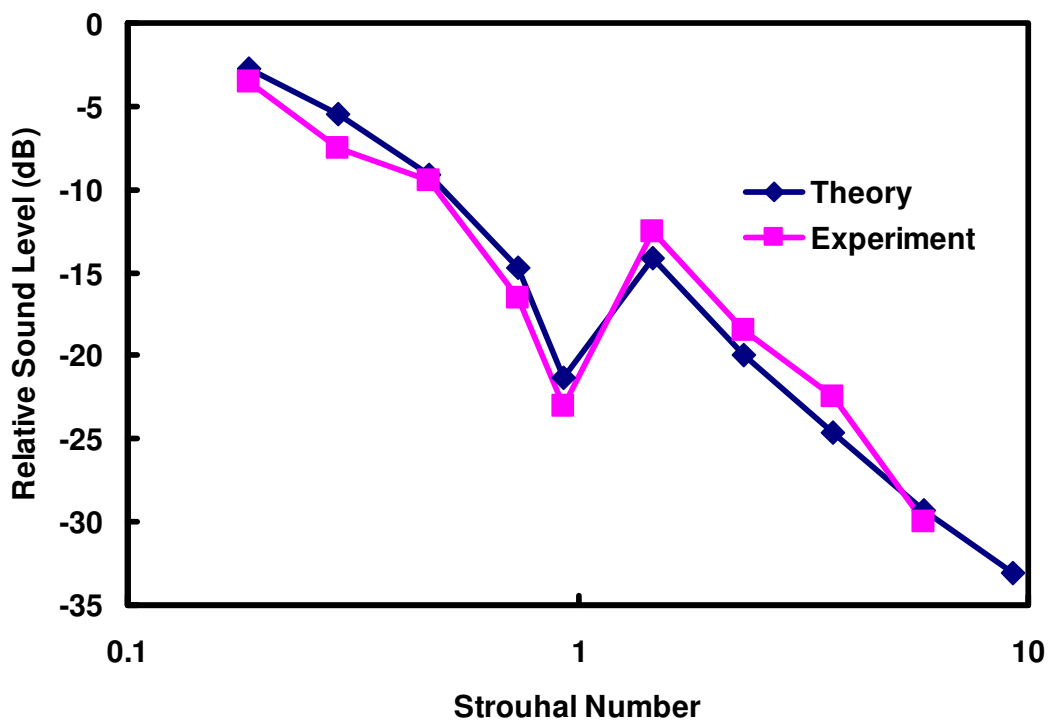


**Figure 3.9:** The sound level at 90° relative to that at 0° as a function of Strouhal number for an unbaffled duct end opening.

Stead's measured reverberation times were used to calculate the average wall absorption coefficients of the room for use in the calculation of the weighting function. The difference between the experimental and theoretical results at coincidence does not occur at low angles of incidence.

Sutton [48] measured the directivity of eight unbaffled duct end openings in an anechoic room. Figure 3.9 shows a comparison of his measurements at 90° for an 80 mm square cross section duct of length 750 mm. Sutton used two sound sources. The sound source directivity was modelled by assuming a source diameter of 300 mm for Strouhal numbers less than one and a source diameter of 30 mm for higher Strouhal numbers. Note that the lower frequency sound source would not have actually been 300 mm in diameter. The 300 mm diameter is used to model the directivity of the sound radiation into the duct. If only plane waves had been excited in the duct, a sound source diameter of infinity would have been used. An absorption coefficient of 0.05 was assumed for the internal walls of the duct.

# 6   CONCLUSIONS

The Simple Harmonic Motion oscillator model of analyses of the current carpet design system shows that there exists a resonance in the 323Hz frequency range which is in the engine or power train noise frequency range. This is verified from the sound Transmission Loss measurements of the carpet variants, using impedance tube method.

Further, the theoretical model presented for panel radiation directivity prediction can be used to successfully predict the sound level radiated at a particular angle to the normal of a panel or opening, relative to the sound level radiated in the direction of the normal. The theory depends on the length of the radiating object in the direction of the observer divided by the wavelength of the sound in air, and is independent of the width of the object at right angles to the direction of the observer. The relative sound level radiated from a panel is relatively independent of the Strouhal number and the angle of radiation apart from a strong peak at coincidence. The relative sound level radiated from an opening decreases as the both the Strouhal number and the angle of radiation increase.

# CHAPTER 4

# DESIGN CONCEPTS FOR REDUCING NOISE FROM FLOOR PANEL SOUND RADIATION

## 1   INTRODUCTION

A set of layered carpet concept designs is proposed for vehicle carpet applications, which are theoretically expected to meet the required acoustic performance targets, and at the same time expected to meet the constraints on various other factors like cost, weight, manufacturability, aesthetics, recyclable etc. Through the design process of deriving a hypothetical concept vehicle carpet having defined layer types, but with variable options for materials and corresponding properties, a set of realizable concept designs are proposed and evaluated with the available materials and infrastructure. The preliminary evaluation is conducted and discussed for the acoustic performance of the layered concept designs.

This chapter outlines the design concepts underlying the vehicle carpet systems and gives a functional analysis report of the designs with respect to the acoustical performance requirements. By explaining the current vehicle carpet design, a baseline is made for further comparison and evaluation. Targets are set with reference to the current production carpet, against which each concept design will undergo analysis for acoustic performance.

Since theoretical explanation and modelling are efficient tools for validating and perfecting the designs, a brief outline of the modelling methods is explained in the context of the layered carpet design techniques.

The expectation is to lay-out key layered concept designs for the future vehicle carpet systems, which can perform superior to the existing layered carpet design, by improving certain acoustic parameters of interest. Further to this stage of conceptual design, a detailed

optimization and functional evaluation stage of the designs is expected, to realize the concept design.

## 2    CURRENT VEHICLE CARPET SYSTEM

The current vehicle carpet system in production is the best starting point for both conceptual design and functional analysis studies. The current production vehicle carpet we have is based on a three material layer design.

The three layers of the current carpet system are from top to bottom, carpet tufting layer, heavy sound barrier layer and the vibration de-coupler/absorber layer.

**Tufting layer**

**Cabin side (top)**                                         **Heavy layer (barrier)**

**Engine side (bottom)**                        De-coupler/absorber layer
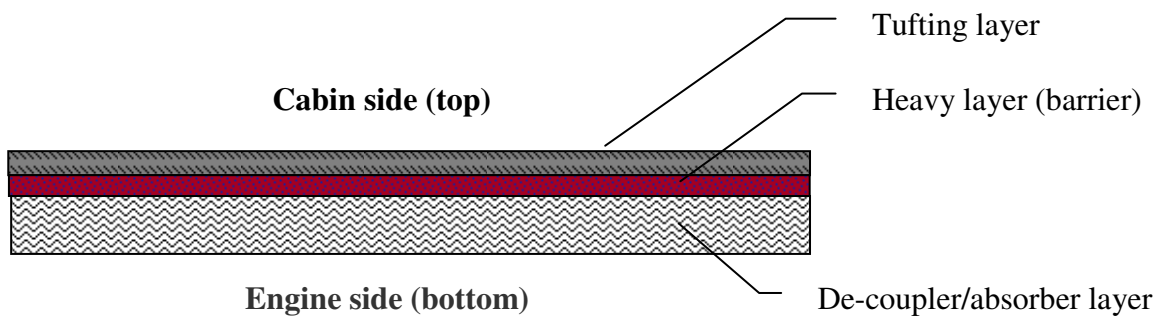
**Figure 4.1 – Current vehicle carpet design**

The materials applied in the current production are,

Carpet tufting layer     - Face 320gm/m$^2$ carpet fabric

Heavy layer                   - 5 kg/m$^2$ heavy layer

De-coupler/absorber   - 1.65 kg/m$^2$ Poly Urethane Foam

Total area density         - 7.5 kg/m$^2$

## *2.1  Functional analysis*

The top carpet tufting layer functionally helps to give the looks, touch & feel and keeps the carpet surface clean and durable to wear. At the same time, in an acoustic point of view, the tufting layer helps, to an extent, for absorbing the sound in the cabin side.

The normal incidence sound absorption coefficient of the various carpet tufting layers are shown below.
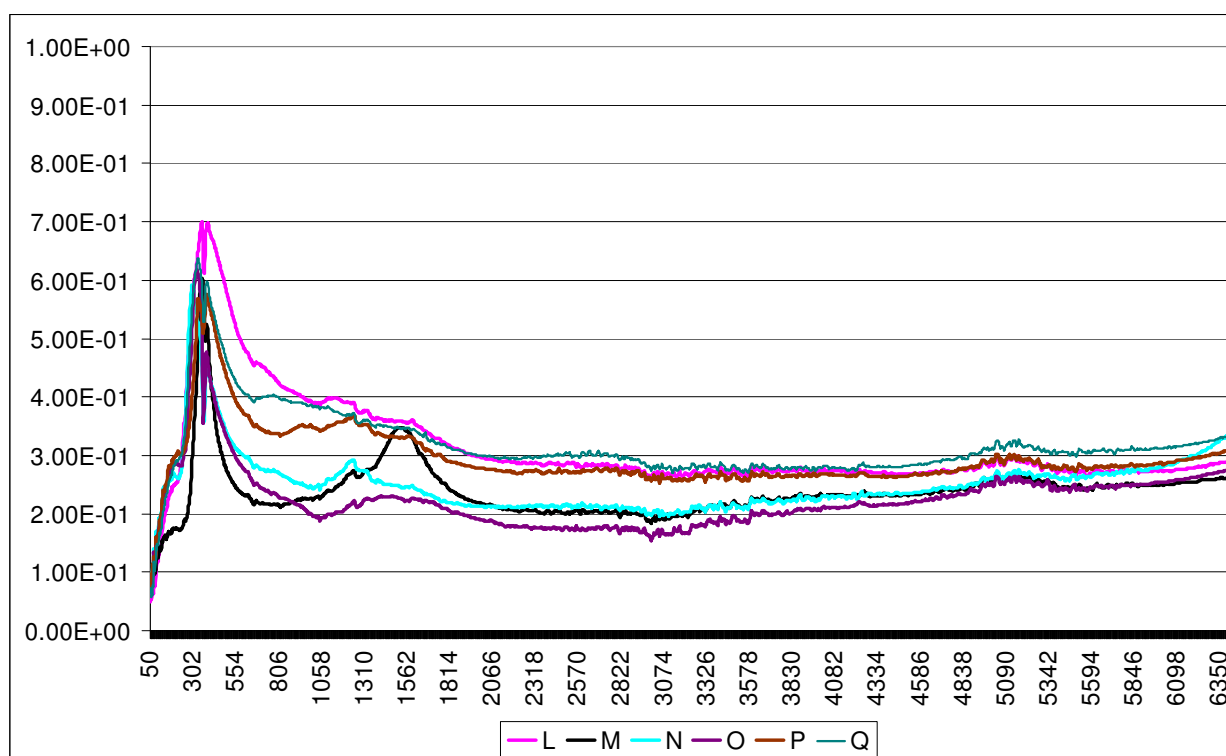


**Figure 4.2 – Normal sound absorption coefficient of
various carpet tufting (L to Q)**

The average sound absorption is relatively less, of only about 30% for the tufting layer.

Meanwhile, the heavy layer functions as a simple sound barrier, where the denser and thicker the layer, the more sound is stopped from entering the vehicle cabin. So the heavy layer contributes to the total weight of the carpet, and so the main parameter would be the surface density of the layer, which is typically between 1.5kg/m$^2$ and 5kg/m$^2$.

The below graph shows the normal incidence Transmission Loss of various heavy layer carpet systems used in current carpet designs. The measured transmission loss ranges from 10dB to 35 dB.
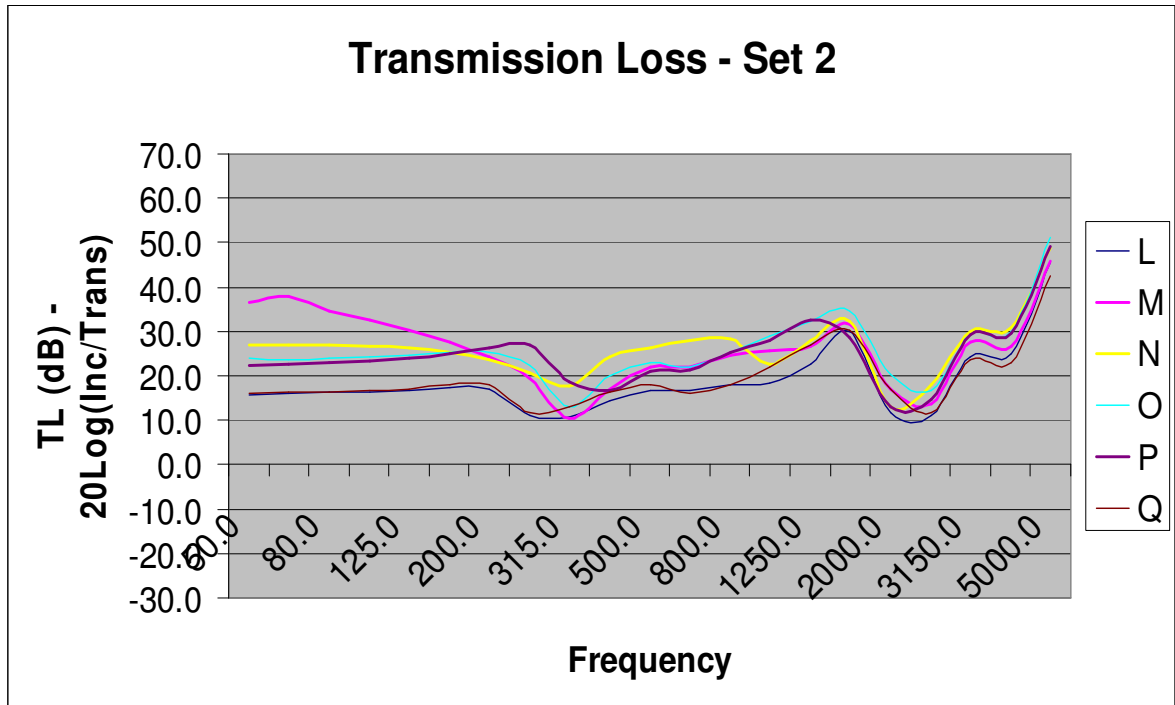
**Figure 4.3 – Normal incidence Transmission Loss
coefficient of various heavy layers**

The bottom final de-coupler layer acts as both a vibration de-coupler/absorber and also helps to fit the carpet bottom well onto the bottom metal floor.

The absorption coefficient for the de-coupler (bottom of carpet) is comparatively high as the below measured result shows. The de-coupler layer can absorb about 80% of the sound incident on it, but mainly in the frequency above 750Hz.
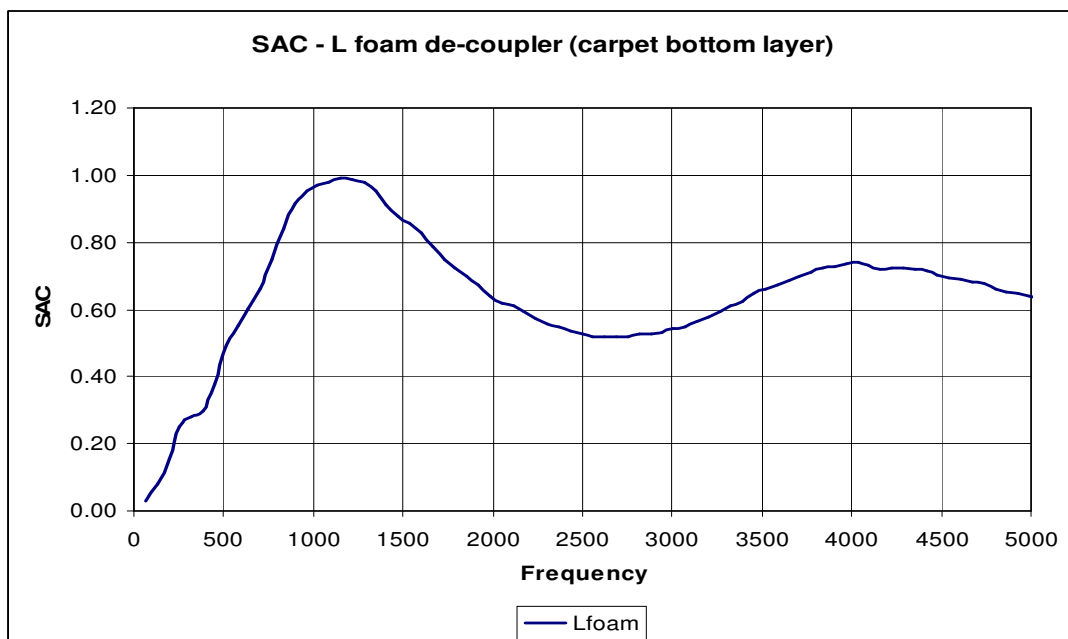


**Figure 4.4 – Absorption characteristics of a typical
de-coupler layer**

## *2.2  Baseline and targets for the carpet design*

The concept design for the vehicle carpet is focussed on improving the acoustic performance of the carpet, both as a power train noise barrier and a cabin noise absorber, while giving highest priority to aesthetics and comfort.

The acoustic evaluation results for current production design can be taken as the baseline for further acoustic performance improvement, at various stages of the conceptual design. For normal incidence absorption coefficient, the best performance curve fit (green line) is taken as the baseline curve, to which the future results will be compared for evaluating improvement. Meanwhile, for Transmission Loss, the minimum curve (heavy layer of 1.7 kgms) and maximum curve (heavy layer of 5 kgms) are considered for defining the baseline and target range. The carpet samples are assumed to have thickness limited to 40mm, and in the pre-moulded stage.

The baseline for power train noise transmission loss and cabin noise absorption are shown as the green lines passing through the best TL and absorption coefficient peaks of the current carpet design.

Absorption coefficient (Cabin/tufting side)
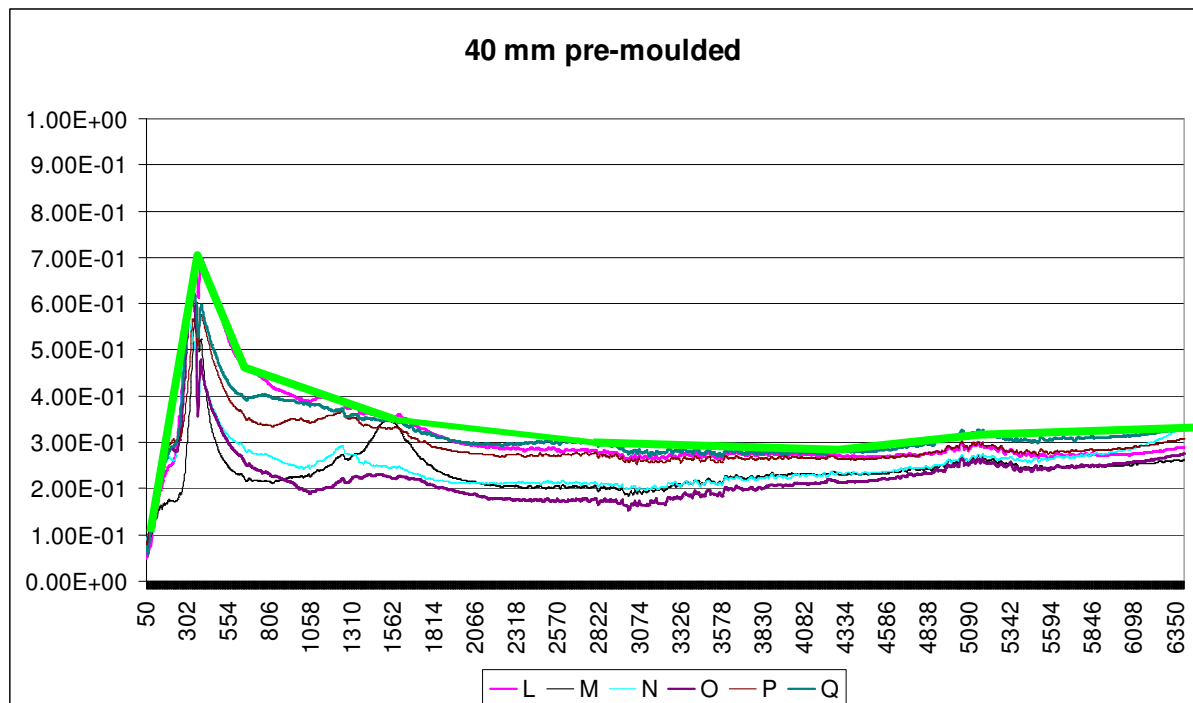


**Figure 4.5 – Cabin side absorption coefficient of
current carpet designs**
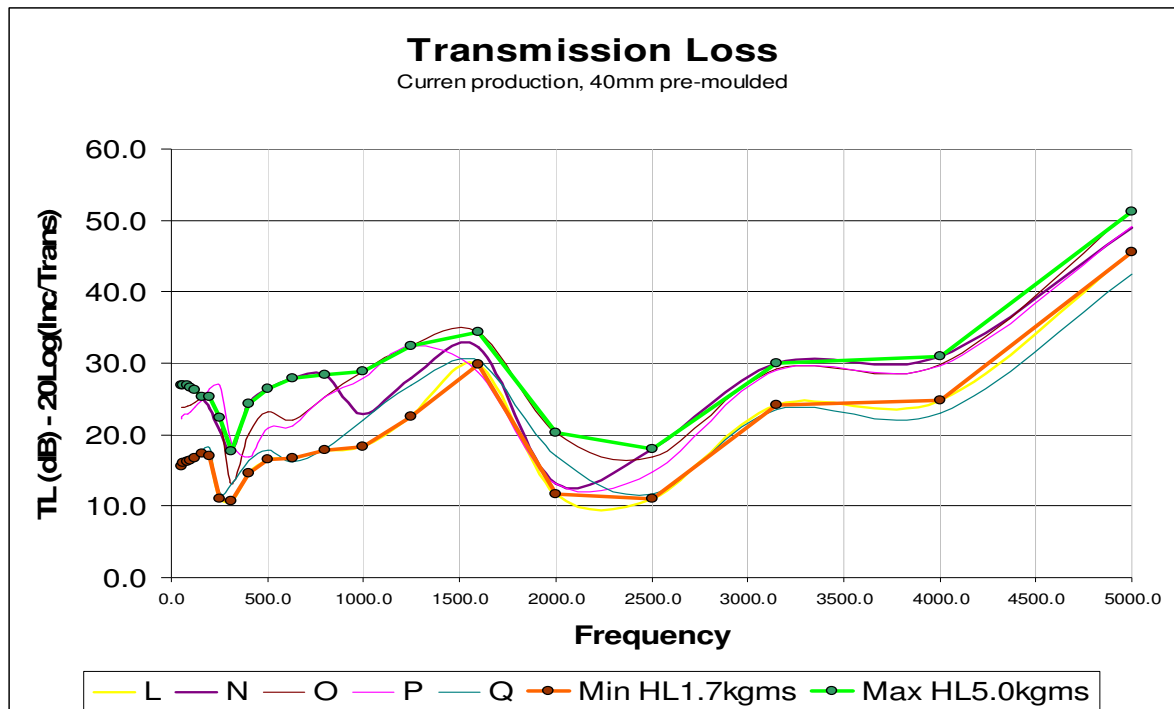
**Figure 4.6 – Transmission loss of various carpet**
**designs, with maximum and minimum defined**

## 3    THEORETICAL BASE FOR FUNCTIONAL ANALYSIS

The acoustic properties, i.e. absorption coefficient and transmission loss, of various layers at the material level can be predicted using existing mathematical models. Meanwhile, the inter-layer interaction and effects are predicted using a mathematical approach based on transfer functions [53].

Fibre & Foam:

Four different models are available to represent foam and fibrous materials [4, 49, 50, 52]:

1.  The elastic porous (foam) model,

2.  The limp porous (fiber) model,

3.  The rigid (fiber) porous model and

4.  The Delany-Bazley (fiber) model [52].

The elastic porous model is used for foam materials where the stiffness of the frame is important in vibro-acoustic response of the noise control material. The energy exchange

between structural energy and acoustical energy within a foam material typically provides much of the desired energy absorption. The full elastic porous model requires all the fluid properties and the elastic bulk properties.

The below diagram gives a basic view of the order of development and application of the mathematical models.
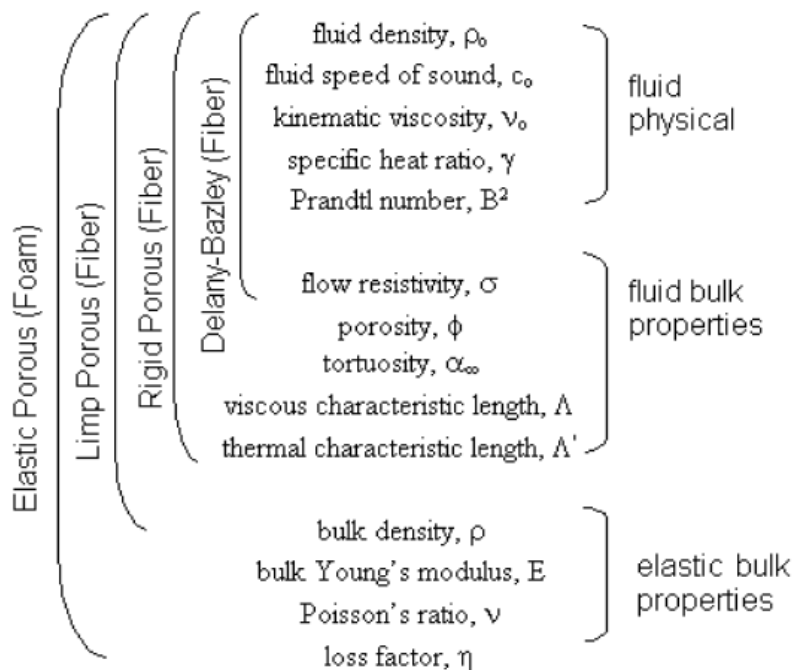


**Figure 4.7 – Material acoustic properties in relevance order for modelling [53]**

For materials in which the frame waves do not carry a significant amount of energy, such as many fiber-based materials, the frame waves may be disregarded altogether and the noise control layer modeled with a single type of acoustic compression wave. In this case one of the fiber models should be used to represent such a material.

When the frame of the porous material can be considered limp, the fluid properties and the bulk density are required to predict the vibro-acoustical behavior. Similarly when the frame of the porous material can be considered rigid, only fluid related properties are required.

The Delany-Bazley model is the simplest fiber model and only requires the fluid density, fluid speed of sound and the flow resistivity of the acoustic material to characterize the performance of a noise control treatment. The Delany-Bazley model is activated when both the viscous and thermal characteristic lengths are zero.

AutoSEA2 acoustic simulation software based on Statistical Energy Analysis method incorporates these mathematical models. Hence, given the required material properties for modelling, any foam or fibre material response in an acoustic field can be modelled and evaluated easily, than working out the tough mathematics.

## 3.1 Layered up material interaction

The layered interaction between various material types, foam, fibre, panel, air gap etc, is solved mathematically using a method called Transfer matrix [4, 30, 35, 39, 57, 59], where the transfer function for the acoustic variable pressures and velocities are parameterised into a 2x2 complex matrix for each layer. The methodology is based on the representation of plane wave propagation in layered media, in terms of transfer matrices. Each layer is assumed to be constructed of a homogeneous and transversely isotropic material. The elastic and fluid layer models are based on classical plane wave propagation. Modelling of the poro-elastic layer is based on the extension of Biot theory to acoustics [4].

Meanwhile, various acoustically known methods and knowledge can be used as a direction for bringing up designs. Adding of new layers for specific requirements, using the double panel separated by a fluid technique, etc are few of them that have relevance. So, theoretically validated or explainable directions have been taken for each concept design.

## 4   PROPOSED CONCEPT DESIGNS

The process of arriving at concept designs is based on the design requirements and by moving in design directions that are theoretically acceptable and that may result in satisfying results on implementation. Hence, the conceptual designs may remain to be hypothetical, to an extent.

**Layered concept 1**:

Introducing minor changes to the existing production vehicle carpet system can improve the cabin side absorption sufficiently, i.e. by adding an absorber layer or air gap (honey comb) just below the tufting layer. This concept design will be more manufacturing friendly.
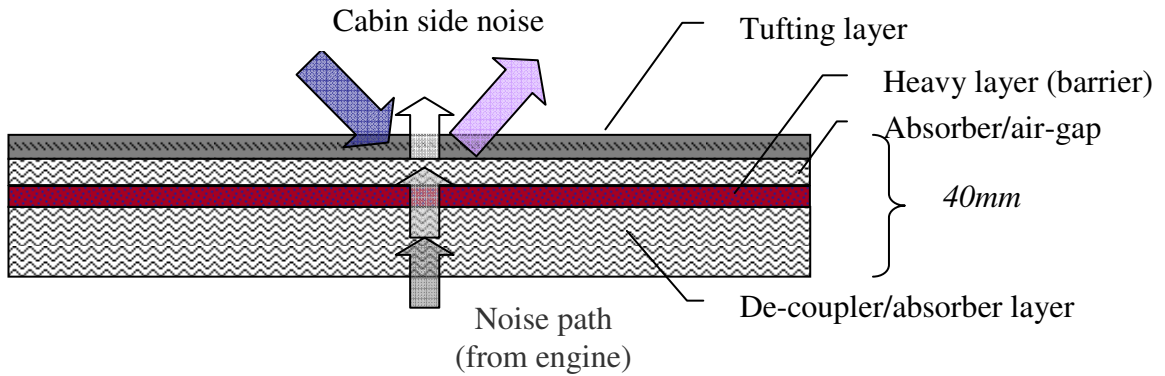
**Figure 4.8 – Concept 1 carpet design**

**Layered concept 2**:

Replacing the heavy layer with a double panel of Air Flow Resistance (AFR) layers, filled with sound absorbing material or air gap (honey comb).
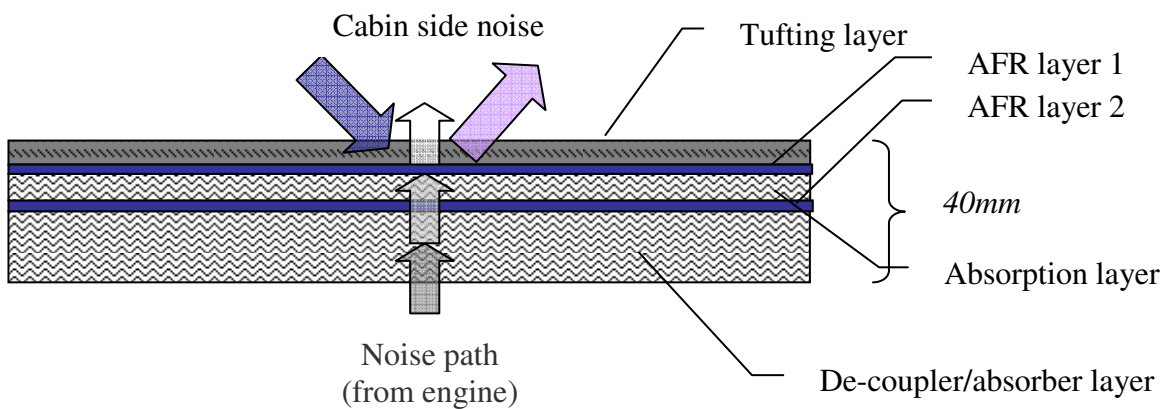
**Figure 4.9 – Concept 2 carpet design**

**Layered concept 3:**

By replacing the thick heavy layer with a double panel system, where the top panel is an AFR layer and the bottom panel is a thin heavy layer. This concept actually tries to make a compromise result of concepts 1 and 2.
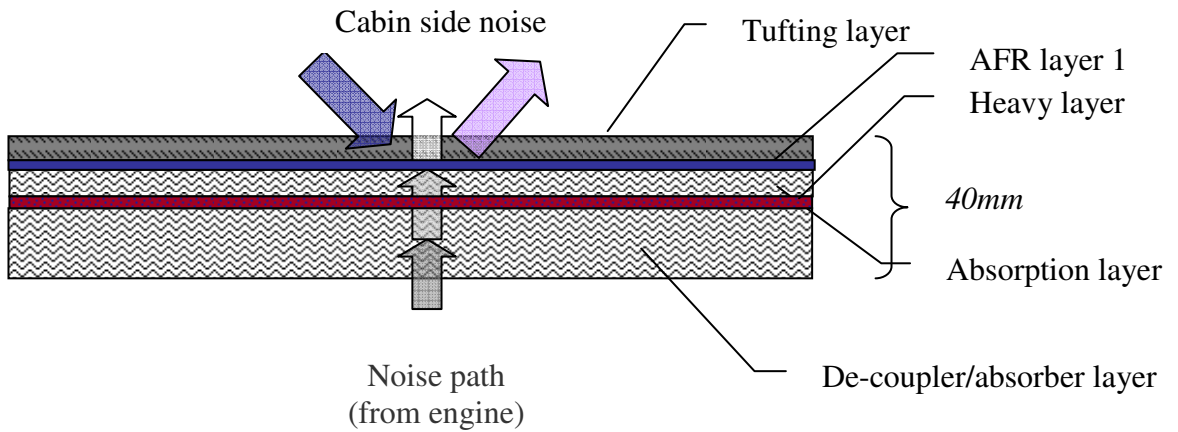


**Figure 4.10 – Concept 3 carpet design**

**Layered concept 4:**

Introducing absorber layer just below carpet tufting and also having a double panel system using AFR panels, separated by an air-gap (honey comb).
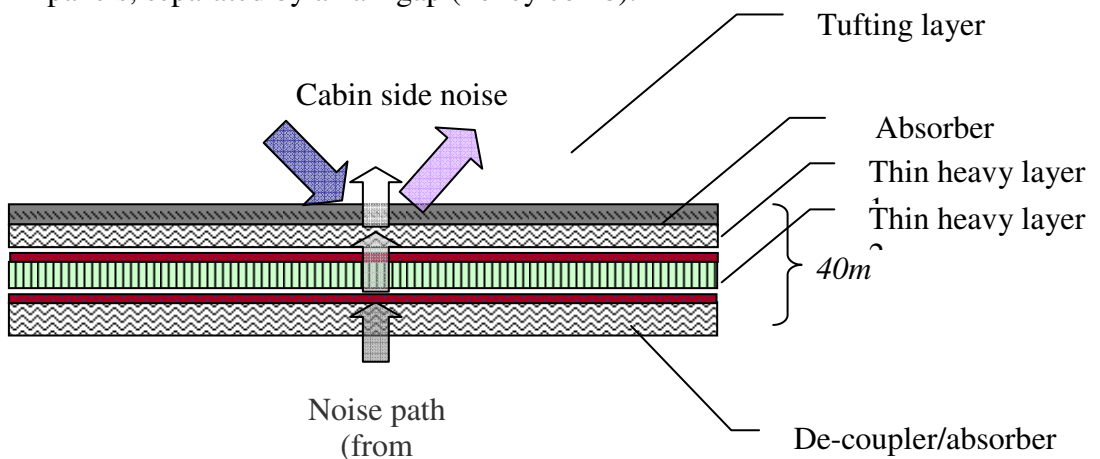


**Figure 4.11 – Concept 4 carpet design**

## 4.1  MATERIAL SELECTION

For the purpose of selecting the best material suiting each concept design layer, a category wise material table is maintained. Referring to the four concept designs laid above, the basic material categories involved are,

1. Carpet tufting type

2. Air Flow Resistant (AFR) type

3. Absorber type

4. Heavy Layer type

5. Air-gap structure type and

6. Scrim/micro-fibre film type, to increase absorption, which is included in later design stage.

As shown below, a simple and direct approach was followed for selecting the best material in each category for building up the concept layers. The carpet or material samples (e.g. Set1 – K)  are listed from top to bottom and the various layer types of these samples are labelled into one of the material type columns (e.g. Foam). For particular design proposals, coloured lines are drawn through the preferred material label boxes, giving a complete view of the materials selected. The material cost, weight, durability, whether its recyclable, etc are expected to be handled after the concept design stage.

| | | Carpet tufting | Structures | Heavy layer | AFR | Foam | Non-woven | Poly Felt | Scrim |
|---|---|---|---|---|---|---|---|---|---|
| Set 1 | | | | | | | | | |
| | B | B1 | | | | B2 (0.4 kgsm) | | | |
| | C | C1 | | | | | C2 | | |
| | D | D1 | | | | D2 (1.5 kgsm) | | | |
| | E | | | | E1 | | | | E2 |
| | F | F1 | | F2 (2 kgsm) LS | | | | | |
| | G | | | | G1 | | | | |
| | H | H1 | | | | H2 (0.51 kgsm) | | | |
| | I | I1 | | I2 (1.7 kgsm) LS | | | | | |
| | J | J1 | | | | | | | |
| | K | K1 | K2 (septum) | | | | K3 | | |
| Set 2 | | | | | | | | | |
| | L | L1 | | L2 (1.7 kgsm) SS | | L3 (1.65 kgsm) | | | |
| | M | M1 | | M2 (1.7 kgsm) SS | | M3 (1.65 kgsm) | | | |
| | N | N1 | | N2 (5 kgsm) SS | | N3 (3.15 kgsm) | | | |
| | O | O1 | | O2 (5 kgsm) SS | | O3 (1.65 kgsm) | | | |
| | P | P1 | | P2 (3 kgsm) SS | | P3 (3 kgsm) | | | |
| | Q | Q1 | | Q2 (3 kgsm) SS | | Q3 (1.65 kgsm) | | | |
| Set 3 | | | | | | | | | |
| | A | | | | A1 | | | | |
| | B | | | | B1 | | | | |
| | C | | | | C1 | | | | |
| | D | | | | D1 | | | | |
| | E | | | | E1 | | | | |
| | F | | | | | | | F1 | |
| | G | | | | G1 | | | | |
| | H | | | | | | | H1 | |
| | I | | | | I1 | | | | |
| | J | | | | | | | J1 | |
| | K | | | | | | | | |
| | L | | | | | | | L1 | |
| | M | | | | | | | M1 | |
| | N | | | | | | | N1 | |
| | O | | | | | | | O1 | |
| | P | | | | | | | P1 | |
| | Q | | | | | | | | Q1 |
| | R | | | | | | | | R1 |
| | S | | | | | | | | |
| | T | T1 (Honeycomb) | | | | | | | |
| | U | U1 (Honeycomb) | | | | | | | |
| | V | V1 (Honeycomb) | | | | | | | |

**Figure 4.12 – Material layer selection matrix**

## 4.2  Evaluation test setup

**Absorption coefficient measurement:**

The normal incidence absorption coefficients of the samples were measured using B&K impedance tube, following the broad-band 2 microphone method.

100mm and 29mm diameter samples were cut and measurements were done inside the large tube set-up (low frequency 50-1.6kHz) and small tube set-up (high frequency 500-6.4kHz).

The microphone and the tube correction factors were considered and compensated throughout the measurements.

At least 2 co-related results were picked up for averaging and combining low and high frequency plots, with the cross-over in 500-6.4 kHz range.

**Transmission loss measurement:**

Impedance tube method is used to measure the normal incidence Transmission Loss of the material sample. This is a newly developed 4 microphone technique, where 2 microphones each measure the wave field on either sides of the sample. This is explained in chapter 6 for reference.

Similar to the absorption coefficient testing, the samples are cut in 100mm and 29mm diameters, and tested for TL in the large tube (50-1.6kHz) and small tube (500-6.4kHz) setups, and the cross over frequency range values are averaged to get a continuous curve.

# 5   PRELIMINARY EVALUATION RESULTS

Acoustic measurements are conducted on the proposed design concepts using various selected material layer samples detailed in the below table.

**Table 1 – Nomenclature of layered material combinations**

| Layer | Code | Material & Specs |
|---|---|---|
| 1. Tufting | Ktuft | Type K, brown tufting, 320gsm |
| 2. Air Flow Resistant layers (AFR) | S3D<br><br>S3F | AFR layer |
| 3. Absorber | MJA316<br><br>Nfoam<br><br>S2M<br><br>S3M<br><br>S3N | CSIRO fibre absorber sample<br><br>1.5 kgsm, close cell polyester foam<br><br>Poly-felt absorber samples |
| 4. Heavy layer | HL1.7<br><br>HL5.0 | 2.5 mm Heavy Layer (1700gsm)<br><br>Heavy Layer (5000gsm) |
| 5. Air gap | HC10mm<br><br>Gap10mm | 10 mm Honeycomb structure (grey)<br><br>10mm air gap |

**Layered concept 1**: Introducing minor changes to the existing production vehicle carpet design, i.e. by adding an absorber layer or air gap (honey comb) just below the tufting layer.
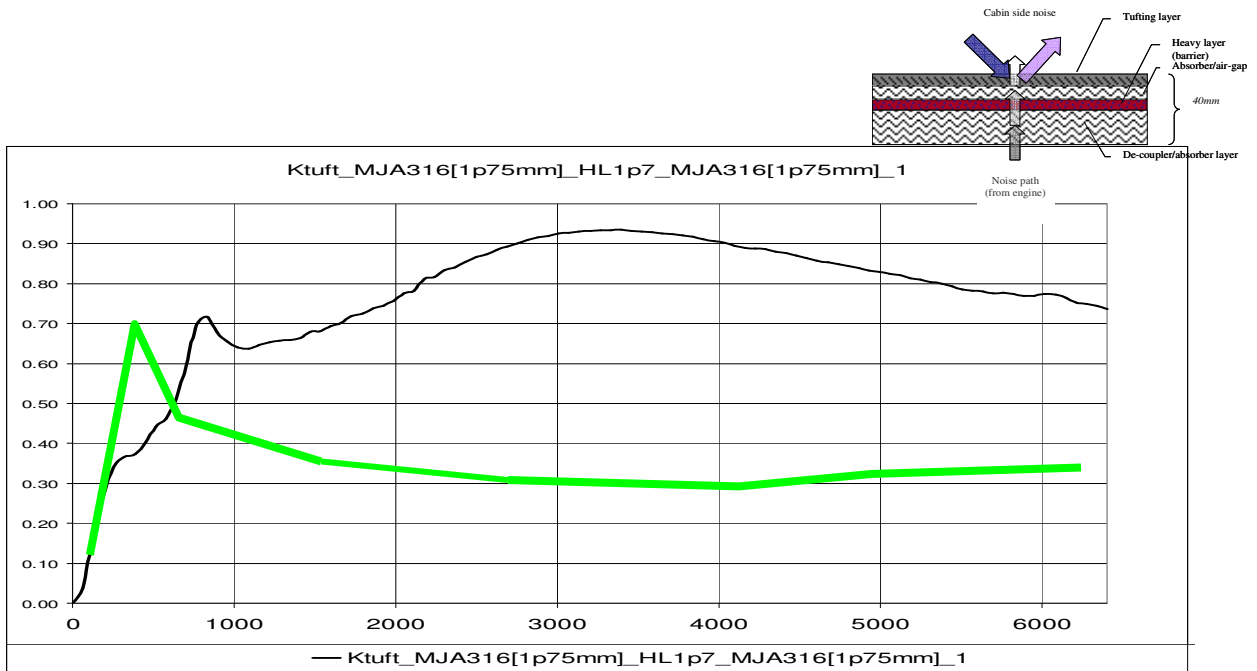


**Figure 4.13 – Cabin side absorption characteristics of Concept 1 carpet design**

Transmission Loss
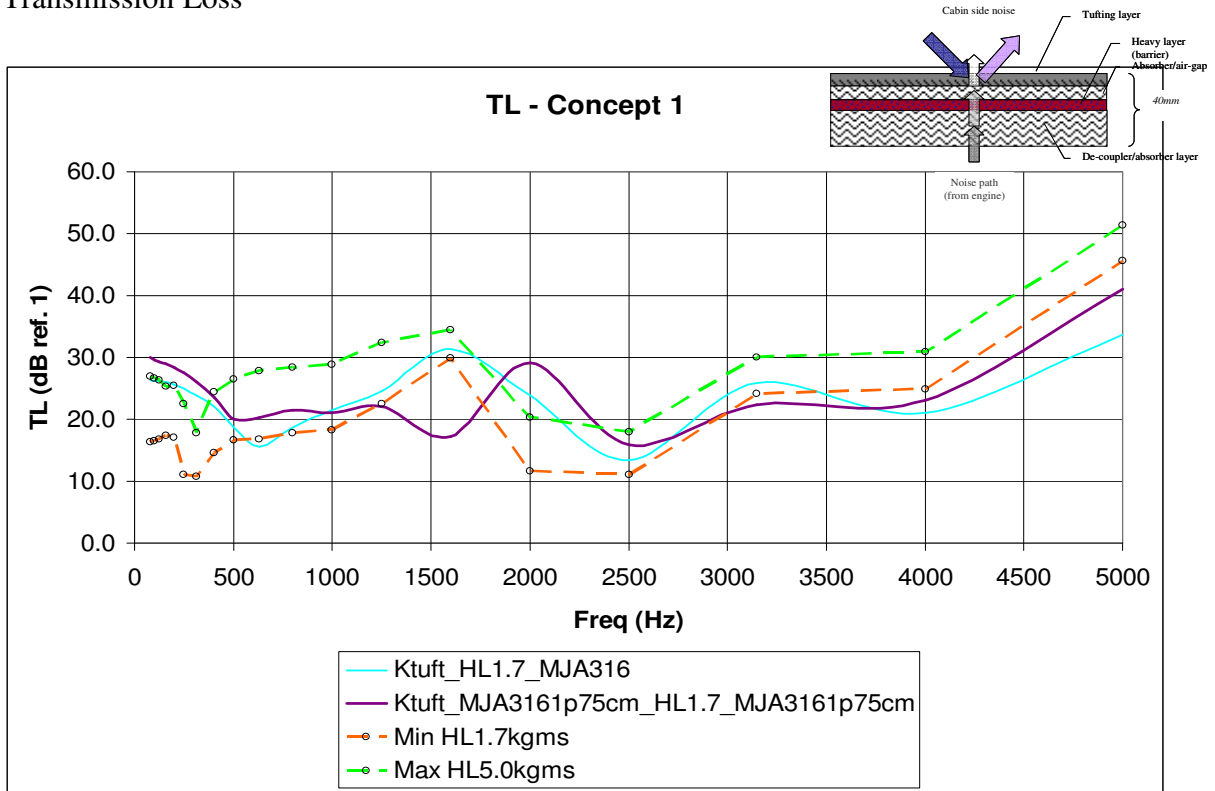


**Figure 4.14 – Transmission loss characteristics of Concept 1 carpet design**

**Layered concept 2:** Replacing the heavy layer with a double panel of Air Flow Resistance (AFR) layers, filled with sound absorbing material.

Absorption coefficient
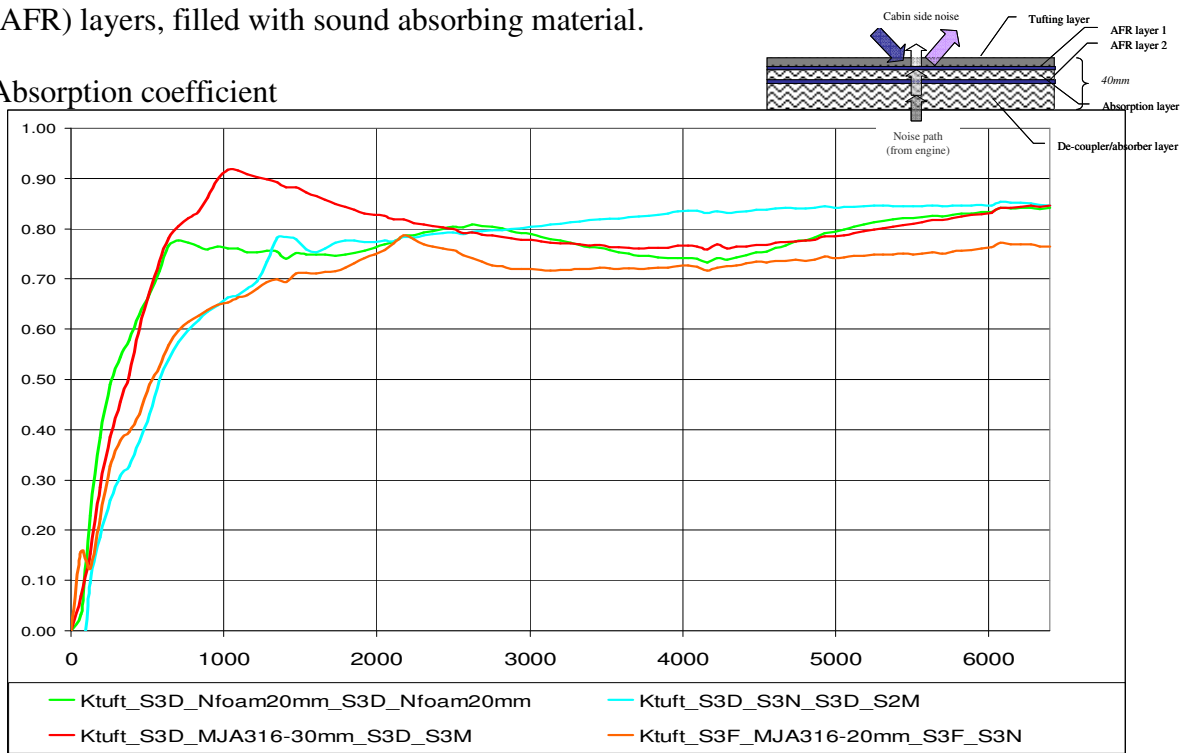


Figure 4.15 – Cabin side absorption characteristics of Concept 2 carpet design

Transmission loss
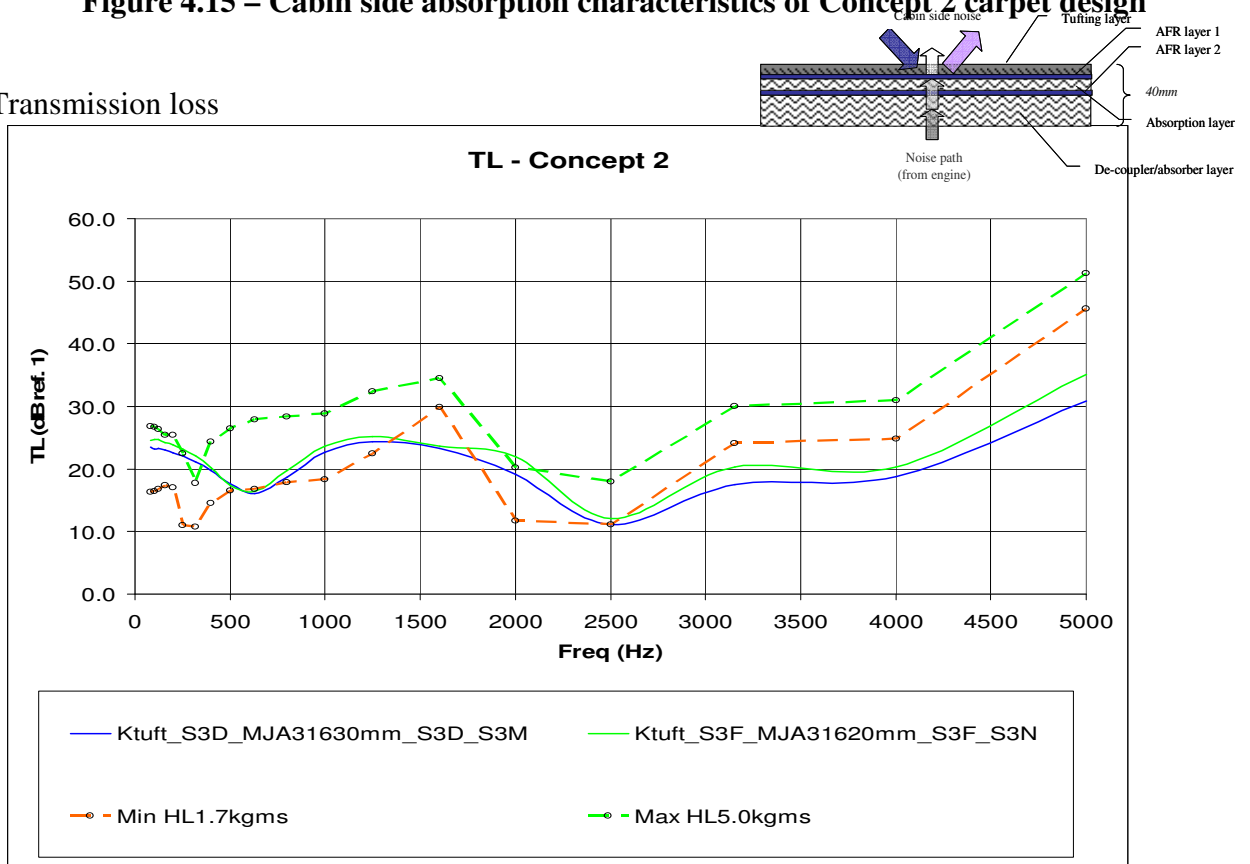


Figure 4.16 – Transmission loss characteristics of Concept 2 carpet design

**Layered concept 3**: Replacing the thick heavy layer with a double panel system, where the top panel is an AFR layer and the bottom panel is a thin heavy layer.

Absorption coefficient
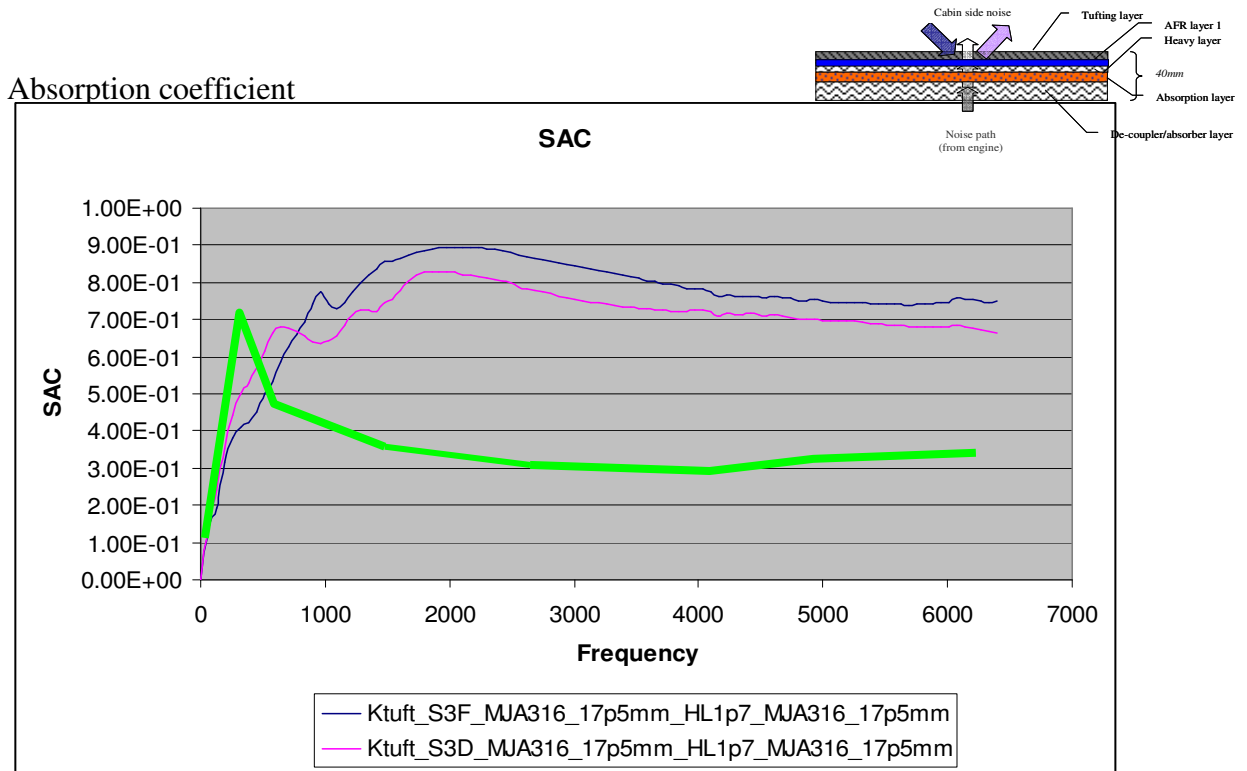


**Figure 4.17 – Cabin side absorption characteristics of Concept 3 carpet design**
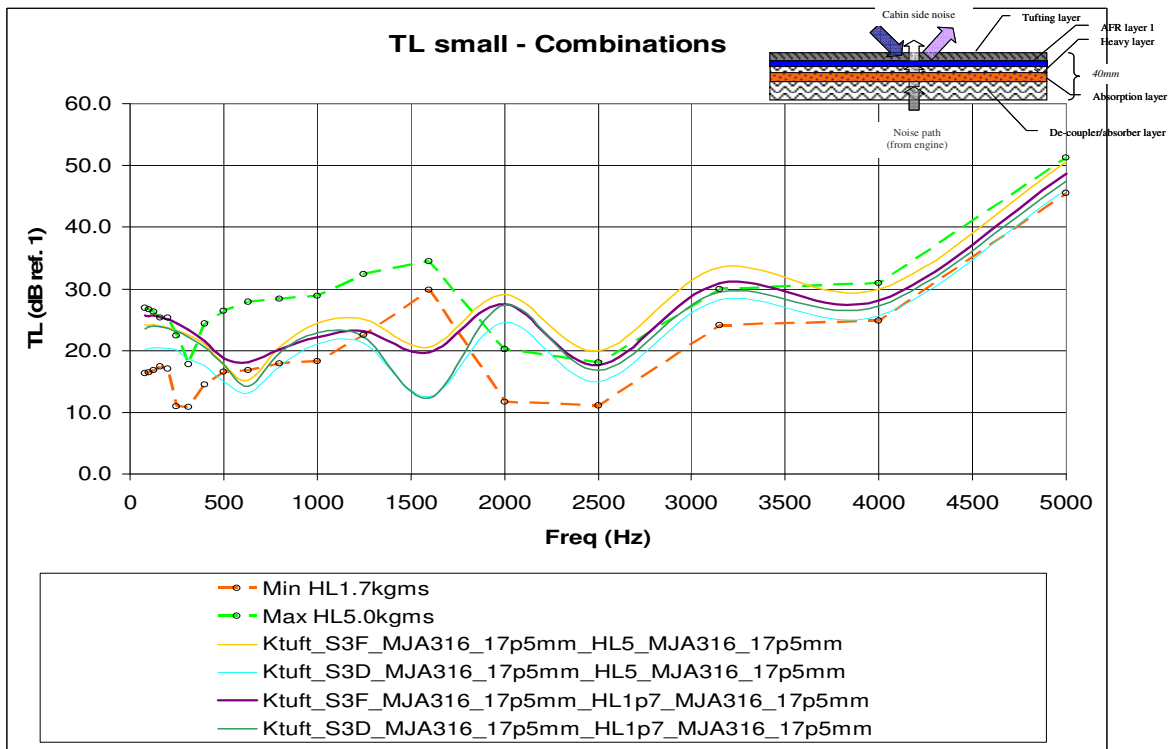


**Figure 4.18 – Transmission loss characteristics of Concept 2 carpet design**

**Layered concept 4**: Introducing absorber layer just below carpet tufting and also having a double panel system using thin heavy layer panels, separated by an air-gap (using honey comb or foam structure).
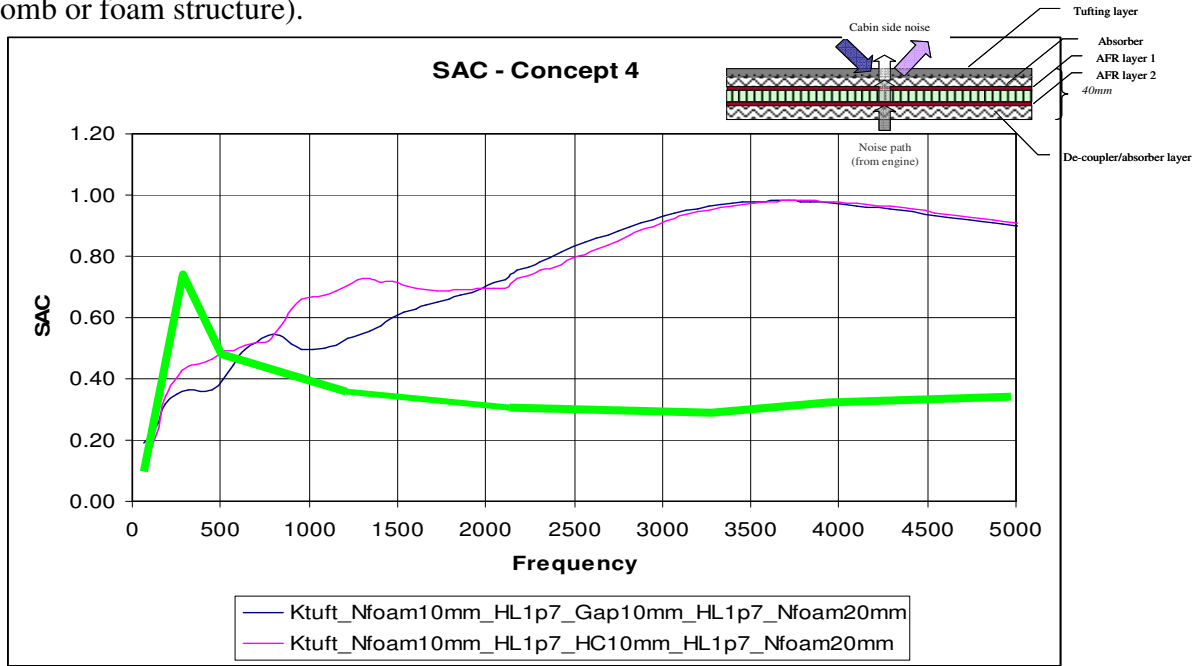


**Figure 4.19 – Cabin side absorption characteristics of Concept 4 carpet design**
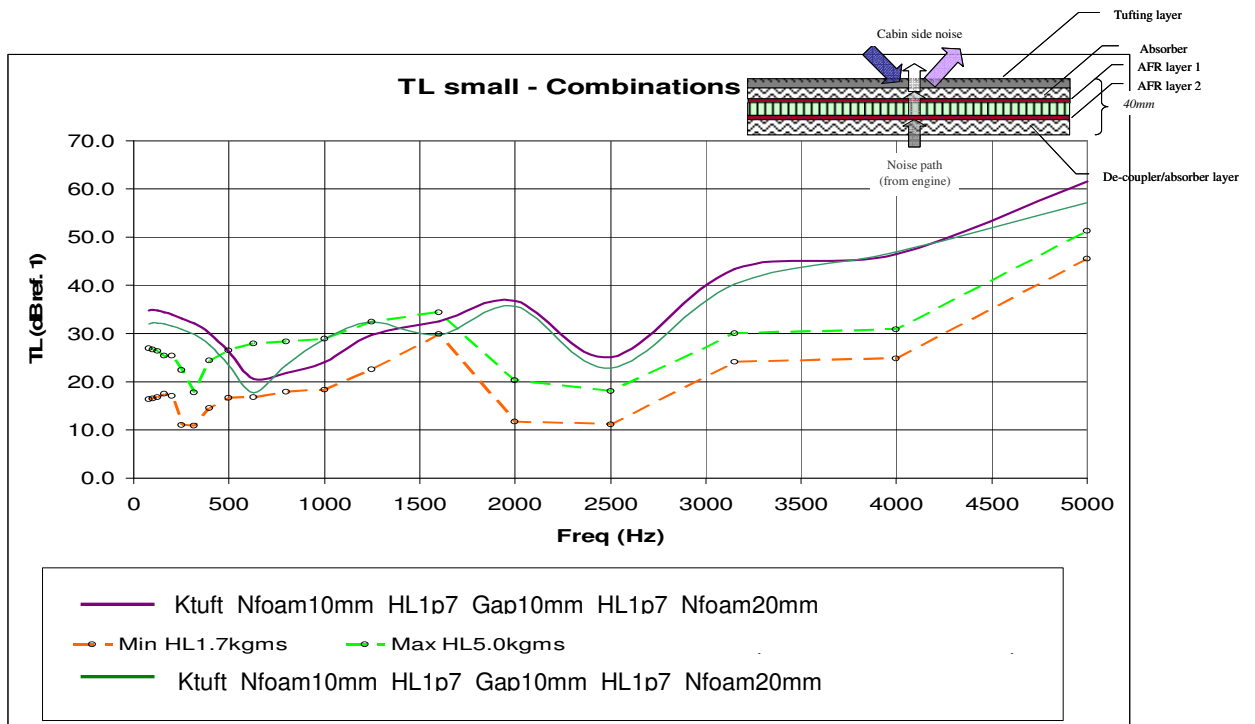


**Figure 4.20 – Transmission loss characteristics of Concept 4 carpet design**

## 5.1  Result discussion

The absorption coefficient measurement results of the new carpet concept designs clearly illustrates that introducing a layer of absorption material between the tufting layer and the heavy noise isolation layer improves the vehicle cabin side sound absorption coefficient to a great extent. Concept 4 carpet design shows the minimal sound absorption coefficient improvement, compared to other design concepts.

Meanwhile, when Concept 1 and Concept2 design Sound Transmission Loss results are not that promising for noise isolation improvement compared to the Heavy Layer (1.7kgsm) noise isolation method, Concept 3 and Concept 4 has a reasonable improvement in Sound Transmission Loss, especially above 2 kHz frequency range. It is to be noted that in the case Concept 4, the measured Sound Transmission Loss is even better than the 1.5kgsm Heavy Layer carpet design, which is a significant improvement in noise isolation.

# 6  CONCLUSION

- Air flow resistance layer in place of heavy layer largely improves the sound absorption coefficients on the cabin side.

- Foam/Fibre Insertion between carpet tufting and heavy layer (Concept 1) improve s largely the sound absorption coefficients on the cabin side, especially in mid-high frequency.

- Concept 2 carpet design, i.e. double air flow resistance layers with absorber layer sandwiched inside instead of heavy layer, is best for SAC at low frequencies.

- Heavy Layer (HL) in the middle could achieve the effect of airflow resistance layer panels separated by MJA 316 (20 mm), for sound transmission loss.

- HL in the middle (Concept 1) will also achieve both good SAC and TL, which is also a development direction.

- The compromised concept design for both cabin side sound absorption and Transmission Loss will be Concept 3, i.e. replacing the thick heavy layer with a double sandwiched panel system, where the top panel is an AFR layer and the bottom panel is a thin heavy layer.

# CHAPTER 5

# DEFINING THE DESIGN PROCESS AND ACOUSTIC TOOLS

## 1    INTRODUCTION

Development of a better acoustic structure involves the introduction of new types of materials or a combination of various materials types to suit the application. The acoustic properties provide important criteria for material selection. The acoustic performance is evaluated by the materials' sound absorption and transmission loss coefficients.

The use of computer simulation to evaluate component layers of materials is a convenient way of optimising acoustic performance. Computer programs like AUTOSEA, require *random* incident sound absorption and transmission loss coefficients and/or intrinsic material property data to run the simulations. Measuring intrinsic property data such as tortuosity, viscous and thermal lengths, among others, are time consuming and require specialized equipment. On the other hand, the evaluation of sound absorption coefficient using a large reverberant chamber requires a large space and facilities [28] and is limited by lower frequency limits. Likewise, sound absorption and transmission loss coefficient measurements using an impedance tube are limited to normal incidence conditions and can not be directly inputted to the simulation programs.

Other issues such as the cost of the facility, portability and ease of operation pose considerable challenges and thereby create a need to explore alternative means to evaluate acoustic properties. It is in this context that a multi-function device is proposed. The proposed 45° SAC device is designed for quick and simple measurement of $\alpha_{\theta,f}$ and $TL_\theta$ – in situ or in laboratory conditions. It can also be used as a portable listening device for subjective analysis.

The proposed V or Y-shaped acoustic wave guide, with which the upper branches forms a 45° angle with respect to the horizontal, is designed to perform the functions of (1) measurement of the sound absorption coefficient (SAC) ($\alpha_{\theta,f}$) and the transmission loss coefficient ($TL_\theta$) of carpet materials, and (2) act as a listening device for subjective evaluation. An acoustic source injects directive sound waves into the duct, hits the sample material at the bottom of the Y-shaped junction, and establishes a standing wave condition. A two-microphone set-up will measure the acoustic pressure and derive the transfer functions needed for the calculation of $\alpha_{\theta,f}$ and $TL_\theta$. The proposed device is portable and can be used for quick in situ measurements.

Further, an overview about the various acoustic simulation tools, especially AUTOSEA 2 acoustic simulation tool, based on the well established Statistical Energy Analysis method, is provided as a platform on which all the design validation is based on.

## 2    REVIEW OF SAC MEASUREMENT METHODS

Literature review for sound absorption measuring devices reveal interesting designs based on the type of measurement methods categorized [29] as follows:

**Reverberation room**

The Sabine equation for estimating the reverberation time, $T_{60}$ is

$$T_{60} = \frac{55.25V}{cS\overline{\alpha}} \dots\dots\dots\dots\dots\dots\dots\dots\dots\dots\dots\dots\dots(1)$$

where $V$ is the volume of the room, $c$=343 m/s is the speed of sound in air, $S$ is the total surface area of the room. $\overline{\alpha}$ is the average absorption coefficient for the room, calculated from

$$\overline{\alpha} = \frac{\alpha_1 S_1 + \alpha_2 S_2 + ... + \alpha_n S_n}{S} \dots\dots\dots\dots\dots\dots\dots..(2)$$

where $\alpha_n$ are the individual absorption coefficients for each surface $S_n$ and $S$ is the total surface area of the whole room.

From Sabine's formula and the definition of absorption, the absorption of the sample can be expressed as:

$$\alpha = \frac{0.16V}{S}\left(\frac{1}{T_s} - \frac{1}{T_e}\right) \dots\dots\dots\dots\dots\dots\dots\dots\dots\dots\dots(3)$$

where:

$\alpha$ is the absorption coefficient of the sample

S is the area of the sample material

V is the volume of the chamber

$T_s$ is the reverberation time, with the sample

$T_e$ is the reverberation time of the empty chamber

There are drawbacks in this method where it is possible to get measurements of $\alpha$ exceeding 100% using the reverberation chamber. This is due to the inherent definition of $\alpha$ hence the uncertainty is at best ±10%. Should we take the physical definition of the absorption coefficient: $\alpha$ = (absorbed energy)/(energy impinging the surface), the reverberation room cannot measure the absorption according to the above definition as there is no real control of either the energy absorbed or impinged in the surface[28]. In addition, large pieces of sample material are needed and the chamber itself is a large and expensive facility.

**Impedance Tube Apparatus**

The impedance tube, or its modern equivalent, is based on the Kundt's tube design and applies the standing wave theory. The Bruel & Kjaer Pulse Impedance Tube – type 4206 and its predecessors are widely used for evaluating both normal sound absorption coefficient ($\alpha_0$) and sound transmission loss properties. Depending on the tube size, the applicable frequency range is 50-6.4kHz. Normal sound absorption ($\alpha_0$) measurements use the two-microphone set-up whist the four-microphone set-up and the associated transfer functions are needed for sound transmission loss evaluation [30].

**Other Devices**

*Microflown PU intensity probe*

The Microflown PU intensity probe is an acoustic particle velocity sensor developed in the University of Twente in 1994 and commercialized in 1997[57]. While traditional method

for measuring sound intensity is to use a PP probe (two pressure microphones) and determines particle velocity to acquire sound intensity, Microflown Technologies introduced an improved sensor using a PU probe (microphone and Microflown) which measures particle velocity instantly. The PU sensor can be used to measure acoustic impedance. The reflection coefficient can then be determined and the absorption coefficient calculated accordingly[57,58,59]. Reliability issues are currently being addressed in an attempt to improve the technology.

*Devices under patent*

Patent search uncovered some types of devices for SAC measurements similar to the impedance tube. Examples are given below.

1.      US Patent 4732039 (Figure 5.1) is a flexible U-shaped channel abutted against a surface to be measured, thereby forming an acoustic duct, with the sample surface forming one wall of the duct. The acoustic wave injected into the duct travels parallel to the surface of the sample and operates on the standing wave theory. The device is claimed for use in acoustic impedance measurement.



Figure 1: US Patent 4732039

2.      US Patent 4537630 (Figure 5.2) is an open-ended acoustic impedance tube abutted against the sample material. It requires a material of known acoustic property for proper



Figure 2: US Patent 4537630

calibration and the unknown sample material measurements is compared to the base readings. This device uses the two-microphone set-up and ascribes to the standing wave theory. An enhanced version of a similar device is shown in Figure 5.3.
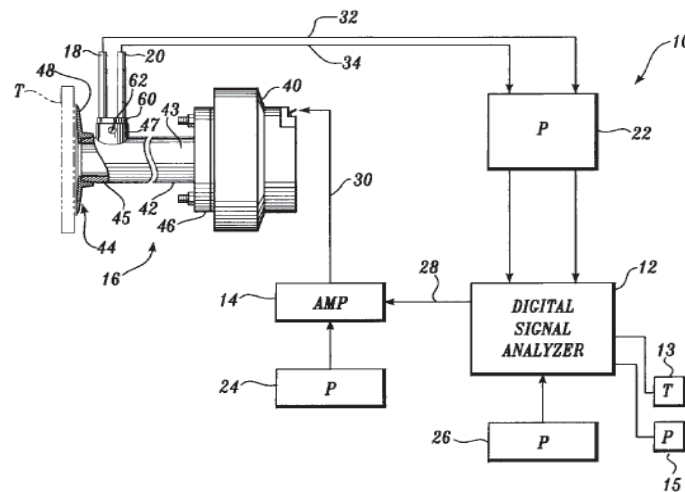


Figure 3: US Patent 6134968

*Diffuse field measurement techniques*

In-situ, diffuse field measurement methods are used particularly in acoustic evaluation of road surfaces[29]. The diagram in Figure 5.4 illustrates the concept.
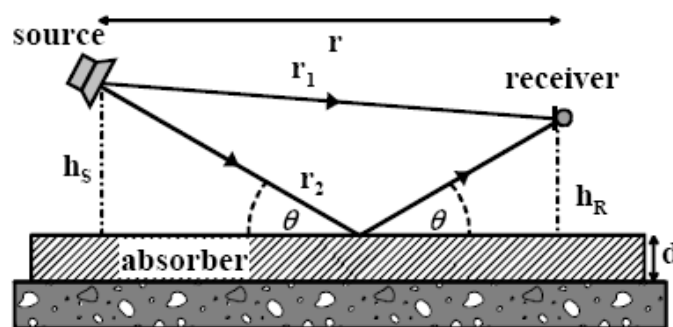


Figure 4: Set-up for transfer function measurement
in front of an absorbing surface [61].

A similar, though simpler, idea was earlier mentioned in the B&K manual. Figure 5.5 shows a similar concept but without the source-receiver leakage pathway.
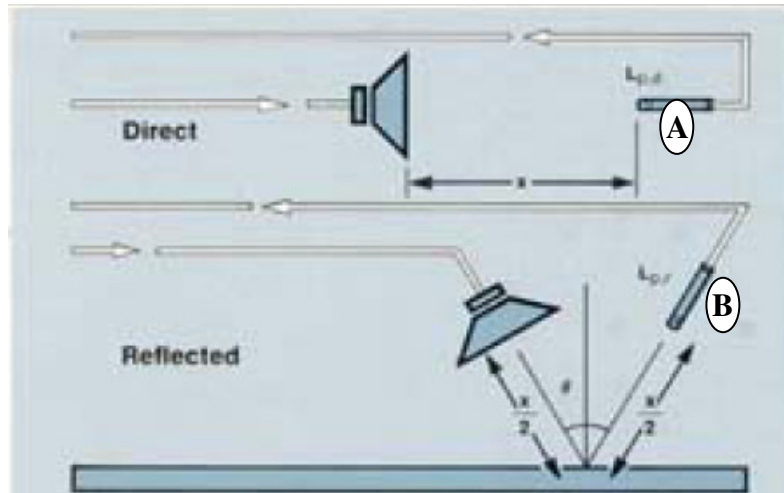
Figure 5. Diffuse field measurement concept (B&K).

The B&K tone burst method[35] can be applied using the following formulation:

Absorption coefficient:

$$\alpha_{\theta,f} = 1 - r_{\theta,f} \quad \text{......................(4)}$$

$r_{\theta,f}$ = the reflection coefficient

$$r_{\theta,f} = 10^{-\frac{(L_{p,d} - L_{p,r})}{10}} \quad \text{..........(5)}$$

$L_{p,d}$ = SPL of direct sound

$L_{p,r}$ = SPL of the reflected sound

The SPL can be expressed as[37]:

$$SPL = 10\log\left|\frac{P^2}{P_{ref}^2}\right| \quad \text{........(6)}$$

If we assign local SPL readings as:

$L_{p,d} \rightarrow P_A$ and $L_{p,d} \rightarrow P_B$, and   substituting (6) into (5), then the sound absorption coefficient can be expressed as:

$$\alpha_{\theta,f} = 1 - \left| \frac{P_B}{P_A} \right|^2 \quad \ldots\ldots\ldots\ldots\ldots\ldots\ldots\ldots\ldots\ldots\ldots\text{(7)}$$

## 3    DESIGN CONCEPT

### 3.1 Theoretical basis

The proposed wave guide operates on the basis of the planar, standing wave theory and assumes that the attenuation in the duct walls is minimal. Acoustic pressure wave measurements are taken from two locations using a two-microphone set-up. Pressure field measurements will be employed to derive the transfer functions (complex, incidence and reflected), impedance, and the reflection factor needed to calculate $\alpha_\theta$ and $TL_\theta$.

Figure 5.6 depicts the planar wave propagation within the proposed device. The sound waves are projected downward at an angle of 45° from the left side ($P_A$), strikes the sample at the bottom junction of the 'V', and resulting in the specular reflection ($P_B$) upwards to the right side. The dominant reflection pathways are also shown as $P_{Ar}$ and $P_{Br}$. Through the use of a semi-anechoic termination cap, it can be further assumed that the magnitude of $P_{Br}$ is small and that the potential leakage back to the source (i.e. similar to the $P_{Ar}$ pathway) is negligible.
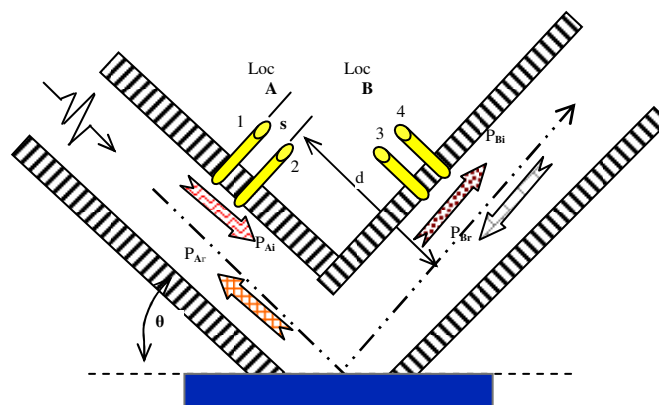


Figure 6. SAC device working principle [62]

The standing wave theory behind the working principle of the proposed SAC device is outlined herein following established methods [30,38,39,40,41].

The sound intensity, at any position inside the waveguide, is the product of the instantaneous pressure and particle velocity at that location, viz:

$$\bar{I}_{(t)} = < P_{(t)} u_{(t)} > \dots\dots\dots\dots\dots\dots\dots\dots\dots\dots\dots\dots\dots(8)$$

Assuming that the sound field is sinusoidal, employing time averaging and using the complex notation, the sound intensity can be written as:

$$\bar{I} = \frac{1}{2} \mathrm{Re}(Pu^*) \dots\dots\dots\dots\dots\dots\dots\dots\dots\dots\dots\dots(9)$$

Time averaging is implicitly given by the factor ½ for rms values of sound pressure and particle velocity, and $u^*$ is the complex conjugate of $u$. The term **Re[…]** means only the real part of the quantity inside the brackets is considered. Referring to Figure 5.6, the absorption coefficient, $\alpha_{\theta,f}$ , can be expressed as the net intensity falling and leaving the sample surface divided by the incoming intensity. The points of reference are at locations A and B.

$$\alpha_{\phi,f} = \frac{\bar{I}_A - \bar{I}_B}{\bar{I}_A} = \frac{\frac{1}{2}\mathrm{Re}(P_A u_A^*) - \frac{1}{2}\mathrm{Re}(P_B u_B^*)}{\frac{1}{2}\mathrm{Re}(P_A u_A^*)} = 1 - \frac{\mathrm{Re}(P_B u_B^*)}{\mathrm{Re}(P_A u_A^*)} \dots\dots\dots\dots\dots\dots(10)$$

The characteristic impedance (in the direction of propagation) in a single plane wave is:

$$Z_0 = \rho_0 c_0 \dots\dots\dots\dots\dots\dots\dots\dots\dots\dots\dots\dots\dots\dots..(11)$$

The particle velocity can be calculated from the pressure using the analogy of Ohm's Law.

$$u = P / \rho_0 c_0 = P/Z_0 \ \dots\dots\dots\dots\dots\dots\dots\dots\dots\dots\dots..(12)$$

The field impedance at any point x within the sound field is:

$$Z_{(x)} = P_{(x)} / u_{(x)} \ \rightarrow \ 1/Z_{(x)} = u_{(x)}/P_{(x)} \ \dots\dots\dots\dots..(13)$$

Using the relation $u^*/P^* \equiv u/P$, (13), and further simplifying (10) yields:

$$\alpha_{\phi,f} = 1 - \left|\frac{P_B^2}{P_A^2}\right| \frac{\mathrm{Re}\left(u_B/P_B\right)}{\mathrm{Re}\left(u_A/P_A\right)} = 1 - \left|\frac{P_B^2}{P_A^2}\right| \frac{\mathrm{Re}\left(1/Z_B\right)}{\mathrm{Re}\left(1/Z_A\right)} \ \dots\dots\dots\dots\dots\dots\dots\dots\dots\dots\dots.(14)$$

The field impedance at location A can be quantified from equations (12) & (13), viz:

$$Z_A = \frac{P_A}{u_A} = \frac{P_{Ai} + P_{Ar}}{u_{Ai} - u_{Ar}} = \frac{P_{Ai} + P_{Ar}}{\left(P_{Ai}/Z_0\right) - \left(P_{Ar}/Z_0\right)} = Z_0 \left[\frac{1 + \left(P_{Ar}/P_{Ai}\right)}{1 - \left(P_{Ar}/P_{Ai}\right)}\right] \dots\dots\dots\dots\dots.(15)$$

The reflected components of the sound waves at locations A & B can be expressed as:

$$P_{Ar} = P_{Ai} R_A \ \text{and} \ P_{Br} = P_{Bi} R_B \ \dots\dots\dots\dots\dots..(16)$$

Then, the expression for the complex reflection coefficients are:

$$R_A = P_{Ar}/P_{Ai} \ \text{and} \ R_B = P_{Br}/P_{Bi} \ \dots\dots\dots\dots\dots..(17)$$

Substituting (17) into (15), the expression for the field impedance simplifies to:

At location A, $Z_A = Z_0 \left[ \dfrac{1 + R_A}{1 - R_A} \right]$ ……………………………………(18a)

Similarly for location B, $Z_B = Z_0 \left[ \dfrac{1 + R_B}{1 - R_B} \right]$ ………………………(18b)

Combining (18) and (14) yields:

$$\alpha_{\phi,f} = 1 - \left| \frac{P_B}{P_A} \right|^2 \frac{\mathrm{Re}\left[ \dfrac{1 - R_B}{1 + R_B} \right]}{\mathrm{Re}\left[ \dfrac{1 - R_A}{1 + R_A} \right]}$$ ……………………………………(19)

Employing a perfect anechoic termination cap on the right hand side of the device will render $R_B \approx 0$ and leaves only the complex reflection function near the source (i.e. $R_A$ at location A) which can be evaluated by the two-microphone set-up and FFT analyser. Sound pressure fields at locations A & B can be measured using standard pressure microphones and the sound absorption coefficient can be calculated using (19).

If all the reflected sound components are neglected (i.e. $R_A$ & $R_B \approx 0$), then equation (19) will simplify to the form similar to (7).

A working prototype model of the proposed measurement device is developed and calibrated, but due to IP issues on pending patents for the design, further detailed specifications are excluded from the document.

## 4    ACOUSTICS SIMULATION AND VALIDATION TOOLS

### 4.1  Scope of vehicle carpet acoustic simulation

Vehicle noise sources are basically categorised as engine/power-train noise, tyre noise, HVAC noise, wind noise, exhaust noise and other external noises. The noise transmission paths to the driver ear include the floor trim, which hence has a role in blocking the noise or absorbing the noise already inside the vehicle cabin. Compared to the other sound package

components, floor trims cover most of the noise-exposed areas of the vehicle, and hence plays a relatively significant role in noise reduction. For a given distribution of noise sources and transmission paths, the acoustic properties of the carpet sections can be locally optimized and thus achieve efficient noise isolation for given constraints of weight and cost.

Virtual modelling and testing is a widely accepted tool for improving product design and predicting performance at early stages of vehicle development, even before prototype build, which saves tooling cost and time caused by design changes. In order to evaluate vehicle trim components in a sound package, intensive vehicle tests are normally conducted, which leads finally to compromised solutions by trial and error methods. New acoustic modelling methods can be used to simulate the component and vehicle tests during early sound package design stages and optimize these trim components, and also provide a highly repeatable standard platform for design comparison and benchmarking.

## *4.2   Simulation process cycle*

An outline of simulation process in vehicle carpet design is given in Figure 5.1. Each block also represents the set of resources and sub-tasks involved at each stage. Referring to the process cycle, the key loops that iterate are the simulation validation  and design optimization loops.
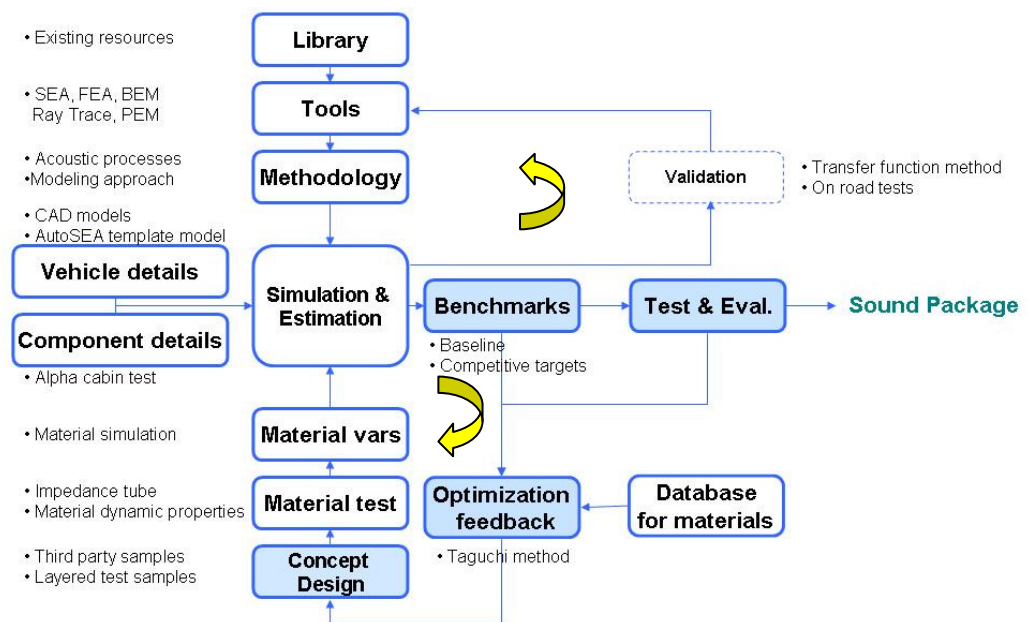


**Figure 7: Simulation process cycle**

The selection of the right simulation tool is an important decision, which largely affects the completion time line of the various processes or stages. Statistical Energy Analysis (SEA) is considered here to provide sufficient resolution (in the frequency range 315Hz - 8kHz) in terms of vehicle noise simulation, and the acoustic modelling software AutoSEA2 from ESI group is used for material (Foam & Fibre modules), component and vehicle (Template Modeller module) level simulations. Re-usability of various simulation resources contribute to the efficiency of the whole modelling process. A detailed discussion is conducted in the following sections regarding the selection of the acoustic simulation tool.

## 4.3   Review of acoustic and vibration analysis simulation tools

Based on the mathematical formulation used for modelling a system there are a variety of options in selecting the appropriate simulation tool. Listing the established methods,

- Finite Element Method/Analysis (FEM or FEA),

- Boundary Element Method (BEM),

- Inverse Boundary Element Method (IBEM),

- Statistical Energy Analysis (SEA),

- Hybrid FEA & SEA method,

- Couple FEM & BEM method and

- Acoustic ray-tracing method.

FEM analysis is an established tool for modelling sheet metal bodies, engines, suspensions and even complete vehicles, but requiring high computation resources, in particular for high frequency modelling, which may take even weeks to evaluate a complete vehicle on a normal personal computer. The accuracy of the results are highly dependent on variation of the model details , and hence could result in erroneous results.
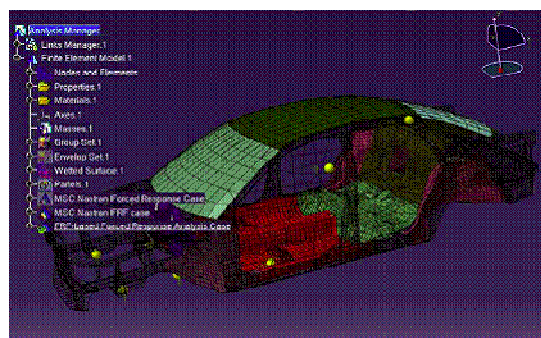


**Figure 8: FEM model of a Sedan (Image courtesy – LMS)**

Meanwhile, Boundary Element Method (BEM) is useful simulation tool for modelling vehicle interior body cavities, interior trim, power train noise, exterior radiation and tyre noise.
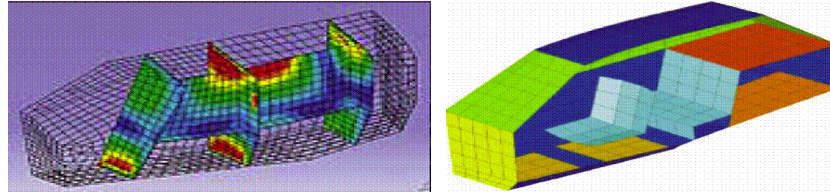


**Figure 9: BEM modelling vehicle interior**
(Image courtesy – LMS & ESI group)

Inverse Boundary Element Method (IBEM) is a modelling tool preferred for predicting surface velocities in applications like power train and tyre acoustic modelling.
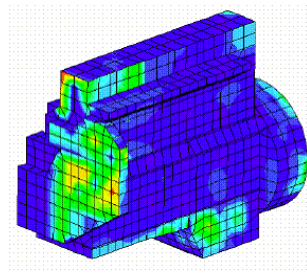


**Figure 5.10: IBEM model of engine**
(Image courtesy – University of Kentucky**)**

Statistical Energy Analysis (SEA) is a proven technology initially formulated for applications in NASA projects. It subdivides the complete model into Systems and sub-systems which interact each other based on energy flow principles. The system and subsystem parameters are derived from experimental measurements. This acoustic modelling method is best suitable for modelling vehicle components like doors, cockpits and also for complete vehicle simulation, both interior and exterior.
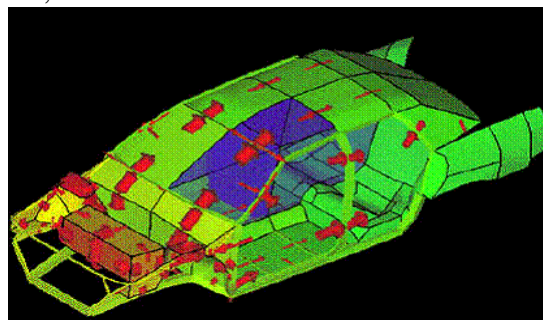


**Figure 5.11: SEA model of a sedan** (Image courtesy – ESI
group)

Hybrid FEM & SEA is a new method of combining the strengths of both the simulation techniques, where rigid junctions and structures are modelled as FE sections and cavities & related high modal density sections are modelled using SEA method.
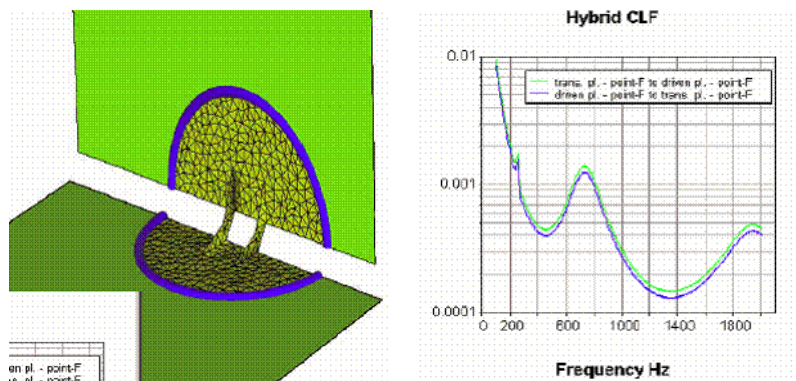


**Figure 5.12: Hybrid FEM & SEA method** (Image courtesy – ESI group)

The important factors for selecting a suitable modelling tool includes the fact that whether it applies to the nature of the acoustic field and its excitation, which are basically categorised as,

- Airborne

OR

- Structure-borne

Further, the complexity of simulating and validating the complete design model, at system or vehicle level, can be selection criteria for defining the scalability of the simulation tool. For the purpose of stage wise simulation, the following are the three levels of modelling and validation to be handled accurately by the single simulation tool.

- Layered material simulation,

- Component or prototype design simulation,

- Complete system or vehicle level simulation

The frequency range of interest, i.e. low frequency, mid frequency or high frequency, is also a primary selection criterion for finalizing the choice of simulation tool. The below table

gives a clear picture of the various simulation tools available and the factors to be considered and compared against.

**Table 1: Comparison of various acoustic simulation methods**

|            | FEM    | BEM  | IBEM | SEA    | FEM+SEA | FEM+BEM | Ray Trace |
|------------|--------|------|------|--------|---------|---------|-----------|
| Lo Freq.   | 10-150 | 10-  | 10-  | No     | 10-     | 10-100  | 20 -      |
| Mid Freq.  | ok     | -500 | -500 | 500 -  | -       | No      | -         |
| High Freq. | No     | No   | No   | -10k   | - 10k   | No      | - 10k     |
| CAD        | Yes    |      |      | NA     |         |         |           |
| Precision  | High   |      |      | High   |         |         | Medium    |
| Computing  | High   | High | High | Low    |         | High    | Low       |
| Time       | High   | High | High | Low    |         | High    | Low       |
| Complexity |        | Low  | Low  | Medium |         | Low     |           |

Thus, referring to the above table for comparison, it is clear that for applications of simulating air-borne vehicle noise (500 Hz and above) and for low computational resources, Statistical Energy Analysis (SEA) is most suitable accommodate modelling method to go forward. AutoSEA from ESI group is one of the recommended SEA modelling softwares in the market, which is used throughout the project.

# 5    CONCLUSIONS

- The proposed $45^{o}$ SAC measurement device provides non-destructive SAC measurement for sound package samples.

- Defining the simulation process cycle and identifying the iterating execution loops is important for project efficiency and result accuracy.

- Statistical Energy Analysis (SEA) is identified as the well suited simulation tool for the vehicle noise frequency range of interest and in terms of computational requirements.

- A stage wise simulation and validation process, i.e. material level, component level and vehicle level, is required for a scalable simulation and validation of the designs.

# CHAPTER 6

# MATERIAL SIMULATION, VALIDATION AND THEORY

## 1   INTRODUCTION

Acoustic materials range from a variety of foams, fibre, poly-vinyl, fabric to other structural material like steel, compressed paper or glass, used to hold these acoustic materials. The visible variables in the layered designs of sound packages are usually thickness, density, number of layers, special surface contours etc. Deriving out the best combination of these variables by experience to solve a particular acoustic problem is normally a time consuming job of trial and error.

For a given homogeneous acoustic material sample, if there is a possibility of simulating these physical variations using a virtual material modelling tool, a huge advantage lies ahead for optimization and quick design validation, compared to conducting experiments.

Acoustic/physical properties of materials are measured and a database of various acoustic package materials has been maintained for the purpose of evaluation.  CSIRO provided test data for material properties of the layers of samples, which is given as input to SEA software to simulate the absorption coefficient (random). The conversion of measured normal incidence sound absorption coefficient to random incidence sound coefficient and comparison of simulated and measured results have been conducted in this chapter.

## 2   MATERIAL LEVEL SEA SIMULATION PROCEDURE

### 2.1  Input parameters for simulation

Material properties like air flow resistivity, porosity, tortuosity and Young's modulus were provided by CSIRO for each possible layer of the carpet sample, so that a material property database was established for calculation of sound absorption coefficient and sound transmission loss. The measured key material properties are explained below [66].

*Air flow resistivity*

Air flow resistivity is defined as the ratio of the pressure drop to the volume flow rate of air through a porous material. We have measured the air permeability of the samples using AS 2001.2.34-90 with an orifice size of 5 cm$^2$ and a differential pressure of 98Pa. The average of 5 repeats and the Coefficient of Variation (CV%) is reported. The Air flow Resistivity is derived from the Air permeability test results. Unit is Ns/m$^3$ or Ns/m$^4$ for unit thickness.

*Porosity*

Porosity $\varphi$ is defined as $\varphi = Va / Vt$ . Where Vt is the total volume occupied by the sample and Va is the volume of the free air within the sample. Va is calculated as (Vt – Vs). Unit dimensionless number in the range 0-1. Vs is s the volume occupied by the test sample material excluding the air. A sample was cut for test its area and thickness are measured to give the total volume Vt, the total volume of the sample in its free state has a unit of ml. The sample was then immersed into a fluid (water and a surfactant to assist wetting) and the displaced volume of liquid is recorded. Unit is ml.

*Tortuosity*

Tortuosity is a measure of the *tortuous* path length of a material see Figure 6.1
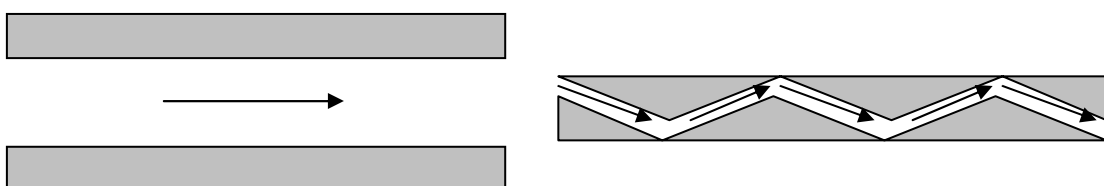


**Figure 6.1: Illustrating Tortuosity Left: Tortuosity = 1 Right: Tortuosity > 1**

Tortuosity has a dimensionless unit, typically larger than one and in the range of 1 - 2. Tortuosity is a property of a porous material it has no meaning if the sample is not permeable.

*Poisson's ratio*

Poisson's ratio is the ratio of the relative contraction strain, or transverse strain (normal to the applied load), divided by the relative extension strain, or axial strain (in the direction of the applied load). Poisson's ratio for the materials concerned are normally very small in value.

*Dynamic modulus (Young's modulus and Loss factor)*

Young's modulus is calculated using the equation, $E = k \times d / A$, where d is the sample thickness, A is its area and k is the stiffness calculated from the resonant frequency of the sample. Similarly, the damping is characterised by the loss factor, $\eta$, which is given by the 3dB bandwidth divided by the resonant frequency: $\eta = \Delta f / f_o$.

## 2.2  Simulation

Further, noise treatment layers were formulated in basis of the materials and their property database and applied to a circular metal plate, for which a script was run to simulate random incidence absorption coefficient values, i.e. inside AutoSEA2 software, select pull down menu sequence as Scripts->UtilitiesQuery->VTL. Note that the noise treatment layer, i.e. like sample B foam, is assumed to have a homogeneous property. Similar material layers are used to simulate multi-layered noise control treatments.
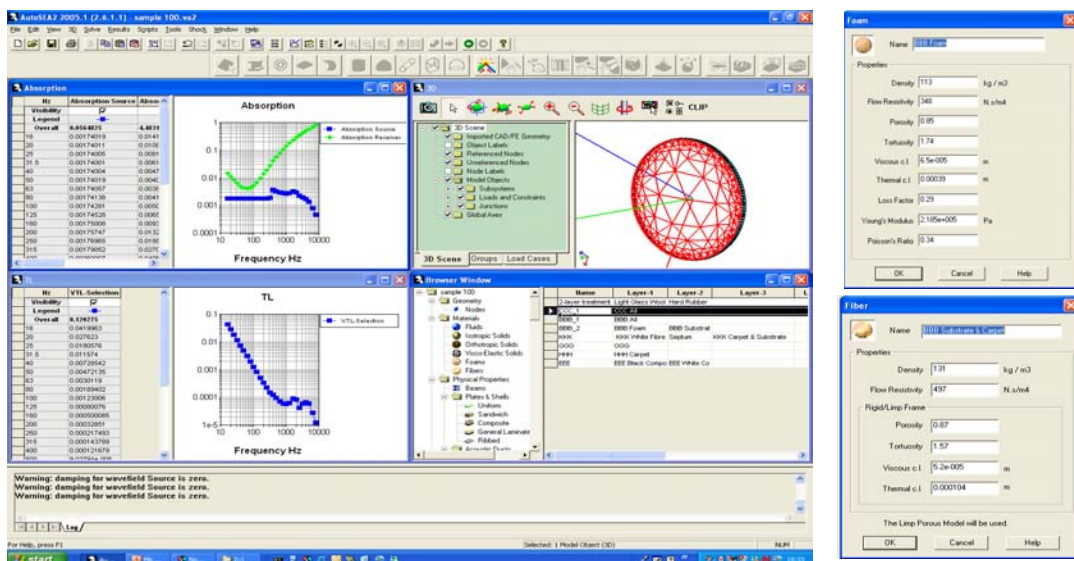


**Figure 6.2 – Material simulation using AutoSEA2**

## 3  VALIDATION PROCEDURE

### 3.1  *Absorption coefficient measurement using impedance tube*

The normal incidence absorption coefficients of the samples were measured using B&K impedance tube, following the broad-band 2 microphone method.

100mm and 29mm diameter samples were cut and measurements were done inside the large tube set-up (low frequency 50-1.6kHz) and small tube set-up (high frequency 500-6.4kHz). The microphone and the tube correction factors were considered and compensated throughout the measurements. At least 2 co-related results were picked up for averaging and combining low and high frequency plots, with the cross-over frequency in 500-1.6 kHz range. Refer Chapter 5 for specific details on normal absorption measurement procedure.

### 3.2  *Normal to random incidence absorption conversion*

According to AutoSEA software manual, simulated sound absorption is random incidence sound absorption coefficient. In order to compare the simulated results with the measured results, the measured normal incident sound absorption coefficients have to be converted to the random incident sound absorption coefficients.

Oblique incident sound absorption coefficient is given by,

$$\alpha_\theta = 1 - \left| \frac{(Z/\rho c)\cos\theta - 1}{(Z/\rho c)\cos\theta + 1} \right|^2 ;$$

where, **Z** is the impedance to the sample material, **ρ** is sound medium density, **c** is velocity of sound in medium and **θ** is the angle of incidence with reference to normal to sample.

Normalized impedance ratio of the sample is also given as,

$$Z/\rho c = z = r + jx.$$

where, r and x are the real and imaginary variables of the normalized impedance ratio, given from the measured impedance ratio.

Thus, after substituting for impedance ratio, we have

$$\alpha_\theta = \frac{4r \cos\theta}{(r \cos\theta + 1)^2 + x^2 \cos^2\theta}.$$

Since we are interested in random incidence absorption coefficient, integration for 180 degrees is to be done.

$$\bar{\alpha} = 2 \int_0^{\pi/2} \alpha_\theta \cos\theta \, \sin\theta d\theta \qquad \text{Refer [53]}$$

Hence, the random incidence absorption coefficient by Paris method [53] is

$$\bar{\alpha}_P = \frac{8r}{x^2+r^2} \left\{ 1 + \frac{r^2-x^2}{x(x^2+r^2)} \tan^{-1}\left(\frac{x}{1+r}\right) \right.$$
$$\left. - \frac{r}{x^2+r^2} \ln[(1+r)^2+x^2] \right\}$$

PARIS method, Refer [63]

Albert method of calculating random incidence sound absorption coefficient is given below.

$$\alpha^* = \frac{4r}{x^2+r^2} \left\{ \frac{1}{2} \ln[x^2+(r+1)^2] - \frac{r}{x} \tan^{-1}\left(\frac{x}{1+r}\right) \right\}.$$

ALBERT method
Refer [53]

Detailed and lengthy derivation and explanation of Albert method is given in [63].

## 4   RESULTS AND DISCUSSION

### 4.1  Normal incidence vs. random incidence

Random incidence absorption coefficient calculation was tried using two different but related methods, Paris and Albert methods. Comparing with the simulated results and as per the support documents supplied with the AutoSEA material software package, it seems that the calculated measurement results using Paris method matches well with the AutoSEA simulation results. So a statistical angular averaging of sound absorption, following Paris

method (AS/NZS 1935.1:1998/Appendix) can be used to convert measured normal incidence absorption coefficient. (Ref: E. T. Paris, Proc. Roy. Soc. 115, 407 (1927) )
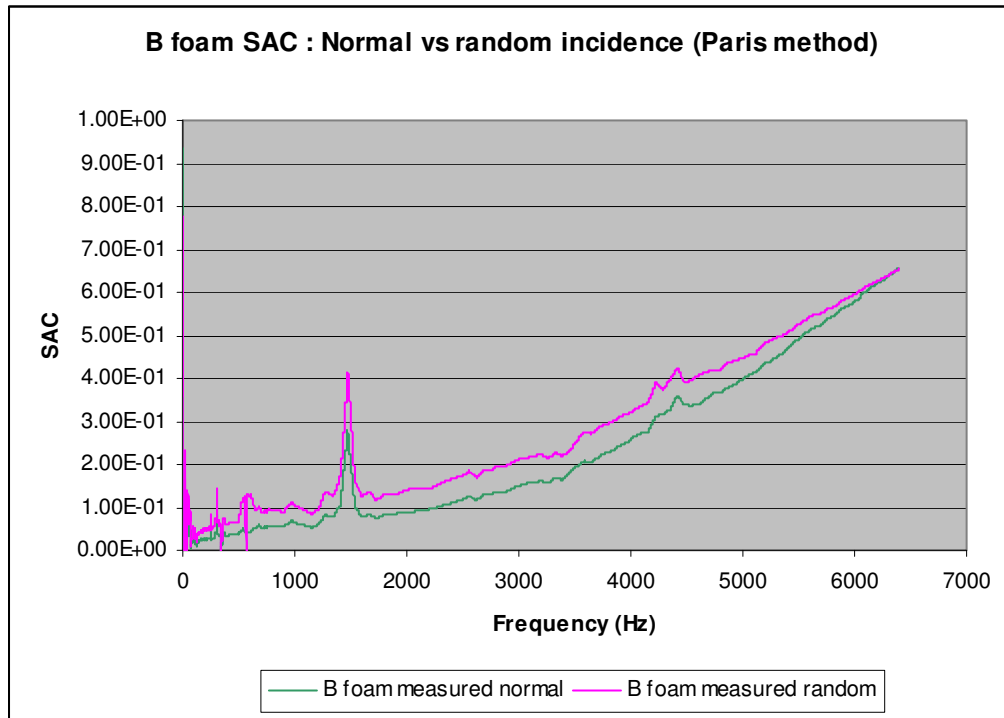


**Figure 6.3: Sample B foam measured normal vs. measured random (Paris method)**
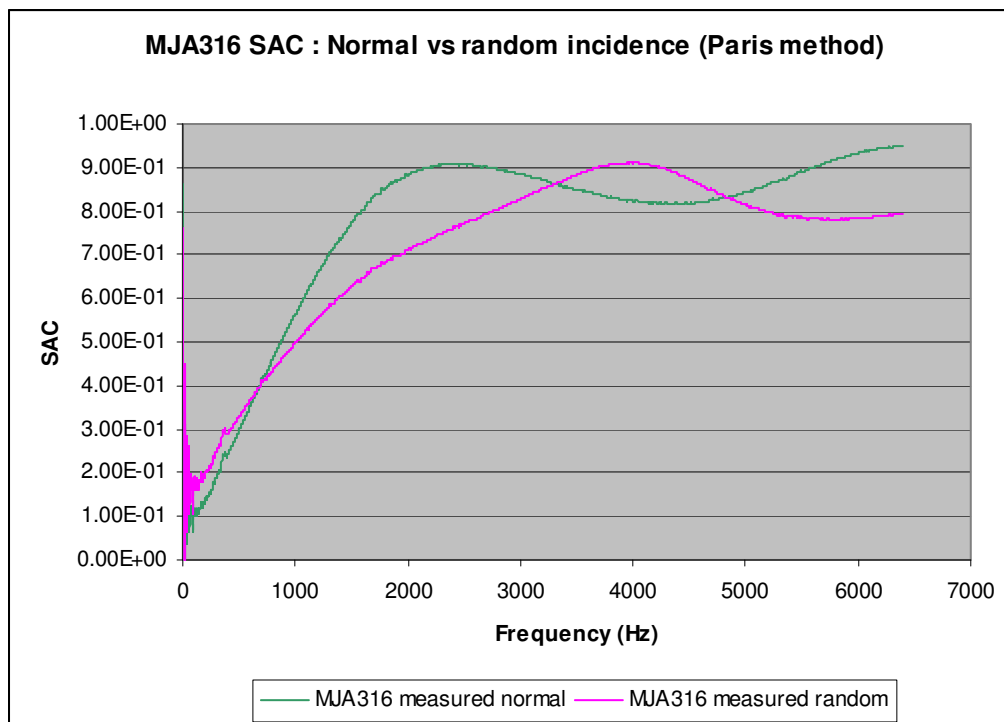


**Figure 6.4: MJA316 SAC measured normal vs. measured random (Paris method)**

## 4.2  *Simulation vs. measured results*

From the results obtained for both simulation and calculated measurements, they show similar trend for various samples, including foam, fibre, felt and Air Flow Resistance (AFR) layers, with a variation of about 10-15%. The simulation results do not include the low frequency resonance peaks, observed in normal incidence absorption measurements. This could be because AutoSEA uses statistical averaging across frequencies, which averages out the peaks.
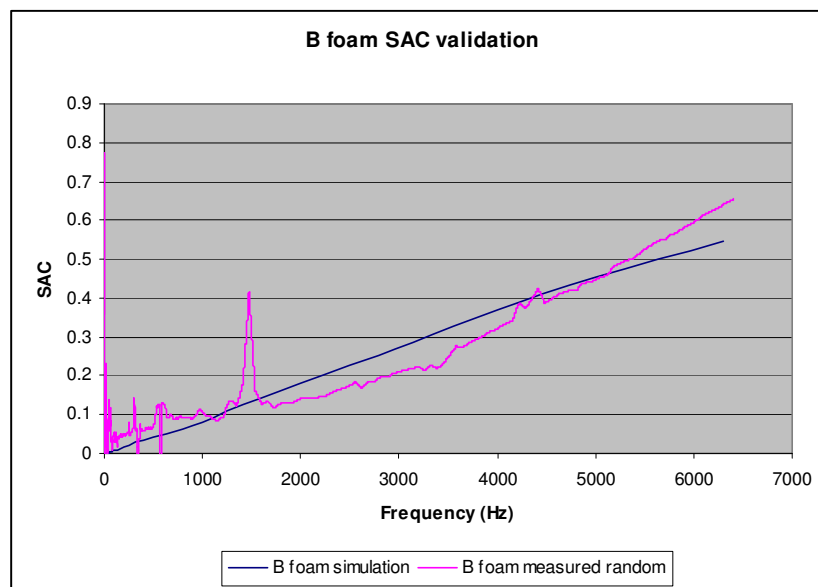


**Figure 6.5: Foam (open cell) sample B foam simulation vs. measured SAC**
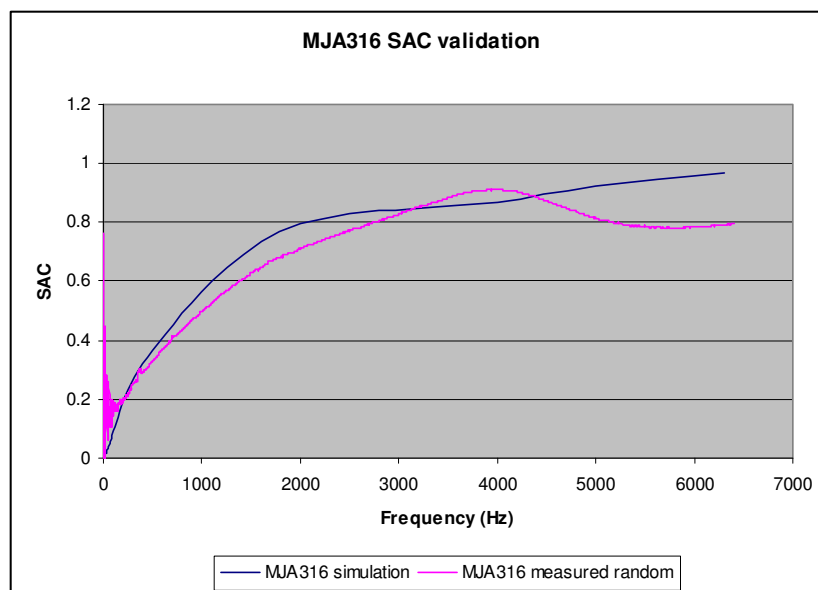


**Figure 6.6: Sample MJA316 fibre simulation vs. measured SAC**

Air Flow Resistant - Fibre (AFR) sample
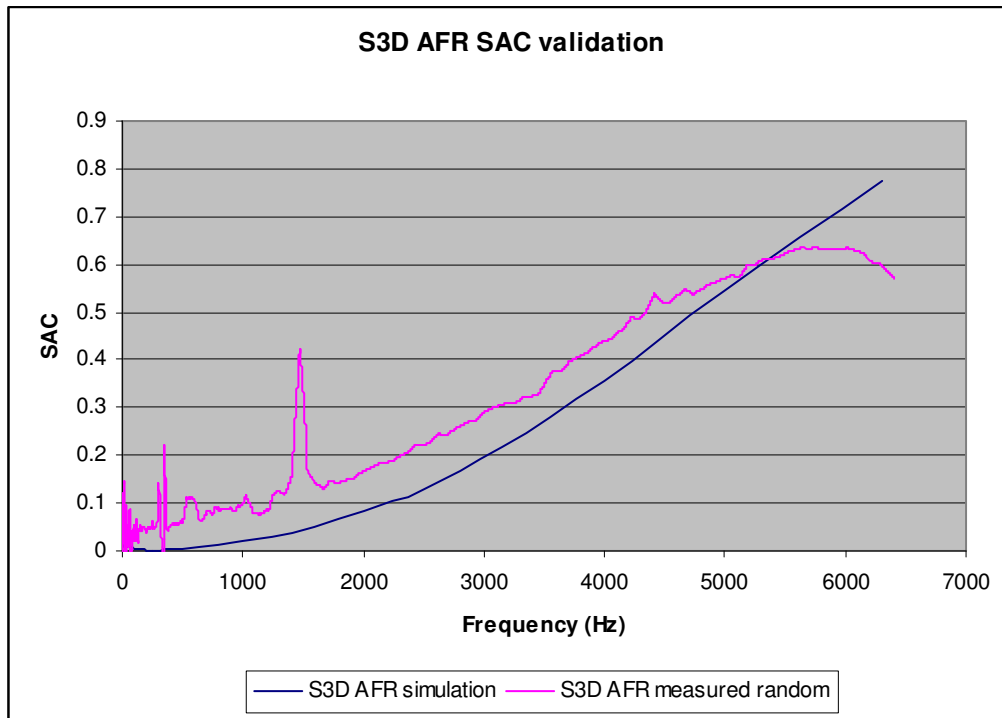


**Figure 6.7: Sample S3D AFR simulation vs. measured SAC**

Air Flow Resistant – Compressed poly-felt (AFR) sample
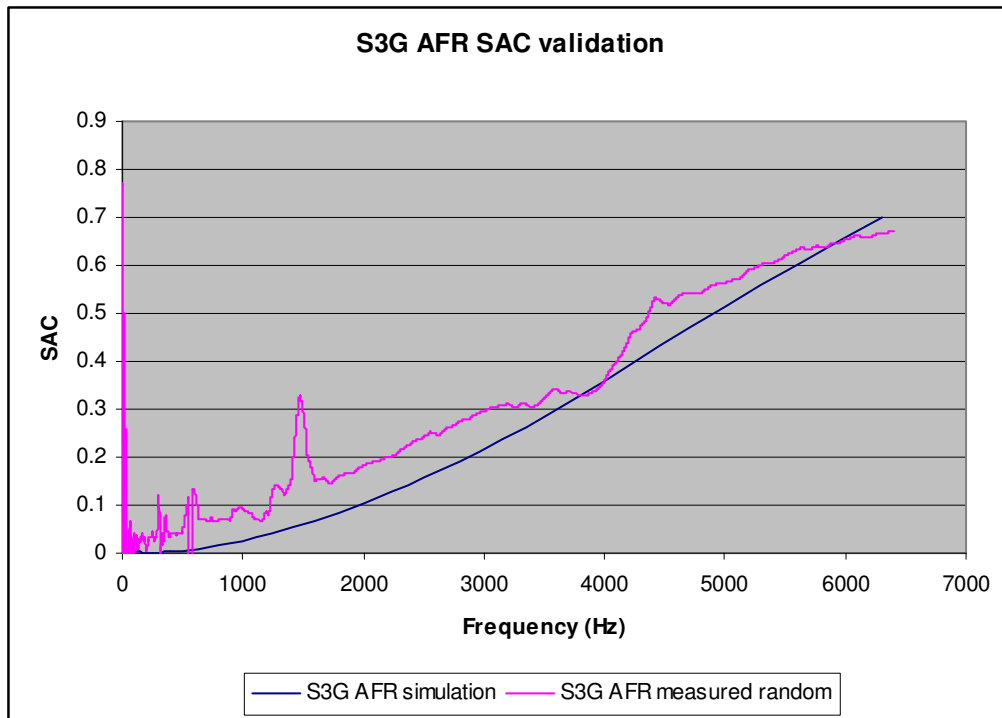


**Figure 6.8: Sample S3G AFR simulation vs. measured SAC**

Poly-felt absorber sample
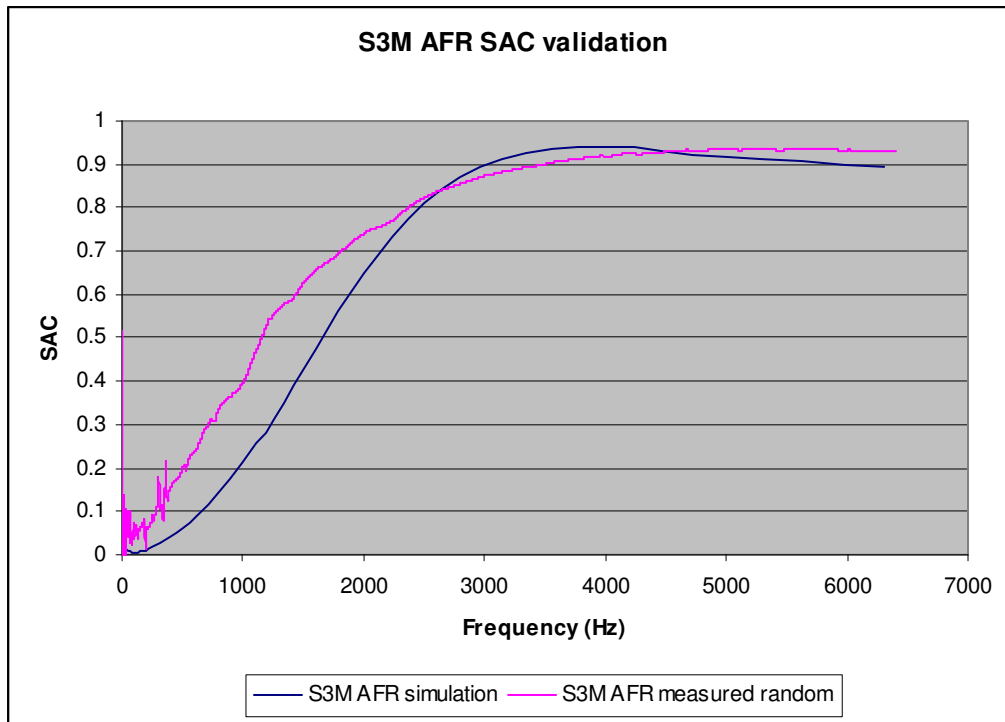


**Figure 6.9: Sample S3M AFR simulation vs. measured SAC**

Foam (closed cell) sample
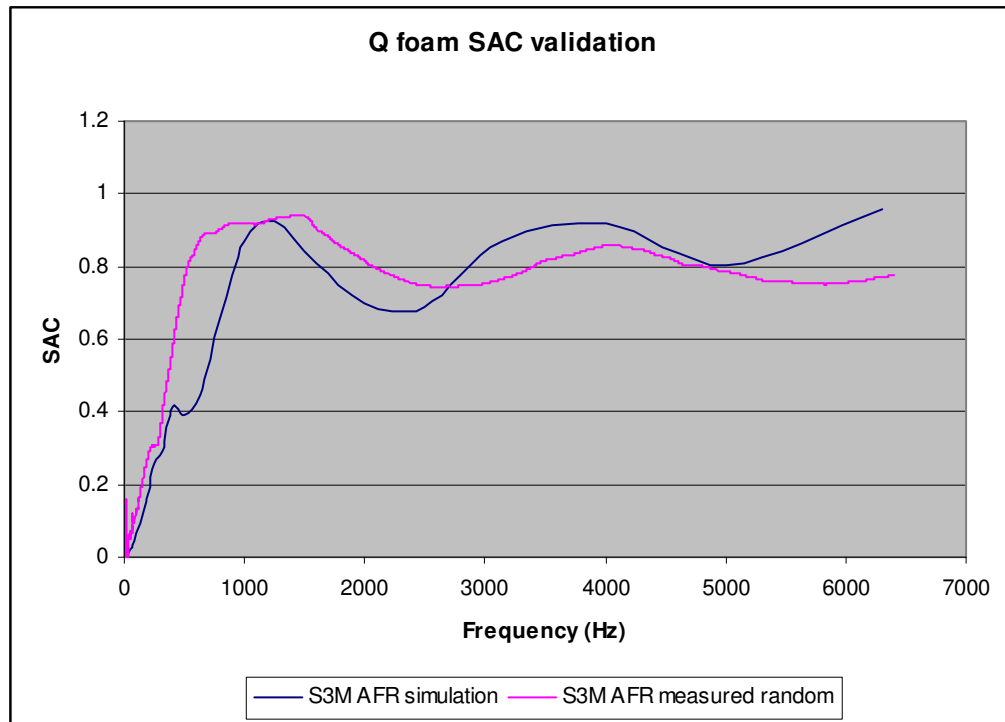


**Figure 6.10: Sample S3M AFR simulation vs. measured SAC**

It should be noted that the comparison of homogeneous materials is considered, i.e. multi-layered or mixed samples are avoided, because AutoSEA assumes the bulk properties of the material to be continuous throughout the sample.

## CONCLUSIONS

- Simulated and measured results of material sound absorption show the similar trend for various samples, with a variation of only about 10-15%.

- The simulation results do not include the low frequency resonance peaks, observed in normal incidence absorption measurements.

- Material samples should be simulated for homogeneous samples only. Multi-layered or non-homogeneous samples will give erroneous results, if simulated as a single material.

- A statistical angular averaging of absorption, following Paris method (AS/NZS 1935.1:1998/Appendix) can be applied to convert measured normal incidence absorption coefficient into random incidence absorption coefficient. (Ref: E. T. Paris, Proc. Roy. Soc. 115, 407 (1927) )

# CHAPTER 7

# VIRTUAL MODELLING AND VALIDATION, AT COMPONENT AND VEHICLE LEVELS

## 1   INTRODUCTION

This chapter outlines the various aspects about virtual modelling of component and vehicle level acoustics using the Statistical Energy Analysis models for carpet design evaluation. Alpha Cabin simulation is used for component level comparative study of the carpets and the results are discussed. A brief explanation of the various stages of the simulation process is provided for a better understanding of the virtual modelling and evaluation cycle. The vehicle virtual SEA model is validated by a transfer function based model evaluation process and finally the vehicle level evaluation of various carpets is conducted and the comparative results are analysed.

Virtual modelling and testing is a widely accepted CAE (Computer Aided Engineering) tool for improving the product design and predicting performance at early stages of vehicle development. This tool allows for early identification of design problems, solving the problems before prototype build, which saves the tooling cost and time, caused by the design changes at the later stages. Vehicle sound package includes floor trims, head liners, door trims and other acoustic components, which are usually tested at component level in acoustic labs, according to various international & national automotive design standards. For example, the reverberation room or Alpha Cabin for measuring sound absorption coefficient and anechoic room/reverberation room test for measuring sound transmission loss. However, this requests tooling for moulding these components for each measurement. In order to evaluate these trim components in the sound package, intensive

vehicle level tests will have to be conducted, which leads to the compromised solutions by trial and error. Further more, any design changes recommended by the test data will induce tooling changes, which are very time and cost consuming.

Virtual modelling tools such as AUTOSEA 2 can be used to simulate the component and vehicle level tests during early sound package design stages and optimize these trim components and thus the sound package design, which saves the time and cost caused by the later changes and provides a highly repeatable standard platform for design comparison and benchmarking.

Following sections also illustrates how to use the software AUTOSEA 2 for carpet design evaluation at the component and vehicle level for design concepts developed in the previous sections.

## 2   COMPONENT LEVEL (ALPHA CABIN) MODELLING

The random incidence absorption coefficient of automobile trims is preferably measured inside smaller versions of the Reverberation chambers, called Alpha Cabin. Normally it is approximately 1/3rd the size of a standard Reverberation chamber. A typical Alpha Cabin has a sample size area of 1.2 m$^2$, which is sufficient for testing vehicle trim parts individually.

As a part of the project, an Alpha Cabin has been designed for physical tests [67], and its CAD isometric view is shown below.
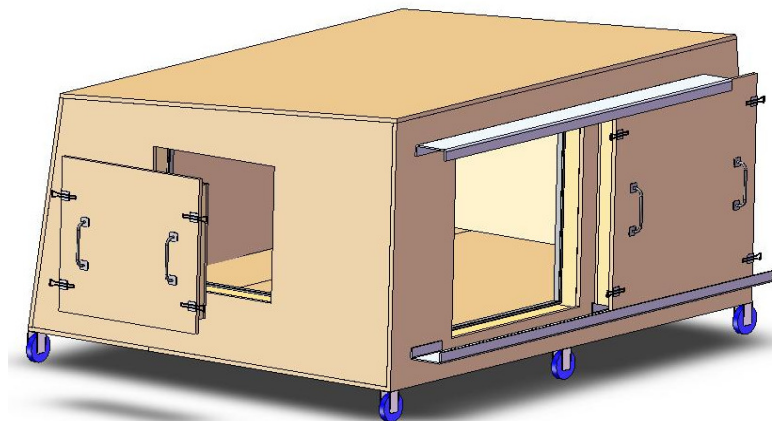


**Figure 7.1: Alpha Cabin CAD design drawing [67]**

The following are the peculiarities of the Alpha Cabin design, which are also considered while developing the SEA model.

- None of the cabin walls are parallel to each other, in order to avoid standing waves

- The cabin wall absorption is kept low by using sheet metal surface.

- The noise sources are small speakers, placed in different points, preferably corners, to generate a diffused sound field

A SEA model of the Alpha Cabin, having similar dimensions as the real Alpha Cabin design and the cabin walls made of sheet metals, is developed. The nodal points and structural components were first designed in CAD and then imported to AutoSEA acoustic software. This was opted, as AutoSEA geometrical modeling interface is not as efficient as CAD.
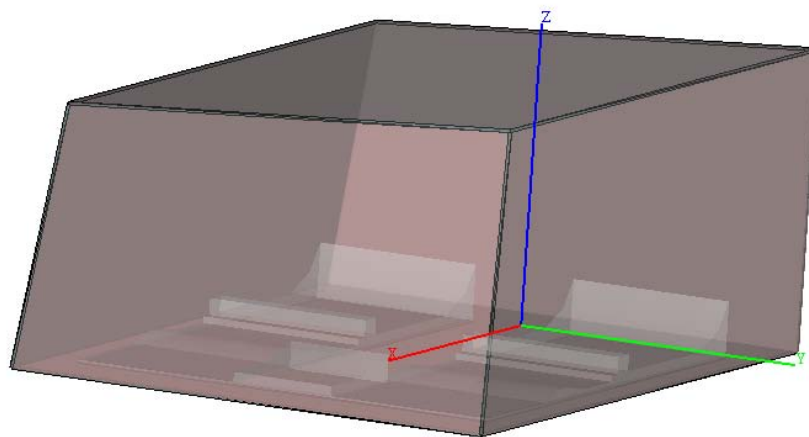


**Figure 7.2: SEA model of Alpha Cabin**

The Alpha Cabin is modeled in such a way that it encloses a single fluid (air) cavity inside, into which the carpet or sound package will be introduced. The below figure is the modeled Alpha Cabin, with the cabin walls made semi-transparent, for through visibility.

Further, a SEA model of the current production carpet, i.e. the Mitsubishi 380 carpet as shown below, is developed, having about 18 zones/sections in total. These are sheet metal sections, applied with Noise Control Treatment, are made such a way that they correspond to the sections on the real carpet, for which the section wise absorption coefficient and transmission loss were measured separately.

**Figure 7.3: Current production (M380) carpet**
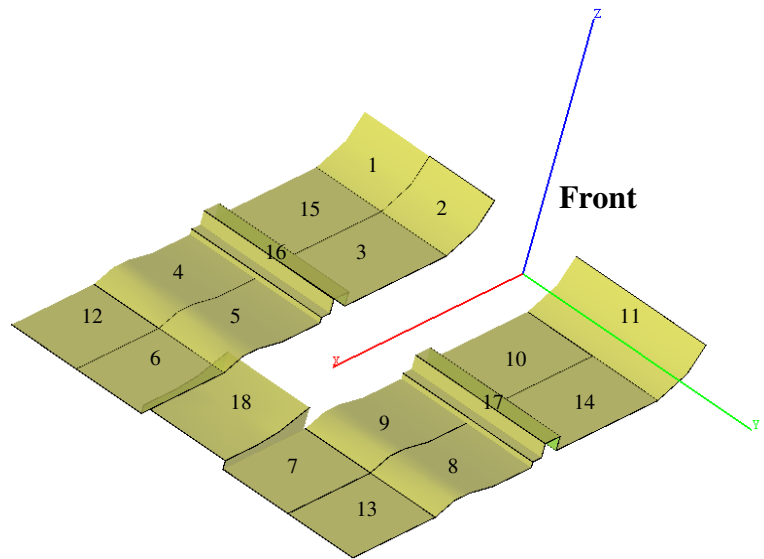


**Figure 7.4: Carpet model labelled into 18 sections**

## *2.1 Cavity modelling*

The modelling of the fluid (air) cavities properly plays a key role in getting the right SEA model of a system. Each cavity is a fluid subsystem, which connects with the other
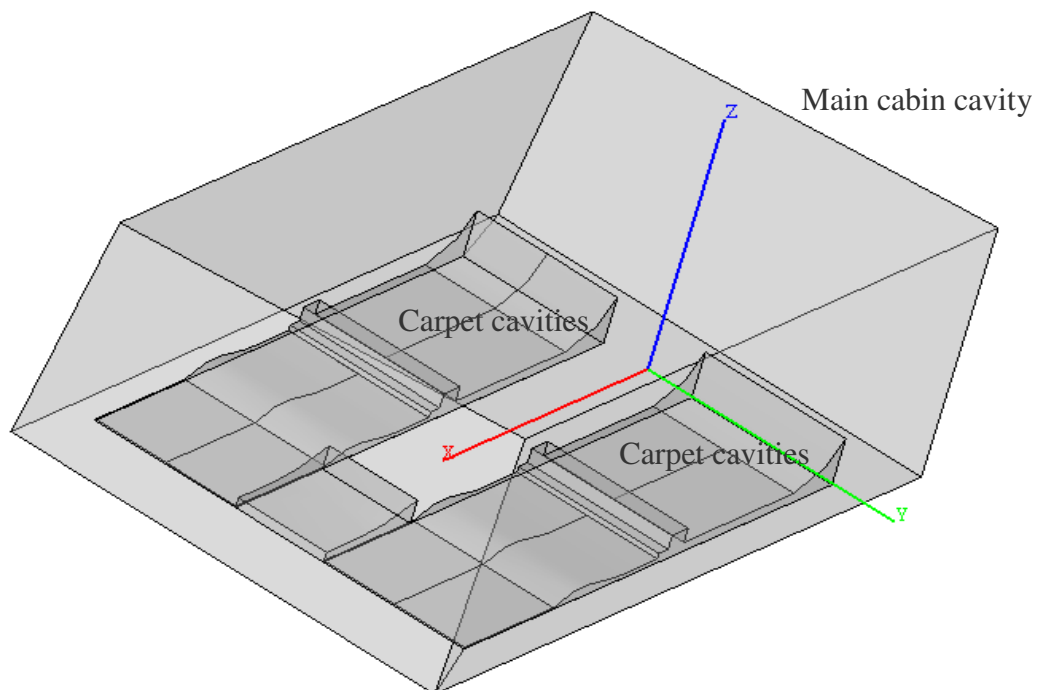


**Figure 7.5: Cavity sections in the SEA model of the Alpha Cabin**

subsystems through the area junctions of the cavity faces.

Similar to the single big cavity that the Alpha Cabin encloses, there are a few cavities that fill the bottom of the carpet structure. These form the connection between the main cabin cavity and the bottom wall of the cabin. These cavities are required, as the carpet bottom is not assumed to be flat, but curved as the real carpet. The grey semi-transparent sections are the cavities, as shown in Figure 7.5.

## 2.2  Noise sources

Similar to the physical Alpha Cabin, three noise sources of equal power (1V reference) are placed on three different faces of the cabin cavity walls. Compared to one noise source, three sources improve the diffused field of sound in the cabin. The absolute powers of the noise sources are not important as we are evaluating for comparative results only.

Figure 7.6 illustrates the noise source locations and gives an idea of the virtual Alpha Cabin test setup. The procedure involved further is to solve for the SEA parameters, which takes a minute or two, and then to select the main cabin cavity for plotting the sound pressure level results, under Engineering Units heading.
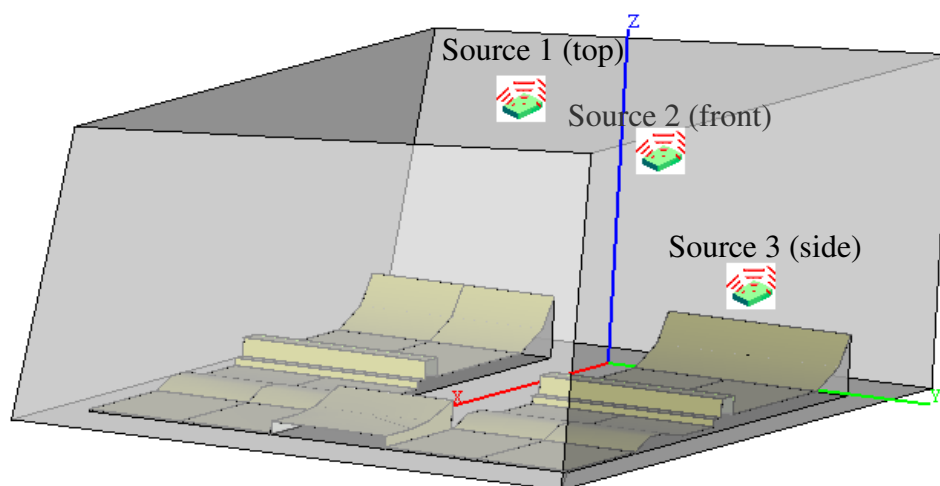


**Figure 7.6: Complete virtual Alpha Cabin SEA model, with noise sources and test carpet**

## *2.3  Virtual modelling test results*

Virtual Alpha Cabin tests were conducted for 4 different cases, which would aid a comparative study of the noise reduction by the carpet. The reference for the noise level in the comparative study is the case where there is no NCT (Noise Control Treatment) on the sheet metal sections of the carpet structure. This is equivalent to no sound package inside the cabin.

The current production carpet of Mitsubishi 380 is tested in two forms, one with the best absorption coefficient of all the sections (i.e. section 5) applied throughout the carpet
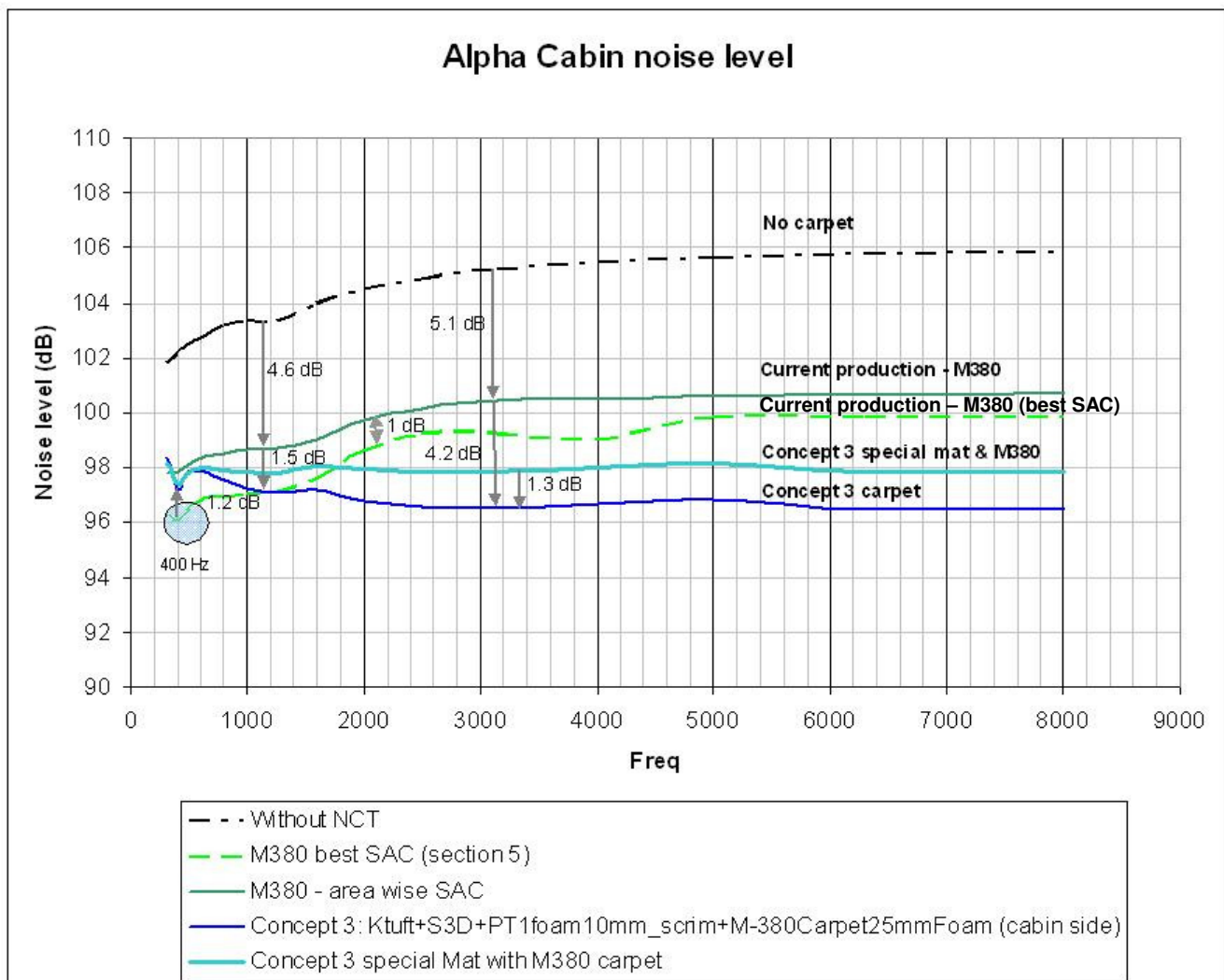


**Figure 7.7: Test results of the virtual Alpha Cabin**

and the second form where each section (1 to 18) is assigned a user defined NCT data, which are the impedance tube measured absorption coefficient and transmission loss values.

Acoustic parameters of the Concept 3 carpet material were measured using impedance tube and applied as a user defined NCT data for modelling and testing. It is to be noted that, since we are using the experimentally measured sound absorption and transmission loss data as user defined NCT data, the layered material level acoustic predictions are expected to match perfectly. The resulting plots are compared in the figure below.

## 2.4 Result discussion

The graph plot in the Figure 7.7 shows the sound pressure levels measured in the Alpha Cabin cavity for various carpet materials, which are compared with those without carpet/noise control treatment.

There are two current production (MITSUBISHI 380) carpet SPL results for comparison, the dark green curve is the actual current production carpet, with each section (1-18) having impedance tube measured absorption coefficient and TL values; meanwhile the light green curve represents the noise level when the best sound absorption coefficient of all the 1-18 sections, i.e. section 5 SAC coefficient, is used for all the other sections also. These two differ by only about 1.5dB in the low frequencies and about 1dB at higher frequencies.

The current production carpet seems to reduce the SPL in the cabin by 4-5 dB at both the low and high frequencies, in comparison with the cabin without the carpet. An SPL reduction of this range, i.e. greater than 3dB, will be reasonably an audible noise reduction for an average listener. At 400 Hz, highlighted by the grey circle, there is a SPL dip as expected, because the best sample of current production carpet (section 5) has a peak absorption coefficient at this same frequency.

It is shown by the curve in blue that the Concept 3 carpet consistently reduces further the SPL by about 4.2 dB above 2 KHz and reduces only 1.5 - 2 dB SPL below 2 KHz, in comparison with the section wise simulated current production carpet. At low frequencies, i.e. less than 1 kHz, the sound absorption performance of both current production and concept 3 carpets are in the similar range.

Meanwhile, for the Concept 3 special mats padded with current production MITSUBISHI 380 carpet, SPL curve is shown in Figure 7.7 as the bluish green line. The Concept 3 special mats reduce the noise levels by 3dB SPL above 2 kHz and by 1 dB SPL at 1 kHz.

Thus, the random incidence Alpha Cabin simulation tests indicate that concept 3 carpet design can reduce the noise level (SPL) inside a vehicle cabin by up to 4.2 dB at high frequencies ( above 2 kHz) and up to an average of 1 dB at low frequency range (below 1kHz), in comparison with the current production carpet.

# 3   VEHICLE LEVEL MODELLING

Virtual simulation and validation for acoustics is a developing field, and is well applied in building acoustics and component level design. Compared to these applications, vehicle acoustic prediction and design based on virtual validation demands highly accurate simulation software, as there are variety of acoustic package components and structural components, which interact in the acoustic field.

The AutoSEA modelling and acoustic simulation software is a well suited tool for the purpose. Based on Statistical Energy Analysis models for each component of the vehicle, AutoSEA generates a subsystem matrix of SEA parameters, which is solved for arriving at noise levels at a particular location in the vehicle. The frequency range of SEA based acoustic simulation is 500Hz-20kHz, as the modal density of air-borne sound is less below 500Hz, and hence can give less accurate results for lower frequencies. But this frequency range (500Hz-20kHz) is sufficient for air-borne acoustic simulations of vehicles. AutoSEA acoustic simulation is becoming a standard acoustic simulation tool of vehicle designers.

The vehicle model used for simulation is a generic sedan model, which would be the preferred popular vehicle model. Geometric details of the car model can be directly imported from CAD or CATIA model of a car. AutoSEA has provided with the Template Modeller module, which is a powerful tool to morph the generic SEA model to the required imported car geometry. So, for simulating the acoustics of sound packages like floor trim, seats etc, which are not vehicle specific, it is preferred to do simulation on a generic SEA model.

This document will try to outline the key sections of the modelling process and will keep aside SEA software specific details. A brief explanation about each vehicle model section is given below.

## 3.1  Engine compartment

Figure 7.8 will help to give a picture about the engine compartment model of the vehicle. For clarity, the vehicle sections, other than the engine compartment, have been replaced by a semi-transparent grey section.
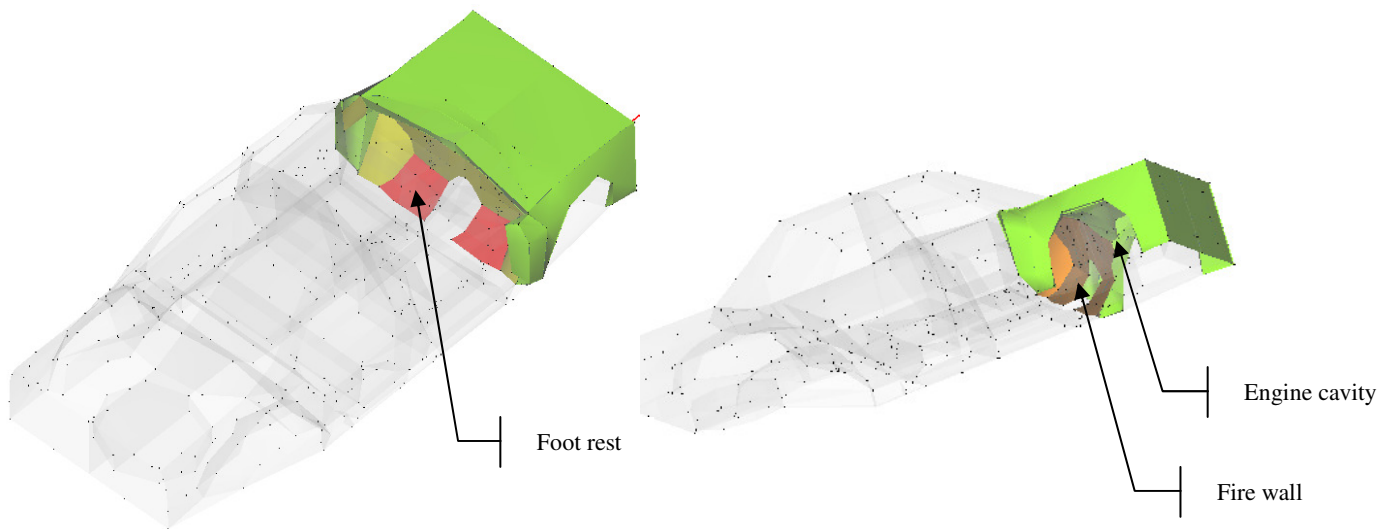
**Figure 7.8: SEA model of engine compartment**

This vehicle SEA model is for air-borne acoustic simulation, and hence a noise source in the location of the engine cavity is sufficient to run the virtual validation of engine noise. The engine compartment has followed a box structure in general, as the actual shape doesn't make a significant difference in the generated acoustic field, other than its directivity.

The firewall, in orange shade, is made up of a curved multi plate structure, which matches a normal car fire wall structure. The firewall is applied with specific noise control treatment, which is explained below. Meanwhile, the red shaded section forms the foot rest area for the front passengers, and is normally covered with the carpet section.

## *3.2  Passenger cabin*

The passenger cabin model includes almost all the components, i.e. the front and back seats, control dash, chassis, roof, doors with loud speaker vents, floor carpet, pillars, glass windows (not shown) etc, which are found in a usual sedan car, except for specific details like the steering wheel, air conditioning vents, mirrors etc, which are not important in an acoustic point of view.

The acoustic modelling has been done inside the passenger cabin, especially the driver side, and so compared to the engine and vehicle rear compartments, the passenger cabin is expected to be closer in detail to the real car cabin. A transfer function analysis is conducted as a part of the validation process for the vehicle model, where the measured

acoustic path transfer functions from the engine and tyre locations to the driver ear are compared with the simulated ones from the SEA model. The results are provided in the following sections.
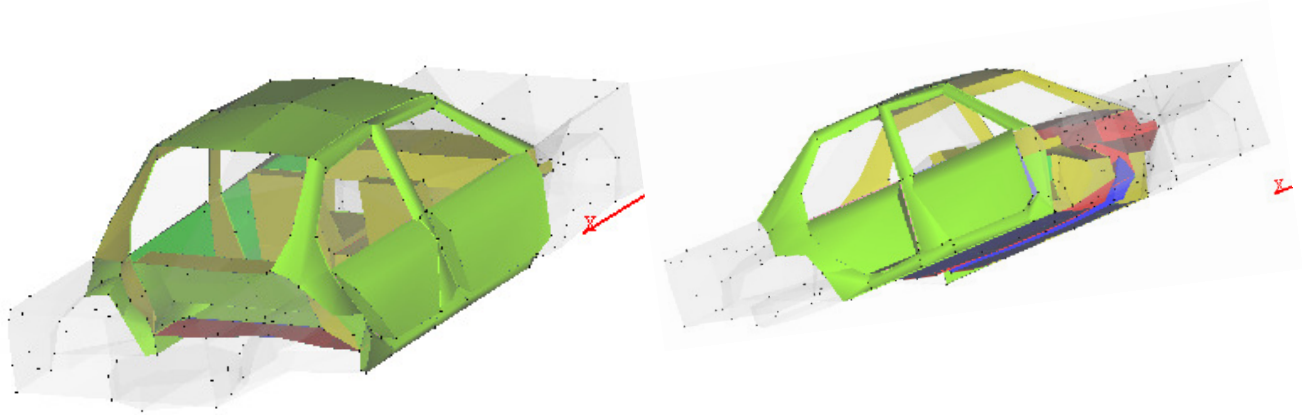


**Figure 7.9: Passenger cabin simulation SEA model**

## 3.3 Vehicle rear compartment

Similar to the engine compartment, the rear compartment is a simple box shaped structure, which includes the trunk, the spare tyre cabin and the wheel arches. The red coloured section is the section beneath the back seats, which will be covered with the floor carpet.
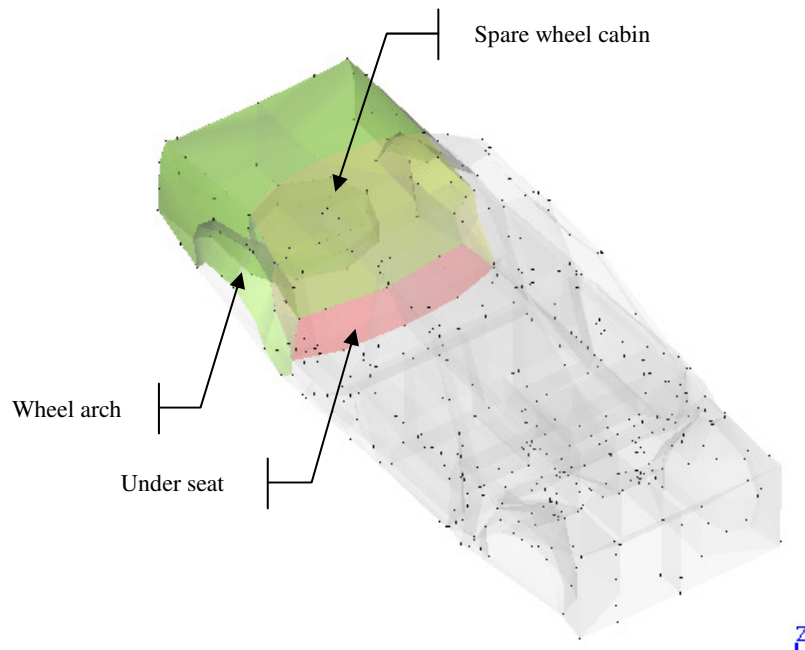


**Figure 7.10: Rear compartment of vehicle SEA model**

The complete vehicle SEA model is illustrated in Figure 7.11, one model with opaque surfaces and the other with semi-transparent surfaces. It is difficult to give a detailed picture of the full model, as it includes a lot of components or sub-systems. A basic statistics of the components involved is given in Table 1.

**Table 1: Statistic of vehicle SEA model**

| Statistics of vehicle SEA model | |
|---|---|
| Nodes | 802 |
| Materials | 91 |
| Physical Properties | 46 |
| Noise Control Treatments | 83 |
| Sound Packages | 11 |
| Groups | 14 |
| Subsystems | 468 |
| Junctions | 1619 |
| Loads & Constraints | 5 |
| Load Cases | 0 |
| Spectra | 100 |
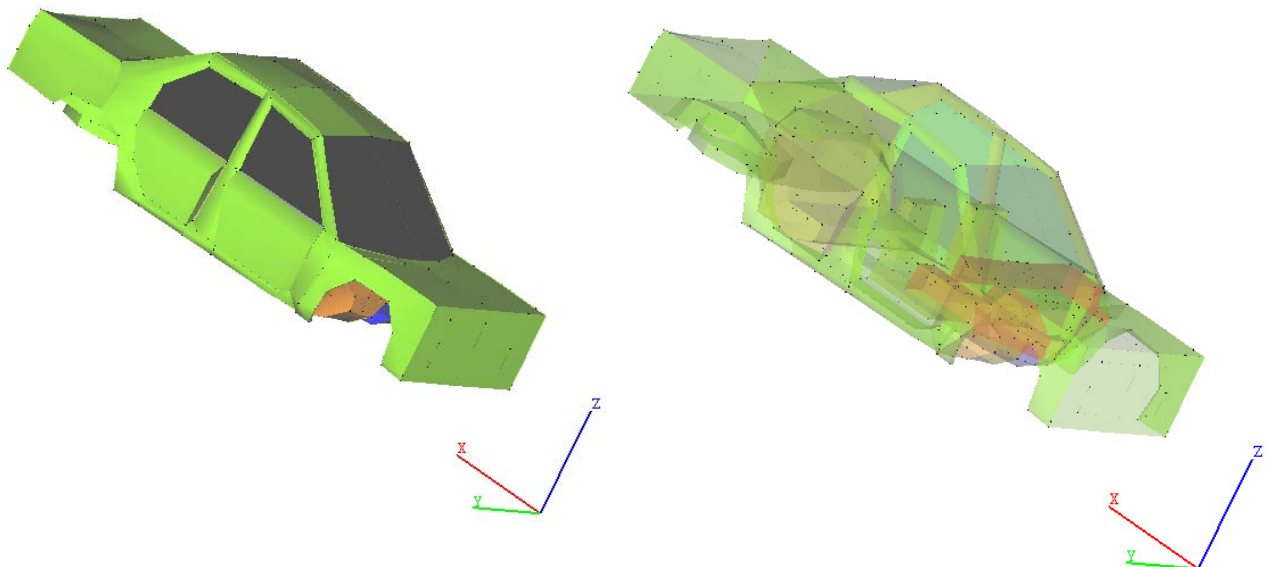


**Figure 7.11: Complete vehicle, sedan car, SEA virtual model**

## 3.4  Acoustic cavity modelling

The acoustic cavity modelling is a key to the accuracy of the SEA modelling process, as air-borne transmission paths between sub-systems depend on how well placed and connected are the acoustic cavities and the vehicle body components.

The vehicle cavities can be separated into interior and exterior cavities, for convenience, as explained below.

### 3.4.1  Vehicle interior cavities

As shown in Figure 7.12, the vehicle interior cavities are expected to fill up all the empty spaces between the vehicle components and make the air-borne connection between the SEA sub-systems. The cavities are modelled by specifying the closed nodes surface which encloses the cavity.
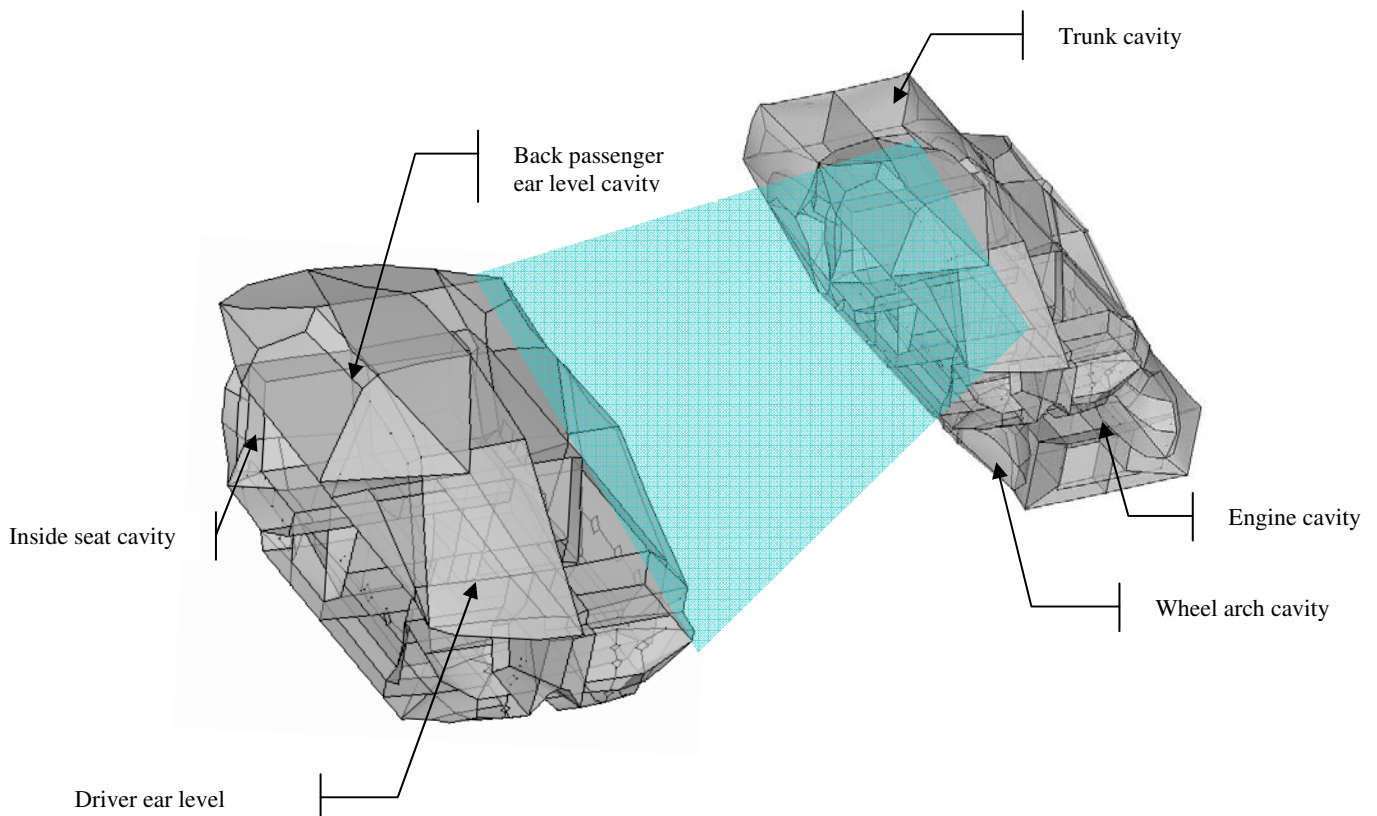


**Figure 7.12: Vehicle interior acoustic cavities**

The cabin cavity has been divided into totally 8 zones, i.e. there are upper and lower cavities for each of the four passenger spaces. The number of cavities can be increased for more accuracy, but in our evaluation process this number is sufficient for measuring average SPL levels at the driver's ear.

## 3.4.2 Exterior cavities

Engine and tyre noise that escapes into the air or space surrounding the vehicle can enter into the vehicle cabin by various acoustic phenomena like diffraction or by indirect coupling of the vehicle component with the cavity of interest. So the vehicle is made surrounded by cavities similar to the vehicle interior cavities, as shown in Figure 7.13. Each exterior cavity is connected directly to the external surface of the vehicle body
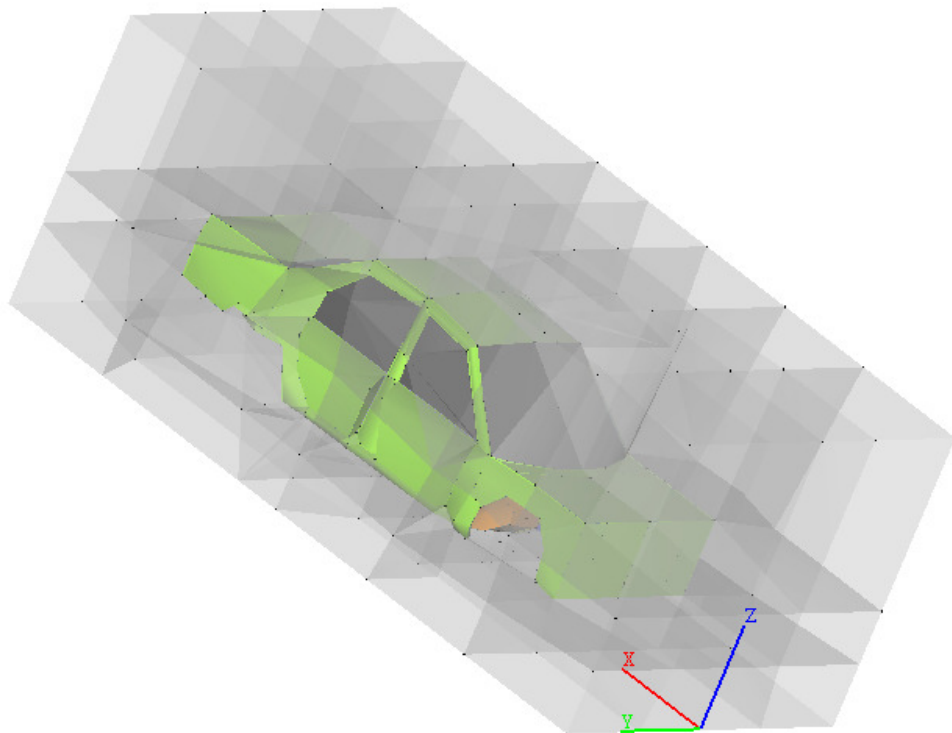


**Figure 7.13: Vehicle exterior acoustic cavities**

## *3.5  Sound Packages*

The vehicle sound package of interest is a collection of the passenger cabin interior trim components. Each section is treated using different material combination for noise reduction, and hence has different sound absorption and sound transmission loss coefficients. The interior vehicle sound package can be divided into 8 sets, for ease of modelling, as follows.

1. **Vehicle floor carpet** – This covers the complete vehicle floor, below the seats and a portion of the fire wall as foot rest area, and normally acts as a sound barrier.

2. **Headliner** – This covers the vehicle roof area and is normally absorptive.

3. **Passenger seats** – These are expected to be the most absorptive of all.

4. **Trunk cover –** This normally has a similar absorption as the floor trim.

5. **Pillars –** They are usually treated with plastics or similar synthetic material.

6. **Control board –** This area is mostly made of plastics or leather sections.

7. **Doors –** The doors are normally made in a double panel structure, with a leather or synthetic leather skin, of low absorption.

8. **Firewall –** This is a more barrier like treatment, than an absorptive layer, which separates the passenger from the engine compartment.

Refer the figures in the following two pages, to get a figurative idea of the sound package sections and the measured sound absorption coefficient curves used for the inputs of each section.
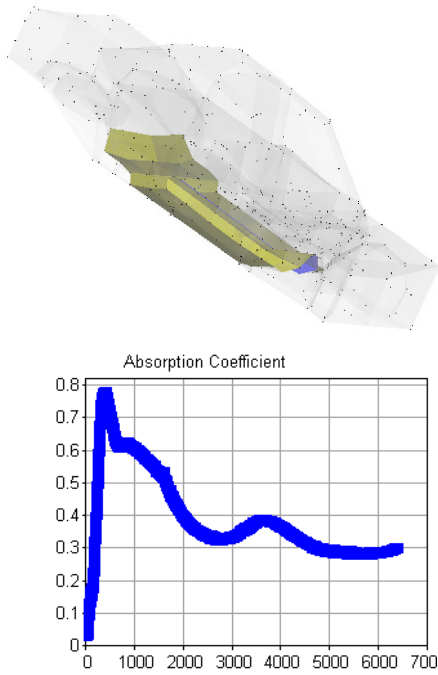
**Figure 7.14: Carpet section of sound package**
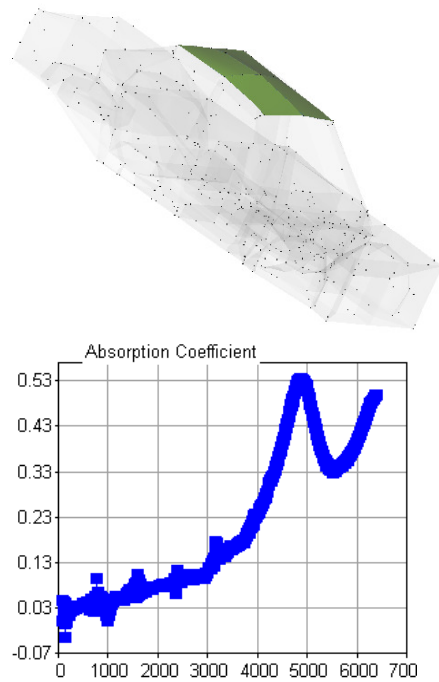


**Figure 7.15: Headliner section of sound package**
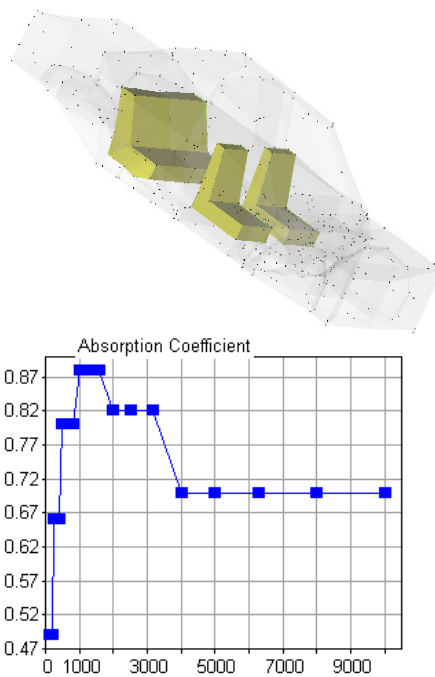




**Figure 7.16: Seats section of sound package Figure 7.17: Trunk cover section of sound package**
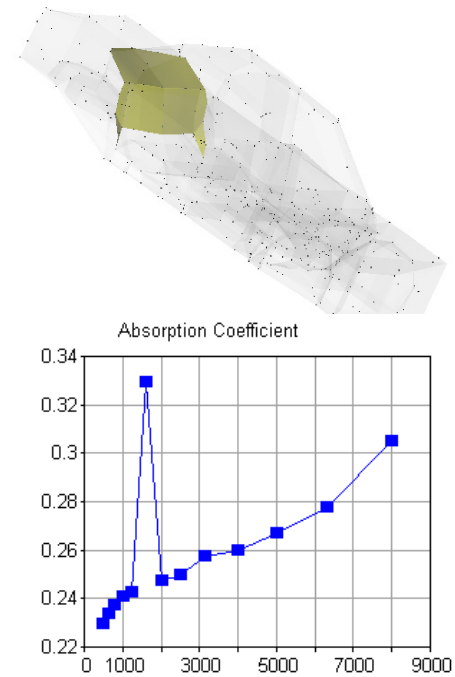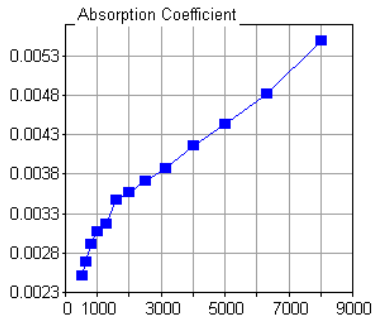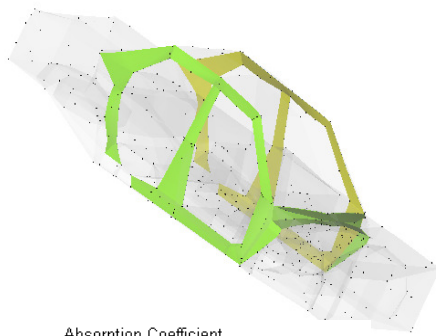
**Figure 7.18: Pillars section of sound package**
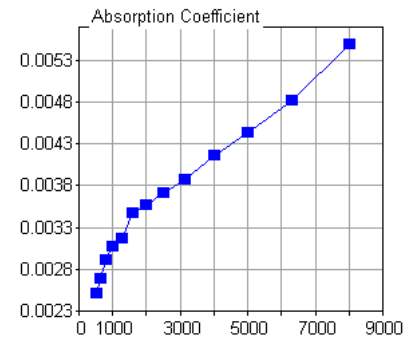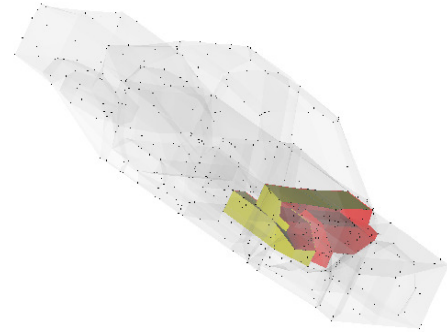


**Figure 7.19: Control dash board section of sound package**
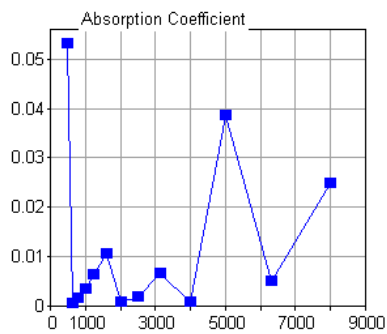


**Figure 7.20: Doors section of sound package**
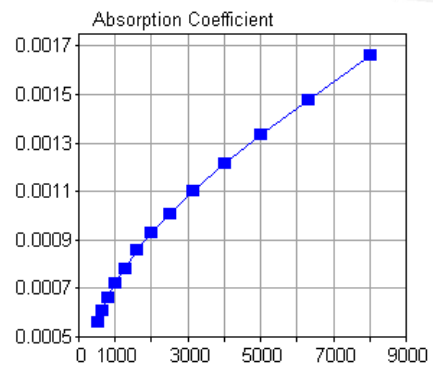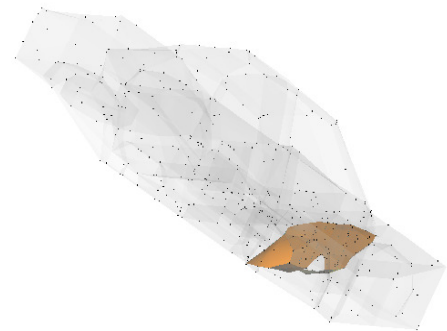


**Figure 7.21: Fire wall section of sound package**

It is notable that the last 4 sound package sections are having almost zero absorption coefficients, as these sections are normally covered with plastics or leather like synthetic skins.

## 3.6  Noise sources

Vehicle noise sources consist of mainly power train (engine) noise, tyre/road noise, wind noise, external traffic noise, vehicle exhaust noise and wiper noise. Out of these, we are interested in the primary noises only, i.e. engine noise and tyre noise.

Figure 7.22 and 7.23 illustrate the engine and tyre noise source locations in the vehicle simulation model. Since we are conducting comparative analysis and transfer function model validation, instead of the actual noise source spectrum, the diffused field noise sources are assigned to be white noise of 1V reference power.
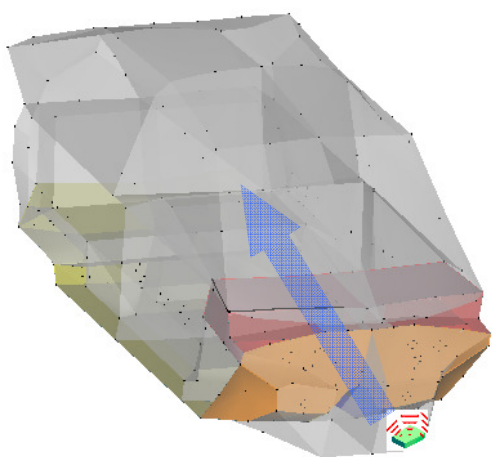


**Figure 7.22: Power train (engine) noise source**
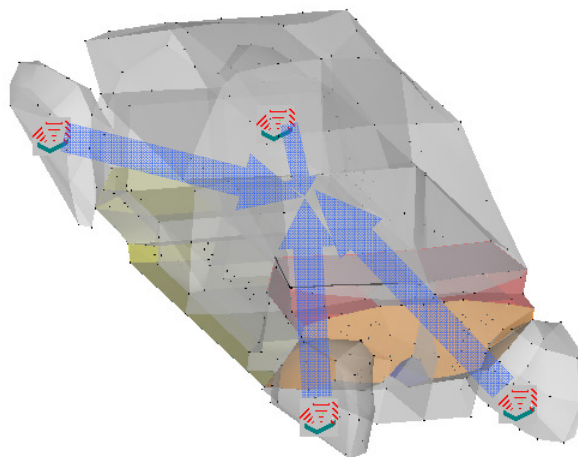
**Figure 7.23: Tyre noise sources**

## 3.7  SEA model validation using transfer function method

Virtual model validation is an important stage in the modelling process and there are various techniques used for the same purpose. Transfer function method is a method used in acoustics to find the spectral ratio of the source to receiver noise path. Once the transfer function of a noise path is known, it can be applied to predict the noise spectrum at the receiver for any other noise source type at the same source position. The transfer function is normally an array of complex numbers, having both magnitude and phase, but here we are

interested only in the magnitude ratio and represented in dB, where the reference is the noise power at the source location.



**Figure 7.24: Transfer function test setup**
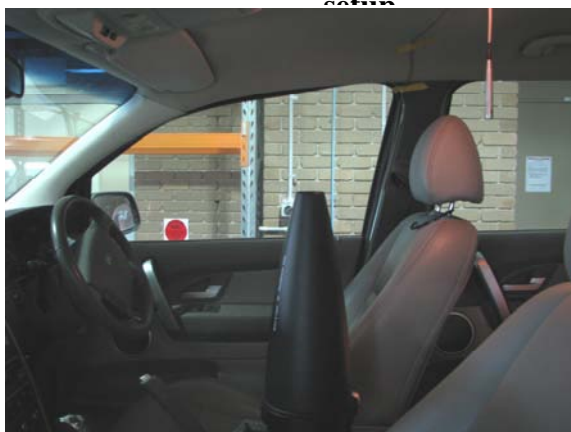


**Figure 7.25: Omni directional loudspeaker at the driver's ear**



**Figure 7.26: Microphone at wheel arch**

In the test setup, since linear acoustic systems obey the reciprocity of source and listener position, the Omni directional loudspeaker source (by Bruel & Kjaer) is placed at the driver ear position, as shown in Figure 7.25. This also helps to avoid moving around the loudspeaker across various parts of the vehicle. The microphones were placed at the engine bay and four wheel arches, for measuring the noise level at those locations, as shown. A microphone was also placed at the driver's ear position to record the reference SPL at the source location.

Measurements were done using both sine sweep and pink noise sources, as sine sweep helps to improve the signal to noise ratio and pink noise helps to keep the power focused in the low frequency range of interest.

The resulting ratio of the noise spectra, at the engine bay and four wheel arches, over the noise spectra at the source location of the driver's ear, are calculated and compared with the virtual SEA model results, as shown in the Figures 27 and 28.
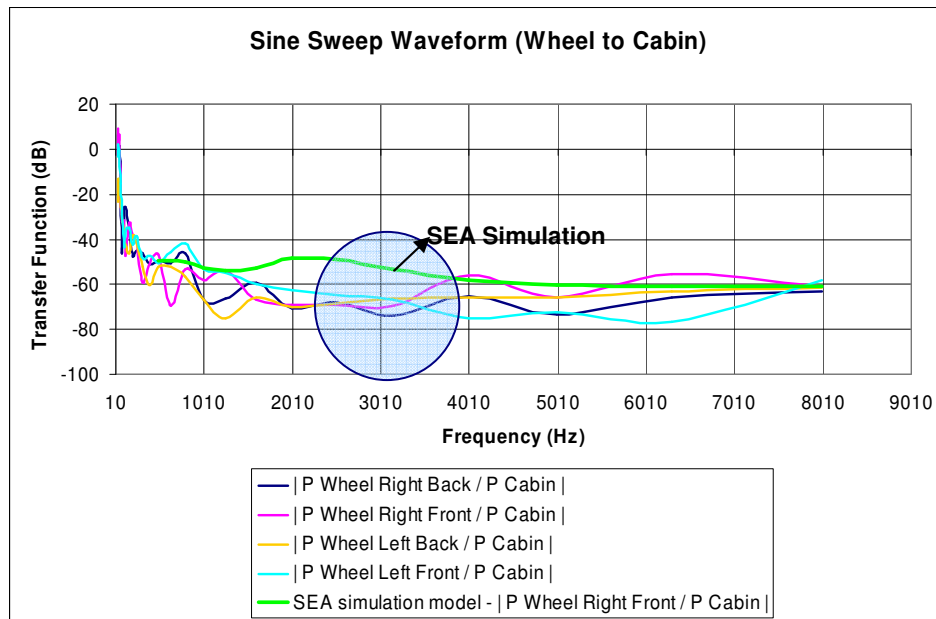


**Figure 7.27: Wheel arch to driver's ear, transfer function**
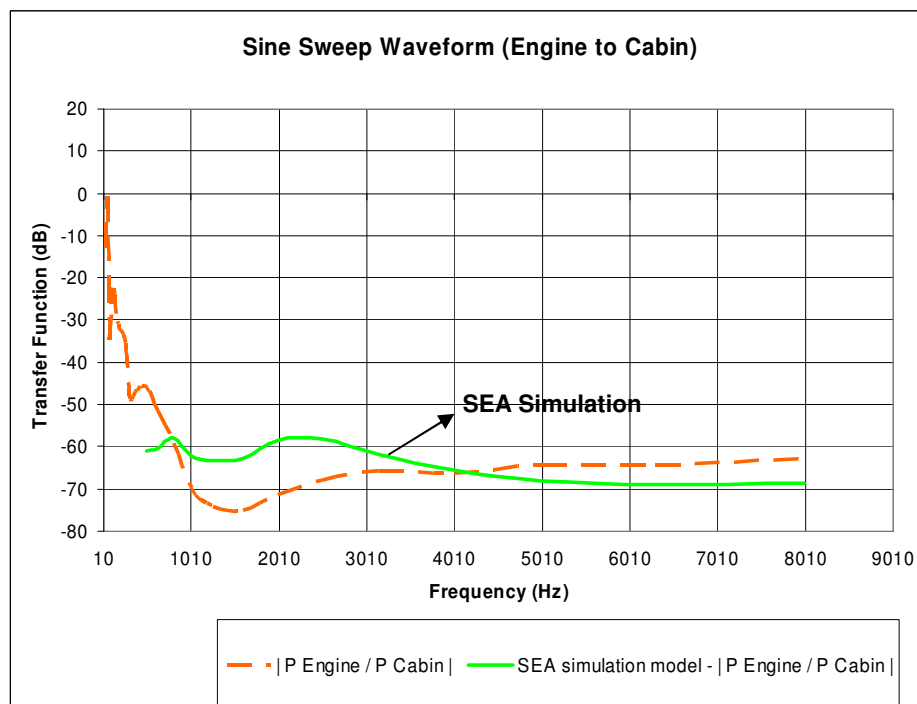


**Figure 7.28: Engine to the driver's ear transfer function**

The transfer function results for both the engine to the ear and the wheel arch to the ear show a good level of match between the real experimental tests on the vehicle and the simulation. As shown by the light blue shaded area in Figure 7.27, there seems to be a deviation for the simulation of right front wheel arch to the driver's ear transfer function at about 2 - 3 kHz range. This could be because of the coincidence frequencies of the sheet metal panels used in simulating the vehicle. Averaging out the transfer function results for all the 4 wheel arches to driver ear simulation is expected to reduce this deviation from the actual measured transfer function for tyre/road noise.

## 3.8  Evaluation of carpets using Vehicle SEA modelling

Once the vehicle model is validated to show matching results with the real car test results, we are at a good position to run evaluation tests for the various carpet designs and to see the effects of introducing each carpet. Since we are interested in a comparative study of the carpet contribution in noise reduction, we start with noise level without the carpet as the reference noise level, against which other carpets are compared with. This is shown in Figure 7.29 as a black dot-dashed line, which shows the highest dB noise level.

The ideal carpet is the one when floor noise control treatment having 100% sound absorption at in-cabin side and having infinite (450dB) transmission loss. The SPL results of this carpet help to know the maximum possible noise reduction potential offered by the floor trims.
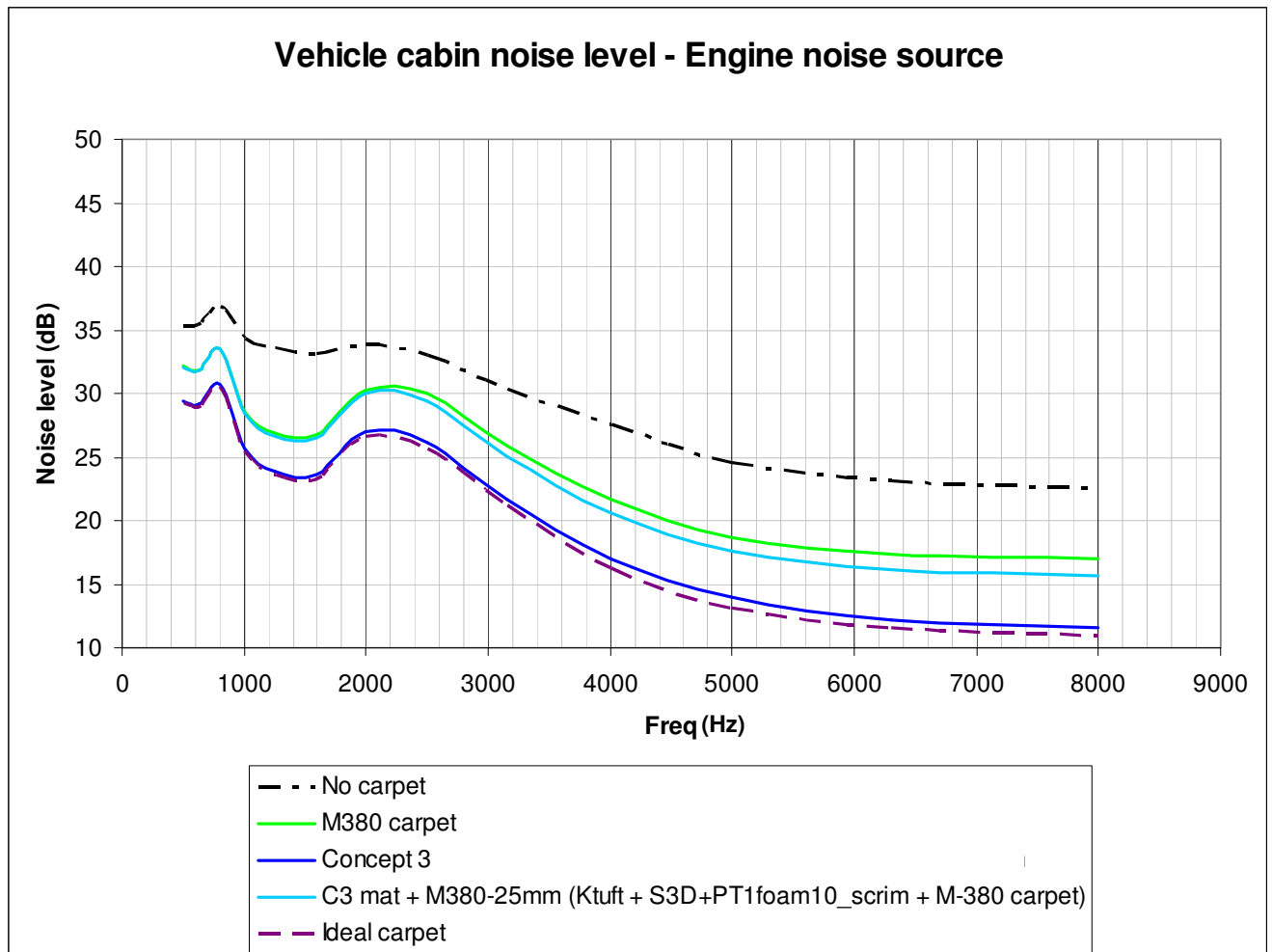
**Figure 7.29: Noise spectrum at the driver's ear, for engine noise source**

Referring to Figure 7.29 for engine noise reduction by carpets, it is clear that the Concept 3 design reduces the noise level by about 3-5 dB compared to the current production MITSUBISHI 380 carpet design. It is worth noting that the Concept 3 results are very close to the ideal carpet results. The Concept 3 mat with current production carpet seems to give only about 1dB of improvement at high frequencies, compared to the carpet only.
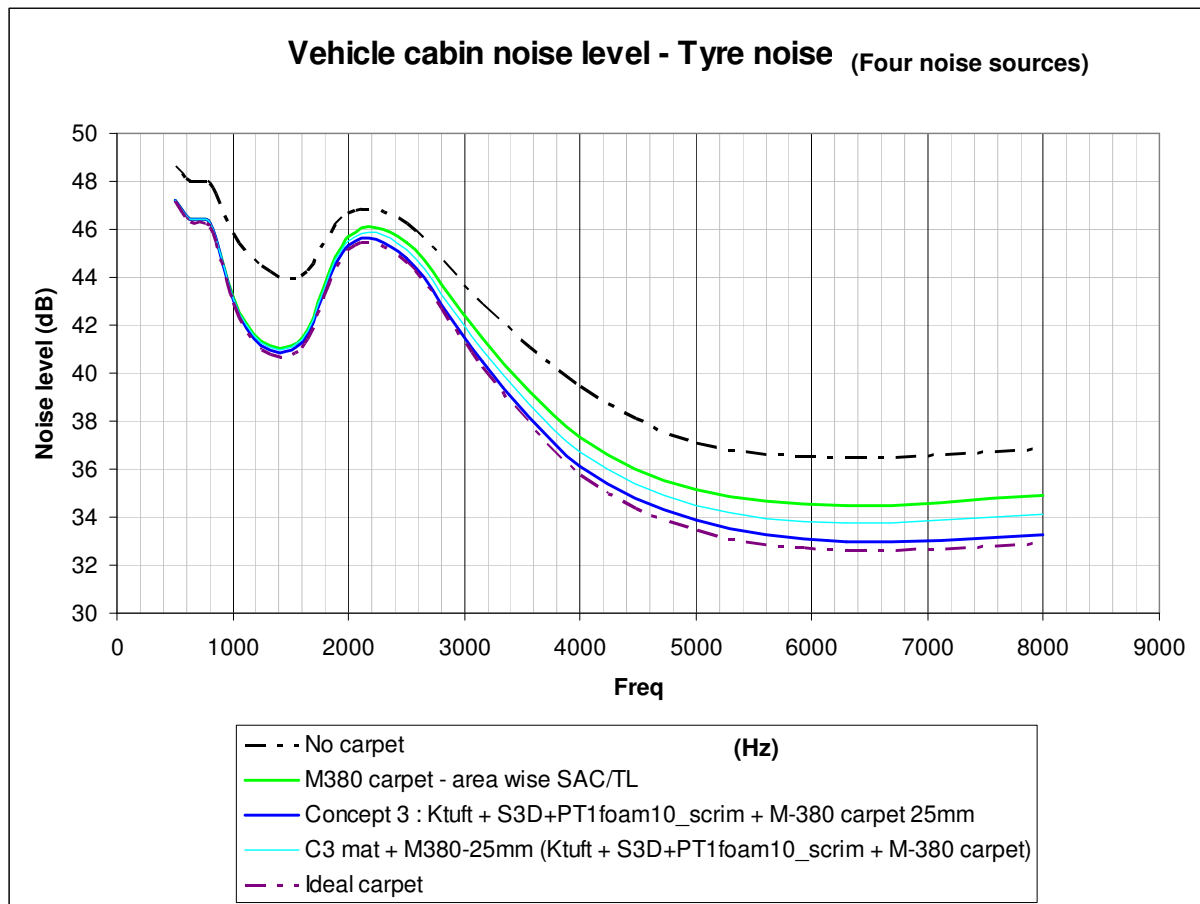
**Figure 7.30: Noise spectrum at the driver's ear, for tyre noise**

Figure 7.30 shows the tyre noise results for various carpets. The noise reduction improvement from carpets is not significant, and the difference in the driver's ear SPL for the no carpet case and the ideal carpet is just 2-4dB.

So these virtual vehicle model tests indicate that floor trim can reduce the sound pressure level inside the vehicle cabin caused by engine or power train noise, but not much caused by tyre noise.

### 3.8.1 Thermo grams of engine and tyre noise paths

Figure 7.31 shows the thermo gram of the air-borne noise paths/levels for 500Hz, 1kHz and 2 kHz frequencies. The colour contour extends from red (high-94dB) to blue (low-10dB) SPL noise levels. A close analysis can help in identifying noise zones, silent zones and key transmission paths.

**Engine noise @ 500Hz**        **Engine noise @ 1kHz**        **Engine noise @ 2kHz**

**Tyre noise @ 500Hz**          **Tyre noise @ 2 kHz**          **Tyre noise @ 1 kHz**
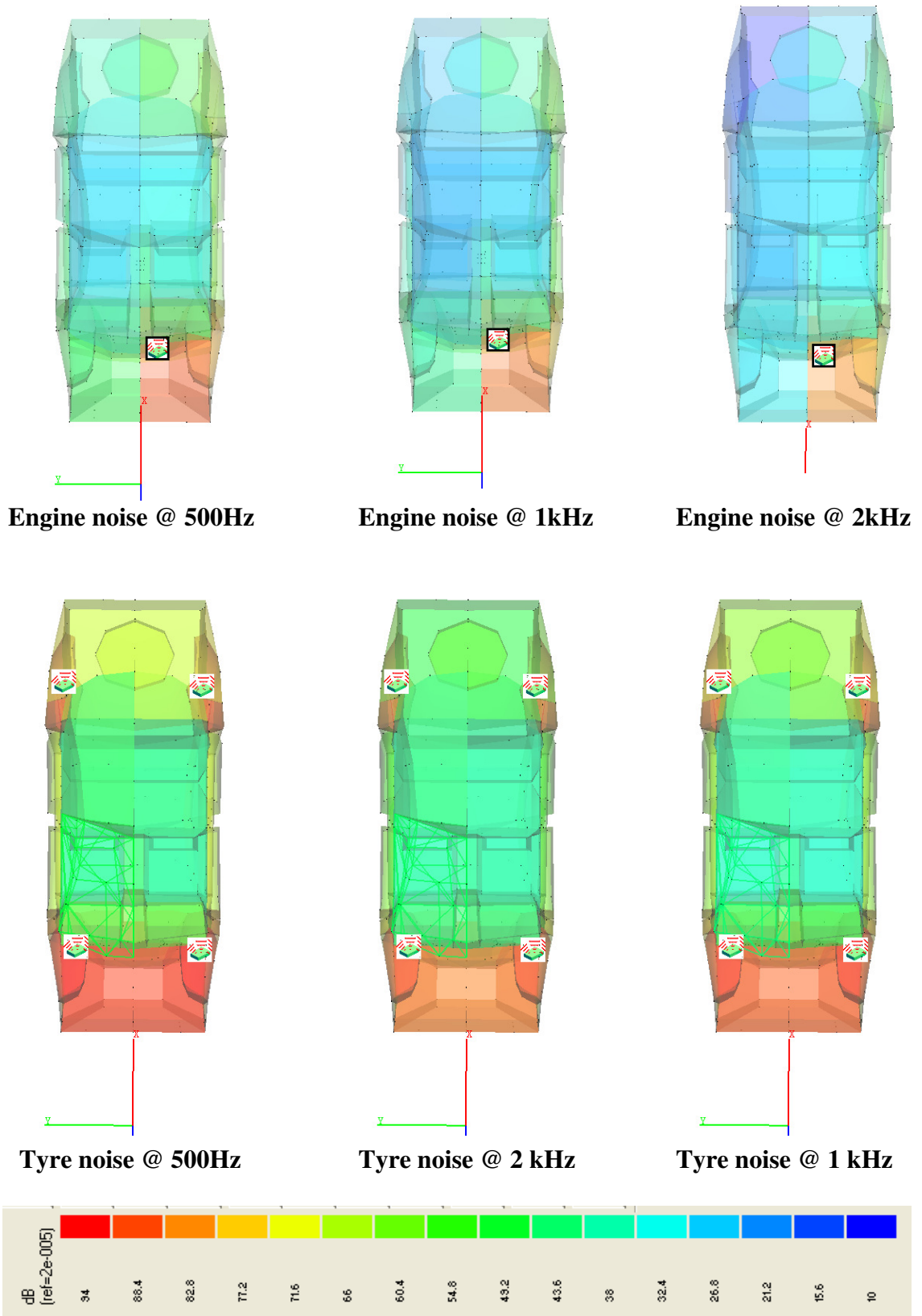
**Figure 7.31: Thermogram for engine and tyre noise, at various frequencies**

# 4  CONCLUSIONS

*Alpha Cabin evaluation*

- In comparison with the current production carpet (MITSUBISHI 380 carpet), Concept 3 carpet consistently reduces about 4.2 dB SPL above 2kHz and reduces up to average of 1 dB below 1 kHz.

- Concept 3 special mats reduce the noise level by 3 dB above 2 kHz and up to an average of 1 dB below 1kHz, in comparison with the current production carpet (MITSUBISHI 380 carpet).

*Vehicle level modelling and carpet evaluation*

- The vehicle virtual SEA model was evaluated/validated using transfer function method and well matching results were achieved for engine and tyre noises, except for the coincidence frequency ranges of the backing sheet metal floor.

- Concept 3 carpet evaluation at the vehicle level shows the reduction of the in-cabin noise level further by up to 3-5 dB, compared to the current production MITSUBISHI 380 carpet design, for power train noise.

- The Concept 3 carpet evaluation at the vehicle level shows the reduction of the in-cabin noise level further by 2 dB at high frequencies, compared to the current production MITSUBISHI 380 carpet design, for the tyre-road noise.

- The Concept 3 mat padded with the current production carpet (MITSUBISHI 380) reduces noise level by about 1dB SPL at high frequencies, compared with the carpet only case for the power train and tyre-road noise.

The concept 3 carpet SPL results are very close to the ideal carpet SPL results, which mean that the concept 3 carpet has nearly reached the noise reduction limit.

# CHAPTER 8

# PROTO-TYPE VALIDATION AND EVALUATION OF DESIGN CONCEPT

## 1   INTRODUCTION

The design concepts proposed for the acoustically improved vehicle carpet system has been proto-type built factory moulded carpet samples, following the standard manufacturing procedures, and validated by the test results of both the laboratory made samples and the proto-type samples. This is required to verify the manufacturing process related factors that can alter or degrade the acoustic performance.

In addition to verifying manufacturing process effects, it is required to test the moulded carpet system in a real life test environment, and compare the psycho-acoustical measurement results with the benchmark carpets. In case the complete carpet could not be moulded following the standard manufacturing process, it is proposed to build proto-type special mats, having the required additional top layers only, which can be placed on top of existing carpet, to form a carpet system similar to the proposed concept design.

Two construction methods were undertaken to produce samples for the C3-Special mat, designated as C3-Special_mat_Lab-made and C3-Mat_Prototype, respectively. The physical testing program consisted of material acoustic property and in-situ vehicle tests. The former was designed to evaluate the acoustic effectiveness of the prototypes through the measurement of the sound absorption coefficient (SAC), whilst the latter aims to provide direct comparison of noise reduction performance among various mat types fitted to the vehicle floor carpet.

## 2  TEST SAMPLES

Based on practical considerations, the development and construction of the C3-Special mat was pursued because of limitations in the production of a full C3 type vehicle floor carpet. Concept 3 (C3) carpet design is explained in previous chapters. The prototype mat (C3-Mat_Prototype), having similar material specifications as the proposed C3 carpet, was intended to also demonstrate improved acoustic performance over other contemporary/standard mat products.

Specimens were cut to size per requirement of the testing procedure. For the impedance tube, a 29mm and 100mm diameter samples were needed. The alpha cabin test require a 1x1m sample and the vehicle test demands that specimens be cut to the size and shape of conventional car mats.

### 2.1  Standard Mat (reference)

Physical characteristics of the standard mat are summarized in Table 1. Standard mat specimens were provided as reference to compare the acoustic performance of the new design concepts. These were cut to size to conform to the requirements of the testing regimes outlined in the following section.

### 2.2  Prototype Mat (Concept 3 design)

The proof of concept for an acoustically improved carpet is embodied on the proposed C3-Special mat. The C3-Mat_Prototype is a simplified version of the Carpet Design Concept 3 floor carpet, i.e. without the thin heavy layer and de-coupler. In addition, absorber layer thickness was reduced (e.g. 7mm) to conform to conventional mat overall thickness of 15mm.

The development of the C3-Mat_Prototype follows the material and construction specification previously described in the concept design explained in previous chapters. The following two versions of the product concept were realized and were subjected to the testing protocols.

### 2.2.1 C3-Special_mat_Lab-made

The C3-Special_mat_Lab-made specimen was constructed under laboratory conditions. The material specifications and order of layered construction (see C1-07 RMIT M06_addendum report) was followed but the components were bonded by glue instead of

thermal lamination. The 3M spray adhesive was used for this purpose. Due to practical considerations, only specimens for use in the impedance tube tests were made and tested. Description of the C3-Special_mat_Lab-made is given in Table 1.

### 2.2.2 C3-Mat_Prototype

The C3-Mat_Prototype specimen was constructed by employing the expertise of professional laminator recommended by *Futuris*. Material components and construction details were followed from the C1-07 RMIT M06Addendum report recommendations. Various material components were either sourced locally or provided by *Futuris*.

A technical problem encountered during the lamination process was that when the AFR layer (Air Flow Resistance layer; material P830N is a high performance mouldable acoustic material sourced from a third party supplier in Melbourne) was heated, it does not develop a "gummy" consistency to facilitate bonding with the other layers (namely the tufting and the absorber layer, i.e. 7mm thick open cell foam with scrim on top (labelled PT1withScrim); sourced from a supplier in Melbourne). Nevertheless a C3-Mat_Prototype Model 1 was successfully laminated with the use of polyethylene (PE) dusting. The second attempt using only thermal bonding was not successful hence the only usable specimen was designated as C3-Mat_Prototype. Relevant physical properties are listed in Table 1.

## 2.3  Constraints and Limitations

Discrepancies in the material properties between the proposed and actual materials used in the construction of the prototype mat were noted. Shrinkage to the final product due to heat treatment during the lamination was also observed. The specified overall thickness of the C3-Mat_Prototype was 15mm but due to shrinkage during lamination the specimen thickness was measured at 11.94 mm (see Table1).

The thin layer of PE as backing for the tufting and the use of slight PE dusting during the lamination process for the C3-Mat_Prototype is duly noted. The presence of added PE may degrade the performance of the AFR resulting to reduced sound absorption potential.

### 2.3.1  Tufting

The K type tufting without backing was originally proposed for the mat prototype. However, the tufting provided by *Futuris* for the construction of the C3-Mat_Prototype had a shorter pile length (see Table 1) and had a thin layer of PE as backing. Due to time

constraints, it was decided to use this tufting material for the construction of the C3-Mat_Prototype. The C3-Special_mat_Lab-made specimen used the K tufting (with the longer pile length) without backing.

## 2.3.2 Lamination

Since thermal bonding/lamination trials failed, the use of polyethylene (PE) powder to facilitate the lamination of C3-Mat_Prototype was resorted to. A second attempt to construct the mat prototype by thermal lamination was not successful. The use of scrim/web could be a future alternative to help the lamination and was suggested by the laminator and the supplier of the AFR material.

**Table 1 -  Sample Specimen Properties**

## Mat Specimen Properties

| Sample | Particulars | Average gsm | Thickness | Pile Length |
|--------|-------------|-------------|-----------|-------------|
|  |  | (g/m$^2$) | (mm) | (mm) |
| Standard Mats | Production Carpet Mats | 2997.28 | 8.71 | 4.5 |
| C3-Special_mat_Lab-made | K-Tufting plus AFR layer plus open cell foam (label:PT1) with scrim, bonded by spray adhesive |  | 15.00 | 5.1 |
| C3-Mat_Prototype (Model 1) | Tufting plus AFR layer plus open cell foam (label:PT1) with Scrim, laminated with PE dusting | 2218.07 | 11.94 | 2.4 |
| C3-Mat_Prototype (Model 2) | Tufting plus AFR plus open cell foam (label:PT1) with scrim, thermally bonded | ****   Final product "unusable" | | |

## 3   PROTOTYPE TESTING

The testing protocols employed were designed to directly compare the acoustic performance of the prototype mat with that of the standard mat. The testing regimes consisted of material property tests and performance testing inside a vehicle cabin.

The metric of primary concern is the sound absorption coefficient (SAC). This metric is decidedly more important than transmission loss (TL) when evaluating the relative performance of the mats, as variable in the tests was the top layer which is the absorptive side. In addition, it was expected that the floor carpet of the Mitsubishi 380 (supplied by *Futuris*) had been optimised for good TL performance.

## *3.1  Material Acoustic Property Testing*

### 3.1.1  Impedance Tube Test

Normal incidence sound absorption coefficients (SAC) were measured using the B&K impedance tube (PULSE™ Acoustic Material Testing in a Tube Type 7758).

The mat specimen samples were subjected to impedance tube testing namely: C3-Special_mat_Lab-made, C3-Mat_Prototype and the standard mat. The impedance tube set-up is shown in Figure 8.1. For more details about the test setup, please refer to the B&K manual and Chapter 5.



**Figure 8.1: Impedance tube setup**

### 3.1.2  RMIT Alpha Cabin Test

The newly built RMIT Alpha Cabin testing chamber [67], shown in Figure 8.2, was used to measure the random incidence sound absorption coefficient of the sample specimens. Direct comparisons will be possible because of identical measurement conditions and standard specimen sizes employed. The C3-Mat_Prototype and the standard mat specimens were tested in the alpha cabin. The C3-Special_mat_Lab-made specimen was excluded from this test because of lack of appropriate sample size. The alpha cabin test required a 1x1m material specimen.

The procedure developed during the alpha cabin tests employed the B&K PULSE set-up to measure T60 decay time measurements, done similar to a reverberation room measurement and following the strict guidelines contained in AS ISO 354-2006 "*Australian Standards: Acoustics – Measurement of sound absorption in a reverberation room*". The RMIT Alpha Cabin has three 50-W co-axial speakers for sound source and three microphones were used to monitor the SPL inside the chamber. The reverberation time measurements were taken in three (3) replications for each sample. The method also required three (3) different configurations, i.e. the microphone and sound source placement variations inside the Alpha Cabin. Overall, for each sample specimen, the T60 decay time measurements were repeated 9 times, for statistical averaging. The random incidence SAC was then calculated from the averaged T60 decay times, using Sabine's equations.



**Figure 8.2: RMIT Alpha Cabin**

### 3.1.3  Vehicle testing using in-situ methods

In addition to the material acoustic property tests, in-situ vehicle cabin performance testing was conducted on the C3-Mat_Prototype and the standard mats. The "mats-on/mats-off" technique was employed, which was previously done in carpet vehicle benchmarking. This involved changing the car mats and taking repeated acoustic measurements, to obtain relative performance measures of the different car mats for direct comparison.

The vehicle tests were conducted under stationary and on-road conditions. The former will focus mainly on the effects of the engine noise while the later will take into account the contributions of tyre-road interaction noise also. In addition, $2^{nd}$ gear slow acceleration tests were also conducted specifically to monitor the distinctive engine noise i.e. combustion cycle noise. The stationary tests were conducted in a quiet and open spot at RMIT Bundoora campus itself, away from the reflective buildings. The on-road tests were conducted in a relatively quiet, well paved suburban road, on sunny and fair weather days. The road surface is representative of normal smooth bitumen paved arterial roads in Victoria with a roughness level of <4.2 IRI (International Roughness Index, taken from VIC Roads Annual Report 2007).

Two test set-ups were also employed – Aachen HMS (Head Measurement System) III psychoacoustic measurements and the PULSE Acoustic measurement system using



**Figure 8.3a: Aachen HMS III and KMT Tachometer set-up**

calibrated pressure condenser microphones (2.5", 200V polarization). The HMS set-up is shown in Figure 8.3a and the test run way specifics are shown in Figure 8.3b, while the PULSE set-up is illustrated in Figure 8.4. The HEAD acoustics measurement system details and its requirement are explained in [55].
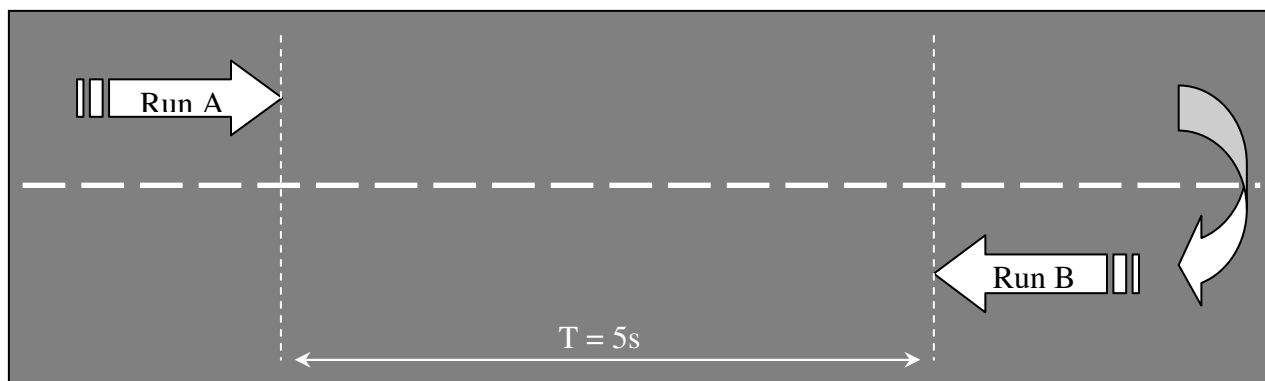


**Figure 8.3b: Test run way specifics**



**Figure 8.4: PULSE set-up (left); Microphone position on floor carpet (right)**

The car used during the vehicle testing is a Mitsubishi 380 Series III, 2007 Model SX with a 3.8L V6 engine. The mileage is 26765 km. Before the testing, the car tyres were inflated to the recommended normal operating conditions of 32psi (220kPa) for all tyres. This particular test vehicle was chosen because its floor carpet is reportedly optimized for dealing with vehicular noise in specific problem frequencies, and hence considered as the reference design.

## 4    TEST RESULTS

### 4.1  *Impedance Tube Tests*

The normal incidence SAC measured for the three mat specimens are shown in Figure 8.5. The C3-Mat_Prototype gave better SAC than the standards mat at the low to middle frequency ranges. This can be an advantage in managing low frequency noise, such as engine or power-train noise.
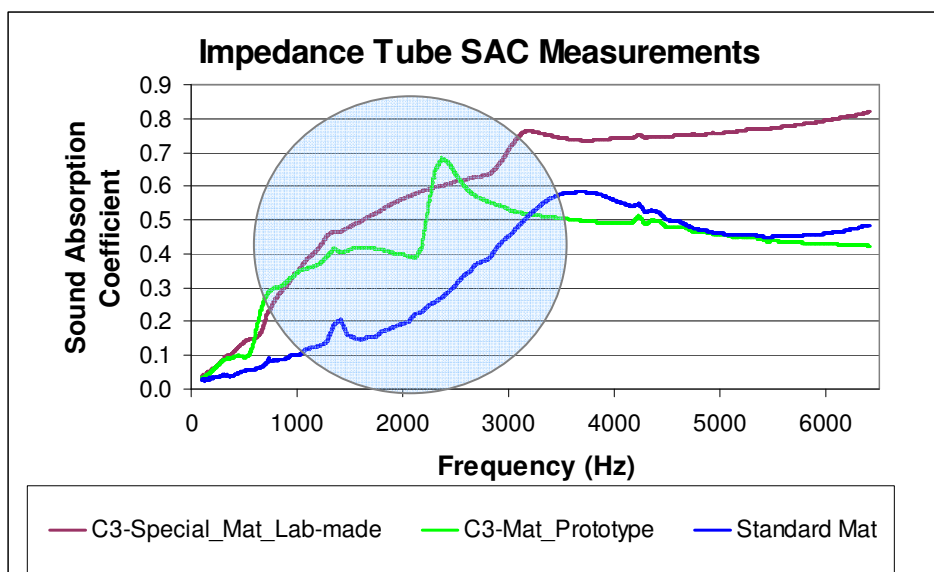


**Figure 8.5: Impedance tube SAC of mat specimens**

The lab made Concept 3mat specimen (C3-Special_mat_Lab-made) had the better SAC at high frequency range compared to either the C3-Mat_Prototype mat or the standard mat. This can be due to the fact that the lab made specimen uses K-tufting having longer pile thickness, which eventually can improve sound absorption. Figure 8.6 show that the pile length influences the SAC of tufting materials. In addition, some form of degradation occurred in the C3-Mat_Prototype during lamination, e.g. shrinkage as evidenced by the reduced mat thickness, which might have a negative impact on its sound absorption capability. The shrinkage of the absorber layer, in this case the foam with scrim component, can degrade the SAC potential of the prototype mat.
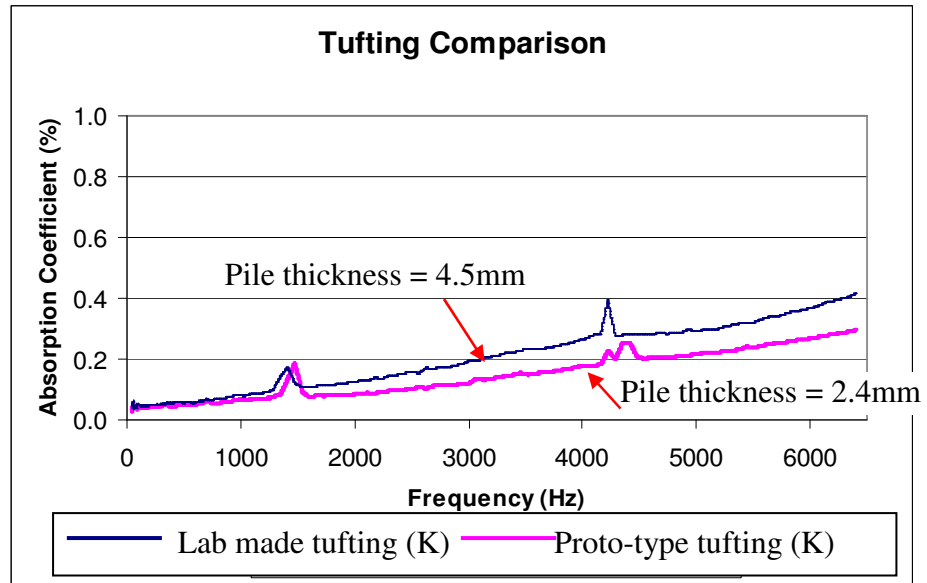
**Figure 8.6: Effect of tufting pile length on SAC**

## 4.2  Alpha Cabin Tests

SAC measurements from the RMIT Alpha Cabin for the C3-Mat_Prototype and standard mat specimens are shown in Figure 8.7. The C3-Mat_Prototype SAC showed an average improvement of about 14.2 % over that of the standard mat. Highest improvement is about 40 % in SAC at 800 Hz.
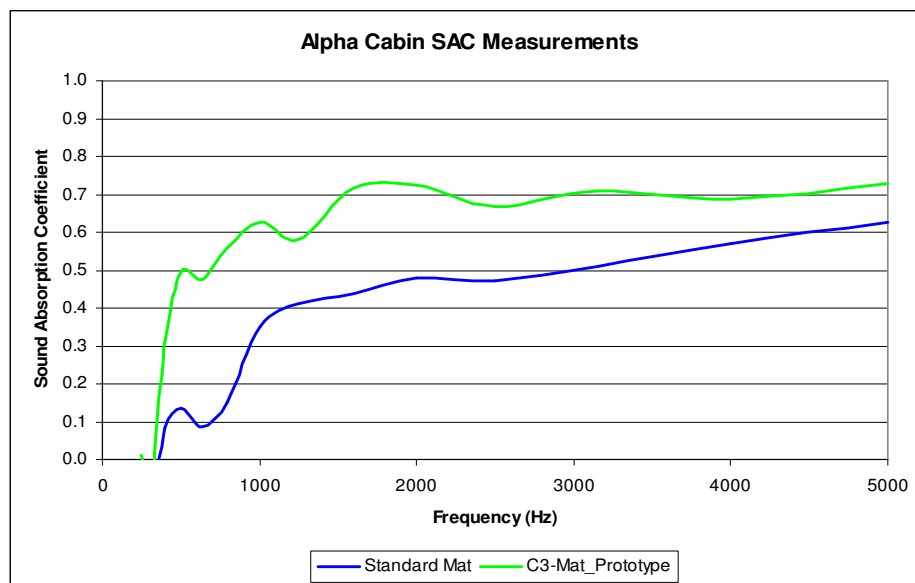


**Figure 8.7: Alpha cabin SAC of mat specimen**

The advantage of the standard mat having a longer tufting pile length, which enhances SAC performance, is to be offset while comparing the constructions; whereas the C3-Mat_Prototype has a distinct absorber layer beneath the AFR. The standard mat construction consists of the tufting backed by a thin heavy layer on a rough underlay. This construction limits the penetration of sound waves into the interior of the carpet/mat mass for further absorption or dissipation, and hence the less SAC performance on cabin side.

## 4.3  In-situ Vehicle Tests

Sound pressure levels (SPL) near the driver's ear were monitored as an indication of noise levels inside the car cabin. Repeated measurements, while different mats were fitted into the floor carpet, will indicate the relative performance levels of the test mats.

### 4.3.1  Stationary Conditions

Figure 8.8 shows the typical SPL levels at the driver's ear level during stationary conditions, with the engine revved up at various rpm's as measured using PULSE Acoustic measurement system. The C3-Mat_Prototype showed improved noise reduction capability compared to the standard mat. It is particularly effective in the low frequency ranges (e.g. < 1 kHz) where the engine noise is prevalent.
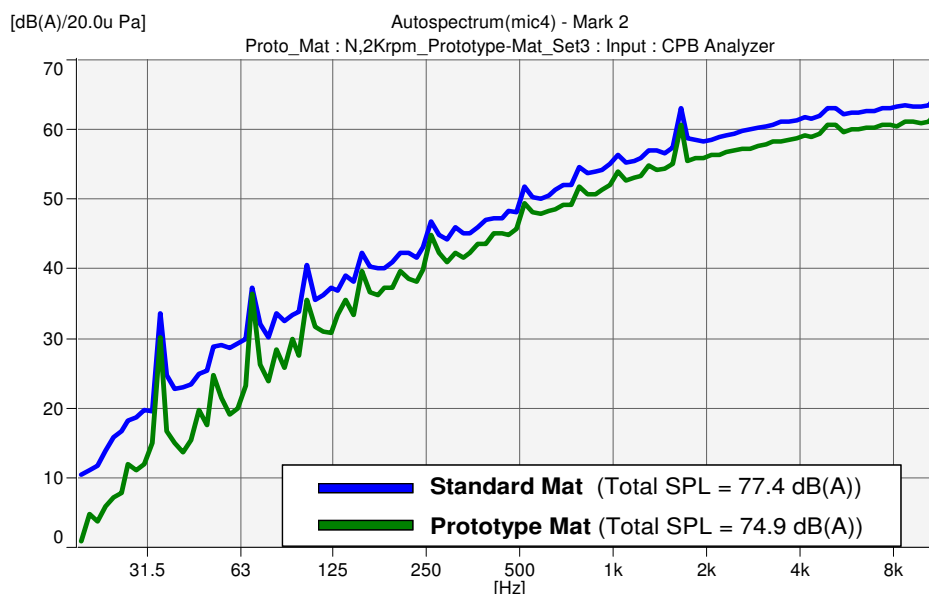


**Figure 8.8: Total SPL at Driver's Ear level during stationary conditions at 2000 engine rpm (PULSE data)**

This trend is applicable to other engine rpm levels where the C3-Mat_Prototype outperforms the standard mat. Please refer Appendix 1 for more results. Figure 8.9 shows the consolidated SPL data for the stationary tests at various engine rpm's. The C3-Mat_Prototype consistently reduces the noise level inside the car cabin for various engine rpm's. The average reduction in the total SPL is about 2.1 dB (A) compared to that of the standard mat.

It is notable that the vehicle level simulation results of concept 3 mat on M380 standard carpet, for engine noise, showed similar possible improvement of around 1dB, especially at the higher frequency ranges. These predictions are compared to standard carpet system (M380), rather than standard mat. However, the simulation results are quite practical in predicting the SPL range.
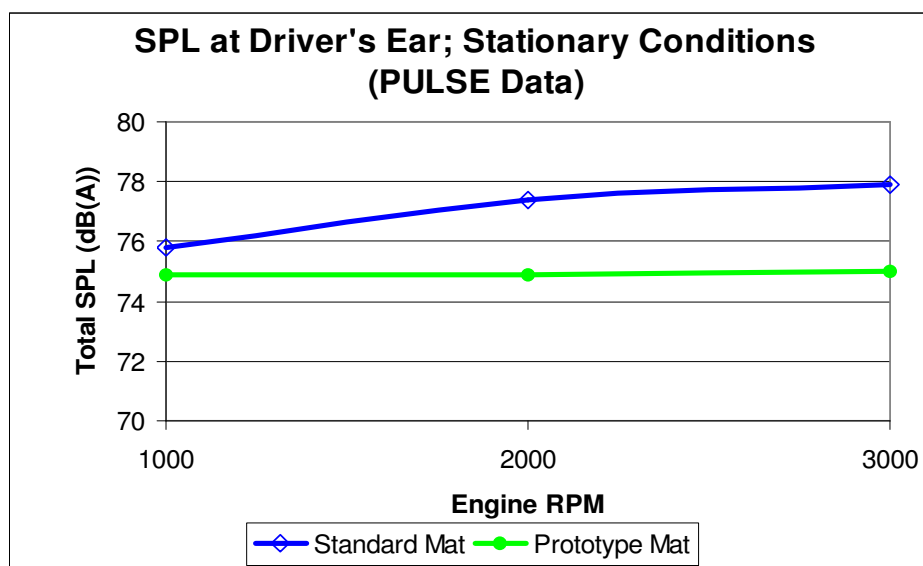


**Figure 8.9: Summary of total SPL at driver's ear level for various engine rpm's during stationary tests (PULSE data)**

Analyses of data for stationary conditions using HMS III followed the trend observed in PULSE data although at a generally lower SPL level. Note that the ArtemiS 4.00 Head Analyser software, used on the HMS III data, calculates the average SPL, while the PULSE system calculates total (peak or sum) SPL, and hence the different numerical values for SPL level quantification. Figure 8.10 shows the consolidated HMS III data for various engine rpm's during stationary tests. The reduction in the average SPL, obtained from HMS III data, attributed to the use of C3-Mat_Prototype as compared to the standard mat is 0.46 dB(A), for all engine rpm's considered.
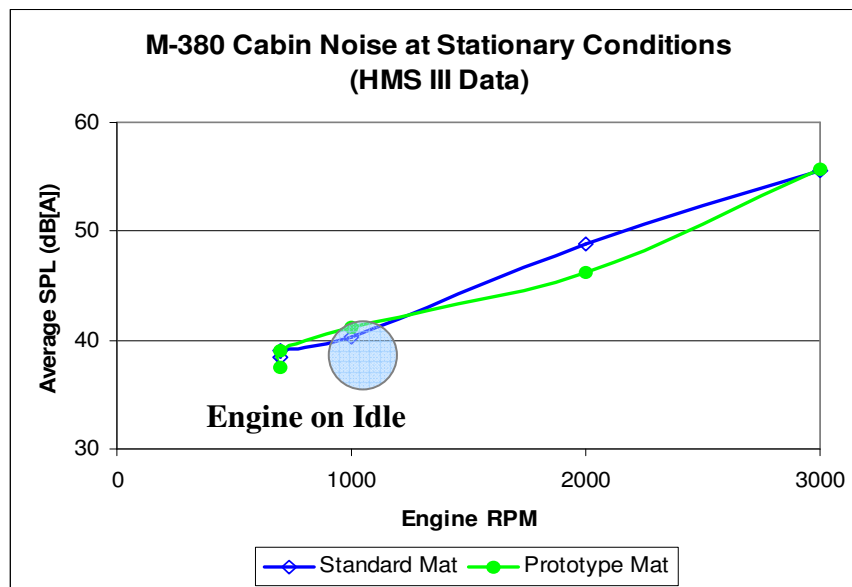
**Figure 8.10: Summary of in-cabin average SPL at various engine rpm's during stationary tests (HMS III data)**

This improvement can be further illustrated when looking at the Articulation Index (AI) report shown in Figure 8.11. Use of the C3-Mat_Prototype consistently improves the in-cabin AI compared to that of using the standard mat. Other HMS data for the stationary tests are provided in Appendix 2.
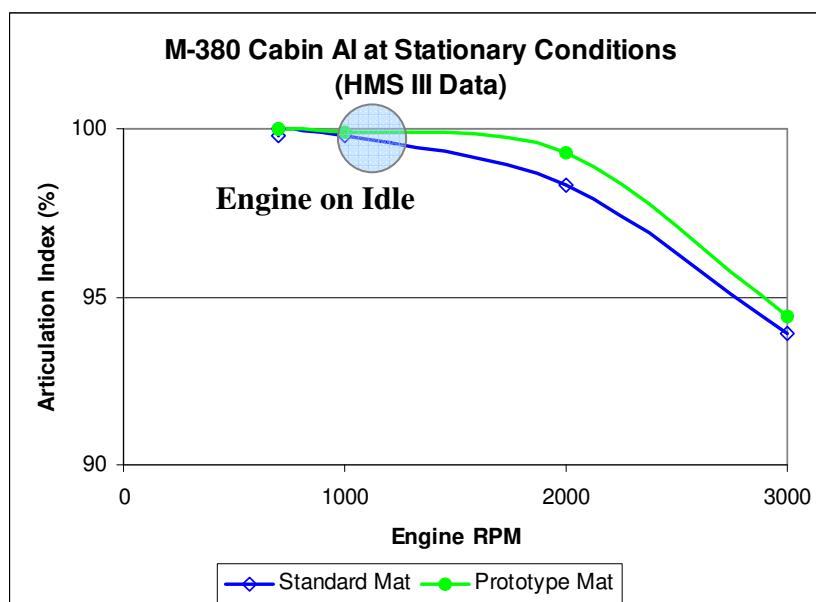


**Figure 8.11: Summary of in-cabin articulation index (AI) during stationary tests (HMS III data)**

### 4.3.2  On-Road Constant Speed test results

A summary of in-cabin noise levels from PULSE measurements are shown in Figure 8.12. The C3-Mat_Prototype performed better than the standard mat for all range of constant speeds. The averaged improvement in noise reduction, in the form of total SPL, is about 0.625 dB (A). Individual total SPL plots for the driving speed tests are provided in Appendix 3.
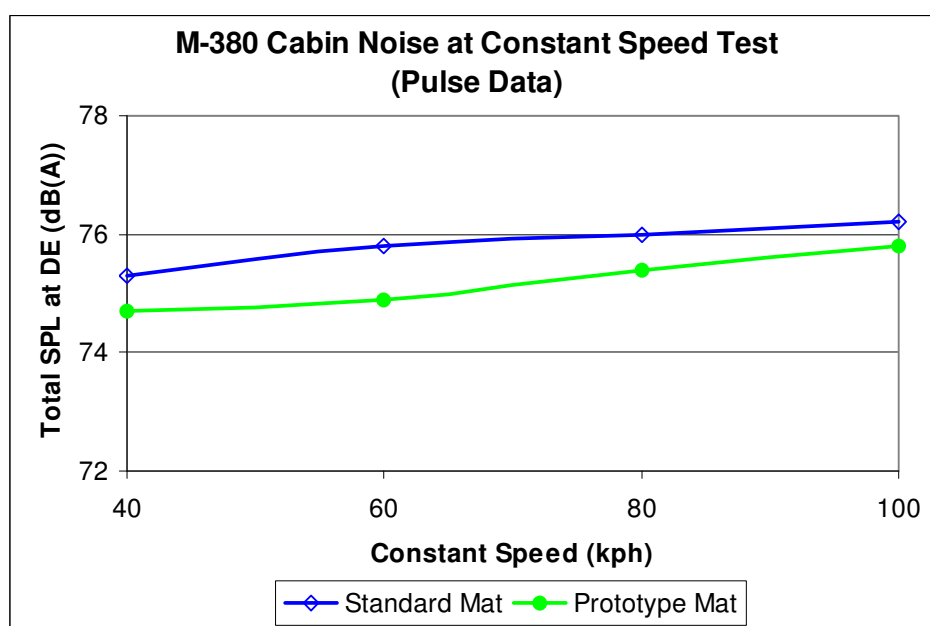


**Figure 8.12: Summary of total SPL at driver's ear level during on-road constant speed tests (PULSE data)**

Results from the analyses of HMS III for constant speed tests were not conclusive. Figure 8.13 shows the in-cabin averaged SPL plotted against the driving speeds considered. It appears that the differences in the performance of C3-Mat_Prototype and the standard mat are marginal. The measured AI at 3000 rpm in Figure 8.14 shows a marginal advantage of using the C3-Mat_Prototype over standard mat. However, overall analyses of AI results indicate that the performances of the mats are comparable, as shown in Figure 8.15. Relevant HMS III data during constant speed tests are shown in Appendix 4.
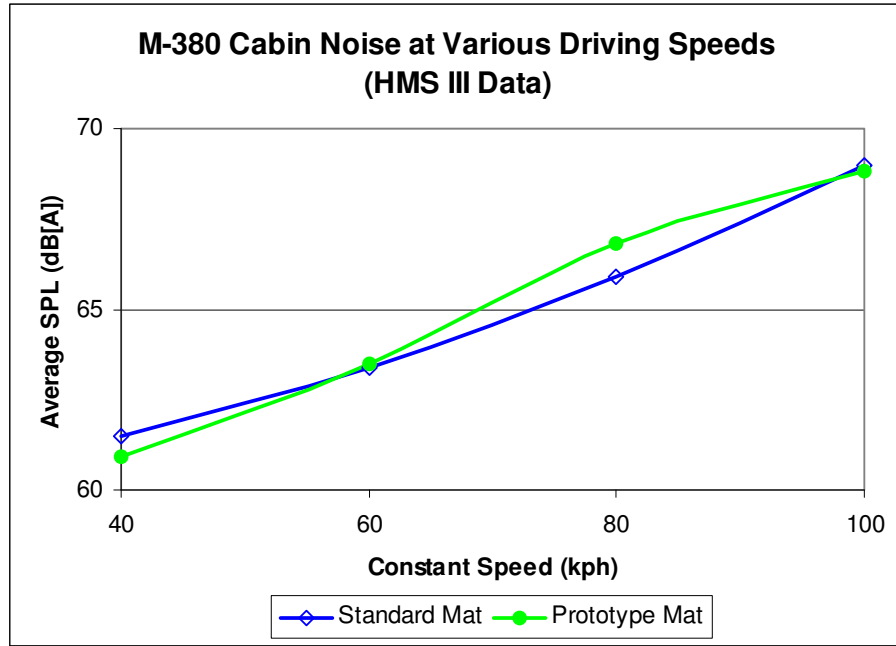
**Figure 8.13: Summary of in-cabin average SPL during on-road constant speed tests (HMS III data)**
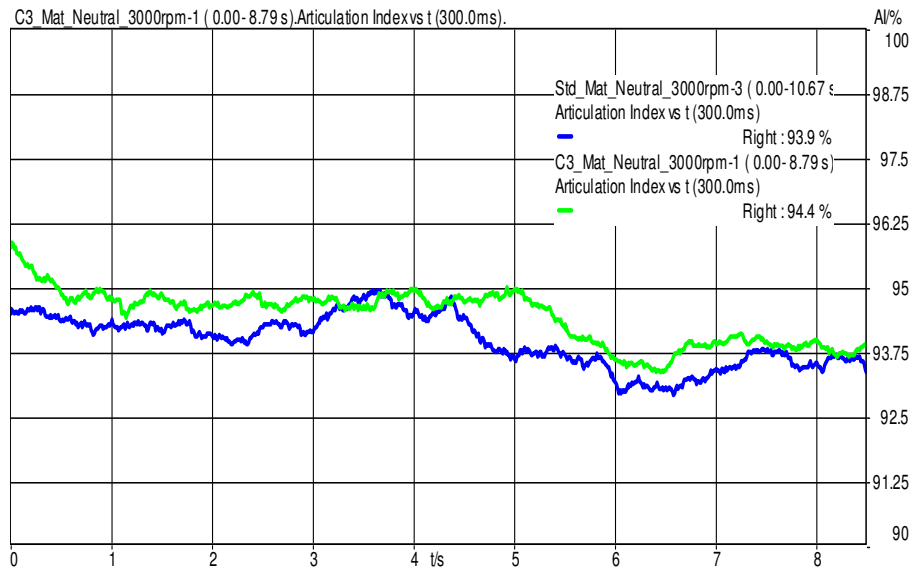


**Figure 8.14: Measured AI at 3000 rpm, stationary conditions (HMS data)**
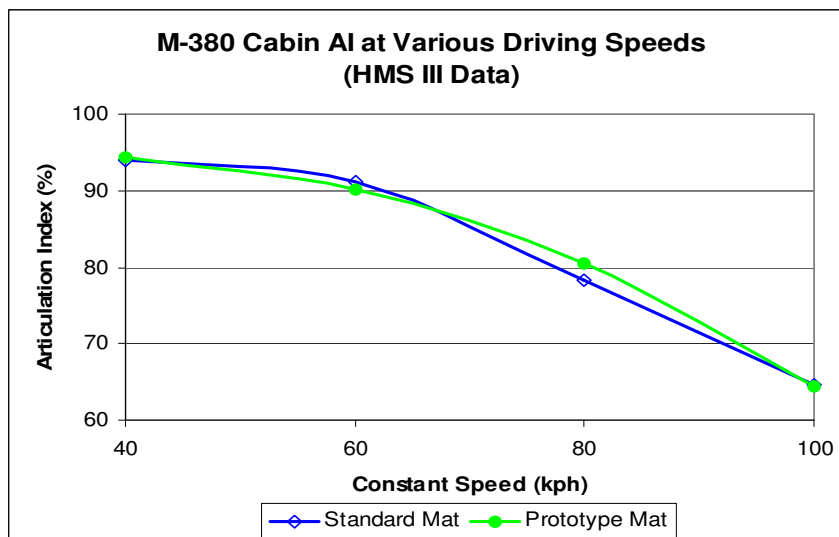
**Figure 8.15: Summary of in-cabin Articulation Index (AI) during on-road constant speed tests (HMS III data)**

### 4.3.3 2<sup>nd</sup> Gear Slow Acceleration Test

Figure 8.16 shows the 2<sup>nd</sup> order SPL inside the vehicle cabin, measured near the driver's ear level, during the 2<sup>nd</sup> gear slow acceleration on-road tests. The 2<sup>nd</sup> order SPL isolates the specific engine noise frequencies, thus making it possible to analyse its effect to the overall noise reduction strategy. The graph in Figure 8.16 indicates that the C3-Mat_Prototype provided a distinct advantage over the standard mat at the frequency range of 2.1-3.0k rpm (100~156 Hz). This can be useful in managing low frequency engine noise entering the vehicle cabin. Such insight is important for developing future improvements in mat/carpet acoustic capability.
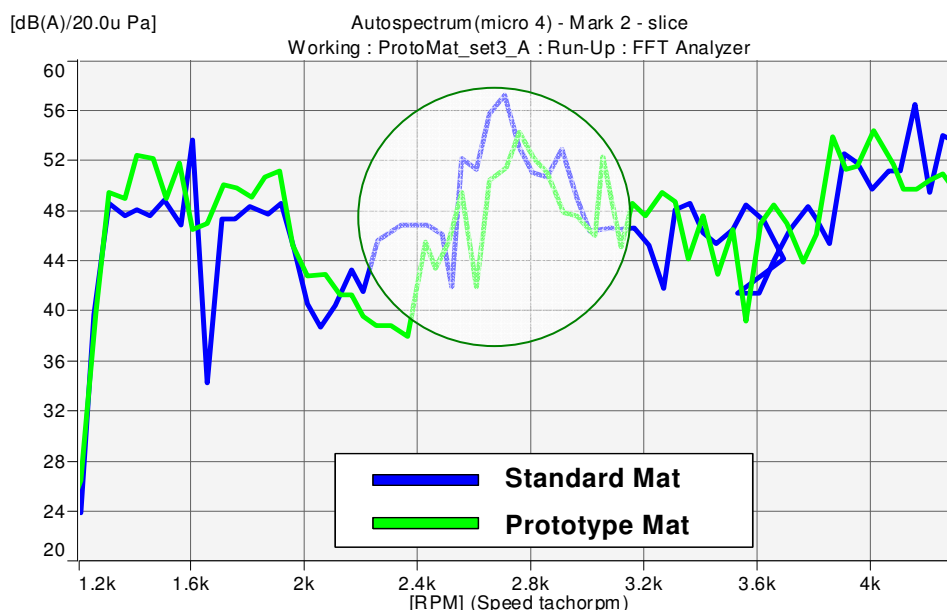


**Figure 8.16: 2<sup>nd</sup> order SPL at driver's ear level for run-up test (PULSE data)**

## 5   CONCLUSIONS

- A proof of concept mat (C3-Mat_Prototype) was constructed albeit slight modifications from the original specifications due to material, time and technical constraints. These deviations pertaining to tufting pile length, presence of thin PE at the back of the tufting, and shrinkage during lamination were noted.

- In the impedance tube SAC test, the C3-Mat_Prototype performed better than the standard mat in the low to mid frequency ranges (up to 3000Hz).

- RMIT Alpha Cabin SAC test showed that the C3-Mat_Prototype outperformed the standard mat by an average of 14.2 percentage points. Highest improvement is about 40 percentage points in SAC at 800 Hz.

- On-road vehicle tests show that the C3-Mat_Prototype has better sound absorption at the low to mid frequency range than Standard mat. PULSE data indicates an improvement in the reduction of in-cabin total SPL by the prototype mat by about 2.1 dB(A) during stationary tests and 0.625 dB(A) during constant driving tests.

- HMS III results are consistent with PULSE results during stationary vehicle tests.

•

# Appendix 1. Stationary Test – PULSE Results

Comparative plots of in-cabin total SPL, from PULSE™ data measured in the vicinity of the driver's ear, during stationary tests on the vehicle fitted with a standard mat and C3-Mat_Prototype. A separate binaural test is conducted using Head Acoustics (HMS III), which will takes into consideration of subjective and directivity parameters of the vehicle noise perceived by an average human listener.
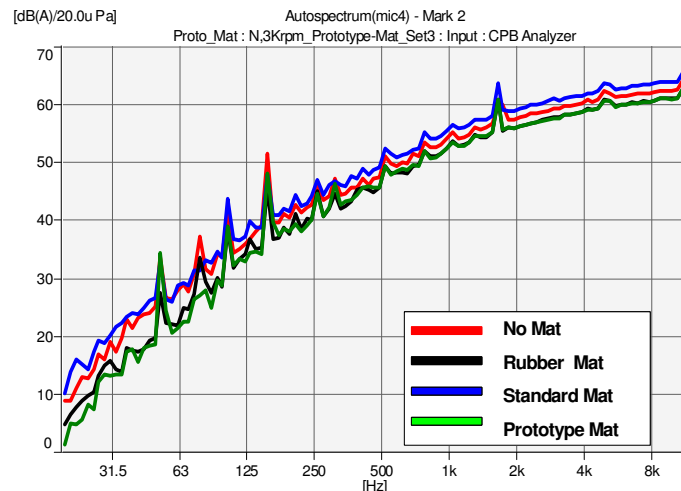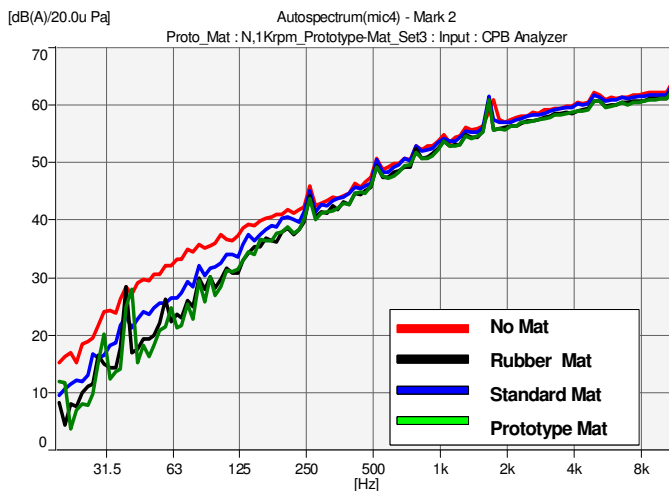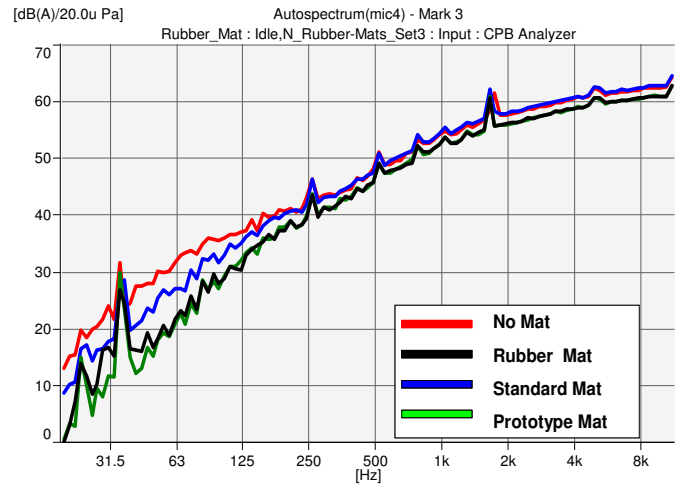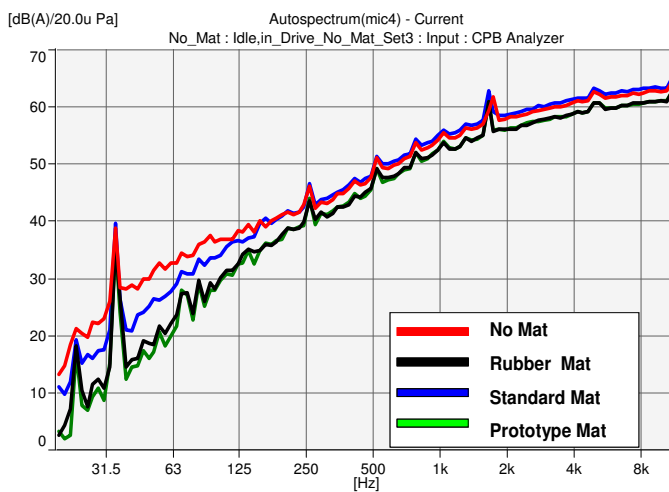
## Appendix 2. Stationary Test – HMS III Results

Average SPL and AI results for standard mat and C3-Mat_prototype at stationary conditions.
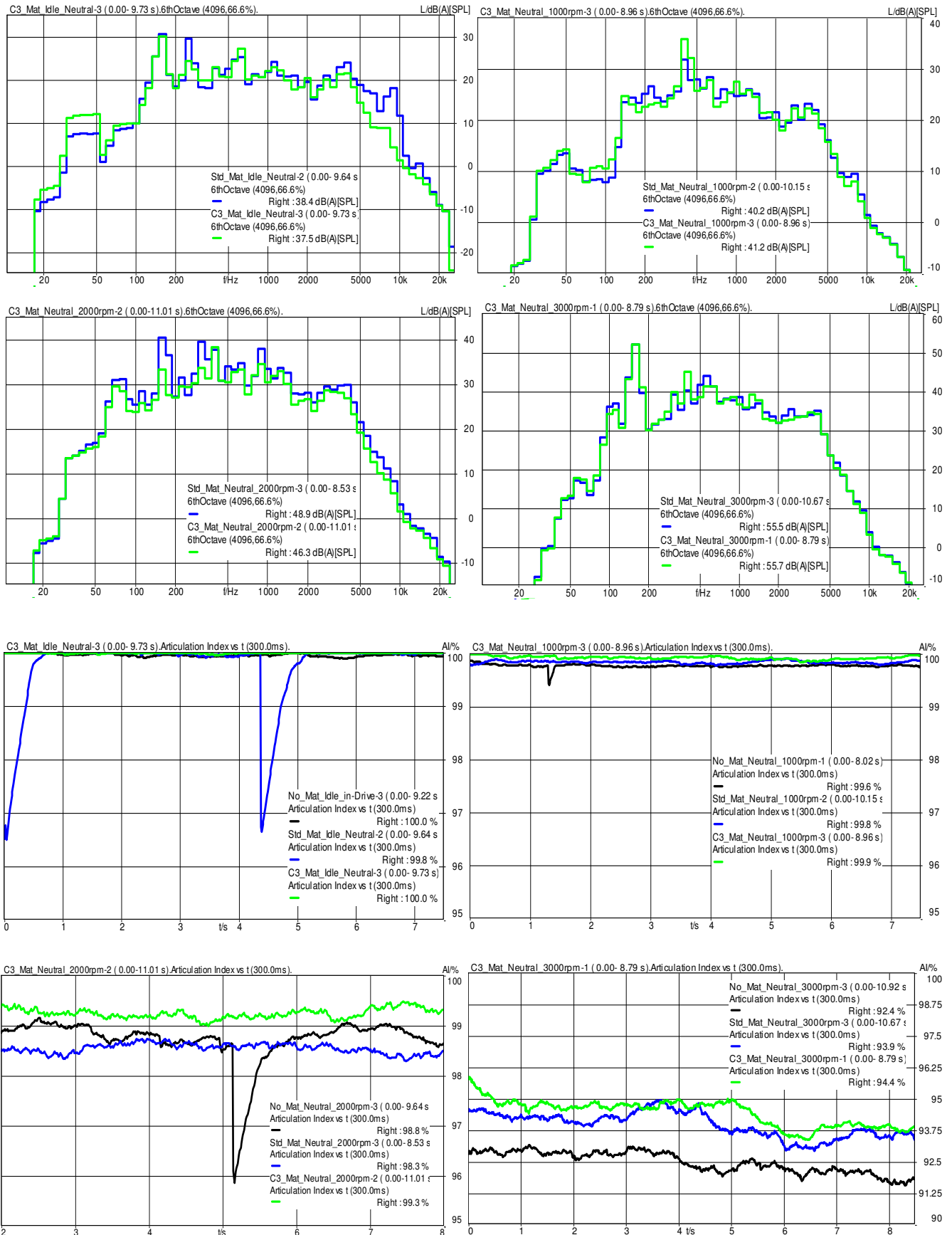
## <u>Appendix 3</u>. Constant Speed Test – PULSE Results

Comparative plots of in-cabin total SPL, from PULSE™ data measured in the vicinity of the driver's ear, during constant speed tests on the vehicle fitted with a standard mat and C3-Mat_Prototype.
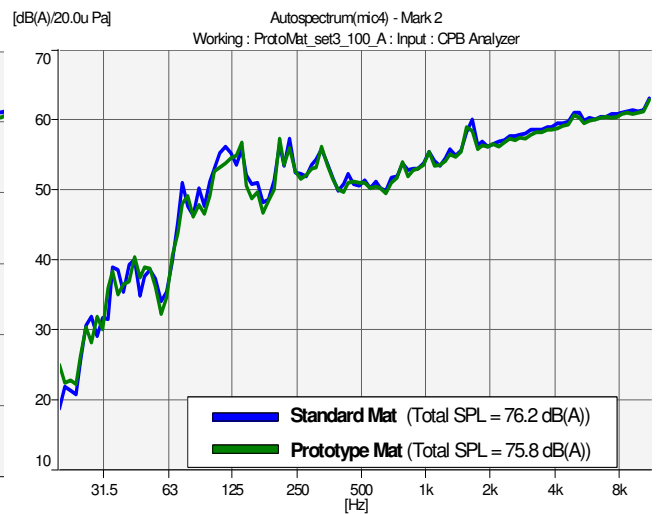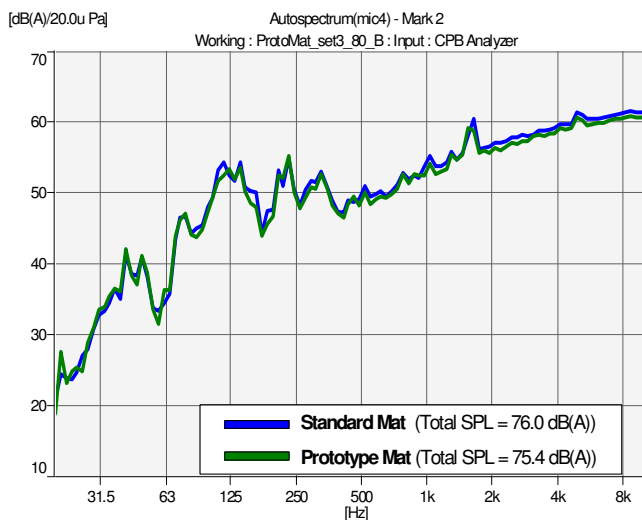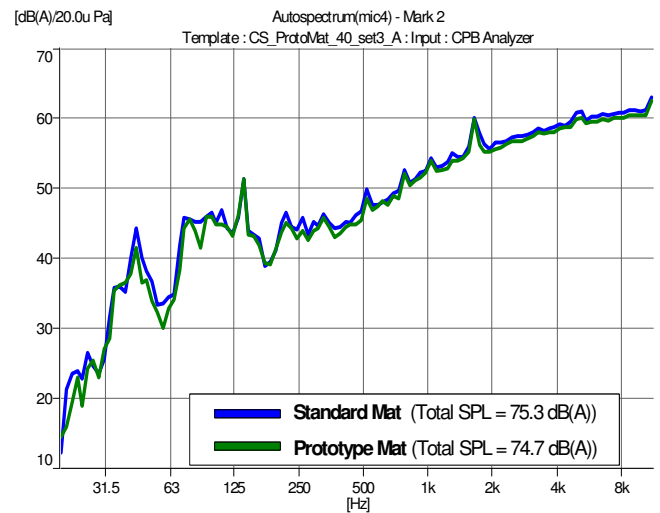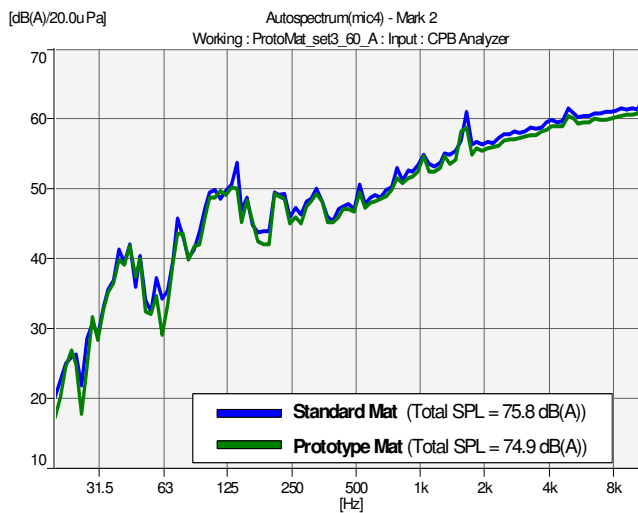
## <u>Appendix 4</u>. Constant Speed Test – HMS III Results

Average SPL and AI results, for standard mat and C3-Mat_prototype samples, at various driving speeds.
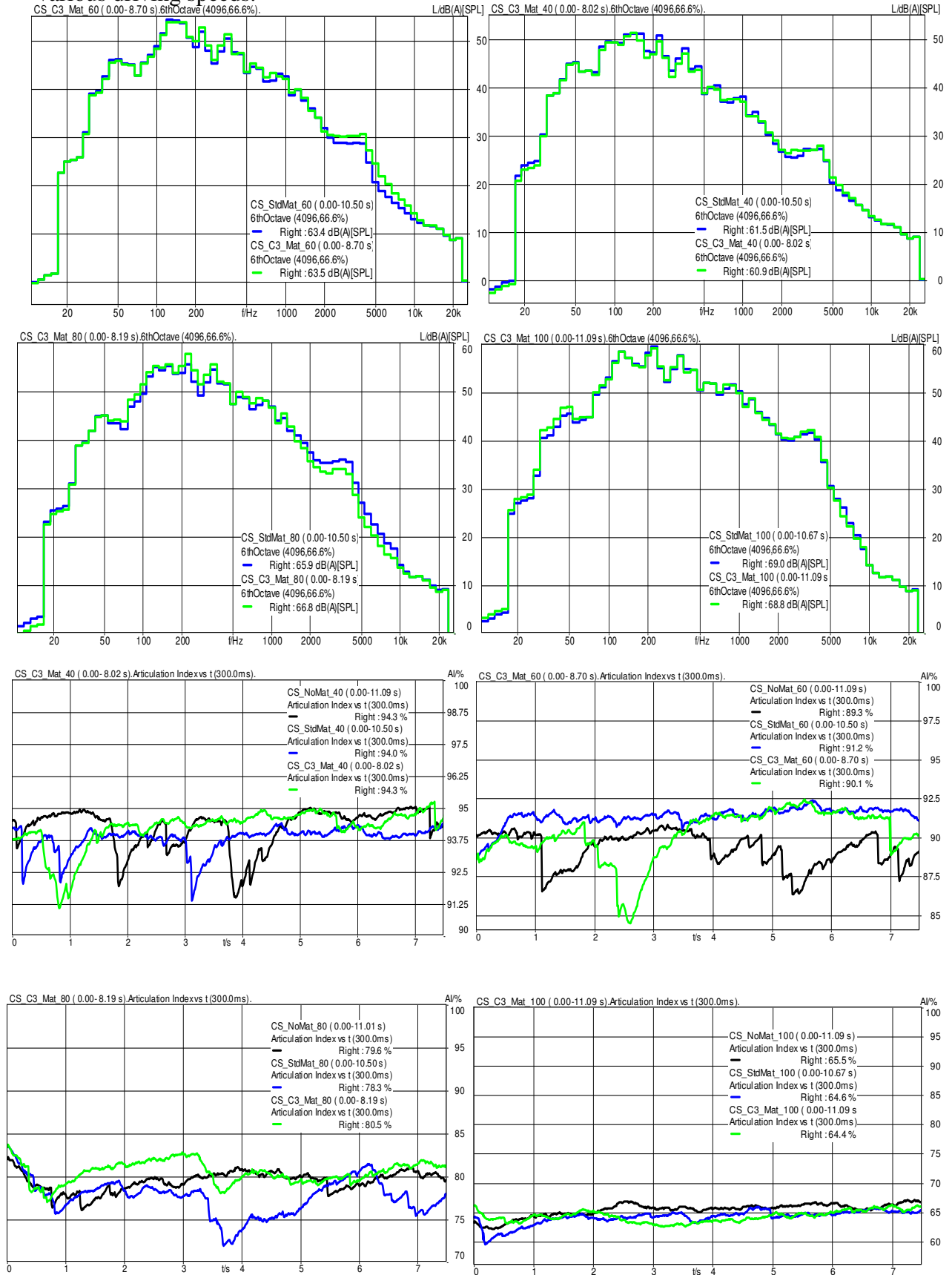
# CHAPTER 9

# DESIGN OPTIMIZATION (TAGUCHI METHOD BASED), AT MATERIAL, COMPONENT AND VEHICLE LEVELS

## 1     ABSTRACT & INTRODUCTION

This chapter outlines the design constraints for the proposed concept 3 carpet design and discusses about how to go forward improving the acoustic performance. The need for efficient optimization techniques is introduced and Taguchi loss function method is explained with brief theoretical background. A detailed Taguchi method analysis is conducted on concept 3 design for cabin side sound absorption performance and Transmission loss performance separately, using a simulated model from Statistical Energy Analysis tools. The results are analysed to reach at conclusions regarding the optimization directions for future design improvement or customization for specific noise control issues in vehicles.

Optimization of the carpet concept design against various constraints is a key to an acoustically efficient design. Taguchi analysis method is considered as the suited statistical optimization tool and applied for component level and sound package level analysis also. The sound package and carpet section wise Taguchi analysis procedure and results are outlined, which can provide directions for further optimization of the concept design. The

analysis is conducted using Statistical Energy Analysis models of Alpha Cabin for component level analysis and generic Sedan model for vehicle level analysis.

Outlining the performance requirements and constraints for the design and conducting an analysis using optimization techniques gains insight into the key parameters that contribute to meet the performance requirements, while adhering to the constraints. The basic design concept labelled **Concept 3,** which has 2 additional layers, i.e. Air Flow Resistant (AFR) layer and Absorber layer, added to the current production carpet design, is the basis for going forward with the detailed analysis and optimization of the carpet design. The Concept 3 carpet design, chosen from the earlier proposed four concepts, is shown below.
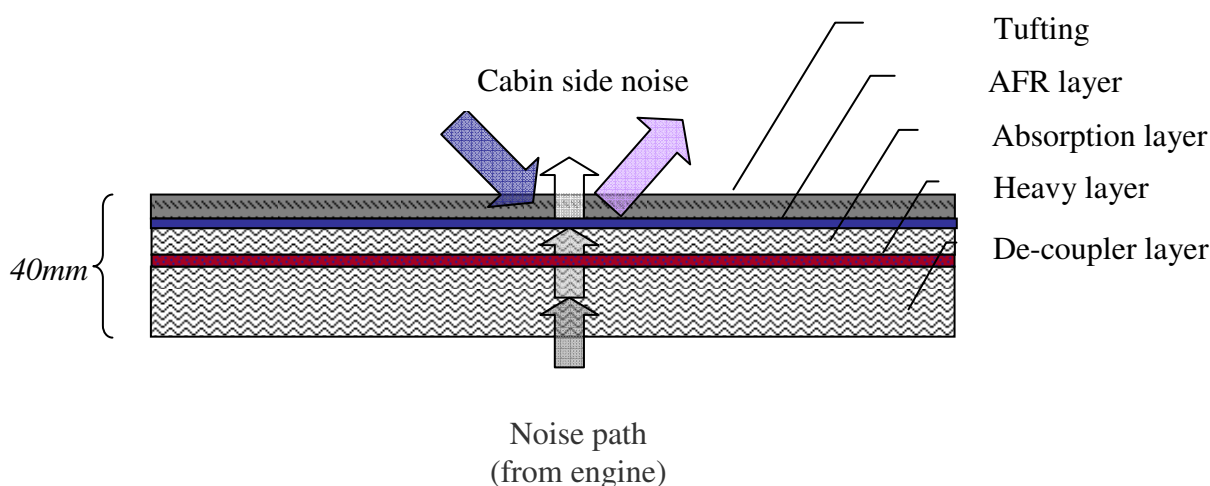


**Figure 9.1 – Concept 3**

Refreshing briefly, **Concept 3** design introduces an Air Flow Resistant (AFR) layer and Absorber layer just below the carpet tufting, compared to the current production carpet design. This design approach was taken because the current production carpet design has a relatively low sound absorption coefficient on the cabin side of the carpet. The measurement results of the proposed **Concept 3** design (40mm thick) in Figure 9.2 below show evidently the improved sound absorption coefficient in cabin side, compared to the current production (40mm thick) carpet shown in green line. The two concept-3 combinations of interest, having different AFR layers, are

Sample 1

Tufting layer (sample K) + AFR layer (sample **S3D**) + Absorber layer (sample SA_sx - Visco Elastic foam 20mm with scrim) + SL - ( Heavy Layer 1.7kgsm and De-coupler layer N foam of 20mm)

Sample 2

Tufting layer (sample K) + AFR layer (sample **S3E**) + Absorber layer (sample SA_sx - Visco Elastic foam 20mm with scrim) + SL - ( Heavy Layer 1.7kgsm and De-coupler layer N foam of 20mm)
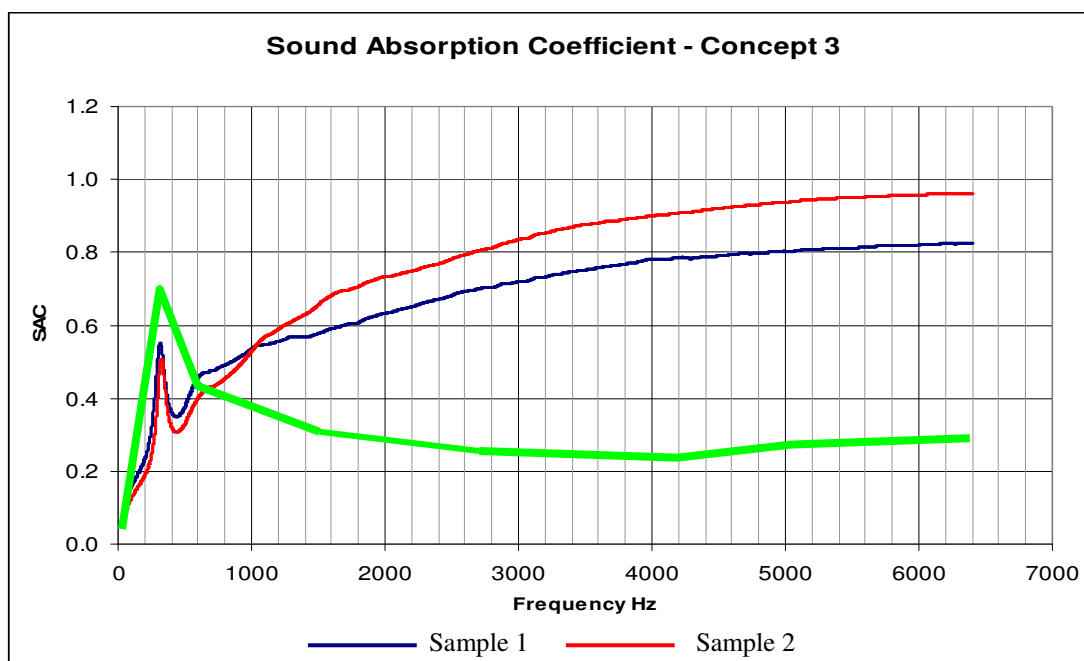


**Figure 9.2 – Concept 3 absorption measurement results**

## *1.1  Optimization requirement & techniques*

Once the basic carpet design concept is formulated, with the given constraints like weight, thickness, cost and performance targets, we need to reach the best layered material combination that provides the most competitive performance from the design. This special combination of materials with appropriate parameters is expected to perform the best, while meeting the defined constraints.

Various approaches can be taken to discover this right combination of layers, but time and resources are always natural constraints. So, we try to rely on existing and proven efficient methods or models, to get directions regarding optimizing for performance.

A Statistical Energy Analysis (SEA) model has been developed for the proposed **Concept 3,** to conduct simulated performance measurements. The **Concept 3** simulation model is initially tuned up and matched with the corresponding experimentally measured performance results. Thus, further optimizing techniques can be worked out using this simulation model, at a faster pace.

Performance sensitivity analysis for various parameters of the layered materials is one way of studying the critical parameters to be optimized. Taguchi Loss Function method is one such optimal sensitivity analysis technique, based on statistical mathematical observations for quality improvement. Taguchi method involves running a few minimum test cases and arriving at a weighted table for the various parameters controlling the quality or performance of a system. A theoretical background is also given in the next sections.

Meanwhile, a possible optimization procedure for sound-package level is to identify the acoustically significant sections of the carpet which contribute in reducing the cabin noise and to apply the treatment in those carpet sections in an extensive manner, compared to the less significant sections. Special noise reduction structures or materials can be applied to these significant sections, to attain a better noise isolation while maintaining an optimum trade-off with various constraints.

## *1.2  Concept 3 constraints and performance targets*

The key constraints for the concept design are

1.  Weight

2.  Thickness

3.  Cost of manufacturing

At the current stage of design, only the weight and thickness are considered as variables of concern as we are conducting the optimizing process on a generic **Concept 3** carpet design. Though there has not been a defined constraint for weight, the current production carpet having a heavy layer of 1.7kgsm, which would measure totally 4.56kgsm for the whole carpet, is taken as the reference weight constraint. The thickness constraint has been defined as 40mm ($\pm$5mm). The optimization techniques will be worked out around these design constraints.

Meanwhile, Taguchi Analysis for both Alpha cabin and vehicle level analysis are conducted on the carpet sections for the cavity Sound Pressure Level (SPL) as the output. In

the carpet section ON/OFF Taguchi analysis, the carpet is divided into 7 different zones of approximately equal area and each carpet section zone noise control treatment is switched ON or OFF according to the setting in the Taguchi table. Meanwhile, for Sound Package analysis, the complete vehicle cabin trim is divided into 7 categories, and each category treatment is switched ON or OFF. Separate Taguchi analyses are conducted for engine noise and tyre noise sources, at low (315 Hz - 1 kHz), mid (1 kHz - 4 kHz) and high (4 kHz - 8 kHz) frequency ranges.

## 2   TAGUCHI METHOD - THEORY

Based on the principles of experimental design and statistical methods, and from his years of research experience, Prof. Genechi Taguchi [60, 61] introduced an approach for

1.  Designing products or processes so that they are robust to environmental conditions

2.  Designing and developing products so that they are robust to component variation

3.  Minimizing variation around a target value

These three goals of Taguchi method are referred to as "parameter design" goals. Designing of experiments to meet the goals are sometimes made unnecessarily complicated, inefficient and sometimes ineffective. Taguchi's method advocates some novel methods of statistical data analysis and approaches to the design of experiments.

Taguchi considers three stages in a product's development to meet a target or goal:

1.  System design (basic configuration)

2.  Parameter design (specific values for system parameters)

3.  Tolerance design (determine best tolerances)

Taguchi recommends that statistical experimental design methods be employed to assist in quality improvement, particularly during parameter design and tolerance design. Taguchi method is already being applied in a variety of applications by corporate firms, including areas like automobile engineering, web design services etc [60, 61].

Generally, each product or process performance characteristics will have a target or nominal value that delivers the customer with maximum value. The objective is to study the variance or sensitivity around this target value. Taguchi method tries to model the departure that may occur from this target value with a "loss function". Taguchi method imposes a

quadratic loss function of the form as shown below, which also quantifies the customer response to the variance from the target,

$$L(y) = k(y - T)^2,$$

where, L(y) is the Taguchi loss function of variable parameter y, k is a statistically derived constant that controls the slope of the quadratic curve and T is the target for the design parameter y that bring maximum customer satisfaction.
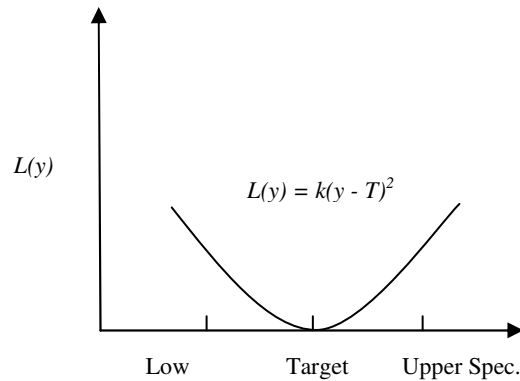


**Figure 9.3 – Taguchi loss function**

The Taguchi loss function is evaluated by running a set of test runs on the product being evaluated, by which the variance of the product's performance is measured for a defined variation of each parameter in the product. The parameters are selected in such a way that they are orthogonal in nature, in the context of the tests undertaken. This process is made efficient by running only the necessary tests, following a Taguchi table.

Below is a "7 parameters - 8 runs" Taguchi table. Each parameter (P-1 to P-7) is considered to have two possible values (A and B). For example, if P-1 is the testing temperature, then 18 degree Celsius (A) and 20 degree Celsius (B) are the two temperature values for running the tests. So a test run can be designed by a combination of these 7 parameters, each having the A or B value. The below Taguchi table has 8 such different test runs. Note that though the total permutation of 7 parameters (A & B) involves $2^7$ test runs, the below 8 test runs are selected for running the orthogonal set of Taguchi tests.

**Table 1 – Taguchi loss function table**

| | | **Input variables** | | | | | | | **Performance** |
|---|---|---|---|---|---|---|---|---|---|
| | **P-1** | **P-2** | **P-3** | **P-4** | **P-5** | **P-6** | **P-7** | |
| Run 1 | A | A | A | A | A | A | A | Output 1 |
| Run 2 | A | A | A | B | B | B | B | Output 2 |
| Run 3 | A | B | B | A | A | B | B | Output 3 |
| Run 4 | A | B | B | B | B | A | A | Output 4 |
| Run 5 | B | A | B | A | B | A | B | Output 5 |
| Run 6 | B | A | B | B | A | B | A | Output 6 |
| Run 7 | B | B | A | A | B | B | A | Output 7 |
| Run 8 | B | B | A | B | A | A | B | Output 8 |
| Avg. of **level 1** (A's) | X1 | X2 | X3 | X4 | X5 | X6 | X7 | |
| Avg. of **level 2** (B's) | Y1 | Y2 | Y3 | Y4 | Y5 | Y6 | Y7 | |
| Diff. **Xn - Yn** (effect) | **W1** | **W2** | **W3** | **W4** | **W5** | **W6** | **W7** | |

$$Y1 = (o/p5 + o/p6 + o/p\ 7 + o/p\ 8)/4 \qquad o/p = Output$$

$$X1 = (o/p\ 1 + o/p\ 2 + o/p\ 3 + o/p\ 4)/4$$

The resulting weighting factors **W1** to **W7** indicate the prominence of a parameter in the output performance, by varying the parameters P1 to P7 respectively. So, if the variance ratio (B-A)/A of the parameters are the same, for example 20%, then the parameter which has the largest weight (W) is the most sensitive one. Hence, in an optimization point of view, this parameter will be the one to first work on, in priority order, because a small addition to this parameter should give the maximum output compared to others.

Thus, Taguchi Method helps to find out easily, within a few test cases, the sensitivity order of the parameters for a given product or process being analysed or optimized.

# 3 MATERIAL LEVEL TAGUCHI METHOD OPTIMIZATION RESULTS

In the case of Concept 3 design Taguchi method analysis, the sound absorption coefficient and transmission loss are done separately, in two analysis tables. Further, the frequencies have been subdivided into 3 groups, for which separate Taguchi analysis is done. Note that the analysis is done on a slightly modified version or special case of concept 3 design, where there are two tufting/substrate layers, which can be considered as a mat placed over a carpet, together forming a concept 3 carpet.

Low frequencies - 315 Hz to 1 KHz

Mid frequencies - 1 KHz to 4 KHz

High frequencies - 4 KHz to 8 KHz

For the case where there are more than 7 parameters that cannot fit into the Taguchi table, one option is to increase the table size or the other option is to identify the less significant parameters by first conducting an initial run of Taguchi tests with the first set of parameters, using an ON/OFF Taguchi analysis, where instead of varying the parameter by a percentage, the material layer itself is included (ON) or not included (OFF).

So we have included an ON/OFF Taguchi de-coupling analysis for both cabin side sound absorption and transmission loss, which is followed by a detailed Taguchi analysis.

## 3.1 ON/OFF Taguchi de-coupling analysis

The selected orthogonal parameters, for initial ON/OFF analysis of the proposed concept carpet design, are as shown below. The parameters are selected such a way that they can be used for both cabin side sound absorption and transmission loss analysis of the carpet.

P1 - De-coupler

P2 - Substrate (tufting base)

P3 - Tufting

P4 - Absorption layer

P5      -       Air Flow Resistant (AFR)

P6      -       Substrate (top tufting base)

P7      -       Tufting (top)
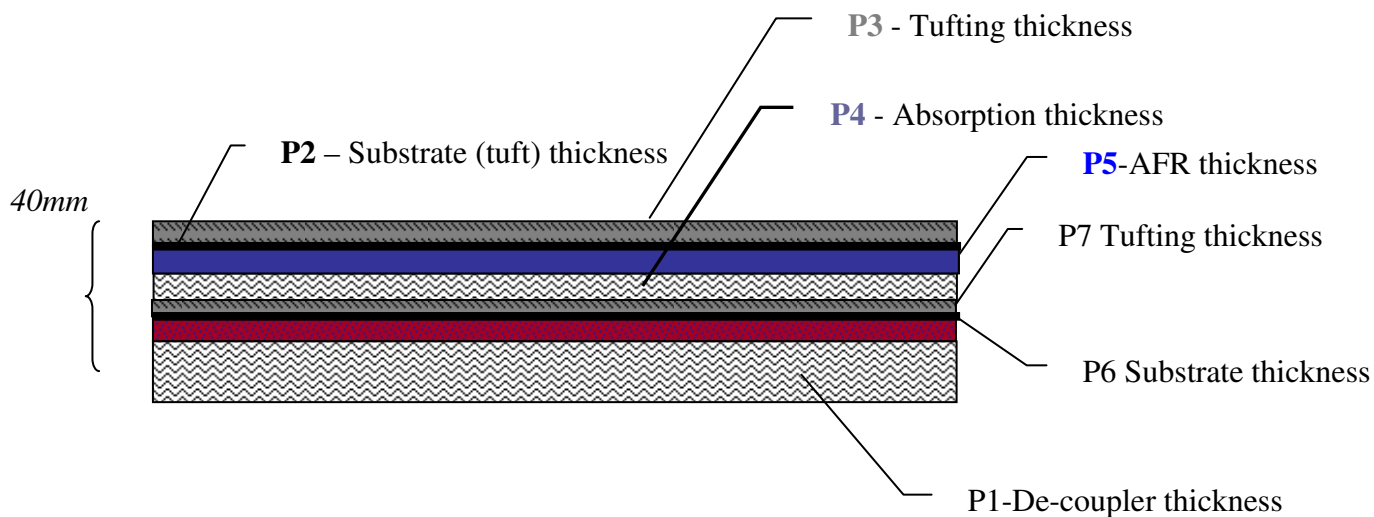


**Figure 9.4: Taguchi orthogonal parameters for carpet concept design**

## 3.1.1 Cabin side absorption: ON/OFF Taguchi tables

Tables 2 & 3 list the ON/OFF de-coupling analysis results for Concept 3 cabin side sound absorption, where the target output is the sound absorption coefficient having frequency average values between 0 and 1. If the material layers are not included (OFF), the material layers are replaced by the same thickness of heavy layer (septum).

**Table 2 – Concept 3 initial ON/OFF Taguchi based test run results**

| | 1. N foam (bottom decoupler) | 2. Substrate (bottom) | 3. Tufting (bottom) | 4. B foam (top absorber) | 5. S3D AFR | 6. Substrate (top) | 7. Tufting (top) | | | |
|---|---|---|---|---|---|---|---|---|---|---|
| | Input variables | | | | | | | Averages | | |
| | **1** | **2** | **3** | **4** | **5** | **6** | **7** | **Low** | **Mid** | **High** |
| Run 1 | 1 | 1 | 1 | 1 | 1 | 1 | 1 | 0.47 | 0.86 | 0.84 |

| | | | | | | | | | | |
|---|---|---|---|---|---|---|---|---|---|---|
| Run 2 | 1 | 1 | 1 | 2 | 2 | 2 | 2 | 0.08 | 0.00 | 0.00 |
| Run 3 | 1 | 2 | 2 | 1 | 1 | 2 | 2 | 0.09 | 0.00 | 0.00 |
| Run 4 | 1 | 2 | 2 | 2 | 2 | 1 | 1 | 0.08 | 0.11 | 0.20 |
| Run 5 | 2 | 1 | 2 | 1 | 2 | 1 | 2 | 0.16 | 0.11 | 0.01 |
| Run 6 | 2 | 1 | 2 | 2 | 1 | 2 | 1 | 0.18 | 0.11 | 0.14 |
| Run 7 | 2 | 2 | 1 | 1 | 2 | 2 | 1 | 0.09 | 0.09 | 0.14 |
| Run 8 | 2 | 2 | 1 | 2 | 1 | 1 | 2 | 0.22 | 0.03 | 0.00 |

**Table 3 – ON/OFF Taguchi loss function table**

| | 1. N foam (bottom decoupler) | 2. Substrate (bottom) | 3. Tufting (bottom) | 4. B foam (top absorber) | 5. S3D AFR | 6. Substrate (top) | 7. Tufting (top) |
|---|---|---|---|---|---|---|---|
| | **1** | **2** | **3** | **4** | **5** | **6** | **7** |
| **Low (315Hz-1KHz)** | | | | | | | |
| Avg. level1 | 0.18 | 0.22 | 0.21 | 0.20 | 0.24 | 0.23 | 0.20 |
| Avg. level2 | 0.16 | 0.12 | 0.13 | 0.14 | 0.10 | 0.11 | 0.14 |
| Diff. (effect) | 0.02 | 0.10 | 0.09 | 0.06 | **0.14** | **0.12** | 0.07 |
| | | | | | | | |
| **Mid (1KHz-4KHz)** | | | | | | | |
| Avg. level1 | 0.24 | 0.27 | 0.25 | 0.27 | 0.25 | 0.28 | 0.29 |
| Avg. level2 | 0.08 | 0.06 | 0.08 | 0.06 | 0.08 | 0.05 | 0.04 |
| Diff. (effect) | 0.16 | 0.21 | 0.17 | 0.20 | 0.17 | **0.23** | **0.26** |
| | | | | | | | |
| **High (4KHz-8KHz)** | | | | | | | |
| Avg. level1 | 0.26 | 0.25 | 0.20 | 0.25 | 0.25 | 0.26 | 0.33 |
| Avg. level2 | 0.08 | 0.09 | 0.09 | 0.09 | 0.09 | 0.07 | 0.00 |
| Diff. (effect) | 0.18 | 0.16 | 0.11 | 0.16 | 0.16 | **0.19** | **0.33** |

Note: The **red** numbers indicate the most sensitive parameters having high or close to high weighting or Taguchi loss function value. The ***blue*** numbers indicate the second most sensitive parameter.

### 3.1.2  Sound transmission loss: ON/OFF Taguchi tables

Tables 4 and 5 list the ON/OFF Taguchi concept 3 sound transmission loss de-coupling analysis, where the target output is sound transmissions loss coefficient. If the material layers themselves are not included (OFF), the material layers are replaced with the same thickness of air gap.

**Table 4 – Concept 3 ON/OFF Taguchi based test run results**

| | 1. N foam (bottom decoupler) | 2. Substrate (bottom, 5mm) | 3. Tufting (bottom) | 4. B foam (top absorber) | 5. S3D AFR | 6. Substrate (top) | 7. Tufting (top) | | Averages | | |
|---|---|---|---|---|---|---|---|---|---|---|---|
| | **Input variables** | | | | | | | | | | |
| | **1** | **2** | **3** | **4** | **5** | **6** | **7** | | **Low freq** | **Mid** | **High** |
| Run 1 | 1 | 1 | 1 | 1 | 1 | 1 | 1 | | 25.94 | 47.27 | 62.45 |
| Run 2 | 1 | 1 | 1 | 2 | 2 | 2 | 2 | | 24.12 | 43.86 | 55.70 |
| Run 3 | 1 | 2 | 2 | 1 | 1 | 2 | 2 | | 25.50 | 46.45 | 61.09 |
| Run 4 | 1 | 2 | 2 | 2 | 2 | 1 | 1 | | 24.20 | 42.19 | 54.07 |
| Run 5 | 2 | 1 | 2 | 1 | 2 | 1 | 2 | | 20.31 | 40.87 | 70.50 |
| Run 6 | 2 | 1 | 2 | 2 | 1 | 2 | 1 | | 22.08 | 37.02 | 66.41 |
| Run 7 | 2 | 2 | 1 | 1 | 2 | 2 | 1 | | 20.95 | 38.65 | 69.24 |
| Run 8 | 2 | 2 | 1 | 2 | 1 | 1 | 2 | | 22.08 | 36.94 | 66.52 |

**Table 5 – ON/OFF Taguchi loss function table**

| | 1. N foam (bottom decoupler) | 2. Substrate (bottom, 5mm) | 3. Tufting (bottom) | 4. B foam (top absorber) | 5. S3D AFR | 6. Substrate (top) | 7. Tufting (top) |
|---|---|---|---|---|---|---|---|
| **Low (315Hz-1KHz)** | | | | | | | |
| Avg. level1 | 24.94 | 23.11 | 23.27 | 23.18 | 23.90 | 23.29 | 23.29 |
| Avg. level2 | 21.36 | 23.18 | 23.02 | 23.12 | 22.40 | 23.16 | 23.01 |
| Diff. (effect) | **3.59** | -0.07 | 0.25 | 0.05 | **1.50** | 0.13 | 0.29 |
| | | | | | | | |
| **Mid (1.25KHz-3.15KHz)** | | | | | | | |
| Avg. level1 | 44.94 | 42.26 | 41.68 | 43.31 | 41.92 | 41.82 | 41.28 |
| Avg. level2 | 38.37 | 41.06 | 41.63 | 40.00 | 41.39 | 41.50 | 42.03 |
| Diff. (effect) | **6.58** | 1.20 | 0.05 | **3.31** | 0.53 | 0.32 | 0.75 |
| | | | | | | | |
| **High (4KHz-8KHz)** | | | | | | | |
| Avg. level1 | 58.33 | 63.77 | 50.78 | 65.82 | 64.12 | 63.39 | 63.04 |
| Avg. level2 | 68.17 | 62.73 | 63.02 | 60.68 | 62.38 | 63.11 | 63.45 |
| Diff. (effect) | **9.84** | 1.03 | **12.24** | 5.14 | 1.74 | 0.28 | 0.41 |

Note: The *red* numbers indicate the most sensitive parameters having high or close to high weighting or Taguchi loss function value. The *blue* numbers indicate the second most sensitive parameter.

### 3.1.3 Parameter elimination discussion

The above ON/OFF Taguchi tables for cabin side absorption and transmission loss helps to identify the parameters that does not play a key role in improving the acoustic performance of the carpet. There are 2 parameters that clearly show low profile in low and mid frequencies, i.e. not coloured *red* or *blue* in the low and mid frequency tables, in terms of the loss function, which are

a) Substrate (bottom),

b) Tufting (bottom) and

So, any of these parameters can be replaced for introducing new parameters, for a detailed Taguchi analysis.

Hence, for going ahead with the detailed Taguchi analysis, the remaining parameters included are,

P6) Heavy layer thickness and

P7) Heavy layer surface density (kgsm)

## *3.2  Detailed Taguchi analysis*

The selected orthogonal parameters, for analysis of the proposed concept carpet design, are as shown below. The parameters are selected such a way that they can be used for both cabin side absorption and transmission loss analysis of the carpet.

P1    -    De-coupler thickness

P2    -    Substrate (top) thickness

P3    -    Tufting (top) thickness

P4    -    Absorption layer thickness

P5    -    Air Flow Resistant (AFR) thickness

P6    -    Heavy layer thickness

P7    -    Heavy layer surface density (in kgsm)
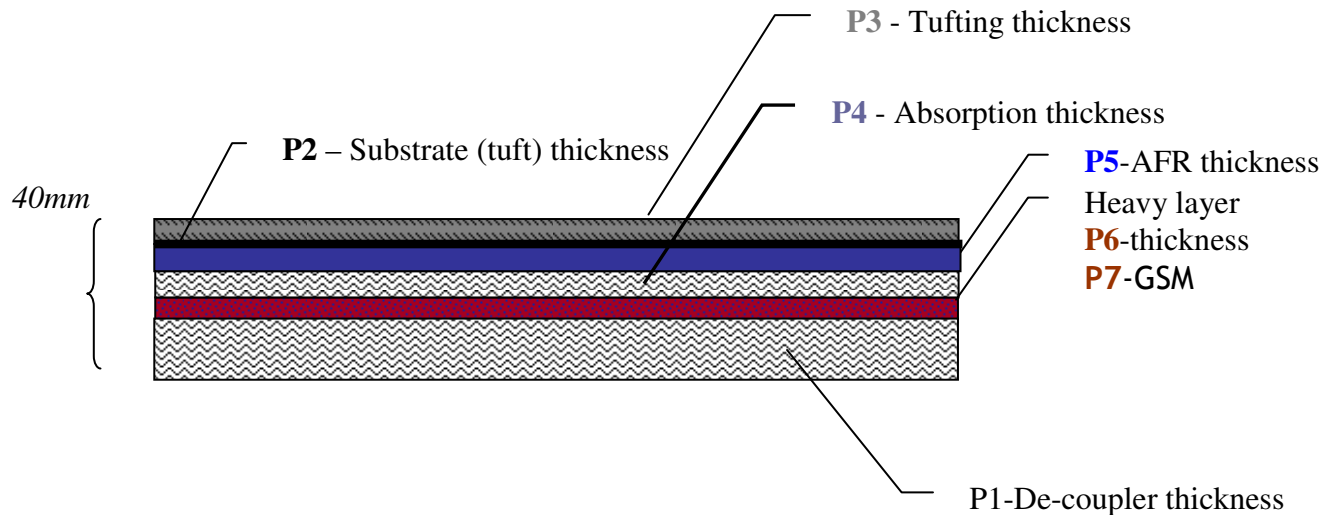
**Figure 9.5: Taguchi orthogonal parameters for carpet concept design**

## 3.2.1  Taguchi analysis: Cabin side absorption

The below tables detail the Taguchi loss function calculations done for the carpet concept in an evident manner.

**Taguchi parameter table**

**Table 6 – Carpet parameters used in Taguchi analysis**

| Input variables | Level 1 | Level 2 |
|---|---|---|
| 1. N foam (bottom de-coupler) thickness (m) | 0.015 | 0.018 |
| 2. Substrate (top) thickness (m) | 0.0005 | 0.0006 |
| 3. Upper (top) tufting thickness (m) | 0.003 | 0.0036 |
| 4. B foam (top absorber) thickness (m) | 0.015 | 0.018 |
| 5. S3D AFR thickness (m) | 0.0032 | 0.00384 |
| 6. Septum (Heavy Layer) thickness (m) | 0.0015 | 0.0018 |
| 7. Septum (Heavy Layer) kgsm | 1.7 | 2.04 |

**Test run table**

## Table 7 – Concept 3 Taguchi based test run results

| | 1. N foam (bottom decoupler) thickness | 2. Substrate (top) thickness | 3. Upper (top) tufting thickness | 4. B foam (top absorber) thickness | 5. S3D AFR thickness | 6. Septum (Heavy Layer) thickness | 7. Septum (Heavy Layer) gsm | Low | Mid | High |
|---|---|---|---|---|---|---|---|---|---|---|
| | **1** | **2** | **3** | **4** | **5** | **6** | **7** | | | |
| Run 1 | 1 | 1 | 1 | 1 | 1 | 1 | 1 | 0.46633 | 0.860225 | 0.841579 |
| Run 2 | 1 | 1 | 1 | 2 | 2 | 2 | 2 | 0.534223 | 0.871294 | 0.83339 |
| Run 3 | 1 | 2 | 2 | 1 | 1 | 2 | 2 | 0.46769 | 0.865318 | 0.8451 |
| Run 4 | 1 | 2 | 2 | 2 | 2 | 1 | 1 | 0.537464 | 0.868971 | 0.837163 |
| Run 5 | 2 | 1 | 2 | 1 | 2 | 1 | 2 | 0.482397 | 0.881431 | 0.835819 |
| Run 6 | 2 | 1 | 2 | 2 | 1 | 2 | 1 | 0.520675 | 0.881431 | 0.845255 |
| Run 7 | 2 | 2 | 1 | 1 | 2 | 2 | 1 | 0.486145 | 0.859206 | 0.834327 |
| Run 8 | 2 | 2 | 1 | 2 | 1 | 1 | 2 | 0.512789 | 0.883313 | 0.843565 |

**Input variables**          **Average absorption coefficients (freq)**

**Table 8 – Taguchi loss function table**

| | 1. N foam (bottom de-coupler) thickness | 2. Substrate (top) thickness | 3. Upper (top) tufting thickness | 4. B foam (top absorber) thickness | 5. S3D AFR thickness | 6. Septum (Heavy Layer) thickness | 7. Septum (Heavy Layer) gsm |
|---|---|---|---|---|---|---|---|
| | **1** | **2** | **3** | **4** | **5** | **6** | **7** |
| **Low** | 315Hz-1KHz | | | | | | |
| Avg. level1 | 0.501427 | 0.500906 | 0.499872 | 0.475641 | 0.077106 | 0.502654 | 0.502654 |
| Avg. level2 | 0.500502 | 0.501022 | 0.502057 | 0.526288 | 0.080424 | 0.502183 | 0.499275 |
| Diff. (effect) | 0.000925 | 0.000116 | 0.002185 | **0.050647** | **0.003318** | 0.00047 | **0.003379** |
| | | | | | | | |
| **Mid** | 1KHz-4KHz | | | | | | |
| Avg. level1 | 0.866452 | 0.873595 | 0.86851 | 0.866545 | 0.872572 | 0.873485 | 0.867458 |
| Avg. level2 | 0.876345 | 0.869202 | 0.874287 | 0.876252 | 0.870226 | 0.869312 | 0.875339 |
| Diff. (effect) | **0.009893** | 0.004393 | **0.005778** | **0.009707** | 0.002346 | 0.004173 | 0.007881 |
| | | | | | | | |
| **High** | 4KHz-8KHz | | | | | | |
| Avg. level1 | 0.839308 | 0.839011 | 0.670572 | 0.839206 | 0.843875 | 0.839531 | 0.839581 |
| Avg. level2 | 0.839741 | 0.840039 | 0.840834 | 0.839843 | 0.835175 | 0.839518 | 0.839469 |
| Diff. (effect) | 0.000433 | 0.001028 | **0.170262** | 0.000637 | **0.0087** | 1.35E-05 | 0.000112 |

Note: The *red* numbers indicate the most sensitive parameters having high or close to high weighting or Taguchi loss function value. The *blue* numbers indicate the second most sensitive parameter.

### 3.2.1.1 Result discussion

Referring to the Taguchi loss function table for Sound Absorption Coefficient, the loss function weighting results indicate that if there is need for improving the sound absorption in low frequencies, we need to first increase the thickness of the absorber layer, just below the carpet top tufting layer, and then if possible try increasing the AFR layer thickness.

It is slightly surprising to note that Taguchi results show that increasing the heavy layer GSM may increase the cabin side sound absorption for low frequency range. This might be because the sound is transmitted through the heavy layer at near natural resonance frequencies of the material, to be absorbed by the de-coupler layer just below the heavy layer.

At mid frequency range, both the absorber layer and de-coupler layer thickness show almost equal sensitivity. The concept 3 carpet sound absorption is quite good at mid and high frequency ranges and the sensitivity of output is only about 0.95%. Similar is the case for the high frequency range, where carpet tufting thickness and AFR layer thickness are the two sensitive areas of improvement, with a higher sensitivity of about 17% for the upper tufting layer.

Referring to the initial ON/OFF Taguchi tables, we can see that few parameters which showed high sensitivity to ON/OFF loss function may show less sensitivity in the detailed Taguchi analysis where a slight variation is applied to the parameters. This can be expected because, like shown in the below Figure 9.6, in ON/OFF Taguchi it is the *absolute* sensitivity or rate of output variation that comes into picture; meanwhile in detailed Taguchi analysis it will be the *local* sensitivity or rate of output variation around the current design parameter value. So, with orthogonally designed parameters, the ON/OFF de-coupling Taguchi analysis gives a sensible for the *effective sensitivity* of the parameter.

run 3
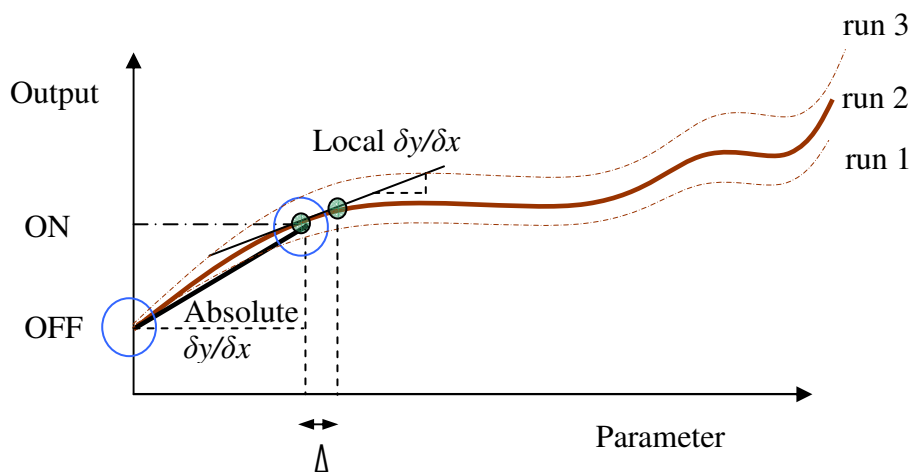
Where,

   ON    - Contribution of parameter to target (output) value is ON
   OFF   - Contribution of parameter to target (output) value is OFF (zero)
   Δ      - Small (delta) deviation for parameter

**Figure 9.6: Taguchi orthogonal parameters for carpet concept design**

**Taguchi parameter table**

**Table 9 – Carpet parameters used in Taguchi analysis (TL)**

| Input variables | | | | |
|---|---|---|---|---|
| | | | Level 1 | Level 2 |
| | | | | |
| 1. N foam (bottom de-coupler) thickness (m) | | | 0.015 | 0.018 |
| 2. Substrate (top) thickness (m) | | | 0.0005 | 0.0006 |
| 3. Upper (top) tufting thickness (m) | | | 0.003 | 0.0036 |
| 4. B foam (top absorber) thickness (m) | | | 0.015 | 0.018 |
| 5. S3D AFR thickness (m) | | | 0.0032 | 0.00384 |
| 6. Septum (Heavy Layer) thickness (m) | | | 0.0015 | 0.0018 |
| 7. Septum (Heavy Layer) kgsm | | | 1.7 | 2.04 |

## Table 10 – Concept 3 Taguchi based test run results (TL)

| | Input variables | | | | | | | Transmission Loss averages (freq) | | |
|---|---|---|---|---|---|---|---|---|---|---|
| | 1 | 2 | 3 | 4 | 5 | 6 | 7 | Low | Mid | High |
| Run 1 | 1 | 1 | 1 | 1 | 1 | 1 | 1 | 25.94 | 47.27 | 62.45 |
| Run 2 | 1 | 1 | 1 | 2 | 2 | 2 | 2 | 26.39 | 50.28 | 65.26 |
| Run 3 | 1 | 2 | 2 | 1 | 1 | 2 | 2 | 25.88 | 49.18 | 64.08 |
| Run 4 | 1 | 2 | 2 | 2 | 2 | 1 | 1 | 26.53 | 48.51 | 63.86 |
| Run 5 | 2 | 1 | 2 | 1 | 2 | 1 | 2 | 26.01 | 49.86 | 67.49 |
| Run 6 | 2 | 1 | 2 | 2 | 1 | 2 | 1 | 25.86 | 48.23 | 66.08 |
| Run 7 | 2 | 2 | 1 | 1 | 2 | 2 | 1 | 25.82 | 48.23 | 65.88 |
| Run 8 | 2 | 2 | 1 | 2 | 1 | 1 | 2 | 26.03 | 49.82 | 67.62 |

Input variable column headings:
1. N foam (bottom decoupler) thickness
2. Substrate (top) thickness
3. Upper (top) tufting thickness
4. B foam (top absorber) thickness
5. S3D AFR thickness
6. Septum (Heavy Layer) thickness
7. Septum (Heavy Layer) gsm

**Taguchi loss function table**

**Table 11 – Taguchi loss function table (TL)**

| | 1. N foam (bottom decoupler) thickness | 2. Substrate (top) thickness | 3. Upper (top) tufting thickness | 4. B foam (top absorber) thickness | 5. S3D AFR thickness | 6. Septum (Heavy Layer) thickness | 7. Septum (Heavy Layer) gsm |
|---|---|---|---|---|---|---|---|
| **Low** | 315Hz-1KHz | | | | | | |
| Avg. level1 | 26.19 | 26.05 | 26.05 | 25.91 | 25.93 | 26.13 | 26.04 |
| Avg. level2 | 25.93 | 26.06 | 26.07 | 26.20 | 26.19 | 25.99 | 26.08 |
| Diff. (effect) | **0.25** | 0.01 | 0.02 | **0.29** | **0.26** | 0.14 | 0.04 |
| | | | | | | | |
| **Mid** | 1.25KHz-3.15KHz | | | | | | |
| Avg. level1 | 48.81 | 48.91 | 48.90 | 48.64 | 48.63 | 48.87 | 48.06 |
| Avg. level2 | 49.04 | 48.94 | 48.94 | 49.21 | 49.22 | 48.98 | 49.79 |
| Diff. (effect) | 0.23 | 0.02 | 0.04 | **0.57** | **0.60** | 0.11 | **1.73** |
| | | | | | | | |
| **High** | 4KHz-8KHz | | | | | | |
| Avg. level1 | 63.91 | 65.32 | 52.24 | 64.97 | 65.06 | 65.35 | 64.57 |
| Avg. level2 | 66.77 | 65.36 | 65.38 | 65.70 | 65.62 | 65.33 | 66.11 |
| Diff. (effect) | **2.85** | 0.04 | **13.14** | 0.73 | 0.56 | 0.03 | 1.55 |

Note: The **red** numbers indicate the most sensitive parameters having high or close to high weighting or Taguchi loss function value. The **blue** number indicates the second most sensitive.

## 3.2.2.1 Result discussion

From the above loss function table it is clear that at low frequencies (315Hz-1kHz), the absorber thickness, AFR layer thickness and de-coupler layer play the key role, with the heavy layer down in the line of sensitivity. This might be because the sound is transmitted through the heavy layer at near natural resonance frequencies, to be absorbed by the absorber layer just above the heavy layer. Further, the heavy layer and the AFR layer forms like a double panel system where the absorber comes in between them, for which the transmission loss increases by the gap between the AFR and heavy layers.

At mid frequency range the heavy layer comes back to picture, with the AFR layer thickness and top absorber layers seconding in improving the transmission loss. The high frequency sound insulation seems to be very sensitive to the increase of carpet tufting layer thickness, seconded by the de-coupler thickness.

## 3.2.3 Summary of detailed Taguchi analysis

- The below table summarises the optimization weighting to be given while trying to improve acoustic performance in each frequency range. Note that the Taguchi loss function values are shown in brackets, beside the layer names placed in priority order.

| | TL | SAC (cabin side) |
|---|---|---|
| Low (315Hz - 1kHz) | 1. Absorber (0.29) | 1. Absorber (0.05) |
| | 2. AFR (0.26) | 2. AFR (0.003) |
| | 3. De-coupler (0.25) | 3. HL gsm(0.003) |

| | TL | SAC (cabin side) |
|---|---|---|
| Mid (1kHz - 4kHz) | 1. HL gsm(1.73) | 1. De-coupler (0.01) |
| | 2. AFR (0.6) | 2. Absorber (0.01) |
| | 3. Absorber (0.57) | 3. Tufting (0.006) |

| | TL | SAC (cabin side) |
|---|---|---|
| High (4kHz - 8kHz) | 1. Tufting (13.14) | 1. Tufting (0.17) |
| | 2. De-coupler (2.85) | 2. AFR (0.01) |

- At low frequency range (315Hz-1kHz), the heavy layer is expected to transmit sound to the next layer and so the de-coupler below the heavy layer might absorb low frequency noise from the cabin side.

# 4   Alpha Cabin based carpet section Taguchi analysis

## 4.1   Carpet section Taguchi analysis procedure

A seven parameter and eight run Taguchi analysis table is used for the carpet analysis. The carpet zones are divided in such a way that it matches physically with the separate areas of the carpet, like the foot rest zone, under seat zone etc, for separate analysis. The orthogonal nature of the Taguchi parameters is not an issue in carpet sections, as physically they are already orthogonal.

The acoustic significance of each carpet section is identified by verifying the loss function results obtained for the ON/OFF Taguchi analysis. ON level is considered as the case where there is carpet or NCT (Noise Control Treatment) on that section and OFF level is the case where there is no NCT, i.e. with sheet metal facing. Following the 7 parameter – 8 runs Taguchi table as shown below, each run test is executed on the simulation model and solved for obtaining the SPL at the cavity of measurement. In the case of Alpha Cabin simulation model, the main cavity is the measurement cavity.

As shown in the sample Taguchi table, for each test run (row) the output, i.e. SPL of the measurement cavity, is noted. After running the 8 test runs and obtaining the corresponding outputs, each parameter loss function is calculated (column) by finding the difference between the average of all the test run outputs with the parameter/carpet section NCT ON and the average of outputs when the parameter/carpet section NCT is OFF. The sample Taguchi table illustrates the loss function calculation procedure. Further, since the carpet zones are not exactly equal in area, while calculating the loss function it is being normalized to the loss function of $1m^2$ carpet sections, by dividing it by the section area.

Table 12 – Taguchi loss function table

| | **P-1** | **P-2** | **P-3** | **P-4** | **P-5** | **P-6** | **P-7** | |
|---|---|---|---|---|---|---|---|---|
| | | | | **Input variables** | | | | **Performance** |
| Run 1 | ON | ON | ON | ON | ON | ON | ON | Output 1 |
| Run 2 | ON | ON | ON | OFF | OFF | OFF | OFF | Output 2 |
| Run 3 | ON | OFF | OFF | ON | ON | OFF | OFF | Output 3 |
| Run 4 | ON | OFF | OFF | OFF | OFF | ON | ON | Output 4 |
| Run 5 | OFF | ON | OFF | ON | OFF | ON | OFF | Output 5 |
| Run 6 | OFF | ON | OFF | OFF | ON | OFF | ON | Output 6 |
| Run 7 | OFF | OFF | ON | ON | OFF | OFF | ON | Output 7 |
| Run 8 | OFF | OFF | ON | OFF | ON | ON | OFF | Output 8 |
| Avg. of ON cases | X1 | X2 | X3 | X4 | X5 | X6 | X7 | |
| Avg. of OFF cases | Y1 | Y2 | Y3 | Y4 | Y5 | Y6 | Y7 | |
| Diff. **Xn - Yn (effect)** | **W1** | **W2** | **W3** | **W4** | **W5** | **W6** | **W7** | |

o/p = Output

$Y1 = (o/p5 + o/p6 + o/p\ 7 + o/p\ 8)/4$

$X1 = (o/p\ 1 + o/p\ 2 + o/p\ 3 + o/p\ 4)/4$

## 4.1.1 Carpet ON/OFF Taguchi sections

The carpet is divided into 7 approximately equal area zones for ON/OFF Taguchi analysis. As shown below, the sections that come into the same zone have the same zone number. Note that, a few similar or symmetric sections may not be included in the Taguchi zones, for equalling the surface areas.
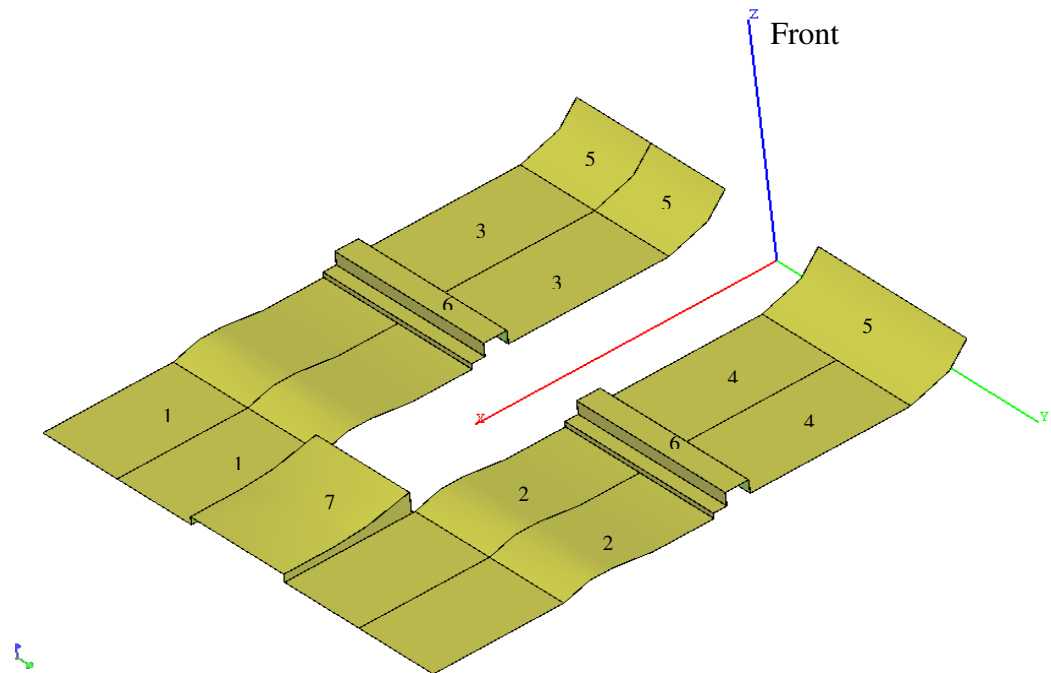
Figure 9.7: Carpet zones for Alpha cabin based ON/OFF Taguchi analysis

## 4.2  Alpha Cabin (component level) Taguchi analysis results

The ON/OFF Taguchi analysis test results in the Alpha Cabin model are given in the tables below.

Table 13: Taguchi Parameter table

| Input variables | | |
|---|---|---|
| Carpet zones | Level 1 | Level 2 |
| | | |
| 1. Zone1 | ON | OFF |
| 2. Zone2 | ON | OFF |
| 3. Zone3 | ON | OFF |
| 4. Zone4 | ON | OFF |
| 5. Zone5 | ON | OFF |
| 6. Zone6 | ON | OFF |
| 7. Zone7 | ON | OFF |
| | | |

Table 14: Taguchi test table

| | 1. Zone1 | 2. Zone2 | 3. Zone3 | 4. Zone4 | 5. Zone5 | 6. Zone6 | 7. Zone7 | | Averages | | |
|---|---|---|---|---|---|---|---|---|---|---|---|
| | Input variables | | | | | | | | Averages | | |
| | 1 | 2 | 3 | 4 | 5 | 6 | 7 | | Low | Mid | High |
| Run 1 | ON | ON | ON | ON | ON | ON | ON | | 101.35 | 102.74 | 103.73 |
| Run 2 | ON | ON | ON | OFF | OFF | OFF | OFF | | 102.09 | 103.96 | 105.20 |
| Run 3 | ON | OFF | OFF | ON | ON | OFF | OFF | | 102.69 | 103.96 | 105.16 |
| Run 4 | ON | OFF | OFF | OFF | OFF | ON | ON | | 103.05 | 104.55 | 105.67 |
| Run 5 | OFF | ON | OFF | ON | OFF | ON | OFF | | 102.49 | 104.24 | 105.27 |
| Run 6 | OFF | ON | OFF | OFF | ON | OFF | ON | | 102.63 | 104.24 | 105.28 |
| Run 7 | OFF | OFF | ON | ON | OFF | OFF | ON | | 102.37 | 103.81 | 105.20 |
| Run 8 | OFF | OFF | ON | OFF | ON | ON | OFF | | 103.07 | 104.42 | 105.39 |

Since the carpet zones are not exactly equal in area, while calculating the loss function it is being normalized to the loss function of $1m^2$ carpet sections, by dividing it by the section area.

Table 15: Taguchi loss function table

| | 1. Zone1 | 2. Zone2 | 3. Zone3 | 4. Zone4 | 5. Zone5 | 6. Zone6 | 7. Zone7 |
|---|---|---|---|---|---|---|---|
| | 1 | 2 | 3 | 4 | 5 | 6 | 7 |
| **Low (315Hz-1KHz)** | | | | | | | |
| Avg. level1 | 102.29 | 102.14 | 102.22 | 102.22 | 102.43 | 102.49 | 102.35 |
| Avg. level2 | 102.64 | 102.79 | 102.71 | 102.71 | 102.50 | 102.44 | 102.58 |
| Diff. (effect) | 0.35 | **0.66** | **0.49** | **0.49** | 0.06 | 0.04 | 0.23 |
| Area normalized (effect) | 1.61 | 3.03 | 2.01 | 1.98 | 0.27 | 0.19 | 1.52 |
| | | | | | | | |
| **Mid (1KHz-4KHz)** | | | | | | | |

| | | | | | | | |
|---|---|---|---|---|---|---|---|
| Avg. level1 | 103.80 | 103.79 | 103.73 | 103.68 | 103.84 | 103.98 | 103.83 |
| Avg. level2 | 104.17 | 104.18 | 104.24 | 104.29 | 104.14 | 103.99 | 104.14 |
| Diff. (effect) | 0.37 | 0.39 | **0.52** | **0.60** | 0.30 | 0.00 | 0.31 |
| Area normalized (effect) | 1.73 | 1.82 | 2.10 | 2.47 | 1.28 | 0.02 | 2.00 |
| | | | | | | | |
| **High (4KHz-8KHz)** | | | | | | | |
| Avg. level1 | 104.94 | 104.87 | 104.88 | 104.84 | 104.89 | 105.02 | 104.97 |
| Avg. level2 | 105.29 | 105.36 | 105.35 | 105.39 | 105.34 | 105.21 | 105.26 |
| Diff. (effect) | 0.35 | **0.48** | **0.47** | **0.55** | 0.44 | 0.19 | 0.29 |
| Area normalized (effect) | 1.60 | 2.23 | 1.91 | 2.24 | 1.89 | 0.83 | 1.86 |

## 4.2.1  Result discussion

ON/OFF Taguchi analysis in Alpha Cabin shows that zones 2, 3 and 4 dominate in the low and high frequencies and zones 3 and 4 dominate in the mid frequencies, in reducing the average SPL inside the Alpha cabin. It is to be noted that the Alpha Cabin simulations are conducted using multiple point sources, to avoid sensitivity to the source location.
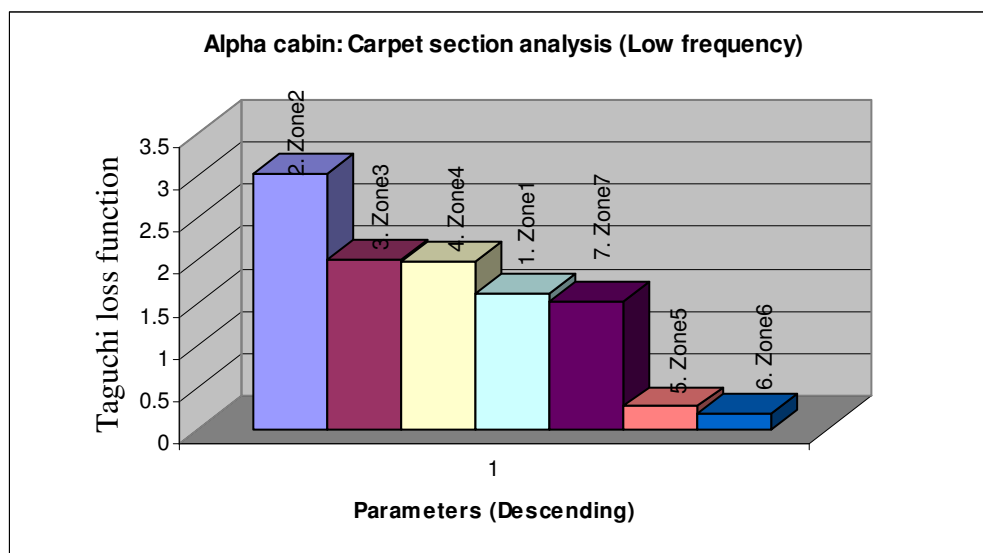


Figure 9.8: Alpha Cabin - Carpet section analysis (Low freq) Taguchi loss function
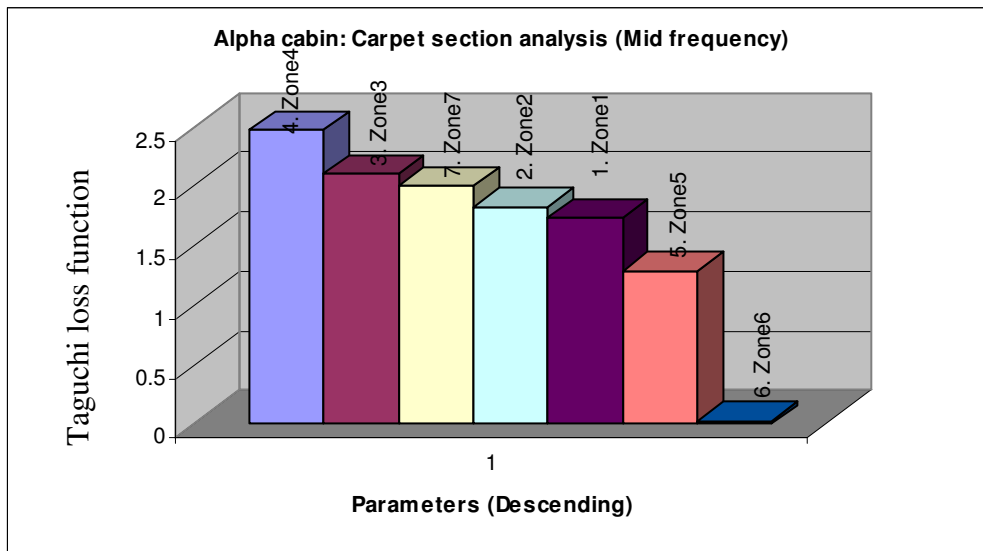
Figure 9.9: Alpha Cabin - Carpet section analysis (Mid freq) Taguchi loss function
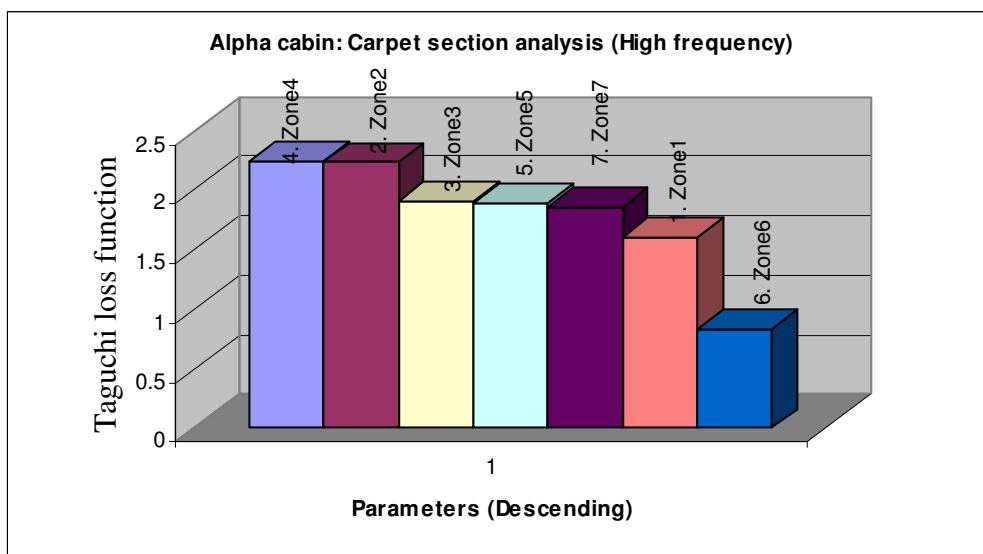


Figure 9.10: Alpha Cabin - Carpet section analysis (High freq) Taguchi loss function

# 5  Vehicle sound package Taguchi analysis

The Taguchi ON/OFF analysis on the vehicle sound package helps to identify the order of significance of each noise treatment in reducing the noise level inside the vehicle

cabin, and also to identify the percentage of contribution in reducing the noise level, in consideration of variable coupling effects.

Compared to the carpet section Taguchi analysis, where the loss functions were normalized with respect to surface area, the sound package Taguchi analysis does not have area normalization.

The in vehicle sound package is divided into 7 sections/categories as explained below.

## 5.1  Sound package Taguchi sections

The following are the sound package sections or parameters (1-7), for which the ON/OFF Taguchi analysis is conducted for both engine noise and tyre noise sources. Note that a separate analysis is conducted for the study of window contribution in cabin noise level.



| 1 | 2 | 3 |
| Seats | Headliner | Door trim |



| 4 | 5 | 6 |
| Carpet | Dash board & firewall | Trunk trim |

**OR**

Chasis pillars                                          Windows
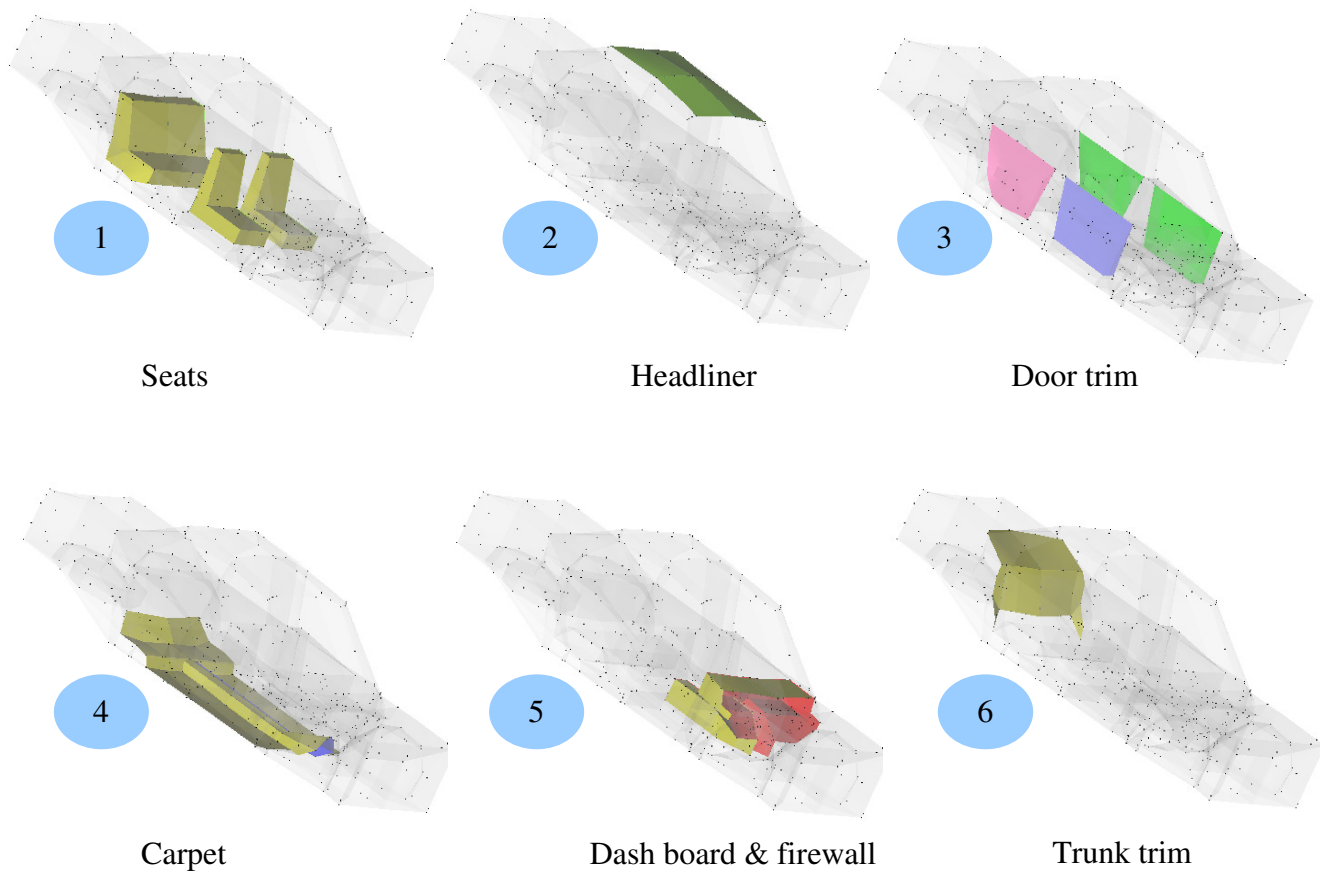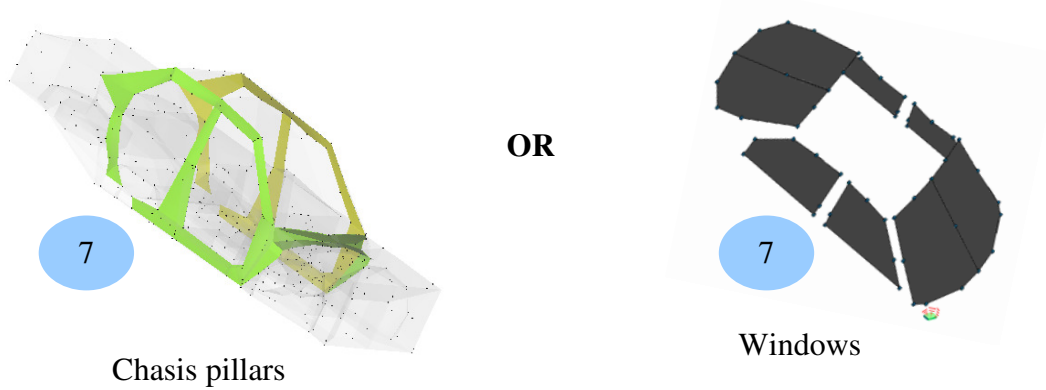
Figure 9.11: Sound package sections/categories for ON/OFF Taguchi analysis

## *5.2  Taguchi analysis results*

The ON/OFF Taguchi analysis test results for vehicle sound package are given in the below tables. The variable and level settings for the vehicle sound package ON/OFF Taguchi analysis are listed in Table 16. The Taguchi test run settings and output results are listed in Table 17.

Table 16: Taguchi Parameter table

| **Input variables** | | |
|---|---|---|
| | Level 1 | Level 2 |
| | | |
| 1. Seats | ON | OFF |
| 2. Head liner | ON | OFF |
| 3. Door trim | ON | OFF |
| 4. Carpet | ON | OFF |
| 5. Dash board + Fire-wall | ON | OFF |
| 6. Trunk | ON | OFF |
| 7. ABC pillars | ON | OFF |

## Engine noise

Table 17: Taguchi test table

| | 1. Seats | 2. Head liner | 3. Door trim | 4. Carpet | 5. Dash board+FireWall | 6. Trunk | 7. ABC pillars | | Averages | | |
|---|---|---|---|---|---|---|---|---|---|---|---|
| | | | | Input variables | | | | | | | |
| | **1** | **2** | **3** | **4** | **5** | **6** | **7** | | **Low** | **Mid** | **High** |
| Run 1 | ON | ON | ON | ON | ON | ON | ON | | 29.84 | 24.32 | 13.56 |
| Run 2 | ON | ON | ON | OFF | OFF | OFF | OFF | | 32.85 | 26.72 | 15.87 |
| Run 3 | ON | OFF | OFF | ON | ON | OFF | OFF | | 30.99 | 24.32 | 10.53 |
| Run 4 | ON | OFF | OFF | OFF | OFF | ON | ON | | 33.34 | 27.55 | 18.80 |
| Run 5 | OFF | ON | OFF | ON | OFF | ON | OFF | | 32.79 | 27.68 | 15.05 |
| Run 6 | OFF | ON | OFF | OFF | ON | OFF | ON | | 30.99 | 24.32 | 10.53 |
| Run 7 | OFF | OFF | ON | ON | OFF | OFF | ON | | 33.19 | 29.05 | 21.71 |
| Run 8 | OFF | OFF | ON | OFF | ON | ON | OFF | | 35.94 | 32.95 | 25.70 |

Since power train or engine noise stays in low-mid frequency ranges, the Taguchi test run results are averaged in the low (315Hz - 1kHz) and mid (1kHz - 4kHz) frequency ranges.

Table 18: Taguchi loss function table

| | 1. Seats | 2. Head liner | 3. Door trim | 4. Carpet | 5. Dash board+FireWall | 6. Trunk | 7. ABC pillars |
|---|---|---|---|---|---|---|---|
| | **1** | **2** | **3** | **4** | **5** | **6** | **7** |
| **Low (315Hz-1KHz)** | | | | | | | |
| Avg. level1 | 31.75 | 31.62 | 32.96 | 31.70 | 31.94 | 32.98 | 31.84 |
| Avg. level2 | 33.23 | 33.36 | 32.03 | 33.28 | 33.04 | 32.00 | 33.14 |
| Diff. (effect) | 1.47 | **1.75** | 0.93 | **1.58** | 1.10 | 0.97 | 1.30 |
| **Mid (1KHz-4KHz)** | | | | | | | |
| Avg. level1 | 25.73 | 25.76 | 28.26 | 26.34 | 26.48 | 28.12 | 26.31 |
| Avg. level2 | 28.50 | 28.47 | 25.97 | 27.89 | 27.75 | 26.10 | 27.92 |
| Diff. (effect) | **2.77** | **2.71** | **2.29** | 1.54 | 1.27 | 2.02 | 1.61 |

## Tyre noise

Table 19: Taguchi test table

| | 1. Seats | 2. Head liner | 3. Door trim | 4. Carpet | 5. Dash board+FireWall | 6. Trunk | 7. ABC pillars | | Averages | | |
|---|---|---|---|---|---|---|---|---|---|---|---|
| | **Input variables** | | | | | | | | | | |
| | **1** | **2** | **3** | **4** | **5** | **6** | **7** | | **Low** | **Mid** | **High** |
| Run 1 | ON | ON | ON | ON | ON | ON | ON | | 45.82 | 42.21 | 32.95 |
| Run 2 | ON | ON | ON | OFF | OFF | OFF | OFF | | 47.43 | 42.70 | 30.54 |
| Run 3 | ON | OFF | OFF | ON | ON | OFF | OFF | | 47.44 | 42.17 | 29.41 |
| Run 4 | ON | OFF | OFF | OFF | OFF | ON | ON | | 48.32 | 43.66 | 35.26 |
| Run 5 | OFF | ON | OFF | ON | OFF | ON | OFF | | 47.44 | 46.30 | 31.64 |

| Run 6 | OFF | ON | OFF | OFF | ON | OFF | ON | | 49.03 | 46.30 | 38.91 |
| Run 7 | OFF | OFF | ON | ON | OFF | OFF | ON | | 48.32 | 44.83 | 38.51 |
| Run 8 | OFF | OFF | ON | OFF | ON | ON | OFF | | 49.83 | 46.01 | 37.22 |

Table 20: Taguchi loss function table

| | 1. Seats | 2. Head liner | 3. Door trim | 4. Carpet | 5. Dash board+FireWall | 6. Trunk | 7. ABC pillars |
|---|---|---|---|---|---|---|---|
| | **1** | **2** | **3** | **4** | **5** | **6** | **7** |
| **Low (315Hz-1KHz)** | | | | | | | |
| Avg. level1 | 47.25 | 47.43 | 47.85 | 47.25 | 48.03 | 47.85 | 47.87 |
| Avg. level2 | 48.65 | 48.47 | 48.05 | 48.65 | 47.87 | 48.05 | 48.03 |
| Diff. (effect) | **1.40** | **1.05** | 0.21 | **1.40** | 0.15 | 0.20 | 0.16 |
| | | | | | | | |
| | | | | | | | |
| **Mid (1KHz-4KHz)** | | | | | | | |
| Avg. level1 | 42.69 | 44.38 | 43.94 | 43.88 | 44.17 | 44.55 | 44.25 |
| Avg. level2 | 45.86 | 44.17 | 44.61 | 44.67 | 44.37 | 44.00 | 44.30 |
| Diff. (effect) | **3.17** | 0.21 | **0.67** | **0.79** | 0.20 | 0.55 | 0.04 |
| | | | | | | | |
| | | | | | | | |
| **High (4KHz-8KHz)** | | | | | | | |
| Avg. level1 | 32.04 | 33.51 | 34.81 | 33.13 | 34.62 | 34.27 | 36.41 |
| Avg. level2 | 36.57 | 35.10 | 33.80 | 35.48 | 33.99 | 34.34 | 32.20 |
| Diff. (effect) | **4.53** | 1.59 | 1.00 | **2.36** | 0.64 | 0.07 | **4.21** |

## 5.2.1  Result discussion

*Engine noise*

At low frequencies, the headliner and the carpet seem to be the dominating sound package components. Meanwhile, in the mid frequency range of engine noise, the seats, headliner and door trim follow the dominating order.
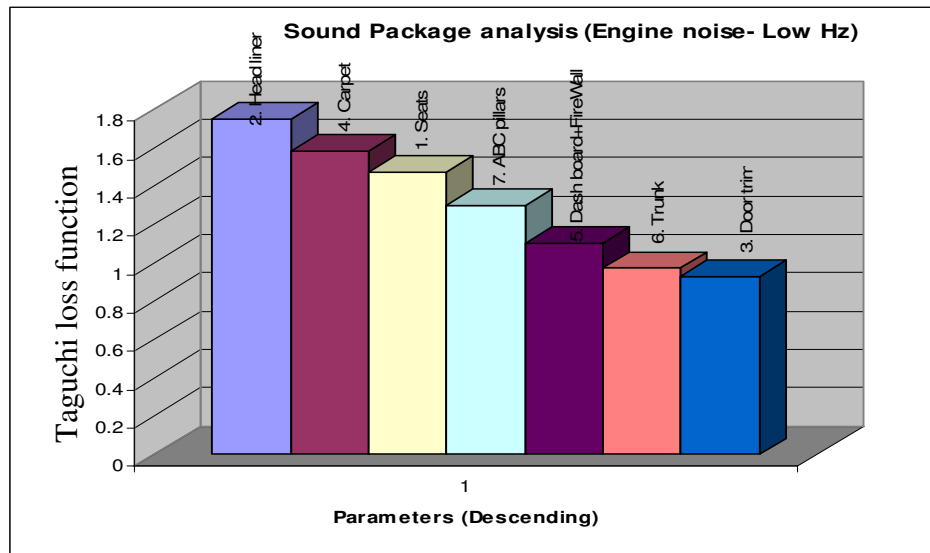


Figure 9.12: Vehicle sound package analysis (Engine noise – Low freq) Taguchi loss function

*Tyre noise*

As expected the seats have the highest loss function in all the frequency ranges of interest. Meanwhile the carpet and headliner are the next two treatments that dominate in the low frequency range. Next to seats, at the mid frequency range, the carpet and the door trim dominate, and the chassis pillars and carpet dominate at the high frequency ranges.
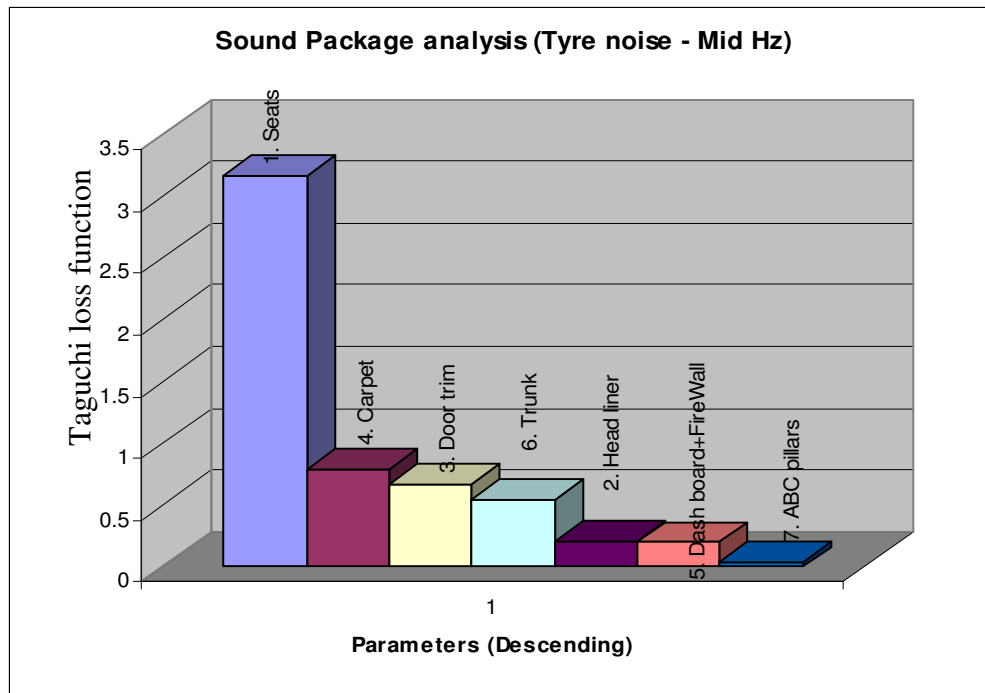
Figure 9.13: Vehicle sound package analysis (Tyre noise – Mid freq) Taguchi loss function

## 5.2.2  Taguchi analysis including window screens

A separate Taguchi analysis is conducted by including the vehicle window glasses, in order to see the contribution of glass absorption and transmission loss. It is to be noted that, similar to the other sound package section, the OFF case for a window is considered as sheet metal (1mm thick) without noise control treatment.

### 5.2.2.1 Taguchi analysis results

The ON/OFF Taguchi analysis test results (engine noise and tyre / road noise) for window contribution study are given in the below tables.

Engine noise

Table 21: Taguchi loss function table

| | 1. Seats | 2. Head liner | 3. Door trim | 4. Carpet | 5. Dash board+FireWall | 6. Trunk | 7. Windows |
|---|---|---|---|---|---|---|---|
| | **1** | **2** | **3** | **4** | **5** | **6** | **7** |
| **Low (315Hz-1KHz)** | | | | | | | |
| Avg. level1 | 33.02 | 32.76 | 33.90 | 33.09 | 33.12 | 34.04 | 31.84 |
| Avg. level2 | 34.29 | 34.55 | 33.41 | 34.22 | 34.19 | 33.27 | 35.47 |
| Diff. (effect) | 1.27 | **1.79** | -0.48 | 1.13 | 1.06 | -0.77 | **3.63** |
| | | | | | | | |
| | | | | | | | |
| **Mid (1KHz-4KHz)** | | | | | | | |
| Avg. level1 | 25.65 | 25.65 | 28.18 | 26.23 | 26.40 | 28.01 | 26.31 |
| Avg. level2 | 28.38 | 28.39 | 25.85 | 27.81 | 27.64 | 26.03 | 27.73 |
| Diff. (effect) | **2.73** | **2.74** | **-2.33** | 1.58 | 1.24 | -1.98 | 1.42 |
| | | | | | | | |
| | | | | | | | |
| **High (4KHz-8KHz)** | | | | | | | |
| Avg. level1 | 16.66 | 15.46 | 20.15 | 17.78 | 16.89 | 19.81 | 16.15 |
| Avg. level2 | 19.78 | 20.99 | 16.30 | 18.67 | 19.56 | 16.64 | 20.30 |
| Diff. (effect) | 3.12 | **5.53** | **-3.85** | 0.89 | 2.67 | -3.18 | **4.15** |

**Tyre noise**

Table 22: Taguchi loss function table

| | 1. Seats | 2. Head liner | 3. Door trim | 4. Carpet | 5. Dash board+FireWall | 6. Trunk | 7. Windows |
|---|---|---|---|---|---|---|---|
| | **1** | **2** | **3** | **4** | **5** | **6** | **7** |
| **Low (315Hz-1KHz)** | | | | | | | |
| Avg. level1 | 48.62 | 48.85 | 49.07 | 48.69 | 49.26 | 49.14 | 47.87 |
| Avg. level2 | 49.94 | 49.71 | 49.49 | 49.87 | 49.30 | 49.42 | 50.69 |
| Diff. (effect) | **1.32** | 0.86 | 0.43 | **1.17** | 0.03 | 0.28 | **2.82** |
| | | | | | | | |
| | | | | | | | |
| **Mid (1KHz-4KHz)** | | | | | | | |
| Avg. level1 | 41.65 | 43.90 | 43.18 | 43.31 | 43.32 | 44.26 | 44.25 |
| Avg. level2 | 45.57 | 43.32 | 44.04 | 43.91 | 43.90 | 42.96 | 42.97 |
| Diff. (effect) | **3.93** | -0.59 | 0.87 | 0.60 | 0.58 | **-1.30** | **-1.28** |
| | | | | | | | |
| | | | | | | | |
| **High (4KHz-8KHz)** | | | | | | | |
| Avg. level1 | 33.71 | 35.24 | 36.32 | 35.09 | 36.36 | 36.07 | 36.41 |
| Avg. level2 | 38.37 | 36.84 | 35.77 | 36.99 | 35.72 | 36.02 | 35.67 |
| Diff. (effect) | **4.65** | **1.60** | -0.55 | **1.91** | -0.65 | -0.05 | -0.73 |

The Taguchi analysis results show that the windows play a very significant role in the low frequency ranges for both the engine and tyre noises.
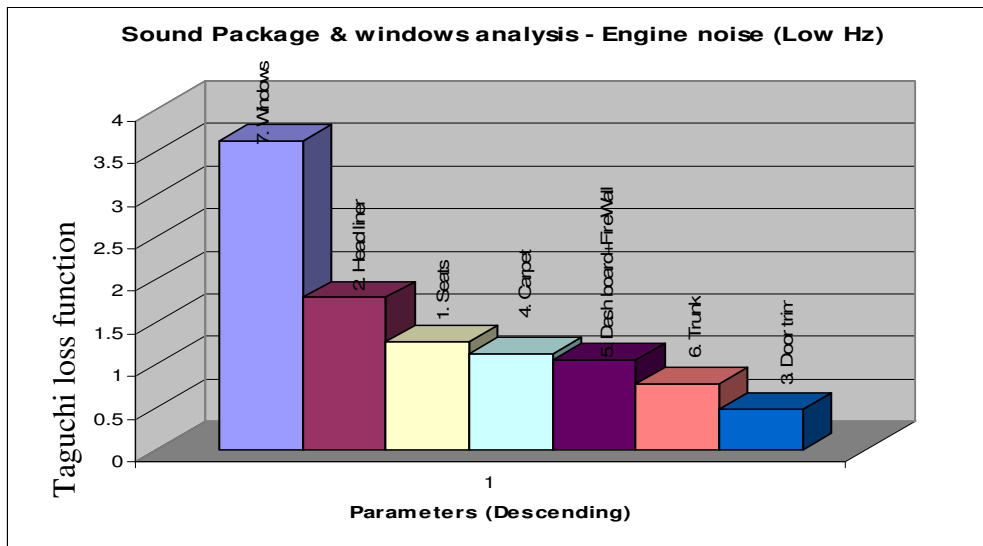
Figure 9.14: Vehicle sound package & window analysis (Engine noise – Low freq)
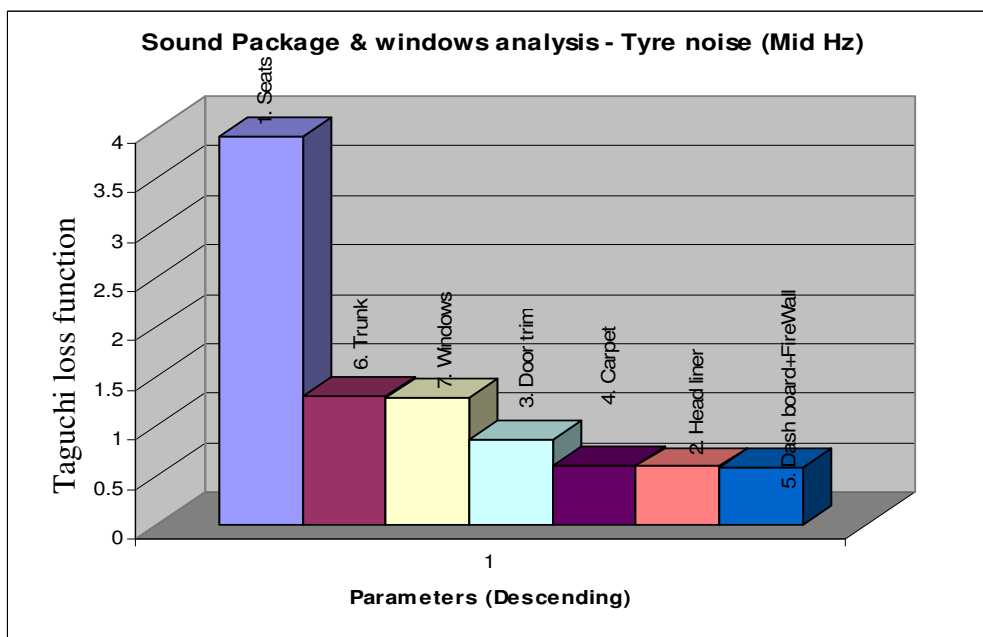


Figure 9.15: Vehicle sound package & window analysis (Tyre noise – Mid freq)

## 5.3  Vehicle carpet section Taguchi analysis

**Carpet sections**

The carpet is divided into 7 approximately equal area zones for ON/OFF Taguchi analysis. As shown below, the sections that come into the same zone have the same zone number.
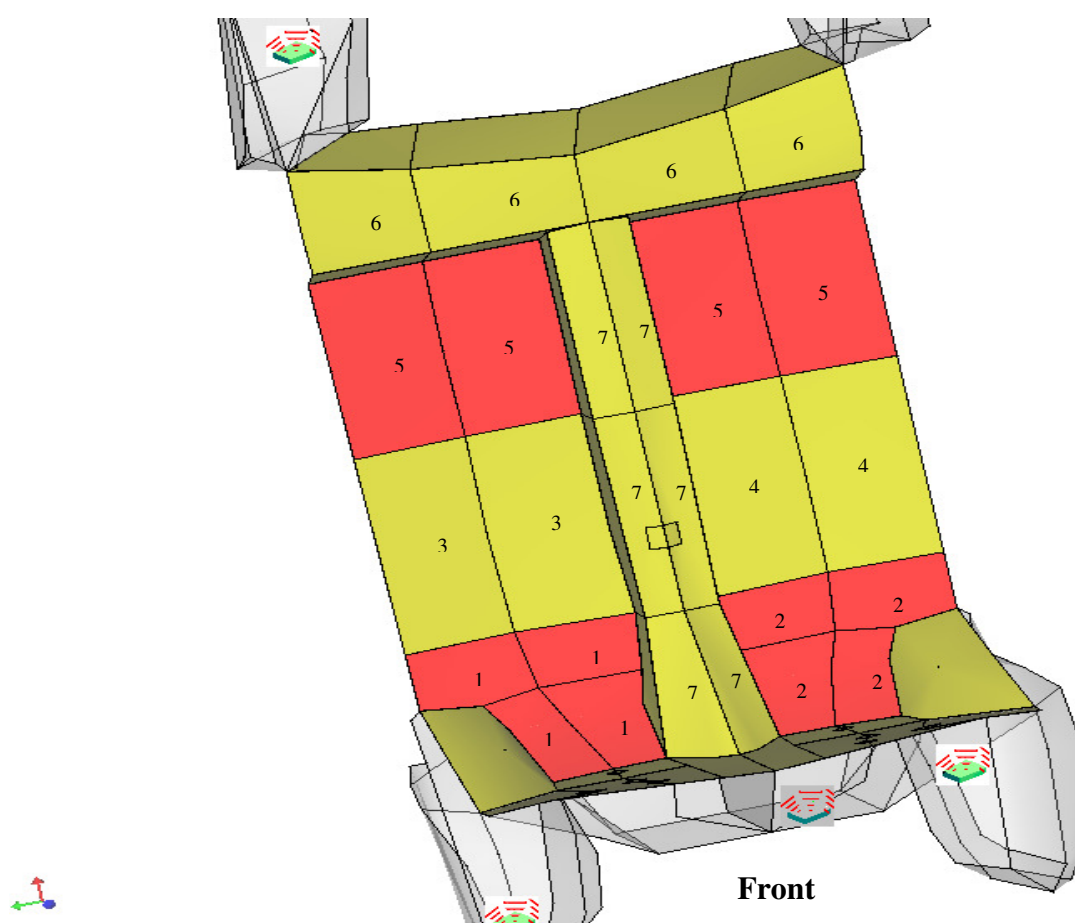


Figure 9.16: Vehicle level carpet section ON/OFF Taguchi zones

Referring to Figure 9.10, the red carpet sections are the areas where normally mats are placed on the carpet. These sections are carefully placed as separate Taguchi zones/parameters, for analysing the contribution of such mat sections. Similar to the Alpha

Cabin Taguchi analysis, the carpet section wise loss function results are normalized to 1m$^2$ as various carpet zones have different surface areas.

Compared to the component level Alpha Cabin Taguchi analysis, where only sound absorption of the carpet is considered, in vehicle level carpet section analysis the Sound Transmission Loss of the carpet also comes into picture. Further, the engine and tyre noise sources are transmitted both as air-borne and structure borne through the vehicle components and cavity subsystems.

## 5.3.1  Taguchi analysis results

The ON/OFF Taguchi analysis test results for vehicle carpet sections are given in the below tables.

*Engine noise*

Table 23: Taguchi loss function table

| | 1. Zone1 | 2. Zone2 | 3. Zone3 | 4. Zone4 | 5. Zone5 | 6. Zone6 | 7. Zone7 |
|---|---|---|---|---|---|---|---|
| | **1** | **2** | **3** | **4** | **5** | **6** | **7** |
| **Low (315Hz-1KHz)** | | | | | | | |
| Avg. level1 | 33.48 | 33.14 | 33.53 | 33.09 | 33.23 | 33.50 | 33.17 |
| Avg. level2 | 33.74 | 34.07 | 33.68 | 34.12 | 33.99 | 33.71 | 34.05 |
| Diff. (effect) | 0.26 | **0.93** | 0.15 | **1.03** | 0.76 | 0.21 | 0.88 |
| Area normalized (effect) | 1.10 | **3.94** | 0.36 | **2.49** | 1.02 | 0.50 | 1.16 |
| | | | | | | | |
| **Mid (1KHz-4KHz)** | | | | | | | |
| Avg. level1 | 30.37 | 29.85 | 30.33 | 29.76 | 30.05 | 30.32 | 30.02 |
| Avg. level2 | 30.54 | 31.06 | 30.58 | 31.16 | 30.86 | 30.60 | 30.90 |
| Diff. (effect) | 0.17 | **1.21** | 0.25 | **1.40** | 0.81 | 0.29 | 0.88 |
| Area normalized (effect) | 0.73 | **5.14** | 0.62 | **3.40** | 1.10 | 0.67 | 1.15 |
| | | | | | | | |
| **High (4KHz-8KHz)** | | | | | | | |

| | | | | | | |
|---|---|---|---|---|---|---|
| Avg. level1 | 21.43 | 20.70 | 21.38 | 20.86 | 21.11 | 21.37 | 20.99 |
| Avg. level2 | 21.63 | 22.36 | 21.68 | 22.20 | 21.95 | 21.69 | 22.07 |
| Diff. (effect) | 0.20 | **1.67** | 0.31 | **1.33** | 0.83 | 0.31 | 1.08 |
| Area normalized (effect) | 0.83 | **7.07** | 0.75 | **3.23** | 1.13 | 0.74 | 1.41 |

*Tyre noise*

Table 24: Taguchi loss function table

| | 1. Zone1 | 2. Zone2 | 3. Zone3 | 4. Zone4 | 5. Zone5 | 6. Zone6 | 7. Zone7 |
|---|---|---|---|---|---|---|---|
| | **1** | **2** | **3** | **4** | **5** | **6** | **7** |
| **Low (315Hz-1KHz)** | | | | | | | |
| Avg. level1 | 47.55 | 47.70 | 47.53 | 47.69 | 47.56 | 47.62 | 47.58 |
| Avg. level2 | 47.94 | 47.78 | 47.96 | 47.80 | 47.92 | 47.86 | 47.91 |
| Diff. (effect) | **0.38** | 0.08 | **0.42** | 0.11 | **0.36** | 0.24 | 0.33 |
| Area normalized (effect) | **1.63** | 0.34 | **1.02** | 0.28 | 0.49 | 0.57 | 0.43 |
| | | | | | | | |
| **Mid (1KHz-4KHz)** | | | | | | | |
| Avg. level1 | 44.82 | 44.85 | 44.77 | 44.82 | 44.78 | 44.78 | 44.82 |
| Avg. level2 | 45.04 | 45.01 | 45.09 | 45.04 | 45.08 | 45.08 | 45.04 |
| Diff. (effect) | 0.23 | 0.16 | **0.33** | 0.22 | **0.30** | **0.30** | 0.21 |
| Area normalized (effect) | **0.96** | 0.66 | **0.80** | 0.54 | 0.41 | 0.70 | 0.28 |
| | | | | | | | |
| **High (4KHz-8KHz)** | | | | | | | |
| Avg. level1 | 36.90 | 36.98 | 36.88 | 36.97 | 36.86 | 36.94 | 36.92 |
| Avg. level2 | 37.22 | 37.13 | 37.23 | 37.15 | 37.26 | 37.17 | 37.19 |
| Diff. (effect) | **0.32** | 0.14 | **0.35** | 0.18 | 0.40 | 0.23 | 0.27 |
| Area normalized (effect) | **1.37** | 0.62 | **0.85** | 0.44 | 0.54 | 0.54 | 0.36 |

## 5.3.2  Result discussion

The results clearly indicate that in the case of engine noise, the front two carpet sections nearer to the engine, i.e. zones 2 and 4, play the key role in noise reduction, which is expected. Meanwhile in the case of tyre noise the front carpet sections nearer to the driver ear, i.e. zones 1 and 3 play significantly in reducing the SPL at the driver ear.
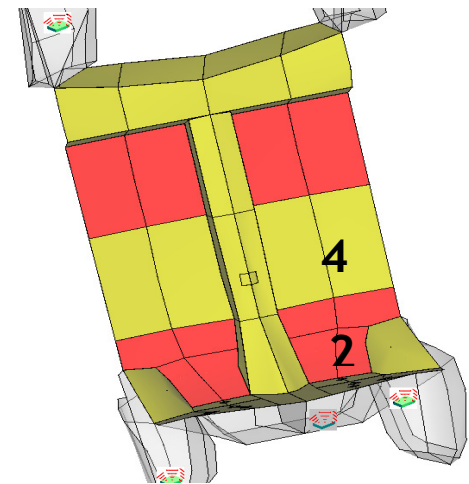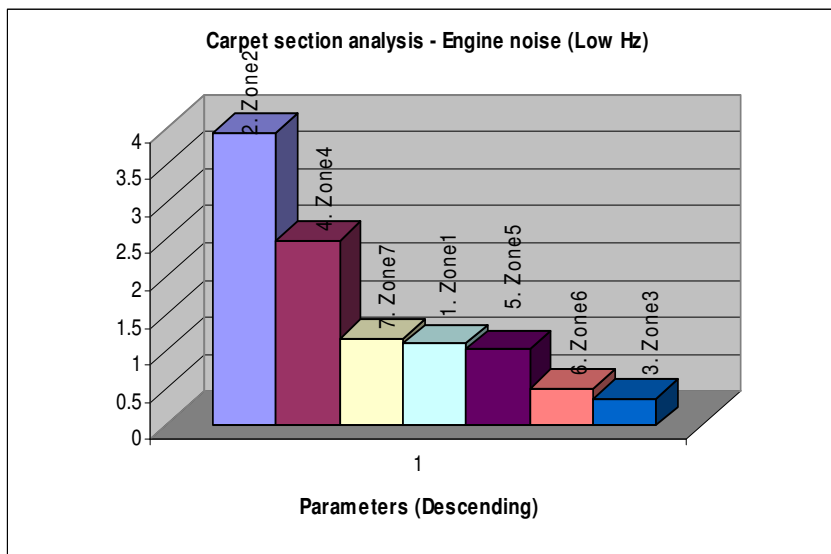


Figure 9.17: Carpet section (Vehicle level) analysis (Engine noise – Low freq)
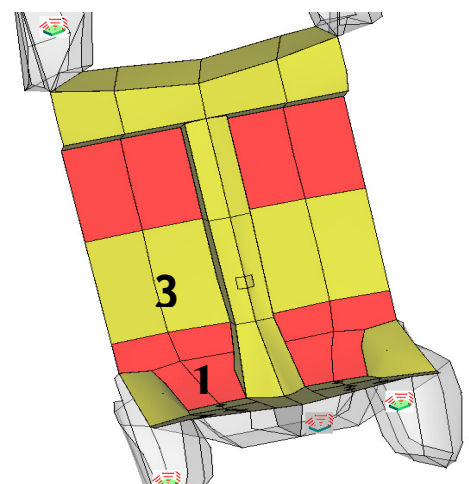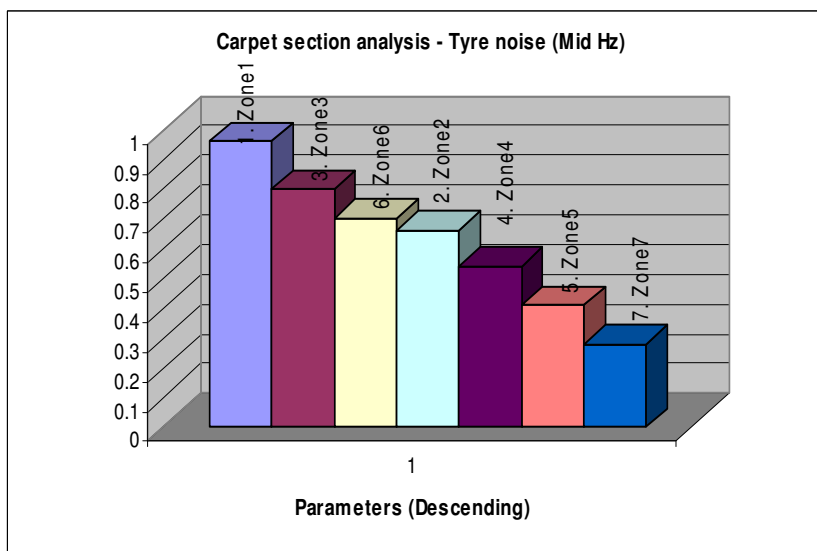


Figure 9.18: Carpet section (Vehicle level) analysis (Tyre noise – Mid freq)

# 6   CONCLUSIONS

- Simulation based Taguchi optimization can give a clear indication for further optimization

- It is preferred that separate Taguchi loss function calculation be done for various frequency ranges, like Low (315Hz-1kHz), Mid(1kHz-4kHz) and High(4kHz-8kHz) frequency ranges

- In Concept 3 carpet layers the AFR and substrate layers have the largest air flow resistivity and there fore they have the largest influence on the sound absorption coefficients in the low frequency range (315 Hz – 1000 Hz). In the mid-high frequencies the tufting & substrate have the largest influence on the sound absorption coefficients (refer Table 3)

- In Concept 3 carpet layers, the foam de-coupler has the largest influence on the sound transmission loss in the low and mid frequency ranges (refer Table 5)

- ON/OFF Taguchi analysis in Alpha Cabin shows that the front foot rest areas (zones 3 and 4) consistently dominate in the low, mid and high frequencies.

- ON/OFF Taguchi analysis for Vehicle sound package shows that for engine noise (low frequencies 315Hz to 1 kHz), the headliner and then carpet seem to be the dominating components.

- ON/OFF Taguchi analysis for tyre noise shows that the seats have the highest loss function in all the frequency ranges of interest, followed by carpet treatment, at the mid frequencies (1kHz - 4kHz)

- The Taguchi analysis results show that the windows play a very significant role in the low frequency ranges, for both the engine and tyre noises.

- The results for carpet section Taguchi analysis indicate that in the case of engine noise, the front two carpet sections nearer to the engine, i.e. zones 2 and 4, play the key role in noise reduction. Meanwhile, in the case of tyre noise, the front carpet sections nearer to the driver ear, i.e. zones 1 and 3, play significantly in reducing the SPL at the driver ear.

# CHAPTER 10

# CONCLUSIONS AND RECOMMENDATIONS FOR FURTHER RESEARCH

## 1   CONCLUSIONS

### *1.1  This thesis*

Initial benchmark analyses and target settings for vehicle cabin noise were conducted to get a clear understanding of the design requirements and constraints. The following observations are worthwhile to be noted from the vehicle tests. Low frequency power train noise has higher sound pressure level (SPL) distribution in the front part of the carpet (front foot well area), which may need more sound barriers. Meanwhile, high frequency tyre-road interaction noise has higher sound pressure level (SPL) distribution in the rear part of the carpet (rear wheel arch and the boot areas), which may need more sound absorption measures.

Theoretical analysis of forced vibration of the carpet system is studied by developing mathematical models based on the simple harmonic response and sound radiation directivity of the floor panel and carpet system. The Simple Harmonic Motion oscillator model of analyses of the current carpet design system shows that there is a resonance around the frequency of 323Hz which is in the frequency range of engine or power train noise. This is verified from the sound Transmission Loss measurements of the carpet variants, using the impedance tube method. Further, the theoretical model presented for panel radiation directivity prediction can be used to successfully predict the sound level radiated at a particular angle to the normal of a panel or opening, relative to the sound level radiated in the direction of the normal.

With a basic theoretical understanding of the current carpet design model, four new concept carpet designs are proposed and evaluated in laboratory for acoustic performance. A concept design for both good cabin side sound absorption coefficients and Sound Transmission Loss, identified as Concept 3 design, is developed.

Material level simulation validation is conducted for various acoustic samples and measured material sound absorption coefficients have a similar trend to simulated ones and have a variation of only about 10-15% for various samples. The simulation results do not include the low frequency resonance peaks, i.e. below 300Hz, observed in normal incidence absorption measurements. Further, since SEA tools use random incidence Sound absorption Coefficient (SAC) values for simulation inputs, Paris method [53] of converting normal incidence SAC to random incidence is used and validated.

The proposed carpet designs are further simulated and evaluated at component and vehicle levels. In the Alpha Cabin simulation (component level) tests, compared with the current production carpet (MITSUBISHI 380 carpet), Concept 3 carpet consistently reduces about 4.2 dB SPL above 2kHz and reduces up to average of 1 dB below 1 kHz. Concept 3 special mats reduce the noise level by 3 dB above 2 kHz and up to an average of 1 dB below 1kHz, in comparison with the current production carpet (MITSUBISHI 380 carpet).

The vehicle virtual SEA model was evaluated and validated using acoustic transfer function method and well matching results were achieved for engine and tyre noises, except for the coincidence frequency ranges of the backing sheet metal floor. Concept 3 carpet evaluation at the vehicle level shows the reduction of the in-cabin noise level further by up to 3-5 dB, compared to the current production carpet design, for power train noise. The Concept 3 carpet simulation at the vehicle level shows the reduction of the in-cabin noise level further by 2 dB at high frequencies, compared to the current production carpet design, for the tyre-road noise. The Concept 3 mat padded with the current production carpet reduces noise level by about 1dB SPL at high frequencies, compared with the carpet only case for the power train and tyre-road noise. It is illustrated that the proposed the concept 3 carpet has nearly reached the noise reduction limit.

As the component and vehicle simulation results are giving promising results, the proposed Concept 3 mat design is proto-typed for on-road evaluation. A proof of concept mat based on the proposed Concept 3 design (C3-Mat_Prototype) was factory moulded, albeit slight modifications from the original specifications due to material, time and

technical constraints. In the impedance tube SAC test, the C3-Mat_Prototype performed better than the standard mat in the low to mid frequency ranges (up to 3000Hz). Meanwhile, RMIT Alpha Cabin SAC test showed that the C3-Mat_Prototype outperformed the standard mat by an average of 14.2 % for in-cabin side SAC, with the highest improvement of about 40 % of SAC at 800 Hz. On-road vehicle tests show that the C3-Mat_Prototype has better sound absorption at the low to mid frequency range than Standard mat. On road tests using both B&K Pulse and binaural head acoustics were conducted and the data indicates a reduction of in-cabin total SPL by the prototype mat is about 2.1 dB(A) during stationary tests and 0.625 dB(A) during constant driving tests. It is noted that these improvements are measured for the proof of concept factory moulded mat, which points to the fact that a Concept 3 carpet system as a whole can give promising results, as predicted by the simulation model results.

Sensitivity and optimization of the proposed carpet design (Concept 3) are conducted by the Taguchi method. Simulation based Taguchi optimization gives a clear indication for further optimization directions.

In Concept 3 carpet layers the AFR and substrate layers have the largest air flow resistivity and therefore they have the largest influence on the sound absorption coefficients in the low frequency range (315 Hz – 1000 Hz). Meanwhile, the foam de-coupler has the largest influence on the sound transmission loss in the low and mid frequency ranges.

Based on the sensitivity analysis studies and prototype evaluation of the Concept 3 carpet design, acoustically improved carpet designs are being proposed for further research, in the following sections.

## 1.2  Research questions

The thesis has addressed the following research questions:

- What is the role of vehicle floor carpet in eliminating engine and tyre noise and how good is the current design in achieving it?

- Is virtual modelling and validation an effective tool for designing and evaluating a vehicle carpet acoustically at vehicle level?

- What could be the theoretical limits of noise reduction in the vehicle cabin by acoustically improved vehicle carpets and where are we now?

- Are there simple and efficient methods for in-situ measuring the acoustic performance of carpet design, non-destructively?

- What are the future possibilities in introducing tuned acoustic layers for vehicle carpets?

The conclusions drawn regarding the above questions are summarised below.

### 1.2.1 What is the role of vehicle floor carpet in eliminating engine and tyre noise and how good is the current design in achieving it?

ON/OFF Taguchi sensitivity analysis for Vehicle sound package shows that for engine noise (low frequencies 315Hz to 1 kHz), the headliner and then carpet seem to be the dominating components. Meanwhile, analysis for tyre noise shows that the seats have the highest loss function in all the frequency ranges of interest, followed by carpet treatment, at the mid frequencies (1kHz - 4kHz).

The average in-cabin sound absorption is relatively less, of only about 30% for the tufting layer. The measured transmission loss ranges from 10dB to 35 dB. The underlying de-coupler layer absorbs about 80% of the sound incident on it, but mainly in the frequency above 750Hz.

Referring to the vehicle simulations results, the no carpet noise level is **4-6 dB** higher compared to the current production MITSUBISHI 380 carpet design, for engine noise. The tyre noise reduction improvement from carpets is not significant, and the difference in the driver's ear SPL for the no carpet case and the ideal carpet is just **2-4dB**.

### 1.2.2 Is virtual modelling and validation an effective tool for designing and evaluating a vehicle carpet acoustically at vehicle level?

It is notable that the vehicle level simulation results of concept 3 mat on M380 standard carpet, for engine noise, showed similar possible improvement of around 1dB, especially at the higher frequency ranges.

### 1.2.3 What could be the theoretical limits of noise reduction in the vehicle cabin by acoustically improved vehicle carpets and where are we now?

It is clear that the Concept 3 design reduces the engine noise level inside the vehicle cabin by about **7-10 dB** compared to the no carpet case. It is worth noting that the Concept 3 results are very close to the ideal carpet results.

The ideal carpet is the one when floor noise control treatment having 100% sound absorption at in-cabin side and having infinite (450dB) transmission loss. The SPL results of this carpet help to know the maximum possible noise reduction potential offered by the floor trims.

From the simulation results for *tyre noise* reduction by vehicle floor carpets, the noise reduction improvement from carpets is not significant, and the difference in the driver's ear SPL for the no carpet case and the ideal carpet is just 2-4dB.

### 1.2.4  Are there simple and efficient methods for in-situ measuring the acoustic performance of carpet design, non-destructively?

The existing principles and devices for measuring the acoustic properties of materials are reviewed in detail. The proposed $45^{o}$ SAC measurement device provides non-destructive SAC measurement for sound package samples. A working prototype model of the proposed measurement device is developed and calibrated.

### 1.2.5  What are the future possibilities in introducing tuned acoustic layers for vehicle carpets?

A dedicated study is being carried out on tuned absorbers and double panel noise isolation layers in the following sections, as recommendations for further research.

## 2   RECOMMENDATIONS FOR FURTHER RESEARCH

This document outlines the continuing developments and possibilities of improving the vehicle carpet design, in an acoustic point of view, by incorporating existing and proven acoustic techniques or by introducing novel design concepts. This design process is not restricted to the normal production constraints, which includes cost, manufacturability, material availability etc. This helps to keep acoustic performance as the key focus, while raising the concept design platform to a higher level. It is hoped that all of the results can be kept aside for future production proposals or as applicable to specific sections of the current carpet system.

## 2.1  Scope for an improved design

Improving or trying to improve a design ahead of an existing proven carpet design should be driven by a reason-based analysis of the current design and its issues. A few of the key reasons behind working on the current design are,

- Sound isolation using heavy layer is a simple acoustic design.

- Increasing area density (GSM) of the heavy layer can improve sound isolation. But the weight penalty is high for the sound isolation obtained.

- More layers helps more energy dissipation

- Utilizing air-gap or double panel techniques have almost zero weight over-heads

- Application of existing aerospace noise reduction techniques

- There are various other novel acoustic structures that can be tried in a carpet design.

  All the above reasons should justify going forward with a concept design for continuing research.

## 2.2  Concept 4 carpet design constraints and targets

The regular constraints for vehicle carpet design such as manufacturing cost, aesthetics, durability, strength etc are not kept as constraints for coming up with an acoustically superior vehicle carpet design. But at the same time, the weight and total thickness are expected to be maintained the same as the current production carpet.

Total carpet thickness constraint              - 40mm

Total carpet weight (GSM) constraint          - 4.6 kgsm

Further, a reasonable acoustical improvement is considered, if it shows at least a 3dB improvement compared to the current production carpet transmission loss, especially the low frequencies (25Hz – 4kHz).

## 3    DOUBLE PANEL AND AIR-GAP THEORY

There are various acoustic techniques applied in building and aerospace industry, which are yet not tapped in vehicle acoustics, which could be due to various design constraints, implementation practicalities or mere process issues. Double panelling is a popular technique used in building acoustics, which involves placing two sound barrier panels close to each other with a fixed air gap in between. If a single barrier layer has a transmission loss of **X dB**, then this double layer system with air gap is expected to reduce sound transmission by **2X dB**, compared to the transmission loss by placing the two barriers on each other which will be only X + 10*log $2^2$ = **X + 6dB**. So, as long as X > 6dB, then it becomes practical to introduce the air gap between the barrier layers.
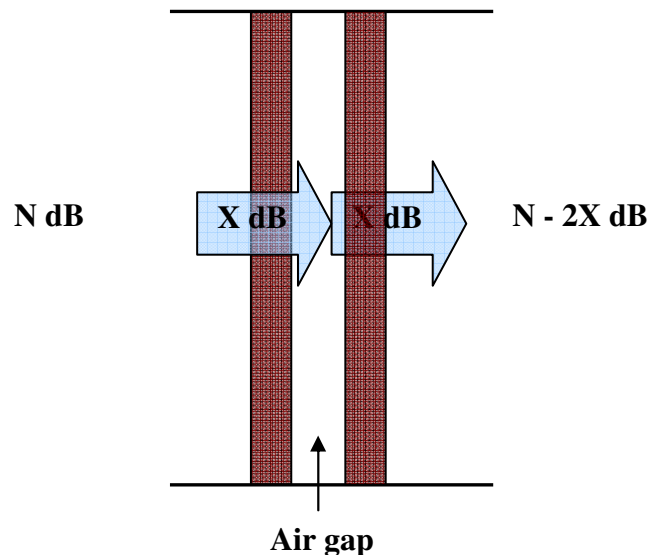


**Figure 10.1 – Double panel sound barrier**

In the case of carpet applications, the heavy layer acts as the heavy and thin sound isolation layer. Since vehicle floor carpets undergo step-on pressures from passengers and the edges are not fixed to the walls like in building acoustics, an air-gap structure is required to hold the two sound barrier layers at a fixed favourable distance. Honey-combs are popular structures in industry, normally used to increase the structural strength while keeping the weight low. So, honey-comb structures made of light materials like polycarbonate, polyester or polypropylene etc can be used for the same purpose.

In the experimental concept 4 case, we use a poly-carbonate honey-comb which is quite rigid and also has a comparable weight with foam. Below is the proposed concept 4 diagram.
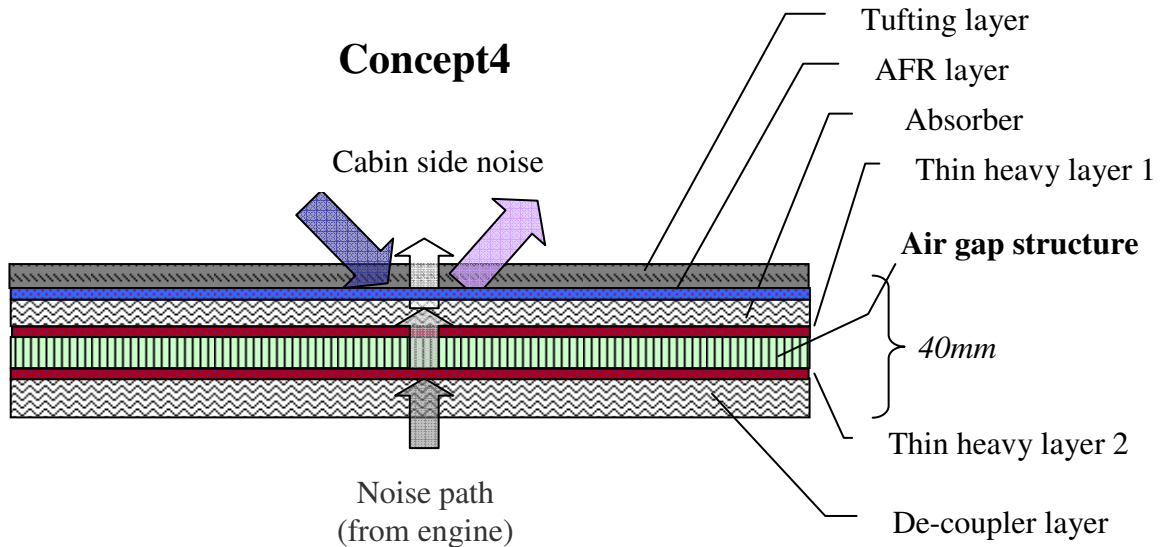


**Figure 10.2 – Concept 4 carpet design**

In concept 4, instead of the single heavy layer in concept 3 which is up to 5kgsm, we can split the heavy layer into two separate lighter layers, i.e. two heavy layers of 1.7kgsm each.

## 4   RESULT ANALYSIS

The below graph plots show the impedance tube test results for Transmission Loss, which also includes the transmission loss of the air-gap plus heavy layer alone (dashed line), without the foam or tufting layers. The layer nomenclatures and abbreviations are briefly explained in Table 1. For example, 2HL&HCg10 means two heavy layers (2HL) separated by the grey (g) honey comb (HC) structure of 10mm.

From the below plots in Figure 10.3, the best four layered combinations are highlighted for detail analysis. It is clear from the graph that there is a steadily increasing transmission loss from 500Hz to approximately 1.5 kHz, at a rate of 20dB per octave, with two local minima at about 400Hz and 2.5 kHz. Note that even the current production carpet having 5kgsm heavy layer is quite low in Transmission Loss through out the frequency ranges and even up to 50dB less at mid frequencies. This clearly illustrates that Concept 4

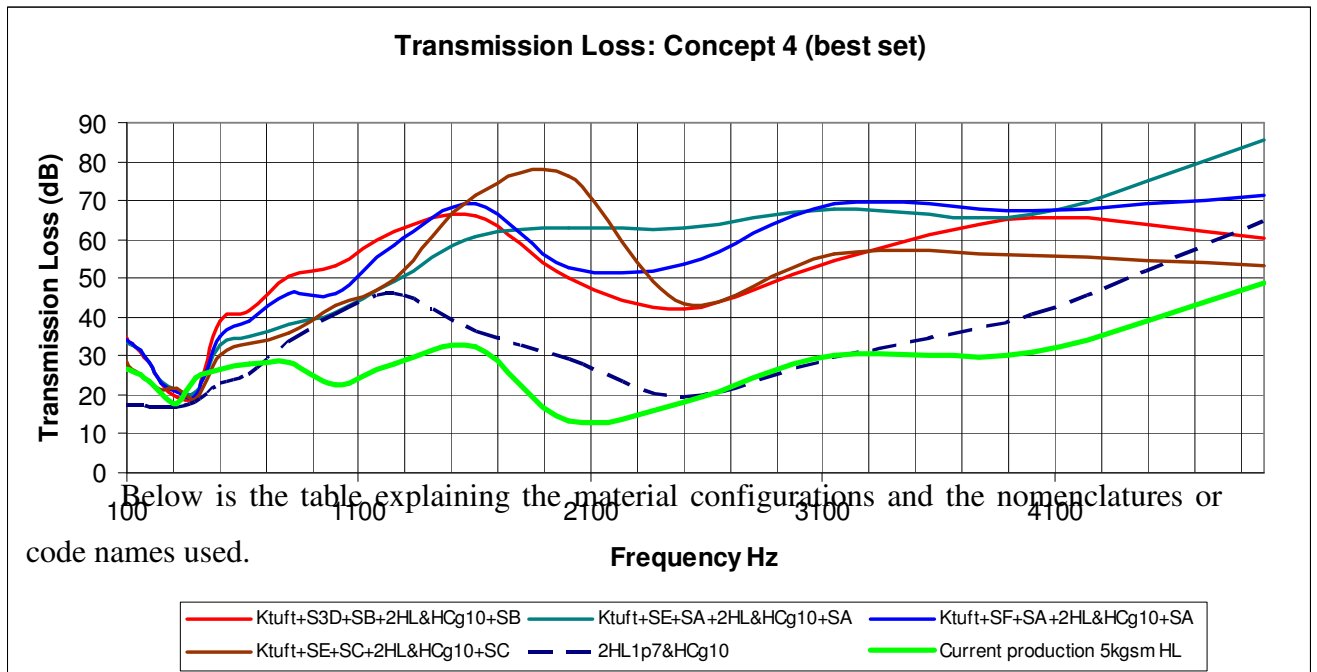carpet design using a honey comb air-gap structure is quite superior in acoustic performance of Transmission Loss.
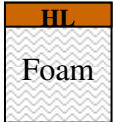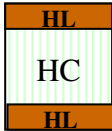


**Figure 10.3 – Transmission Loss measurements of Concept 4 design models**

Below is the table explaining the material configurations and the nomenclatures or code names used.

**Table 1 – nomenclature of layered material combinations**

| Layer | Code | Material & Specs | Construction |
|-------|------|------------------|--------------|
| 1. Tufting | Ktuft | Type K, brown tufting, 320gsm | N/A |
| 2. Air Flow Resistant layers (AFR) | S3D<br><br>S3E | 1237gsm AFR layer<br><br>1146gsm AFR layer | N/A |
| 3. Absorber | SA_scrim<br><br>SB_scrim<br><br>SC_scrim<br><br>SD_scrim<br><br>Scrim = ks<br><br>Scrim = sx | Visco-elastic foam with scrim, 20mm<br><br>Visco-elastic foam with scrim, 20mm<br><br>Fibre with scrim, 20mm<br><br>Fibre with scrim, 20mm |  |

| | VE10_ks | 100 gsm scrim | |
| | PT1f10_scrim | 44 gsm scrim | |
| | | Visco-elastic foam + scrim, 10mm | |
| | | PT1foam+scrim, 10mm | |
| 4. Heavy layer (HL)& decoupler | SL | 2.5 mm Heavy Layer (1700gsm) +1.5 kgsm close cell polyester foam (Nfoam), 20mm |  |
| | Nf20 | Nfoam, 1.5 kgsm, close cell polyester foam, 20mm | |
| 5. Air gap | 2HL&HCg10 | 2.5 mm Heavy Layer (1700gsm) + 10 mm Honeycomb structure (grey) + 2.5 mm Heavy Layer (1700gsm) |  |
| 6. Heavy layers | HL x kgsm | X kgsm Heavy layer |  |

It is to be noted that it should be verified whether the cabin side sound absorption is affected in any form by the air-gap introduced between heavy layers. So absorption tests were conducted on the concept 4 designs to verify this. The below graph shows that absorption coefficient above 1kHz has gone down by about 10% compared to the concept 3 design with single heavy layer. As the tests were done by just replacing the Concept 3 heavy layer with new Concept 4 heavy layer, it can be expected that some sound is normally transmitted through the heavy layers and absorbed by the de-coupler foam behind, i.e. in the reverse direction of engine noise path into the cabin, and since the dual heavy layer structure of Concept 4 gives higher transmission loss, this high TL makes sound energy be absorbed by the layers above the dual heavy layer only; the de-coupler play little role in absorption.
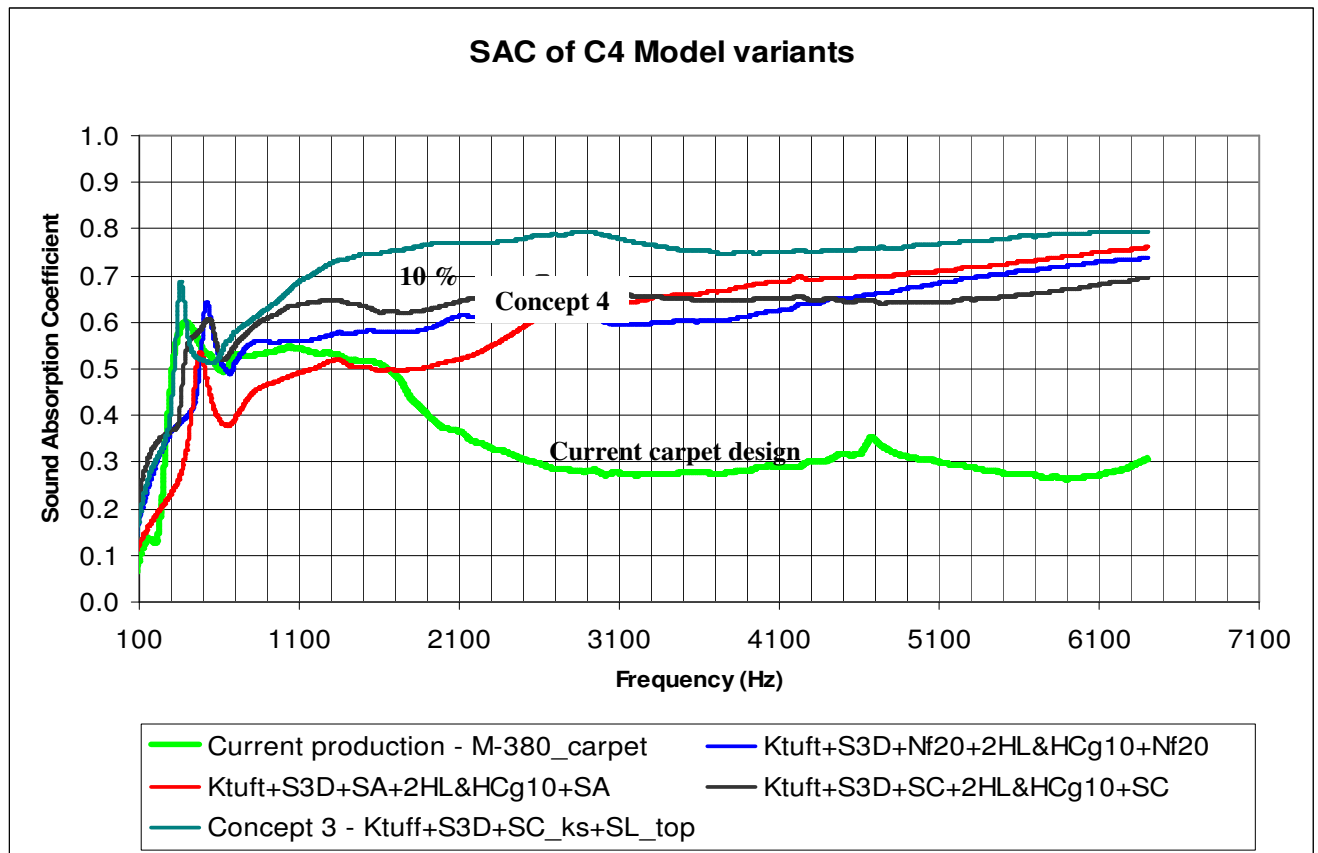
**Figure 10.4 – Sound Absorption Coefficient measurements of Concept 4 design models**

## 5    EVALUATING AGAINST CONSTRAINTS: Foam VS Honey comb

The design constraints we have in hand for concept 3 design are weight and total carpet thickness, against which we could compare **concept 4** design weight penalty. So a brief study is done in comparing between concept 3 and concept 4, where 10mm of absorber or de-coupler foams in concept 3 have been replaced by the honeycomb structure 10mm thick, as shown below in Figure 10.5.

It is to be noted that with regards to weight constraints both 10mm honeycomb structure and 10mm foam showed about the same gsm or weight. So the honey-comb is expected not to introduce any weight penalty, other than manufacturability. The heavy layers used are 1.7kgsm of area density.
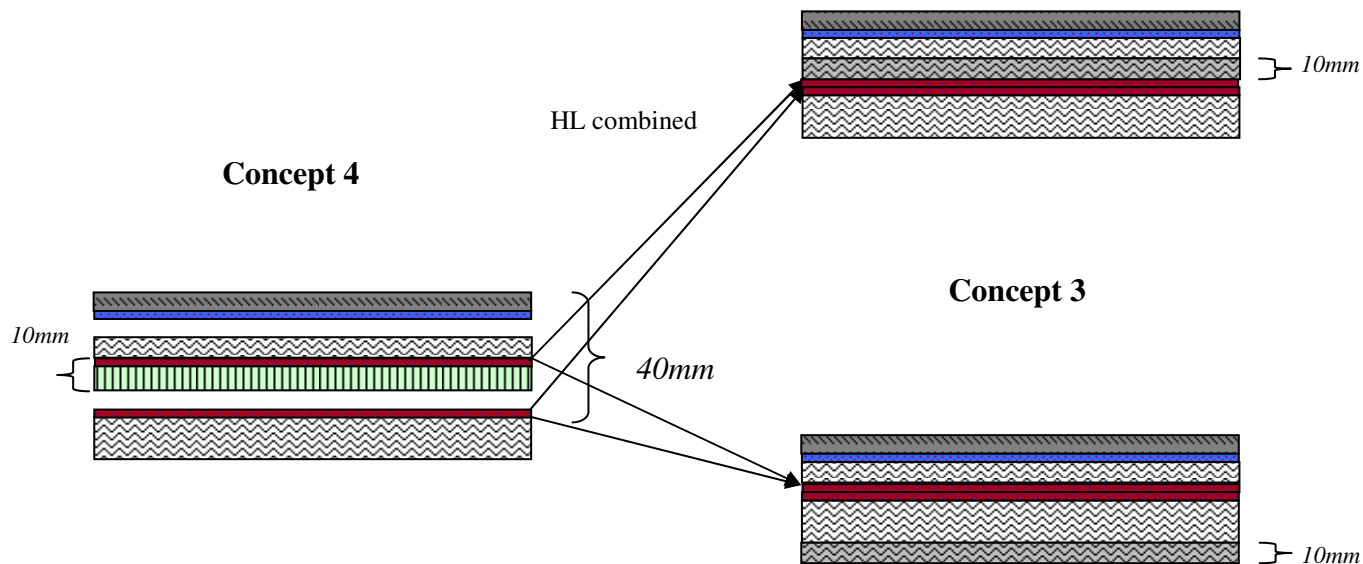


**Figure 10.5 – Concept 3 absorber/de-coupler layer replaced by honey-comb**

Further, transmission loss measurements were conducted to have direct comparison of introducing the honey-comb into concept 4 without any constraint overheads, and the results are as shown in below figure

It can be seen that concept 4 gives about 20dB of improvement in TL, compared to concept 3, at mid frequency ranges. It is notable that this increment in acoustic performance is without any weight or thickness increase introduced by the honeycomb layer of 10mm. Concep4 and concept 3 are close in transmission loss across the high frequency range. Thus this quantifies that the new concept 4 is superior to concept3 in terms of acoustic performance (TL) for the given weight and thickness constraints, and hence is a design for future acoustically improved vehicle carpets.

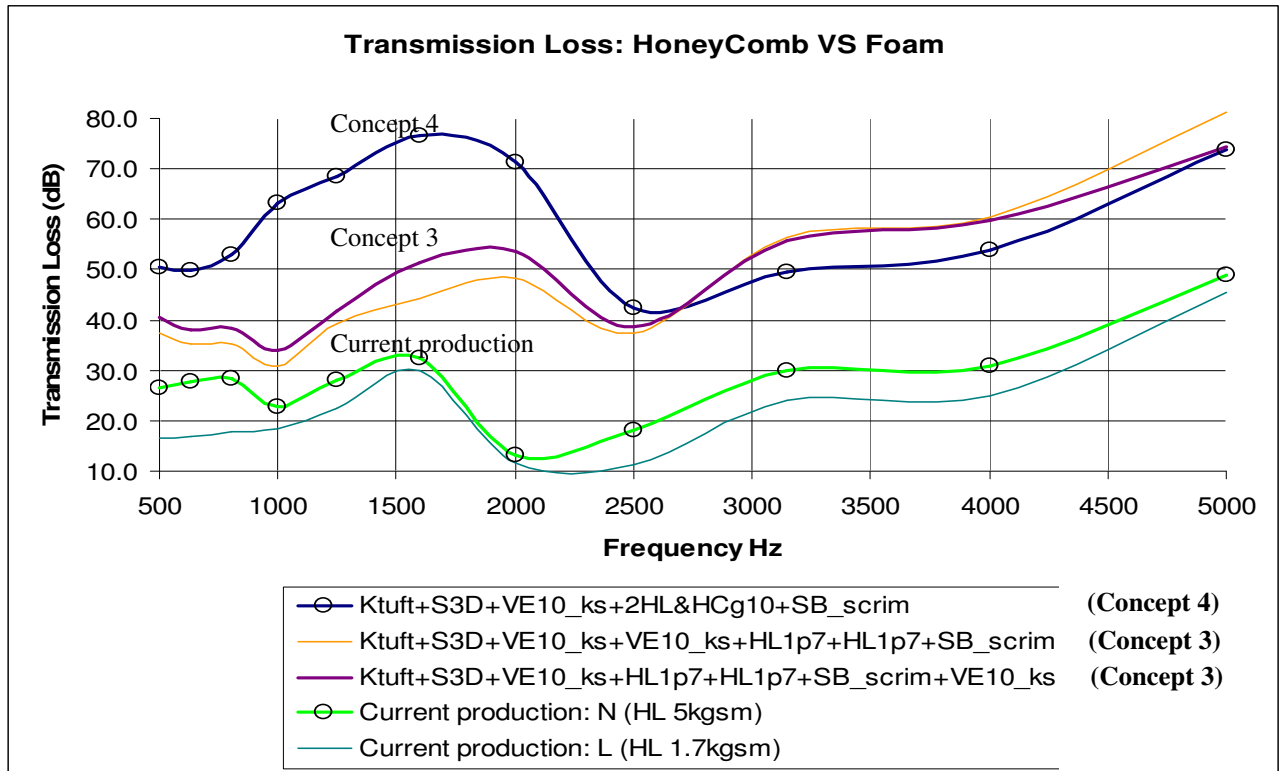**Figure 10.6 – Comparison of concept 4 and concept 3, without new weight or thickness overheads**

## 6   SPECIAL TUNED RESONANT ABSORBER LAYERS

Acoustic absorber structures have been widely used in applications like building acoustics, where specific frequencies are the target of absorption, like the room modal frequencies. Literature for resonant absorber structures point to mainly two successfully applied resonant absorbers, the Helmholtz resonator panels and the membrane (bass-trap) absorbers. These special structures and their performance at low frequency ranges is worth investigating.

The Helmholtz absorption principle is well known for its results and hence the realization of its application to a vehicle floor trim depends on how well it can be included into the current carpet layers, meanwhile adhering to the weight and cost constraints.

A possible way of introducing a Helmholtz resonator structure tuned for compensating for the weak transmission loss of the heavy layer material, i.e. measured to be around 323 Hz, is given below.
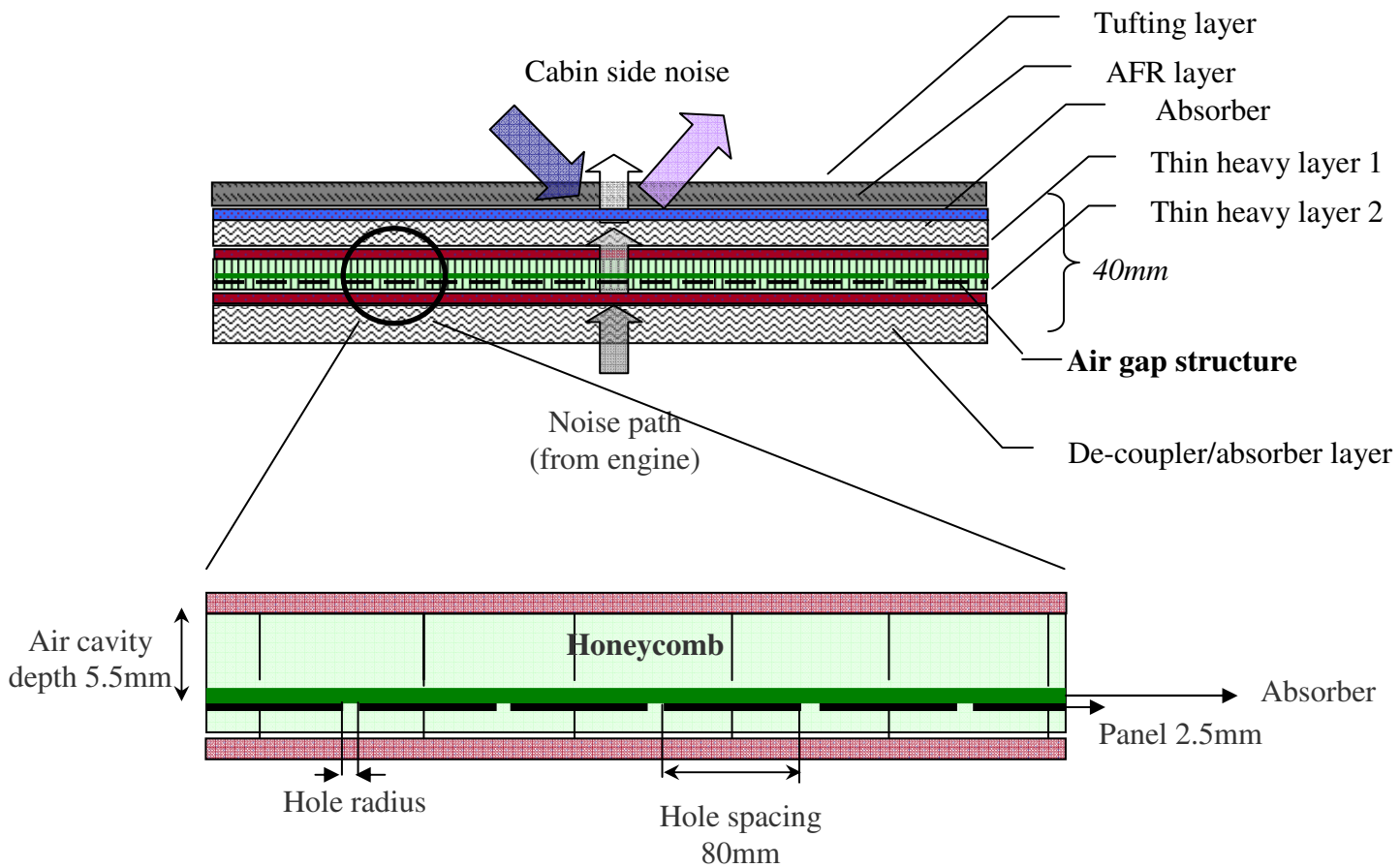
**Figure 10.7 – Tuned Helmholtz resonant absorber layer included in the Honey Comb dual panel structure**

**Example calculation of the Helmholtz resonator parameters :**

Frequency of resonant absorption $f = c/2\pi * \sqrt{(\pi*a^2/(t*D^{2*}d))}$,

Where,

C = Velocity of sound (343m/s)

a = hole radius

t = Panel thickness

D = Hole spacing

d = cavity depth

Frequency tuned for – 250Hz

| | |
|---|---|
| Panel thickness | 2.5mm |
| Cavity depth | 5.5mm |
| Hole spacing | 80mm |
| Hole radius | 0.8mm |
| Absorber thickness | 2mm |
| Total thickness | 10mm |

From the above calculation of the Helmholtz resonator layer parameters for a frequency range around 250 Hz, it is clear that the dimension like panel thickness (2.5mm), cavity depth (5.5mm) and absorber thickness (2mm) all can fit into the dimensions of the current vehicle carpet structure.

Construction of such a structure is quite involved and sophisticated equipment is required to get the matching hole radius. Hence, perforated material samples were out-sourced from third party building acoustic material providers. Such a sample (V white micro 25mm), open cell foam with a perforated synthetic facing, was tested to verify it. The specifications and details of the sample is not presented due to IP concerns.
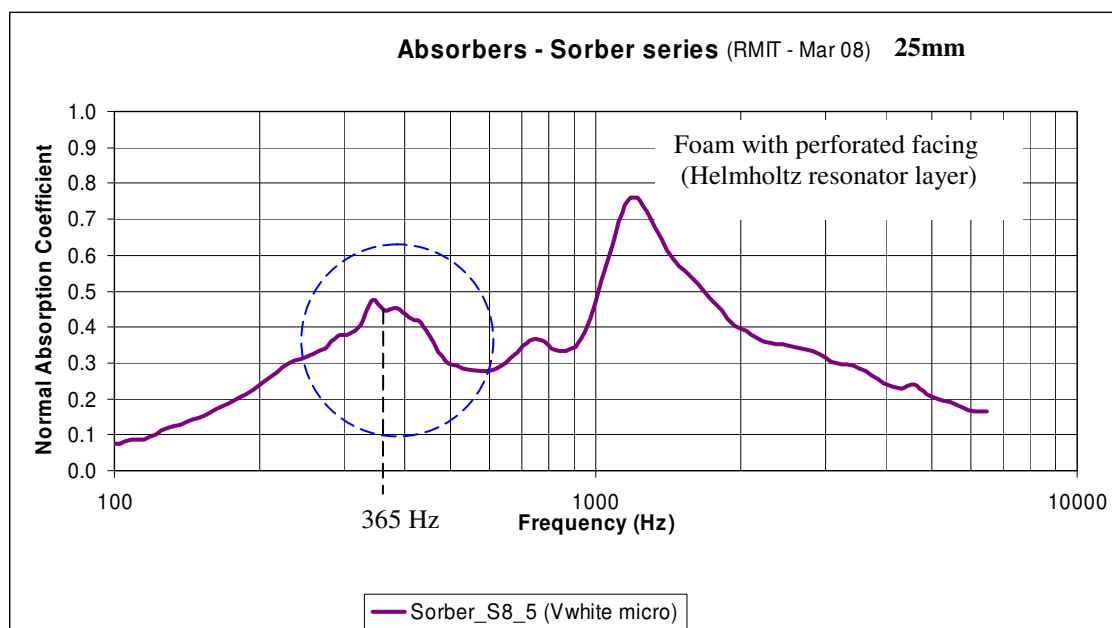


**Figure 10.8 – SAC result of perforated facing foam (25mm) Helmholtz resonator**

Similarly, the possibility of introducing resonant membrane absorber layers was investigated briefly. The below graph illustrates the improved low frequency absorption by a 25mm thick open cell foam having a thin corrugated foil membrane facing.
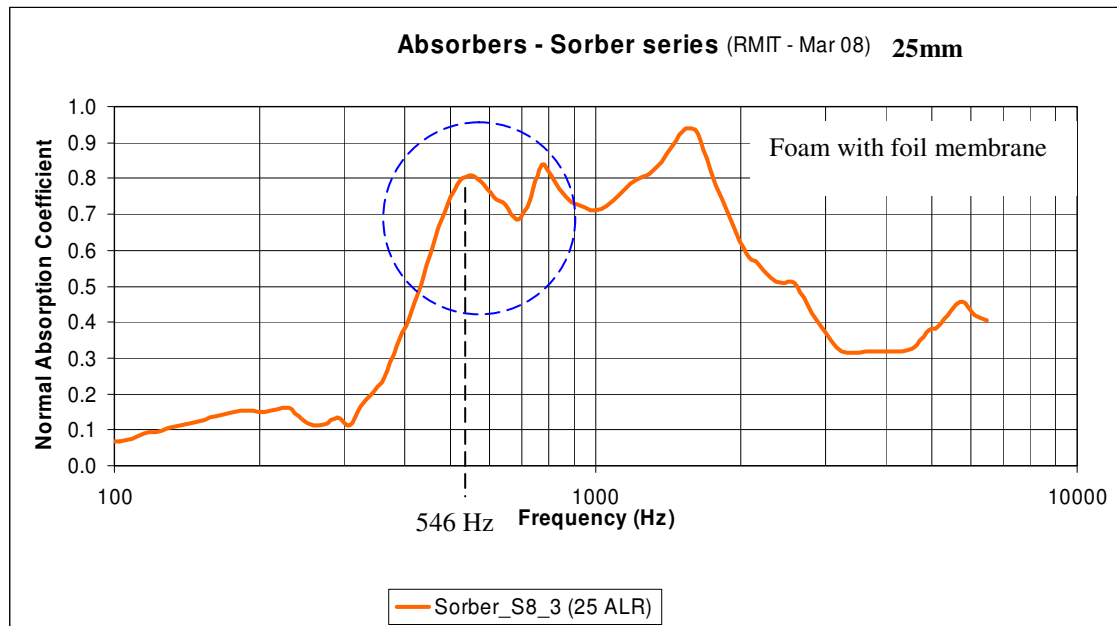


**Figure 10.9 – SAC results of *corrugated foil facing foam* resonant membrane absorber**

The SAC results for the special resonant absorbers indicate that introducing these layers into the vehicle carpet system or even other noise prone areas of the vehicle, can extend the noise reduction capability of the noise treatment to specific low frequency ranges. Further research in the direction of making these structures manufacturing friendly and cost effective can definitely give promising results.

Summarizing the recommendations for further improvement of vehicle carpet designs,

- Introducing air-gap in between the heavy layers improves the transmission loss by up to 20dB in the frequency range of 1kHz – 2kHz, and up to 10dB in the frequency range of 500Hz – 1kHz, and so is the best for these frequency ranges.

- The introduction of honey-comb structure as an air-gap structure doesn't add any over-head in terms of weight or thickness, compared to foam.

- Replacing a part of absorber or de-coupler layer by a honey-comb structure doesn't affect much the sound absorption.

- Special tuned absorber layers like the perforated facing foam Helmholtz resonator and the corrugated foil faced foam membrane absorbers are excellent in extending the noise reduction into specific low frequency ranges of interest.

# REFERENCES

[1]   Name, Initial and name, initial (year), *The title of document.* Journal, serial page section

[2]   De Bree, H.-E., (1996), *The microflown, a noval device measuring acoustical flows, sensors and actuators.* A. Physical, SNA054/1-3:552-557.

[3]   Duval, A. and al.(2005), *Vehicle acoustic synthesis method 2nd generation: an effective hybrid simulation tool to implement acoustic lightweight strategies.* Journee SFA/Renault/SNCF/-Guyancourt.

[4]   Lannoye, R. and al. (2004), *A practical device to determine the reflection coefficient of acoustic materials in-situ based on a microflown and microphone sensor*, I.S.M.A. - Leuven.

[5]   Allard, J.-F. (1993), *Propagation of Sound in Porous Media*, Applied Science.

[6]   Kampl, R. and Leitner, J. (1999, Sept. 15-17), 38th International Man-made Fibres Congress, Dombim/Austria.

[7]   Buck, K. A. and Wellman, R. A. (1997). ICI Polyurethanes, *Importance of Durability on Acoustical Performance for Carpet Underlay*, SAE-970148.

[8]   Hilyard, N.C. and Cunningham, A. (1991), *Design Optimisation of MDI-Based Polyurethane Foam Backed Automotive Carpet Systems*, SAE 911087.

[9]   Balte, R., Choe, J. and Cherng, J.G. (2003), *Investigation and Benchmarking for Vehicle Floor Coverings*, SAE 2003-1-1575.

[10]  Nick, A., Becker, U. and Thomas, W., (2002, July), *Improved Behaviour of Interior Parts of Renewable Resources in the Automotive Industry,* Journal of Polymers and the Environment, Vol 10, No.3.

[11]  Skinner, C., Peters, J., Vandenbroeck, J. (2006, Mar), Acoustic Absorbers: *A third way for the management of sound in automobiles*, Paper for UTECH Europe.

[12]  Sureshkumar, S. and Raveendra, S.T. (2003). *Modelling Noise Control Materials*, SAE 2003-01-1580.

[13]  Duval, A., Rondean, J.-F., Bishoff, L. Dejaeger, L. (2006, 30th Nov), *In Situ Impedance and Absorption Coefficient Measurement Compared to Poro-elastic Simulation in Free, Diffuse or Semi-statistical Fields Using Micro-flown p-u Probes*, Journee

SFA/Renault/SNCF.

[14] Trevor, J. Cox and Peter, D'Antonio, *Acoustic Absorbers and Diffusers - Theory, design and application*, Taylor & Francis Group.

[15] Veen, J. R. and Saha, P., (2003), *Feasibility of a Standardized Test Procedure for Random Incidence Sound Absorption Tests Using a Small Size Reverberation Room*, SAE 2003-01-1572.

[16] Caprioli, D., Bertolini, A. and Gaudino, C. (2005), *Improved NVH Performance Via Genetic Optimization of Damping and Shape of Vehicle Panels*, SAE 2005-1-2329.

[17] Gansen, P. and McCullough, D. (1990), *Viscoelastic MDI Based Polyurethane Foam for Sound and Vibration Dampening in Automobiles*, SAE 900093.

[18] MacFarland, D. R. (1994), *Cost Effective Moulded Polyurethane Foam for Automotive Acoustical Carpet Underlay and Dash Insulators*, SAE 940700.

[19] Pendergast, P. L. (1989), General Motor Corp*., Use of Taguchi Techniques as a Process Development Tool for Carpet-Covered Door Panel Production*, SAE-890238.

[20] Dempsey, M. P. and Hurley, M. F. (1991), Mobay Corp., *Advances in Urethane Foam Composites for Interior Trim*, SAE 910520.

[21] Bohm, R. (1989). *Foam Backed Automotive Carpets in Europe*, SAE 890237.

[22] John, T. Long (2003), *SEA for Design: A Case Study,* 2003-01-1565

[23] Chadwyck, T. Musser (2003), Cambridge Collaborative, Inc., *Sound Package Performance, Weight, and Cost Optimization Using SEA Analysis,* 2003-01-1571

[24] *Development of Quiet Sound Package Treatments for Class 8 Trucks*, SAE 2001-01-1541

[25] *Case Study on Airborne Road Noise Reduction of a Passenger Vehicle,* SAE 2003-01-1407

[26] *Tuning of Multi-layered Acoustic Systems,* SAE 2003-01-1437

[27] *Object- Oriented SEA Modelling,* SAE 2003-1-1551

[28] *Acoustical Optimization of Perforated Laminate Material and its Application to Vehicles,* SAE 2003-01-1567

[29] Bruel, PV and Mattia, G. M. (1998), *Bruel Acoustics Technical Review 97-01*. (web-link www.bruel-ac.com/tr/tr9701.html)

[30] Garai, M. (1993), *Measurement of the Sound-Absorption Coefficient In Situ: The Reflection Method Using Periodic Pseudorandom Sequences of Maximum Length.*

Applied Acoustics Vol. 39.

[31] *User Manual -. B&K Impedance/Transmission Loss Measurement Tubes-Type 4206.*

[32] De Bree, H-E, Lanoye, R ,de Cock, S and Van Heck, J. (2005), *In situ, broad band method to determine the normal and oblique reflection coefficient of acoustic materials.* SAE International 2005-01-2443.

[33] Lanoye, R, Vermeir, G, Lauriks, W, Kruse, R and Mellert, V. (2006), *Measuring the free field acoustic impedance and absorption coefficient of sound absorbing materials with a combined particle velocity-pressure sensor.* J. Acoustical Society of America 119(5): 2826-2831

[34] Lanoye, R, de Bree, H-E, Lauriks, W & Vermeir, G. (2004), *A practical device to determine the reflection coefficient of acoustic materials in situ based on a Microflown and microphone sensor.* (web-link : www.microflown.com/data/ISMA_2004_10177 )

[35] Garai, M, Berengier, M, Guidorzi, P and L'Hermite, PH. (1998, 4th – 7th Oct), *Procedure for measuring the sound absorption of road surfaces in situ. Proc*. Euro Noise'98 Conference. Munchen.

[36] Volker, M and Nocke (2007), C. *Applications of in-situ measurement techniques of absorption.*(web-link: www.akustikbuero.info)

[37] Bruel & Kjaer (1998), *Application note: Measurements in building acoustics.* (web-link: www.bk.de)

[38] Blake, W.K. (1986), *Mechanics of Flow-Induced Sound and Vibration*: Vol. I. Academic Press.

[39] Fisher, K. (2004), *Broadband acoustic impedance tube comparison of two microphone broadband method with conventional discrete frequency traversing technique and development of broadband analysis software.* MS Thesis. Applied Physics. RMIT University.

[40] Schultz, T, Cattafesta, LN and Sheplak, M. (2006), *Comparison of the two-microphone method and a modal decomposition method for acoustic impedance testing.* © University of Florida, Published by American Institute of Aeronautics and Astronautics.

[41] Cooke, M. (2001), *Frequency range of the acoustic impedance tube.* MS Thesis, University of Queensland.

[42] AS/NZS 1935.1:1998 (ISO 10534-1:1996), *Acoustics – Determination of sound absorption coefficient and impedance in impedance tubes. Part 1: Method using*

*standing wave ratio.*

[43] Internet resource web-link: http://www.phys.unsw.edu.au/music/.

[44] Rindel, J.H. (1975), *Transmission of traffic noise through windows – Influence of incident angle on sound insulation in theory and experiment.* Report No. 9, The Acoustics Laboratory, Technical University of Denmark, Lyngby, Denmark.

[45] Davy, J.L. (2004, 3-5 November), *The radiation efficiency of finite size flat panels.* Acoustics 2004, Transportation Noise and Vibration – The New Millennium, Proceedings of the Annual Conference of the Australian Acoustical Society, Gold Coast, Australia, Publisher Australian Acoustical Society, Castlemaine, Victoria, Australia, ISBN 909882-21-5 pp 555-560.

[46] Cremer, L. and Heckl, M. (1973), *Structure-Borne Sound*, Springer-Verlag Company, New York.

[47] Davy, J.L. (2007, 28-31 August), *A model for predicting diffraction on a finite flat surface as a function of angle of incidence and surface size.* Inter-noise 2007, Istanbul, Turkey.

[48] Stead, M. (2001), *Sound Reduction for Reverberant, Direct and Diffracted Sound through Single Isotropic Glass Panels of Finite Size*, Master of Engineering Science Thesis, Department of Mechanical Engineering, Monash University, Melbourne, Australia.

[49] Sutton, M. (1990), *Noise Directivity of Exhaust Stacks.* Final year thesis for the Honours Degree of Bachelor of Engineering, University of Adelaide, Adelaide, Australia.

[50] Bolton, J. S. et al. (1996), *Sound Transmission Through Multi-Panel Structures Lined with Elastic Porous Materials.* Journal of Sound and Vibration 191(3), pp. 317- 347.

[51] Bolton, J. S. and Kang, Y. J (1997)., *Elastic Porous Materials for Sound Absorption and Transmission Control*, Proceedings, SAE Noise and Vibration Conference, 971878, pp. 77-91.

[52] Lawrence, E. Kinsler, Austin, R. Frey, Alan, B. Coppens and James, V. Sanders (2000), *Fundamentals of Acoustics*, Fourth edition - John Wiley & Sons.

[53] Delany M. E., Bazley E. N. (1970). *Acoustical properties of fibrous absorbent materials*. Appl. Acoust. 3, 105-116.

[54] AutoSEA2 Foam 2005, *User's guide.* Theory and Q/A.

[55] *Practical Designed Experiments*, Alan Long Quality Pty. Ltd.,1999.

[56] HEAD Acoustics, *Application Note: Binaural Measurement, analysis and playback*, (web-link: Application-notes@HEAD-acoustics.de).

[57] AS ISO 354-2006 *"Australian Standards: Acoustics – Measurement of sound absorption in a reverberation room"*

[58] De Bree, H-E, Lanoye, R ,de Cock, S & van Heck, J. (2005), *In situ, broad band method to determine the normal and oblique reflection coefficient of acoustic materials.* SEA International 2005-01-2443.

[59] Lanoye, R, Vermeir, G, Lauriks, W, Kruse, R and Mellert, V. (2006), *Measuring the free field acoustic impedance and absorption coefficient of sound absorbing materials with a combined particle velocity-pressure sensor.* J. Acoustical Society of America 119(5): 2826-2831.

[60] Lanoye, R, de Bree, H-E, Lauriks, W and Vermeir, G (2004), *A practical device to determine the reflection coefficient of acoustic materials in situ based on a Microflown and microphone sensor.* (web-link:www.microflown.com/data/ISMA_2004_10177 )

[61] Genichi Taguchi (1993), *Taguchi on Robust Technology Development*, ASME Press, New York.

[62] Dr. Genichi Taguchi and Yuin Wu (1989), *Taguchi methods: Case Studies from the U.S. and Europe*, Japaneese Standards Association, ASI Press.

[63] Edsil, Dilla and Xu, Wang (2007), *$45^o$ SAC device concept paper (Report C1-07/M5D)*, AutoCRC Carpet Acoustics Project Report.

[64] Cordioli, J. A.  andM. T. Jr., et al. (2004). *Applications of the Statistical Energy Analysis to Vibro-Acoustic Modeling of Vehicles,* SAE.

[65] Paris, E. T. (1927), Proc. Roy. Soc. 115, 407.

[66] Albert, London (1950), *The Determination of Reverberant Sound Absorption Coefficients from Acoustic Impedance Measurements,* JASA vol. 22, no.2.

[67] Dr. Stuart, Lucas (2007), *CSIRO Material Test Results, Samples B-K,* Project Report.

[68] Chris, Murphy and Ross (2007), *Final Year Thesis*, SAMME RMIT Melbourne.